This is to certify that the

thesis entitled

FIELD INVESTIGATION OF TRANSVERSE CRACKING IN JOINTED CONCRETE PAVEMENTS (JCP's)

presented by

Michael Anthony Frabizzio

has been accepted towards fulfillment
of the requirements for

Masters degree in Civil Engineering

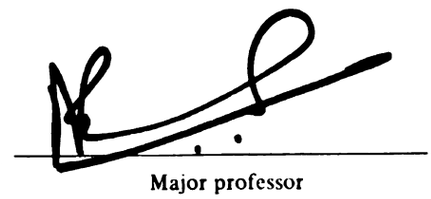

Major professor

Date 12/14/98

FIELD INVESTIGATION OF TRANSVERSE CRACKING IN JOINTED CONCRETE PAVEMENTS (JCP's)

By

Michael Anthony Frabizzio

A THESIS

Submitted to
Michigan State University
in partial fulfillment of the requirements
for the degree of

MASTER OF SCIENCE

Department of Civil and Environmental Engineering

1998

ABSTRACT

FIELD INVESTIGATION OF TRANSVERSE CRACKING IN JOINTED CONCRETE PAVEMENTS (JCP's)

By

Michael Anthony Frabizzio

Environmental and/or traffic related stresses can lead to the development of transverse cracking in jointed concrete pavements (JCP's). Deterioration of transverse cracks over time can result in loss of serviceability and loss of structural capacity in such pavements. An understanding of the factors affecting transverse cracking in JCP's and the ability to assess when and how to repair pavements with this distress are therefore two issues of importance to transportation agencies. Addressing these issues, the primary objectives of this research were to study the effects of various factors on transverse cracking in JCP's and to demonstrate methods for evaluating these cracked pavements. Field data collected from in-service JCP's located throughout southern Michigan was used to accomplish these objectives. Joint spacing, concrete coarse aggregate type, and shoulder type were found to have significant effects on transverse crack development and/or performance. Three analysis procedures that are based on the use of falling weight deflectometer (FWD) data - backcalculation of pavement support and stiffness parameters, determination of crack performance parameters, and assessment of void potential near cracks – were demonstrated using data from this study. These procedures allow for evaluation of cracked JCP's. Results from these FWD analyses were used to develop threshold limits necessary for performing evaluations with these procedures.

To my parents,

for their selflessness, support, and love,

and in recognition of their knowledge and wisdom,

for which no degree could ever quantify,

and

to my brother,

who is my best friend,

and is always there for me.

ACKNOWLEDGEMENTS

I would first like to thank Dr. Neeraj Buch for his support and guidance throughout my graduate career at Michigan State University.

I would also like to thank the Michigan Department of Transportation (MDOT) and the Pavement Research Center of Excellence (PRCE) at Michigan State University for sponsoring this research work and providing financial support. In addition, I would like to thank MDOT for performing coring and falling weight deflectometer testing as well as providing the necessary traffic control for carrying out the collection of field data. Thanks must also be given to the various MDOT personnel who assisted me in compiling the inventory data for this research study.

I would also like to give thanks to Dr. Mark Snyder for his work on the Volumetric Surface Texture (VST) testing performed in this study and for the technical support he provided regarding the analysis of the VST test results.

A final thanks is given to the many students, most notably Jacob Hiller, who helped me with field data collection.

TABLE OF CONTENTS

CHAPTER Page

Page

LIST OF TABLES

TABLE Page

LIST OF FIGURES

- CHAPTER I -

Introduction

PROBLEM STATEMENT

Transverse cracks in jointed concrete pavements (JCP's) are discontinuities in the pavement oriented perpendicular to the direction of traffic. These cracks are typically the result of environmental and/or traffic related stresses. Deterioration of such cracks over time can lead to loss of serviceability and loss of structural capacity of the pavement. It is therefore of interest to identify and understand the factors that influence transverse cracking. An additional issue of importance to transportation agencies is the need to assess when and how to repair pavements with this distress.

OBJECTIVES OF RESEARCH

One objective of the research in this study was to use field data to identify the significant factors that affect the occurrence and performance of transverse cracks in JCP's. There have been several other studies performed to determine factors affecting transverse cracking, but they have often been laboratory-based and have often neglected the significance of concrete coarse aggregate type. Thus, a comprehensive field investigation was performed with one objective being to study the effects of various factors, including aggregate type, on transverse cracking. Based upon these results, design recommendations could be given to transportation agencies (particularly the sponsoring agency for this study - the Michigan Department of Transportation (MDOT)) to improve the performance of these pavements with regard to transverse cracking.

Another aim of this investigation was to demonstrate how field data can be used to determine values for selected crack performance parameters. These parameters provide a means for characterizing the integrity of cracks. An agency could compare parametric values with threshold values to evaluate the condition of cracks. Such evaluations could be used to help in deciding when and how to rehabilitate pavements with transverse cracks. It was also the intent of this study to establish thresholds for the performance parameters based on data from this research.

An additional objective of this study was to obtain and analyze field data to demonstrate the use of a voids analysis procedure for evaluating cracked JCP's. This procedure is an evaluation technique that allows for an assessment of the likelihood of loss of support near cracks and joints. By identifying the presence of voids at cracks and joints, this procedure allows appropriate rehabilitation actions to be taken to restore support to a cracked JCP. In addition to describing the methodology for performing this analysis, it was also an aim of this research to use the results from the voids analyses performed herein to check the validity of existing threshold values for determining void potential.

SCOPE OF RESEARCH

To accomplish the research objectives, forty-nine (49) test sites from in-service highway pavements demonstrating transverse cracking were chosen. Inventory data for these test sites was collected and compiled using MDOT construction records. Field performance data was collected for the sites approximately each season over a fourteen

month period. The research objectives were accomplished by utilizing both the inventory and field data.

Various analyses were performed to satisfy the objectives of this research. Methods for determining crack performance parameters were demonstrated and threshold values were established for these parameters. The effect of temperature on the performance parameters was examined using field data from this study. A backcalculation procedure for determining pavement support and stiffness parameters, which are used to determine the crack performance parameters alluded to above, was also demonstrated. A voids analysis procedure was performed and appropriate thresholds were determined for evaluating void potential using this procedure. Several factors affecting transverse crack occurrence and performance were identified through analyses of the field data. Included among these analyses was a relatively new procedure, Volumetric Surface Texture (VST) testing, which was used to investigate the effect of concrete aggregate type on crack performance potential. Results and discussion pertaining to all analyses are contained in Chapters V and VI of this thesis.

CONTENTS OF THESIS

This thesis contains background information on transverse cracking in JCP's, a discussion of the analyses performed and the results obtained from the data collected in this study, and a summary of the conclusions and recommendations derived from this research. A more detailed breakdown of the contents of individual chapters follows. Chapter II includes: background regarding how transverse cracks are formed in JCP's; a summary of the factors that have been found to influence the occurrence and performance

of these cracks in past studies; an explanation of the load transfer mechanisms for transverse cracks; and, a description of the performance parameters associated with crack performance. Chapter III provides a synopsis of some of the common methods used in rehabilitating/resurfacing JCP's with transverse cracks. A description of the test sites used for the research in this thesis is given in Chapter IV. This chapter also includes descriptions of the inventory and field data collected for the test site pavements. The various FWD analysis procedures performed using field data in this study – namely, backcalculation of pavement support and stiffness parameters, determination of crack performance parameters, and assessment of void potential near cracks - as well as the results obtained from performing these procedures are discussed in Chapter V. A discussion of the analyses performed and results obtained in this study pertaining to the investigation of factors affecting transverse cracking in JCP's is provided in Chapter VI. A summary of the conclusions and recommendations arising from the analyses performed in this study as well as a listing of future research needs related to the study of transverse cracking in JCP's are contained in Chapter VII, which concludes this thesis.

- CHAPTER II -

Literature Review I - Overview of Transverse Cracking in JCP's

FORMATION OF TRANSVERSE CRACKS IN JCP's

Jointed Concrete Pavements

Jointed concrete pavements utilize joints, or engineered cracks, to serve a variety of purposes. JCP's can be further categorized as either jointed plain concrete pavements (JPCP's) or jointed reinforced concrete pavements (JRCP's) to distinguish between those JCP's with temperature reinforcing steel and those without such reinforcement. The three basic types of joints utilized in these pavements are contraction, expansion, and construction joints. Contraction joints are the most common joint type encountered in JCP's. These joints are used to control the location of cracking in the pavement, which results from tensile stresses induced by temperature, moisture, and friction [1]. Partial-depth saw cuts cause a weakened plane which cracks through the full slab depth upon subjection to the noted tensile stresses. Expansion joints, which involve full-depth saw cuts, are used in JCP's to allow for thermal expansion of the pavement without buckling of the slab [1]. Where construction must be stopped temporarily, such as at the end of a day's work, construction joints are formed in the pavement [2]. Load transfer devices, most commonly metal dowel bars, are usually placed across all three of these types of joints to maintain the structural integrity of the pavement. Joints are also usually sealed to prevent water and incompressibles from entering the discontinuity. Despite the use of joints, transverse cracking occasionally develops at locations in a slab between the joints

due to environmental and traffic induced stresses. Such midslab transverse cracks were the focus of this research investigation.

Causes of Transverse Cracks in JCP's

Transverse cracks can be induced in JCP's through a variety of mechanisms: fatigue cracking due to a combination of curling, warping, and traffic stresses; plastic and drying shrinkage stresses; friction between the slab and supporting layer (base or subgrade); and, settlement of the supporting layers (base and subgrade). A description of each of these mechanisms follows.

Fatigue Cracking

Repeated applications of tensile stresses, primarily due to curling, warping, and traffic loads, can lead to fatigue cracking in JCP's. Huang explains the curling mechanism by considering a jointed concrete pavement to be a rigid plate supported by a liquid (or Winkler) foundation. The Winkler foundation models the subgrade as a set of independent springs, where deflection at any point is proportional to the force at that point and independent of all forces elsewhere. Downward curling occurs when the top of the slab is warmer than the bottom. In this case the top of the slab is longer than the bottom and the slab consequently curls downward. The springs on the edges are in compression and push the slab upward, while the interior springs are in tension and pull the slab downward. This is illustrated in Figure 1. This results in compression at the top of the slab and tension in the bottom of the slab. The reverse situation, upward curling, occurs when the top of the slab is cooler than the bottom. Here, the springs on the edges

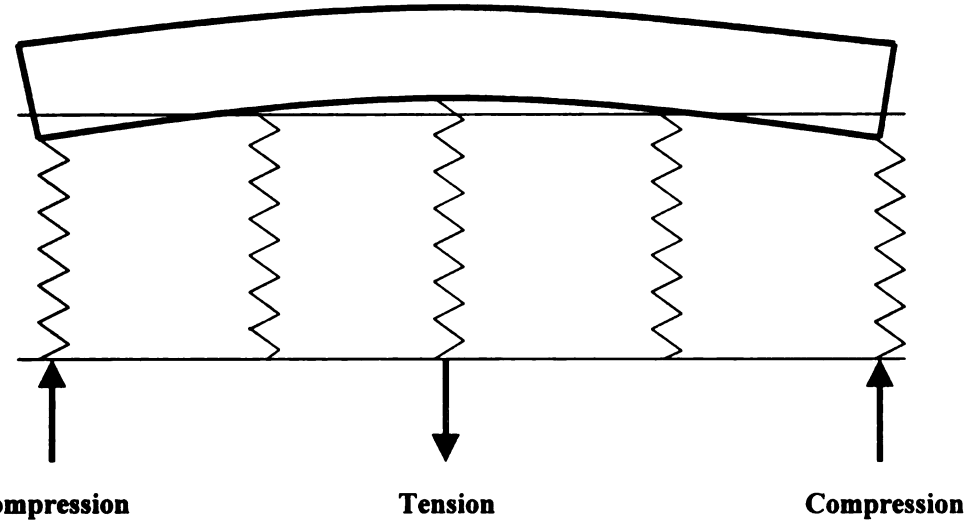

Figure 1 Depiction of Downward Slab Curling. (After Huang [3].)

pull the slab downward, while the interior springs push the slab upward, as shown in Figure 2. This results in tension at the top of the slab and compression in the bottom portion. Curling occurs primarily due to daily temperature variations. [3]

Complex equations for computing the stress in concrete pavements caused by curling were developed by Westergaard [4]. Huang provides simplified equations for computing the curling stress in a slab with finite dimensions [3]. Equations (1) and (2) from Huang are used to compute the curling stress in the x- and y-directions, respectively [3]:

$$\sigma_{cx} = \frac{E\alpha_t \Delta t}{2(1-\nu^2)}\left(C_x + \nu C_y\right) \quad (1)$$

$$\sigma_{cy} = \frac{E\alpha_t \Delta t}{2(1-\nu^2)}\left(C_y + \nu C_x\right) \quad (2)$$

where:

σ_{cx}	=	curling stress in x- (longitudinal) direction for a finite slab, kPa
σ_{cy}	=	curling stress in y- (transverse) direction for a finite slab, kPa
E	=	concrete modulus of elasticity, kPa
α_t	=	coefficient of thermal expansion of concrete, mm/mm/°C
Δt	=	temperature differential between top and bottom of concrete slab, °C
ν	=	Poisson's ratio for concrete
C_x	=	correction factor for curling in a finite slab, x- (longitudinal) direction
C_y	=	correction factor for curling in a finite slab, y- (transverse) direction.

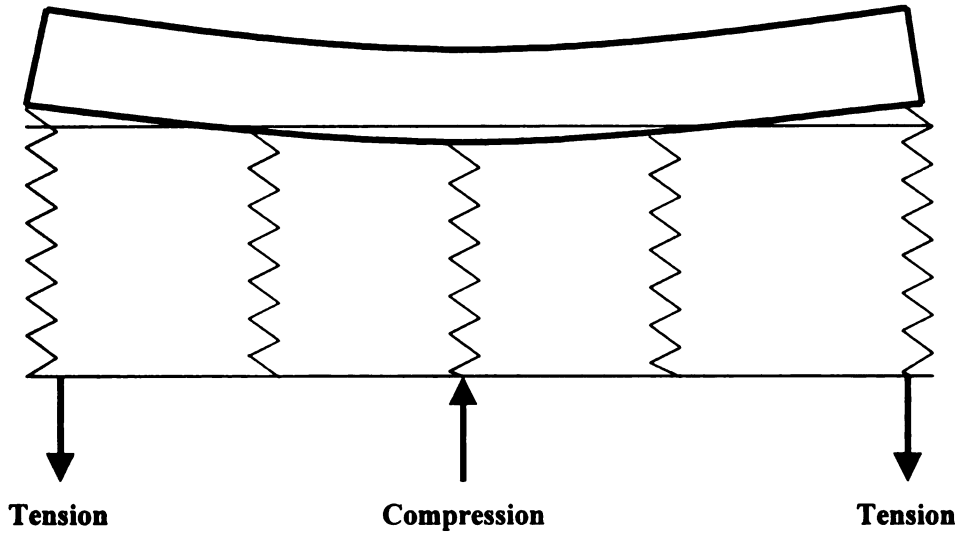

Figure 2 Depiction of Upward Slab Curling. (After Huang [3].)

In these equations, C_x and C_y are correction factors which account for the finite dimensions of a slab [3]. These factors can be determined using a curve developed by Bradbury, which relates C_x and C_y to L_x/ℓ and L_y/ℓ, respectively [5]. L_x and L_y are the respective length and width of the slab, as shown in Figure 3. The radius of relative stiffness, ℓ, is defined by equation (3) in [3]:

$$\ell = \left[\frac{Eh^3}{12(1-\nu^2)k}\right]^{0.25} \qquad (3)$$

where:

ℓ	=	radius of relative stiffness, mm
E	=	concrete modulus of elasticity, kPa
h	=	concrete slab thickness, mm
ν	=	Poisson's ratio for concrete
k	=	modulus of subgrade reaction, kPa/mm.

Warping stresses can also be induced in JCP's due to a moisture gradient. According to Huang, when the top of the slab has a lower moisture content than that at the bottom, the slab warps upward. This causes compressive stresses at the bottom of the slab and tensile stresses at the top of the slab. Warping is a seasonal phenomenon and therefore has relatively few stress cycles. It is difficult to determine the magnitude of warping stresses due to their dependence on many factors, such as relative humidity at the pavement surface, the free water in the concrete, and the moisture content of the support layers. [3]

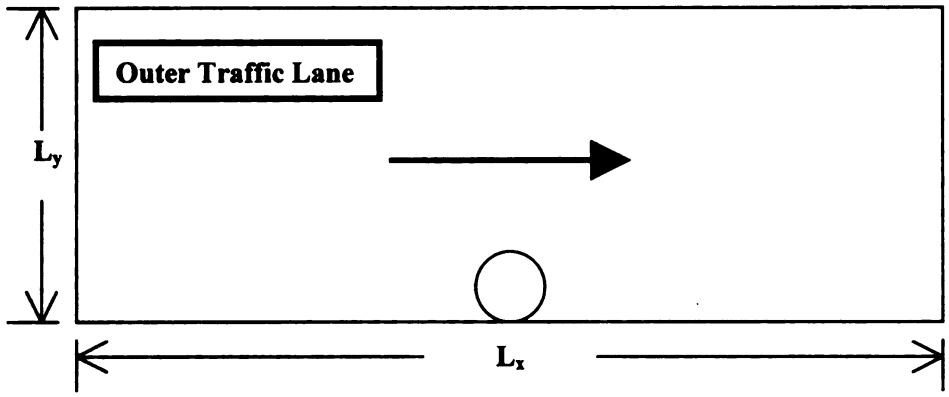

Figure 3 Finite Slab with Circular Edge Load Condition.

Traffic loads are probably the most significant source of damage in causing fatigue cracking. When analyzing the stresses due to traffic loads, three different load conditions are usually considered: interior, edge, and corner. The edge load condition midway between the transverse joints is considered to be the critical load position with regard to fatigue cracking, as this is the location where maximum tensile stress typically occurs [3]. This is because the load is located far away from the joints, and thus does not benefit from the load transfer provided there by dowel bars [3]. It is also the critical load position because the load is placed at a free edge, producing the maximum bending stress. Figure 3 shows the placement of a circular edge load on a JCP. The arrow shows the direction of traffic. Westergaard developed equation (4) to compute the stress due to a circular loading at the critical edge load position [6]:

$$\sigma_e = \frac{3(1+\nu)P}{\pi(3+\nu)h^2}\left[\ln\left(\frac{Eh^3}{100ka^4}\right) + 1.84 - \frac{4\nu}{3} + \frac{1-\nu}{2} + \frac{1.18(1+2\nu)a}{\ell}\right] \quad (4)$$

where:

σ_e	=	stress for circular edge load condition, kPa
ν	=	Poisson's ratio for concrete
P	=	applied load, kN
h	=	concrete slab thickness, m
E	=	concrete modulus of elasticity, kPa
k	=	modulus of subgrade reaction, kPa/m
a	=	radius of loaded area, m
ℓ	=	radius of relative stiffness, m.

As noted previously, it is the repeated application of stresses that causes fatigue cracking in concrete. Damage due to cycles of curling, warping, and traffic stresses accumulates over time and eventually can cause fatigue cracking. The conventional practice used in fatigue analysis for pavements is to use Miner's linear cumulative fatigue hypothesis [7]. In this hypothesis damage due to a given stress level is expressed in terms of a damage ratio, which is the ratio of the predicted to allowable number of load repetitions [7]. The damage ratios from all stress levels for each type of stress are summed. If this sum is equal or greater than 1, fatigue cracking is assumed to occur [7]. According to Ioannides, Miner's hypothesis provides only a rough approximation to reality and is used principally due to its ease of application [8]. Ioannides points to the dependence of fatigue strength on the sequence of loading, among other factors, in disputing the validity of Miner's hypothesis, and suggests that more sophisticated methods of analysis, such as fracture mechanics, are needed to more accurately analyze fatigue in pavements [8].

In any event, Miner's hypothesis is currently the most widely accepted method for analyzing fatigue in concrete pavements. To calculate the damage ratios due to the various stresses on a pavement, the allowable number of load applications for the particular stress level must be determined. This can be done by using an S-N curve, which is a curve relating the stress ratio (S) to the allowable number of load applications (N). The stress ratio is the ratio of the applied stress to the modulus of rupture of the concrete. N is measured in terms of ESAL's (80 kN equivalent single axle loads). ESAL's are described in more detail in [1]. For JCP's the stresses due to curling and traffic can be computed using equations (1), (2), and (4) for each stress level. No readily

available equation for computing warping stresses exists. Stress ratios can be computed for the various stress levels of curling and traffic and the allowable number of load applications can then be computed for the respective stress levels. Damage ratios can then be determined for the various stress levels of curling and traffic by noting the respective number of stress applications. [3]

When calculating the damage due to traffic, it must be remembered that the stress is being computed for the critical edge load condition. Therefore, the number of load repetitions due to traffic must be reduced since only a small portion of the total traffic will be applied at the edge location. It should also be considered that curling (and warping) stresses can be either additive or subtractive from the traffic stresses depending on the orientation of the curling and warping. The sum of the damage ratios must be kept under 1 to prevent fatigue cracking. Warping stresses should also be considered in the analysis. It should be noted that, in practice, curling and warping stresses are often neglected in pavement design for a variety of reasons, as discussed by Huang. [3]

Plastic and Drying Shrinkage

Plastic and drying shrinkage of concrete involve changes in volume of fresh and hardened concrete, respectively, and can lead to transverse cracking in JCP's. According to Mindess and Young, plastic shrinkage is usually associated with surface cracking due to evaporation of water from the pavement surface and/or suction of water from the concrete by the base or subgrade. Such loss of water from the fresh concrete induces negative capillary pressures within the paste, causing it to contract. Contraction of the paste leads to rearrangement of the water particles within the concrete, and surface

cracking occurs. These negative capillary pressures and the associated surface cracking typically result when the rate of surface evaporation exceeds the rate of bleed water rise in the concrete. [9]

Drying shrinkage involves volume changes in concrete due to loss of moisture in hardened concrete. These volume changes are resisted by friction between the slab and the support layer (base or subgrade), which results in tensile stresses in the concrete that cause transverse cracking. Joints are placed to control the location of this cracking. The mechanism of drying shrinkage is not well understood, but it is known that it involves a combination of reversible and irreversible shrinkage. Irreversible shrinkage is believed to result from changes in the bonding and arrangement of particles within the concrete microstructure during hydration. Reversible shrinkage is attributed to changes in capillary stress, disjoining pressure, and surface free energy within the cement paste, as the relative humidity exposed to the concrete changes. [9]

Interface Friction between Slab and Support Layer

Variations in temperature and moisture conditions cause volume changes in a concrete slab. Increases in temperature and/or moisture lead to expansion and thus movement of the slab. Similarly, the slab will tend to contract if the temperature and/or moisture are decreased. As the slab attempts to expand or contract, frictional stresses between the slab and the support layer (base or subgrade) resist the movement. These frictional stresses induce tensile stresses in the concrete, which can lead to transverse cracking. Joints help to control the location of this cracking as well. JRCP's utilize steel reinforcement to hold cracked concrete together under temperature variations. [3]

Settlement of Base and/or Subgrade

Transverse cracking can also occur if the base and/or subgrade material settles or consolidates significantly beneath the concrete slab. This settlement or consolidation causes a loss of support under the slab and cracking can develop upon traffic loading. [10]

Factors Affecting the Occurrence of Transverse Cracks in JCP's

Past studies have found that a variety of factors contribute to the formation of transverse cracks in JCP's. A review of these findings, sectioned by the type of cracking induced, follows.

Fatigue Cracking

The literature reveals that many factors affect the formation of fatigue cracks in JCP's. Those factors which influence curling, warping, and traffic stresses inherently affect fatigue cracking. Bradbury's curve, described earlier, indicates that a larger joint spacing (L_x) corresponds to a higher value for C_x (up to $L_x = 8.5\ell$; increasing L_x beyond this value causes a slight decrease in C_x and eventually a plateauing of C_x when L_x reaches a value of 12.0ℓ) [5]. It can be seen from equation (1) that a higher C_x value causes a higher curling stress. Increasing the joint spacing also causes a larger warping stress [10]. Equations (1) and (2) also indicate that an increase in the temperature differential between the top and the bottom of the slab increases the curling stress. Similarly, an increase in the moisture gradient throughout the slab can be expected to increase the warping stress. Thus, large variations in daily temperatures and seasonal

moisture contents increase the magnitude of curling and warping stresses. These larger curling and warping stresses increase the probability of fatigue cracking.

Support conditions are among the many factors that affect stresses due to traffic loads in JCP's. Darter et al. showed that increasing the k-value leads to a decrease in the amount of transverse cracking [10]. When no temperature gradient is present in a slab, it was found that increasing the subgrade or base stiffness will decrease the tensile stresses in the slab due to traffic loads [10]. However, when a temperature differential does exist, a stiffer subgrade or base can lead to increased combined curling and traffic load stresses [10]. Higher traffic stresses lead to a greater chance of fatigue cracking. Smith et al. found that use of a permeable base layer in combination with a separator layer and a longitudinal edge drain collector system leads to fewer transverse cracks than designs with a dense-graded base layer [11]. This last finding points to the need for providing good drainage to the pavement in addition to reducing stresses in order to avoid cracking.

Increased slab thickness was found to decrease the amount of fatigue cracks by reducing tensile stresses due to traffic, according to a study by Smith et al. Less fatigue cracks were also shown to be associated with higher concrete strengths. This study also showed that widened slabs (4.0 to 4.3 m in width) with traffic stripes painted at 3.7 m lead to fewer transverse cracks. Widened slabs move traffic away from the edge location of the pavement, thus avoiding the critical edge load condition and reducing the potential for fatigue cracking. Poor load transfer at joints can also contribute to transverse cracking in JCP's by increasing the tensile stresses in the slab due to traffic loads. Non-working joints can result from malfunctioning, misaligned, or corroded dowel bars. [11]

Other studies have shown that shoulder designs affect the occurrence of fatigue cracks. Compared to other shoulder types (e.g., asphalt shoulders), tied concrete shoulders lead to lower fatigue stresses and thus fewer fatigue cracks [10]. These shoulders effectively transform an edge loading at the mainline pavement - shoulder joint into an interior load. The slab and shoulder are tied together, effectively becoming one composite support system for the load. The bending stress and thus tensile stress in the concrete is reduced as the load is no longer concentrated at a free edge. The relationship between sympathy joints in concrete shoulders and transverse cracks in the mainline pavement was noted by Darter [12]. Sympathy joints, which are shoulder joints that have joint spacing shorter than that for the mainline pavement, were found to cause transverse cracking in the mainline pavement adjacent to the shoulder joints [12]. Such cracks are the result of differential responses within the slab and the shoulder to thermal expansion and contraction. Since the slab and shoulder are tied together and each responds differently to thermal variations due to the difference in joint locations, cracking results as tensile stresses are induced.

Plastic and Drying Shrinkage Cracking

Several factors are known to contribute to plastic and drying shrinkage cracking. Mindess and Young explain that high wind velocity, low relative humidity, high air temperature, and high concrete temperature are the conditions most likely to cause plastic shrinkage cracking. These conditions lead to a high rate of surface evaporation in the concrete. Drying shrinkage is a more complex phenomenon and is thus influenced by more factors. A high water-to-cement ratio leads to greater porosity in the cement paste

and thus more potential for drying shrinkage. Higher curing temperatures help to reduce the amount of drying shrinkage, especially irreversible shrinkage. Cement composition also affects drying shrinkage. It is believed that sulfoaluminates in the paste contribute to drying shrinkage. The use of admixtures can also affect the amount of drying shrinkage of the paste. A combination of high aggregate content, moderate cement content, and low moisture content lessen the potential for drying shrinkage. Stiffer aggregates reduce the amount of drying shrinkage as well by providing restraint to volume changes in the paste. Thicker slabs decrease the amount of shrinkage as the path of diffusion for moisture loss is lengthened. Drying shrinkage also decreases with increasing relative humidity. The likelihood of cracking due to drying shrinkage is enhanced by higher amounts of friction between the slab and support layer. [9]

Cracking Due to Slab - Support Layer Interface Friction

As was discussed earlier, longitudinal slab movements (contraction and expansion) result from changes in temperature and moisture within the slab. Cracking can occur due to the friction developed between the slab and support layer during these movements. Greater amounts of temperature and moisture change lead to more movement of the slab and thus greater potential for cracking. Also, a higher amount of friction between slab and support layer will increase the likelihood of cracking. This type of cracking will further be more likely as the ratio of slab length (joint spacing) to slab thickness increases. [2]

Cracking Due to Base and/or Subgrade Settlement

Instability of the support layers to the slab can lead to settlement or consolidation of these layers and eventual transverse cracking in the area where such an event occurs. In one report, Darter attributed transverse cracking to settlement caused by the use of a rounded stone base in combination with a sand subbase without a separation layer [12]. The combination of a stone base and sand subbase led to instability of the support structure to the slab under traffic loading. Poor drainage capabilities and improper compaction of dense-graded base layers may also lead to consolidation of support layers.

LOAD TRANSFER ACROSS TRANSVERSE CRACKS IN JCP's

Importance of Load Transfer across Transverse Cracks in JCP's

Load transfer across transverse cracks is critical to the maintenance of adequately performing JCP's. Both sides of a crack share in supporting the load, as part of the load is transferred from one side of the crack to the other, reducing the deflections and consequent damage to the pavement [13]. Raja and Snyder explain how low severity cracks can become medium to high severity fatigue cracks through a loss of load transfer [14]. They explain that hairline transverse cracks often develop in the early life of JCP's due to shrinkage stresses and frictional stresses induced by thermal movements of the slab [14]. Opening of the cracks over time leads to intrusion of water and incompressibles into the cracks and loss of load transfer, which causes increased slab deflections [14].

These conditions can lead to pumping, faulting, and spalling at the crack [14]. Pumping involves the expulsion of water from beneath the pavement due to slab deflections [2]. Support material can become suspended in the lost water, which results

in a loss of support under the slab [2]. This loss of support causes increased stresses due to traffic and thus can lead to fatigue cracking [14]. Corner breaks, which are broken sections of pavement at a slab corner, can also result from increased stresses at the crack due to this loss of support [2]. Faulting is a differential vertical displacement of two sides of adjacent slab fragments [2]. It is caused by a high velocity transfer of water and suspended solids from beneath the leave side to beneath the approach side of a crack as a wheel load crosses the discontinuity [2]. This leads to a buildup of the suspended material under the approach side of the crack [2]. Here, "approach side" refers to the side before a crack as a load approaches the crack, and "leave side" refers to the side after the crack. Crack spalling is the deterioration of a crack usually caused by excessive compressive stresses developed between the concrete and entrapped incompressibles within the crack [2]. Transverse cracks (fatigue cracks, shrinkage cracks, etc.) demonstrating spalling and/or faulting lose serviceability as these distresses cause increased roughness and user discomfort [15]. Loss of load transfer across transverse cracks also increases the internal tensile stresses within the pavement and can lead to more fatigue cracking and loss of structural integrity in the pavement [16]. The next section describes the two common mechanisms of load transfer across transverse cracks: aggregate interlock and to a lesser extent reinforcement dowel action (in JRCP's).

Shear Transfer Mechanisms

Aggregate Interlock

Aggregate interlock is the primary mode of load transfer across transverse cracks in JCP's. For the purposes of this study, aggregate interlock will be considered to be the

only mechanism contributing to load transfer across such cracks. This shear transfer mechanism is effective in providing load transfer as long as the crack faces are kept close to one another [17]. This finding was clearly affirmed by Benkelman in 1933 when he declared, ". . . when roughened edges of two slabs are held firmly together, the aggregate interlock may be expected to function perfectly and permanently as a load-transfer medium" [18]. When a crack develops in a JCP, the two crack faces are usually rough and irregular [17]. Such roughness is due to aggregate protrusions from the crack face and irregular texture of the cement matrix. When one side of the crack is subjected to an approaching wheel load, a differential vertical displacement of the two slab fragments occurs, and results in the protrusions of one crack face coming into contact with the matrix of the other crack face [14]. A combination of bearing and friction between the aggregate particles of the two crack faces inhibits further differential movement between the slab fragments [17]. Aggregate interlock is the name given to this mechanism that allows a portion of the wheel load to be transferred from one side of a crack to the other through shear, as it involves an interlocking of aggregate particles across a crack plane [14]. There are several models that have been developed to describe this mechanism.

Theoretical Models

Laible et al. proposed one model which divides the crack face roughness into "local" and "global" components. Local roughness causes interlocking of the fine aggregates through a crushing or bearing action. Global roughness involves the interlocking of coarse aggregate particles through a sliding and overriding action. Local roughness is presumed to dominate the aggregate interlock mechanism at small crack

widths (less than 0.25 mm), whereas global roughness controls the mechanism for wider cracks. [19]

A second model depicts aggregate interlock as a phenomenon caused by frictional sliding of two rigid surfaces. Jimenez et al. represent these rigid surfaces by a sawtooth shape [20]. Fardis and Buyukozturk use a series of parabolic segments to depict the surfaces [21].

Walraven proposed a model of aggregate interlock that considers concrete to be a two-phase material consisting of aggregate and a cement matrix. Concrete is modeled as a distribution of rigid spheres of a range of sizes embedded to varying depths within a deformable rigid-plastic matrix. Shear forces are considered to be resisted through a combination of sliding and crushing of the aggregates (rigid spheres) into and over the plastic cement matrix. Initially, a sliding of the opposite crack faces occurs, where the aggregates on one side slide against the cement matrix on the other side. High contact stresses develop as the contact area is reduced and crushing of the aggregates into the matrix occurs. Eventually, equilibrium of the forces is reached and further plastic deformation ceases. This model does not consider contact between aggregates from opposing sides of the crack surface. [22]

Millard and Johnson performed a laboratory investigation to test the validity of the above models. Test results did not support the local and global roughness model or the frictional sliding model. However, the two-phase aggregate interlock model did seem to provide consistent agreement with their test results. [23]

Reinforcement Dowel Action

JRCP's usually contain longitudinal reinforcing steel that is designed to prevent widening of transverse cracks by absorbing tensile stresses in the concrete caused by temperature and/or moisture variations. Assuming that this reinforcement does provide such restraint to crack widening, it is reasonable to believe that it also aids the aggregate interlock mechanism by keeping the crack faces in close contact. In this way, reinforcement in JRCP's could affect load transfer. Reinforcement can also restrain crack widening caused by overriding of aggregate particles during aggregate interlock [24]. Here, frictional forces induced by the reinforcement contribute to the aggregate interlock resistance [24]. This is another example of how reinforcement could affect load transfer. However, in each of these cases, the mechanism of load transfer would still be aggregate interlock.

Some investigators believe that reinforcement in JRCP's can provide a mechanism for load transfer by itself through dowel action. Theoretical models for the mechanism of this dowel action are discussed in the following section. It should be noted that this study neglects the effect of steel reinforcement in JRCP's on load transfer and the possible contribution of this reinforcement as a load transfer mechanism for several reasons. First, it is often found that the reinforcement in JRCP's has dropped to the bottom or risen to the top of the slab for a variety of reasons. Where such movement has occurred, the reinforcement will have a minimal effect in restraining crack widening. Due to the seemingly frequent occurrence of this misplaced reinforcement, it was believed to be prudent to neglect its effect on load transfer in this study. It was also believed that it was not appropriate to consider this reinforcement to be a source of load

transfer, as it is designed merely to provide resistance against tensile stresses due to temperature and/or moisture changes. The steel is not necessarily and most likely not able to provide a significant contribution to load transfer through dowel action. Assuming that the reinforcement does provide some amount of load transfer, it would be difficult to differentiate and assess the relative affects of each mechanism (aggregate interlock and dowel action) on load transfer in a field study such as the one described here. A final reason why reinforcing steel in JRCP's was not considered to affect or contribute to load transfer in this study is that in many cases it is found that the reinforcement has actually been sheared off during formation of the crack, thus rendering it useless for either purpose.

Theoretical Models

Three mechanisms - direct shear, kinking, and flexure of the bars - have been proposed to explain the shear transfer of load through dowel action in cracked reinforced concrete [25]. Direct shear and kinking of the bars would be the principal mechanisms of dowel action if the concrete supporting the reinforcement was considered to be rigid [23]. However, it is known that substantial deformation of the concrete occurs, and thus flexure of the bars is the primary mechanism of dowel action [26].

Millard modeled this flexure mechanism by considering the reinforcing bar as a beam on an elastic foundation [27]. Millard and Johnson note, however, that only the initial shear stiffness can be determined using this model. High stress concentrations in the concrete supporting the reinforcement produce non-linear behavior and negate the use of this model at higher stress levels. Such non-linear behavior is attributed to crushing or

splitting of the concrete supporting the bars and/or plastic yielding of the bars. Equations to predict the non-linear shear stiffness were developed and presented in [23]. Test results indicate that these equations provide a good approximation of the shear stiffness due to the dowel action mechanism. [23]

Quantification of Load Transfer

Load transfer across discontinuities in JCP's is commonly quantified by a term called load transfer efficiency (LTE). Expressed as a percentage, LTE gives an indication of the effectiveness of a crack in transferring load. Computation of load transfer efficiency based on deflections near the crack under an applied load is a very useful method of determining the LTE. The load transfer efficiency computed using this approach is termed the deflection load transfer efficiency (LTE_δ) [28].

Use of LTE_δ assumes that the amount of load transfer across a crack is directly proportional to the relative deflections of the unloaded to loaded sides of the crack [18]. LTE_δ was used in this study to characterize the ability of cracks and joints to transfer load. Deflection load transfer efficiency was computed in this study by using equation (5) [28]:

$$\mathbf{LTE_\delta = \frac{\delta_U}{\delta_L} \times 100\%} \qquad \mathbf{(5)}$$

where:

LTE_δ	=	deflection load transfer efficiency, %
δ_U	=	deflection on the unloaded side of a crack or joint, μm
δ_L	=	deflection on the loaded side of a crack or joint, μm.

This definition of load transfer efficiency was adopted for this study for two reasons. First, it is relatively simple in concept and thus easily interpreted. Secondly, and more importantly, it was used because LTE_δ can be easily computed using field data from a falling weight deflectometer (FWD), which was used in this study. An FWD is a device that applies an impulse load, using a 300 mm diameter circular load plate, to a pavement and measures the resulting pavement deflections through a series of sensors. Deflection data for computing LTE_δ is thus readily available when this device is used. Use of the FWD in collecting deflection data to be used for data analysis purposes in this study is discussed in more detail in Chapter IV.

Figures 4 and 5 illustrate the meaning of LTE_δ by considering the two extreme cases - 0% and 100% deflection load transfer efficiency, respectively. In these figures, a load P is shown to be applied on one side of a crack or joint. The resulting deflections are depicted in the figures as well. It is seen in Figure 4 that when there is no load transferred (0% LTE_δ), the unloaded side of the slab has no deflection and thus does not share in the carrying of the load. As noted earlier in this section, this is the worst-case scenario, as all the load must be carried by one side and increased deflections result. This can eventually lead to other distresses in the area of the crack or joint. The best-case scenario is depicted in Figure 5, where the LTE_δ is 100%. Here, it can be seen that the deflections on each side of the crack or joint due to the applied load P are equal. Thus, the load is being equally shared by both sides of the discontinuity, and the minimum amount of damage is inflicted on the pavement.

The ability of a crack to maintain its load transfer efficiency over time is sometimes referred to as load transfer endurance. Several measures of this endurance

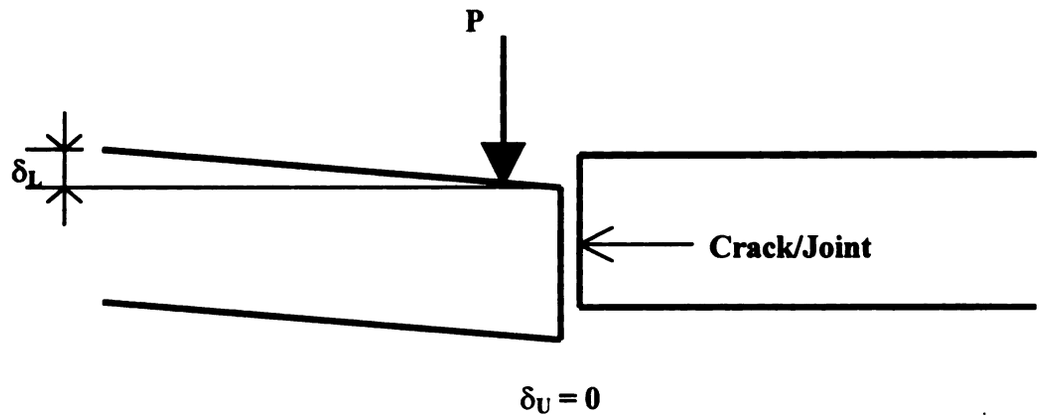

Figure 4 **Depiction of 0% Deflection Load Transfer Efficiency. (After Buch [29].)**

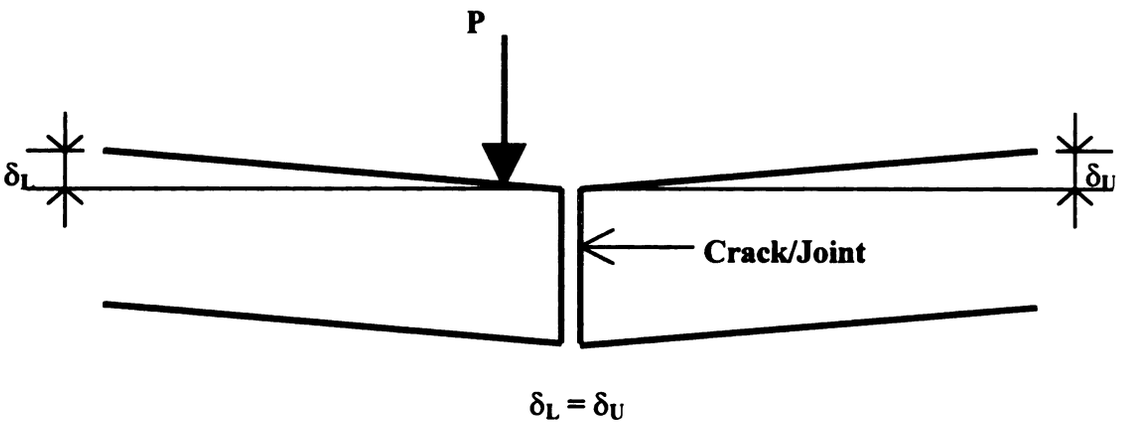

Figure 5 **Depiction of 100% Deflection Load Transfer Efficiency. (After Buch [29].)**

have been formulated by investigators. Colley and Humphrey defined the Endurance Index as one such indicator of load transfer endurance [30]. No such indicators of load transfer endurance were computed in this study, although some of the factors which have been found in previous studies to affect load transfer endurance will be discussed in the next section. Computation of an endurance index requires load transfer data throughout the life of the pavement, and is thus more suited for laboratory studies or long-term pavement field testing.

Besides LTE_δ, other pavement performance parameters were used in this study to characterize the ability of a crack or joint to transfer load. The transferred load efficiency (TLE) was one such parameter [28]. TLE quantifies load transfer efficiency in terms of load rather than in terms of deflection [28]. The total load transferred from the loaded to the unloaded side of a crack or joint along its entire length is given by a parameter termed P_T [28]. This parameter was also considered in this study. AGG, which characterizes the shear stiffness due to aggregate interlock of a crack or joint per unit length of the discontinuity, was another parameter determined in this study [28]. All three of these parameters were derived from LTE_δ values. The procedures and equations used to determine these parameters are discussed in Chapter V. Another parameter, τ, describes the loss of shear stress across a crack or joint under loading [29]. It is defined by equation (6) in [29]:

$$\tau = \frac{(\delta_L - \delta_U) \times \mathbf{AGG}}{\mathbf{h}} \qquad (6)$$

where:

τ	=	loss of shear stress across a crack or joint, kPa
δ_L	=	deflection on the loaded side of a crack or joint, mm
δ_U	=	deflection on the unloaded side of a crack or joint, mm
AGG	=	aggregate interlock shear stiffness per unit length of a discontinuity, kPa
h	=	concrete slab thickness, mm.

τ was not considered in this study, as interpretation of its meaning is somewhat more difficult than that for the other parameters.

Factors Affecting the Efficiency and Endurance of Load Transfer across Transverse Cracks in JCP's

Many factors have been found in previous studies to affect the efficiency and endurance of load transfer across transverse cracks in JCP's. A summary of the findings from these studies is given in this section. These factors are categorized as: crack characteristics, aggregate properties, support conditions, concrete slab properties and parameters, reinforcement properties, environmental conditions, and load conditions.

Crack Characteristics

Numerous investigators have found a relationship between crack width and load transfer efficiency. Colley and Humphrey determined that as joint opening increases, the effectiveness (or efficiency) of load transfer by aggregate interlock decreases [30]. Benkelman also found that increasing the crack width can significantly decrease the load transfer efficiency [18].

Other researchers have noted the same trend, but in terms of shear stiffness. Soroushian et al. found that decreasing the crack width caused a significant increase in the shear stiffness of the aggregate interlock mechanism [24]. Fenwick and Paulay and Paulay and Loeber also found that the aggregate interlock shear stiffness increases as the crack width decreases [31, 17]. Increasing the shear stiffness translates to a lower amount of vertical differential deflection between the opposing sides of a crack plane for a given load. Less differential deflection generally corresponds to a greater efficiency in load transfer across the crack. Snyder explains why increasing crack width causes a decrease in shear stiffness [14]. As the crack width increases, a loss in contact between the opposing crack faces results, and thus more differential vertical movement is required for sufficient contact to be made and load transferred across the crack [14]. NCHRP Synthesis 19 provides threshold limits of 0.9 to 1.0 mm for crack opening, beyond which aggregate interlock is ineffective in transferring load [32].

An interesting relationship between number of cracks per slab and crack width was found by Benkelman. For jointed plain concrete pavements, it was found that crack width decreased as the number of cracks per slab increased. This is likely due to a decrease in the length of the slab fragments with a greater amount of cracks per slab. A shorter slab fragment should result in a smaller crack width than a longer slab fragment when the fragments are contracted due to temperature changes. Noting the relationship described above between crack width and load transfer efficiency, it might be inferred that as the number of cracks per slab increases, the load transfer efficiency of the cracks increases. This relationship between number of cracks per slab and crack width did not

hold true for reinforced pavements, presumably due to the reinforcement effectively restraining crack widening. [18]

Aggregate Properties

Aggregate shape, size, hardness, type, gradation, and treatment as well as the mode of fracture through the concrete (around or through the aggregates) have all been found to significantly affect aggregate interlock load transfer across cracks in concrete. The effect of coarse aggregate shape was studied by Colley and Humphrey [30]. It was found that crushed stone aggregates provided better load transfer effectiveness and endurance than natural rounded aggregates [30]. The increased angularity of crushed aggregates provides more crack face texture for aggregate interlock.

The literature also reveals that the size of the coarse aggregate can significantly affect aggregate interlock load transfer, especially at larger crack widths. Nowlen found that increasing the aggregate size significantly improves load transfer effectiveness, particularly at large joint widths [13]. It was also shown that increased aggregate size improves the endurance of load transfer [13]. Bruinsma et al. concluded in their study that it is likely that the use of large coarse aggregates in the concrete mix provides improved load transfer efficiency and endurance, provided that all other factors are the same, including concrete strength [33]. This improved performance is the result of less vertical differential movement across the crack with larger particles [33]. Soroushian et al. also found that increased aggregate size can improve the shear stiffness, and consequently the load transfer efficiency, due to aggregate interlock [24].

Loss of aggregate interlock occurs over time due to abrasion of the crack faces. Thus, harder aggregates, which are more resistant to wear, would be expected to demonstrate better load transfer endurance than softer aggregates. Nowlen confirmed this notion, as he showed that harder aggregates do indeed lead to improved load transfer endurance. [13]

Bruinsma et al. studied the effect of coarse aggregate type on load transfer efficiency and endurance through a laboratory investigation. Four aggregate types were considered - limestone, natural gravel, slag, and recycled concrete aggregate. Limestone and natural gravel specimens showed better load transfer efficiency and endurance than specimens using slag or recycled concrete aggregates. It was explained that this is probably due to smoother crack faces associated with the slag and recycled concrete specimens. These manufactured aggregates are usually assumed to be weaker than the natural aggregates (limestone and natural gravel). The manufactured aggregate specimens thus have smooth crack faces, as cracks propagate through the relatively weaker aggregates rather than around them. This results in a lower amount of aggregate protrusions from the surface and thus less crack face texture available for aggregate interlock. [33]

The mode of fracture in concrete (i.e., around or through the aggregates) has indeed been cited as an important factor influencing load transfer characteristics [14]. When cracks propagate around the aggregates, more aggregate pullouts occur, which results in a rougher crack face [14]. Increased load transfer efficiency and endurance is generally associated with a rougher crack face. Nowlen found that the age of the concrete at time of fracture has a significant effect on the mode of fracture [13]. It was found that

early fractures result in more aggregate pullouts due to weaker aggregate-paste bond strengths [13]. Fractures occurring at later ages lead to less pullouts as this bond strength has been increased and cracks are more likely to propagate through the aggregates [13]. Thus, it was concluded that early fractures lead to improved load transfer efficiency and endurance [13].

Sutherland and Cashell noted that the mode of concrete fracture can explain why natural rounded gravel aggregates sometimes demonstrate better load transfer behavior than more angular, crushed limestone. The higher aggregate-paste bond strength developed in the limestone specimens leads to more cracks propagating through the aggregates. A greater amount of aggregate pullouts result for the natural gravel specimens, as the bond strength is weaker. Thus, better load transfer efficiency is found for the natural gravel specimens. [34]

The effect of aggregate gradation on shear stiffness due to aggregate interlock was examined by Walraven. Two gradations were considered in his study. One gradation was formulated according to the Fuller curve, and the other had a large proportion of sand. It was found that at large crack widths the finer aggregate gradation had a significantly lower shear stiffness than the gradation using the Fuller curve. Thus, the finer aggregate gradation would be expected to have a lower load transfer efficiency than the coarser gradation. This is due to less available contact area for the finer aggregate gradation at large crack widths. [22]

The effect of coarse aggregate treatment on load transfer endurance was studied by Bruinsma et al. The load transfer characteristics of virgin aggregate specimens, recycled concrete aggregate specimens, and blends of virgin and recycled concrete

aggregate specimens were compared. Virgin aggregate specimens showed significantly better load transfer endurance than recycled concrete aggregate specimens. Blending recycled concrete aggregate with virgin aggregate of equal or greater size resulted in an endurance level between that of the virgin aggregate and recycled concrete aggregate specimens. The differences in performance of the various aggregate treatments was attributed to differences in the crack face textures. The recycled concrete aggregate specimen had the smoothest crack face according to visual observations. The improved performance of the blended specimen over the recycled concrete aggregate specimen was probably due to a rougher crack face texture. It was also found in this study that adding virgin aggregate of a larger size to normally graded virgin aggregate results in improved load transfer endurance. [33]

Vandenbossche and Snyder determined relationships between aggregate properties and load transfer efficiency indirectly by performing Volumetric Surface Texture (VST) testing. This relatively new test procedure, which quantifies the surface texture of a crack face, was utilized in the research for this thesis to determine the effect of aggregate type on surface texture. It is discussed in more detail in Chapter VI. Vandenbossche and Snyder found that increasing the coarse aggregate size leads to a rougher volumetric surface texture. They also determined that stronger aggregates such as limestone result in a rougher volumetric surface texture than weaker aggregates such as slag. Regarding aggregate treatment, a rougher texture was found for virgin aggregate specimens than for specimens with recycled concrete aggregate. This was attributed to the reduced amount of aggregates at the crack face for recycled specimens, as they are composed of not only aggregates but also old mortar. Blending recycled aggregate with virgin aggregates did

lead to improvements in the volumetric surface texture. It was also found in their study that rougher volumetric surface texture corresponds to higher load transfer efficiency. Thus, it may be inferred that increased aggregate size, stronger aggregates, and/or use of virgin or blended aggregates lead to improved load transfer efficiency. [35]

Support Conditions

The support provided to the slab has a significant effect on the endurance of load transfer across transverse cracks in JCP's. Improved support can be accomplished by using a stiff base layer and/or a stiff subgrade. Colley and Humphrey found that use of a cement-treated base significantly increases the endurance of load transfer [30]. They also showed that increasing the modulus of subgrade reaction increases the load transfer endurance [30]. Bruinsma et al. confirmed these findings, as they found through laboratory testing that increasing the foundation stiffness leads to significantly improved endurance of load transfer [33]. The stiffer foundation reduces slab deflections and allows more load to be transferred into the foundation, reducing the amount of load carried by aggregate interlock and the reinforcing steel [33]. It is interesting to note that despite the beneficial effect that increasing the modulus of subgrade reaction has on load transfer endurance, it can actually decrease the deflection load transfer efficiency [28].

Concrete Slab Properties and Parameters

Load transfer efficiency and endurance has also been found to be affected by the concrete slab properties and parameters. It was shown by Soroushian et al. that increasing the concrete compressive strength increases the aggregate interlock shear

stiffness [24]. Walraven also found this relationship to be true [22]. Thus, the load transfer efficiency can be expected to increase with increasing concrete strength.

The slab thickness has been found to affect both the efficiency and endurance of load transfer across cracks. Aggregate interlock load transfer efficiency increases proportionally with the increased cross-sectional area available for shear resistance that is associated with increased slab thickness [2]. Colley and Humphrey determined that increasing the slab thickness also significantly increases the load transfer endurance [30].

Bruinsma et al. studied the effect of slab tension on load transfer efficiency and endurance of transverse cracks for JRCP's. Increasing the slab tension was found to decrease both the efficiency and endurance of load transfer. This was attributed to higher strains and stresses in the reinforcing steel and larger crack widths with high slab tension. Increasing the tension leads to greater strain in the steel, which results in wider crack openings. Larger crack widths are associated with reduced amounts of contact area between the crack faces, and thus, lower load transfer efficiency. Increased abrasion of the crack faces also results and leads to a lower load transfer endurance. It was also suggested that the large crack widths force a greater amount of load to be carried by dowel action of the reinforcing steel. Consequently, fatigue failures of this reinforcing steel are more likely to occur, and reduced load transfer endurance results. Increased slab tension can result from longer slab lengths and/or greater slab-support layer friction. Thus, reducing the joint spacing and/or the slab-support layer friction should lead to improved load transfer efficiency and endurance of transverse cracks. It was also concluded in this study that using both a stiffer foundation and reduced slab tension leads

to an improvement in load transfer endurance greater than the sum of the individual improvements which result from using either alone. [33]

Reinforcement Properties

The amount, size, and type of reinforcement used in JRCP's have been found to affect the load transfer characteristics of transverse cracks in these pavements. Larger wires and a greater amount of reinforcement were found to increase load transfer endurance in a laboratory study by Bruinsma et al. [33]. The increased size and quantity of reinforcement reduces the strain in the steel, which leads to smaller crack widths [33]. Aggregate interlock can thus be maintained longer as abrasion of the crack faces is reduced through smaller crack widths [33]. Fatigue stresses in the steel are also reduced with narrower crack widths [33]. Thus, reinforcement dowel action could also be maintained longer with increased reinforcement size and quantity [33]. Millard and Johnson found that a larger reinforcement size increases shear stiffness (and thus load transfer efficiency), but tends to induce more spalling at the crack faces [23].

Bruinsma et al. also studied the effect of reinforcement type on load transfer endurance. Deformed wire mesh was found to improve load transfer endurance, when compared to smooth wire mesh. The improved bond between the concrete and deformed steel restricts strain in the steel to the vicinity of the crack. This results in a smaller crack width, and thus, improved aggregate interlock and reduced fatigue stresses in the steel. [33]

An innovative design, utilized in the study by Bruinsma et al., using large deformed bars proved to provide significant improvements to load transfer endurance.

An unusually strong bond between the bars and the concrete kept the crack opening very tight. Thus, improved aggregate interlock and reduced stresses in the steel resulted. Use of these large deformed bars also provided substantial improvement to the shear and bending resistance of the steel. These effects led to increased endurance of load transfer across the transverse cracks in the study. [33]

The effect of combining a stiff foundation with an increased quantity of large reinforcing steel on load transfer endurance was also examined by Bruinsma et al. This effect was found to depend on the aggregate type. Recycled concrete aggregate specimens derived benefit from both of the improvements. Gravel specimens were found to be significantly improved only by the use of the stiffer foundation. Hence, it is believed that a stiffer foundation improves load transfer endurance for all aggregate types, but use of increased reinforcement size and quantity mainly improves performance for specimens comprised of aggregates with lower surface texture. [33]

Combining reduced slab tension and a deformed wire mesh was found to provide an increase in load transfer endurance approximately equal to the sum of using either improvement alone. Thus, using both a deformed wire mesh and a shorter slab length and/or reduced slab-support layer friction should result in better load transfer endurance. [33]

Environmental Conditions

Climatic factors such as temperature and moisture also affect the load transfer efficiency across transverse cracks in JCP's. Seasonal variations in the average temperature lead to differences in the shear stiffness across these cracks. As the average

temperature decreases from summer to winter, the shear stiffness (and thus load transfer efficiency) decreases as well. This decrease can be attributed to thermal contraction of the slab at lower temperatures, which results in a greater crack width and thus less load transfer efficiency across the cracks. [36]

Daily temperature variations also affect aggregate interlock load transfer efficiency. If a significant temperature variation occurs between nighttime and daytime, slab curling will take place. For example, high daytime temperatures cause a strong positive temperature differential (top of slab is warmer than bottom), which results in downward curling of the slab fragments for cracked slabs. This curling reduces the crack width at the pavement surface and allows for a higher load transfer efficiency due to the increased amount of contact between the opposing crack faces. [16]

Seasonal moisture variations can cause warping of the slab, which affects load transfer efficiency [37]. Slab warping is particularly an issue in climates that experience dry, low humidity conditions [10]. In such climates, a substantial amount of drying of the slab may occur following a wet season, and this would result in an upward warping of the slab fragments in a cracked slab [10]. Upward warping results in a greater crack width at the pavement surface, which reduces the load transfer efficiency across the crack.

The temperature and weather conditions that existed at the time of paving can also influence the load transfer efficiency of transverse cracks in JCP's. If cold and humid ambient conditions prevail during paving, a lower temperature than usual will be required to cause expansion of the pavement during its service life. Thus, low temperatures in the winter season may be associated with relatively narrow crack widths and high load transfer efficiency in such circumstances. [38]

Load Conditions

The load magnitude, number of load repetitions, and location of load (approach vs. leave side of crack) for inclined cracks have been found to significantly affect load transfer efficiency and endurance across transverse cracks. Colley and Humphrey found that load transfer endurance decreases as the magnitude of the load increases. Furthermore, they found that load transfer endurance is not significantly affected by loads less than some critical value. Such light loads cause little to no degradation of the crack faces and thus have no significant effect on load transfer. [30]

Colley and Humphrey also verified the intuitively obvious relationship between load repetitions and load transfer effectiveness (or efficiency). That is, they determined that as the number of load repetitions increases, load transfer effectiveness decreases. An interesting finding was made, however, that approximately 90% of effectiveness loss occurs during the initial 500,000 load repetitions. [30]

An inclination of a crack throughout its depth affects its deflection load transfer efficiency. Where such an inclined crack exists, the approach and leave side LTE_δ's will be significantly different. An inclined crack subjected to loads P_1 and P_2 on the approach and leave sides, respectively, is shown in Figure 6. In this case, the approach side LTE_δ will be higher than the leave side LTE_δ. When P_1 is applied to the approach side, the loaded side is able to rest on the unloaded side of the slab, and good contact and aggregate interlock results. When P_2 is applied to the leave side, the loaded side has little contact with the unloaded side, and the load is primarily carried by the leave side alone. Thus, for inclined cracks, load transfer efficiency will be higher on the side which rests on the favorably inclined edge of the adjacent slab fragment. [16]

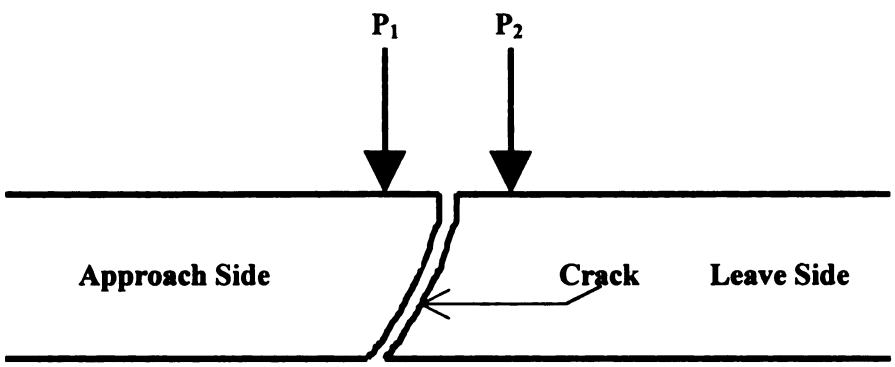

$LTE_{\delta,\ Approach} > LTE_{\delta,\ Leave}$

Figure 6 **Influence of Load Location on LTE_δ for Inclined Cracks. (After Poblete et al. [16].)**

Other Effects

Most of the factors that have been found to affect load transfer efficiency and endurance across transverse cracks in JCP's have been discussed in this section. There are certainly other factors that also have effects on crack performance, but an exhaustive list of these factors is beyond the scope of this thesis. However, two other factors will be briefly discussed here.

The effectiveness of the joints in accommodating slab movements will affect the efficiency and endurance of load transfer across nearby transverse cracks. Misaligned or corroded dowel bars, malfunctioning dowel assemblies, and the presence of expansion joints can each result in substantial crack movements. The resulting opening in the cracks can lead to significant losses in load transfer efficiency and endurance. [14]

The age of a pavement has an indirect effect on decreasing the load transfer efficiency of transverse cracks. As the pavement ages, it is subjected to more cycles of crack opening and closing, more applications of deicing salts which can corrode reinforcement, more freeze-thaw cycles, and so on. Thus, if everything else is held constant, cracks in older pavements would be expected to have lower load transfer efficiencies. [15]

- CHAPTER III -

Literature Review II – Rehabilitation/Resurfacing Methods for JCP's with Transverse Cracking

OVERVIEW

A review of some of the common procedures used in rehabilitating/resurfacing cracked JCP's was conducted in this study. Since this study was partially focused on development and demonstration of methods that can be used to assess when and how to repair cracked JCP's, it was felt that such a review would provide pertinent background information to the reader. Although this review does not cover all available rehabilitation/resurfacing techniques for cracked JCP's, it does provide an indication of some of the types of actions that can be performed to restore integrity to such pavements.

Many alternatives are available for rehabilitating or resurfacing JCP's with transverse cracks. Selection of the appropriate actions to be used on a particular pavement will depend on many factors, such as the overall existing pavement condition, the causes of the various distresses, and the cost/benefit ratio of employing the respective actions. Thus, all distresses associated with a cracked JCP must be identified and an evaluation of the causes of these distresses must be performed prior to selecting the rehabilitation/resurfacing actions to be taken on the pavement. Destructive (e.g., coring) and nondestructive (e.g., deflection testing) test methods can be used to evaluate the condition of the pavement and investigate the causes of the individual distresses.

Several of the common actions used to repair existing transverse cracks and crack-related distresses and prevent their reoccurrence are discussed in this chapter. Frequently, a combination of two or more of these actions are utilized to effectively

rehabilitate the cracked slabs. Some overlay alternatives for resurfacing cracked JCP's are also discussed here. The actions considered here include: "do nothing," full-depth repair, load transfer restoration, slab stabilization, provision of improved edge support, diamond grinding, crack sealing, unbonded concrete overlay, bonded concrete overlay, and asphalt overlay. Each of these alternatives are briefly discussed with regard to: 1) when the action is feasible for use, 2) the procedures involved in carrying out the action, and 3) suggested concurrent work.

REHABILITATION/RESURFACING METHODS

"Do Nothing" Alternative

Feasible Conditions for Use

Transverse hairline cracks that extend only partially through the depth of the slab require no rehabilitation. The suggested action is therefore the "do nothing" alternative. Such cracks, which are often the result of plastic shrinkage, do not allow significant amounts of water to penetrate the pavement substructure and usually have a negligible effect on the serviceability of the pavement. [39]

Full-Depth Repair

Feasible Conditions for Use

Full-depth repairs can be used to restore pavement rideability and structural integrity to a cracked JCP. Transverse cracks demonstrating severe spalling, pumping, corner breaks, and/or faulting are candidates for this repair procedure. This is also an appropriate procedure for cracks that have been deteriorated due to material-related

distresses such as D-cracking or alkali-silica reactivity. Cracks with poor load transfer efficiency (identified through deflection testing) and spalling should also be considered for this type of repair, even if pumping and faulting have not occurred. This method restores pavement integrity, as deteriorated concrete is replaced and load transfer is provided across the transverse joints at the patch boundaries. Note that this procedure can also be used to repair joints that are deteriorated. It should further be noted that partial-depth repairs (not discussed here) are sometimes recommended for cracks having only surface spalling. [40]

Summary of Procedures Involved

A summary of the procedures involved in performing full-depth repairs is provided in the following paragraphs. The first step involves defining the limits for the areas to be repaired. The repair area should be selected to include all distresses that have been identified. Once these areas have been identified, they should be isolated by sawing full-depth cuts along their perimeter. The deteriorated concrete can then be removed by either lifting it out or breaking it up. The liftout method is preferred as it usually imparts no damage to the support layers. If the concrete is too badly deteriorated to be safely lifted out, the breakup method will have to be used. There are several techniques available for carrying out both the liftout and breakup methods. [40]

After the old concrete has been removed, the subbase must be prepared. If the subbase was damaged during concrete removal, new material must be added. The subbase should be uniformly compacted prior to placing the new concrete. Load transfer must be provided across the joints at the patch boundaries. It is recommended that at

least four 38 mm dowels be placed in each wheelpath. Deformed tie bars can be used in lieu of dowel bars on the approach joint, but their use requires special considerations to be made (see [40]). Installation of the dowel bars involves drilling holes into the existing slab edges, cleaning out the holes using compressed air, and placing the dowel bars along with an anchoring material. For long repair lengths (> 4.5 m) or full slab replacements extending only one lane wide, tie bars are usually placed along the longitudinal joints at the patch boundaries. Holes are drilled into the edge of the existing slab and subsequently cleaned. Tie bars are then placed with anchoring material. For shorter repair areas extending only one lane wide, a bondbreaking board is placed along the longitudinal joint. A bond between the existing slab and the patch could lead to cracking in the slab adjacent to the transverse joints at the patch boundaries. A bondbreaker should also be used at longitudinal shoulder joints and at longitudinal joints connecting adjacent patches. [40]

The concrete can then be placed, finished, and textured. Burlap dragging or transverse tining can be used to provide a patch surface texture similar to that of the existing slab. Proper curing measures should then be taken. This may involve the use of a curing compound and insulation boards/mats. A smooth transition should be provided between patch areas and existing slabs. This may require use of diamond grinding (to be discussed later in this chapter). Transverse and longitudinal joints should be sawed and sealed along the patch perimeter as the final step in this procedure. [40]

Suggested Concurrent Work

In addition to repairing the transverse cracks using full-depth patches, other work may be performed to prevent distresses from reappearing at patch locations. Edge drains can be installed outside the outer wheelpath to provide improved drainage to the pavement system [40]. Slab stabilization, which is described later in this chapter, can be used to restore support to the slab if voids exist beneath the patches, cracks, and/or joints [40]. Corner deflections near the transverse joints of the patches can be reduced by constructing a rigid edge support (also described later in this chapter) [41]. Use of any or all of these three actions would lessen the likelihood of pumping, faulting, and corner breaks plaguing the repaired pavement.

Load Transfer Restoration (Dowel Bar Retrofitting)

Feasible Conditions for Use

Load transfer restoration is useful for transverse cracks demonstrating faulting and/or poor load transfer, as this procedure inhibits the occurrence of future faulting and improves the load transfer efficiency of such cracks [42]. It is recommended that this procedure be used when load transfer efficiency drops below 50% [41]. Deflection measurements for computing load transfer efficiencies should be made at cool temperatures (10 to 27°C) [41]. Misleadingly high LTE values can result at high temperatures due to the beneficial effects of thermal expansion and downward slab curling. Load transfer restoration should not be used on cracks where major spalling or material-related distresses exist [39]. Note that this procedure is also valid for poorly

performing joints where dowels were not originally placed or existing dowels are malfunctioning.

Summary of Procedures Involved

The procedure described here involves the use of dowel bars to restore load transfer across cracks in JCP's. It is recommended that three 38 mm dowel bars be used in each wheelpath [43, 39]. The first step in this repair method involves sawing slots in the pavement (parallel to the centerline) across the cracks so that dowels can be placed at mid-depth in the slab. Lightweight equipment should be used to remove the concrete from the slots so that no damage is imparted to the support layers. The slots should then be sand-blasted and cleaned of saw slurry and other material. [43]

Chairs should then be installed in the slots to hold the dowel bars in position when the backfill concrete is placed. The dowel bars should be coated with a parting compound and placed on the chairs. It is suggested that expansion caps be attached to the ends of the dowel bars to allow for expansion of the backfill concrete. Once the chairs are in place, the bottom and sides of the crack within the slot should be caulked. In addition to providing a smooth level surface, the caulking prevents backfill material from entering the crack at the bottom or sides of the slots. A fiber or foam filler-board should be placed around the dowels at mid-length to preserve the form of the crack across the slot [39, 43]. A prepackaged patching material should then be used to fill the slots. Cracks can be sealed by sawing reservoirs and then installing a joint sealant (crack sealing is discussed later in this chapter). [43]

Suggested Concurrent Work

Diamond grinding should be performed to restore rideability at faulted cracks which were repaired using load transfer restoration. Other work may also be performed in addition to load transfer restoration to inhibit the occurrence of future distresses at crack locations. Such work might involve installation of edge drains, slab stabilization, and/or construction of a rigid edge support. These actions, combined with the improved load transfer provided by the dowel bar retrofit procedure described in this section, should effectively combat the development of pumping, faulting, and corner breaks at the repaired crack locations.

Slab Stabilization

Feasible Conditions for Use

Slab stabilization is a nondestructive repair procedure that restores support to a pavement through the injection of grout without raising the slab [44]. Pumping of fines from pavement support layers can lead to voids under transverse cracks and joints, which results in a loss of support. Faulting and corner breaks often result after such voids are created. This repair procedure can be used to restore support where voids exist near cracks and joints in JCP's, leading to a more structurally sound pavement [44]. It is important, however, that slab stabilization is not performed at cracks or joints which have no voids [41]. Such misuse of this procedure could cause slabs to lift off their support and/or create uneven support for the slabs [41]. It might also be noted that at least one study has found that slab stabilization is ineffective at restoring support to JCP's with cement-treated bases [45].

Summary of Procedures Involved

Voids can exist under the approach or leave side of a crack or joint or even under shoulders, but they most frequently occur beneath the corner of the leave side of a transverse discontinuity [41]. Before slab stabilization can be performed, the cracks and joints which have voids must be identified [44]. It is sometimes desirable to estimate the size of the voids as well in order to better estimate the amount of material which will be needed to fill the voids. There are three available methods for detecting void locations – visual inspection, deflection measurement, and ground penetrating radar (GPR) [44].

Visual inspection is the simplest yet most unreliable method for estimating void locations. Transverse crack or joint faulting, corner breaks, lane-shoulder dropoff, and the presence of fines near cracks and joints are indications of the existence of voids. A limitation of this method is its lack of accuracy in estimating void location and size. [44]

Deflection testing can be used to detect void locations and sizes. Large vertical deflections indicate the presence of voids [44]. Static testing can be performed using a Benkelman beam [44]. FWD's and other devices are available for performing dynamic testing. A relatively rapid and simple method can be used to detect void locations using deflection testing [44]. This method was used in this study to detect the presence of voids at selected cracks and joints within the test sites. Results and discussion concerning the use of this method as well as a brief description of the test procedure are given in Chapters IV and V of this thesis. A second, more cumbersome method is available for determining both void locations and sizes [44]. Detailed information regarding this second method can be found in [41]. Deflection testing should be

performed at cool temperatures to avoid the effects of downward curling and slab expansion on deflection measurements [41].

A relatively new method for estimating void locations and sizes is the use of GPR combined with pulsed electromagnetic wave (PEW) technology. This method involves transmission of electromagnetic waves into the pavement, followed by detection of the reflection pattern of such waves from the pavement. Voids can be detected by examining the wave reflection pattern. A more detailed account of this test procedure is provided in [44]. The accuracy of this method must be improved before it becomes a viable option for void detection. [44]

After the void locations have been detected, the next step is to drill holes in the concrete. The hole depths are determined by the base type. Holes must penetrate through stabilized bases into the subgrade, as it has been found that voids form under these stiffened bases. Where granular bases exist, holes should only go through the slab and end at the top of the base layer. Hole patterns depend on several factors, namely pavement type (JPCP or JRCP), joint spacing, and slab condition [46, 47]. Hole locations are selected to allow for filling of voids as well as grout flow between holes or towards cracks and joints. [44]

Once the holes have been drilled, grout injection can begin [44]. The most common types of grout used are pozzolan-cement grout and polyurethane [48]. The grout is pumped into the holes in a sequence which tends to drive away water from under the slab and force it out through the pavement joints [44]. Pumping stops when any of the following conditions occur: the slab starts to lift, the grout ceases to pump at the maximum allowable pressure, or the grout begins to flow out of an adjacent hole [44]. If

the grout is displacing water from under the slab, pumping should stop when an undiluted mixture of grout flows from the pavement [44]. Grout injection should also cease if, after one minute, there is no grout in any adjacent hole, crack, or joint, and no slab movement has been detected [44]. These are indications that a large void exists beneath the pavement, which will require repair measures other than slab stabilization (e.g., full-depth repair) [41]. After grout injection is complete, wooden plugs are sometimes driven into the holes [41]. This prevents the grout from coming out of the holes due to back pressure [41]. The need for using such plugs is questionable [44]. A cement grout is used to fill the holes after the grout has set [41]. Slab stabilization should not take place at temperatures below 4°C or if the subgrade freezes [46].

Deflection testing or GPR should be performed on stabilized slabs twenty-four (24) to forty-eight (48) hours after slab stabilization. This is done to check if the stabilization procedure was effective in restoring support. Testing should also be done on slabs that were not stabilized to allow for comparison. If stabilization was not effective the first time, it can be attempted one or two more times if necessary. After the third attempt, slabs which still suffer from loss of support should be repaired using an alternative method. [44]

Suggested Concurrent Work

Slab stabilization should usually be combined with other repair procedures to effectively restore the functional and structural integrity of a cracked JCP. Pumping of support material out of cracks and joints can be avoided by preventing water from accumulating beneath the slab. Sealing transverse cracks helps to block water from

entering the pavement. Installing edge drains can help to remove water from beneath the slab. Other techniques (full-depth repair, dowel bar retrofitting, and construction of a rigid edge support) are useful in limiting slab deflections and thus inhibiting pumping, faulting, and other associated distresses at crack locations. Diamond grinding can be used to restore rideability at faulted cracks. [44]

Construction of Rigid Edge Support

Feasible Conditions for Use

This repair procedure involves the construction of either a slab edge beam or a tied concrete shoulder to provide improved edge support to an existing JCP [49, 50]. This edge support reduces stresses and deflections at slab edges and corners [49, 50]. By reducing the deflections at transverse crack and joint corner locations, the potential for pumping, faulting, and corner breaks is significantly decreased. The reduced edge stresses will also lessen the likelihood of transverse cracking in the pavement. This repair procedure is thus useful wherever it is suspected that the existing shoulder is not providing adequate support to the mainline pavement. This is assumed to be the case for JCP's having asphalt or untied concrete shoulders and demonstrating a substantial amount of loss of support. If substantial loss of support exists for pavements having tied concrete shoulders, the condition of the shoulder and the tie bars should be investigated to determine if improved edge support is needed.

Summary of Procedures Involved

Either a full-width concrete shoulder or a narrow concrete "beam" attached to the slab edge can be used. Cost and the condition of the existing shoulder will help decide which should be used. For example, if the existing shoulder is in poor condition and will require rehabilitation anyway, a full-width concrete shoulder will likely be more cost-effective. If the edge beam is used, it should have a minimum width of 610 mm. The edge beam can be constructed with or without an undercut lip. The depth of the edge beam should be at least as great as the thickness of the slab. [41]

The base layer must be in good condition prior to constructing the shoulder or beam. If the base material was disturbed during excavation, it must be recompacted to provide uniform support to the shoulder or beam. Following excavation, holes can be drilled into the existing slab at mid-depth for tie bar placement. Deformed tie bars, spaced at 305 to 610 mm, are then placed into the holes and secured using epoxy or nonshrinking grout. Once the tie bars have been secured and the shoulder area has been prepared, the concrete can be placed and textured. Texturing of the shoulder or beam surface should be performed such that drivers can distinguish between the pavement and shoulder. This can be accomplished by texturing the shoulder or beam perpendicular to the mainline pavement. The last step is to seal the longitudinal lane-edge support joint and the transverse shoulder/beam joints. [41]

Suggested Concurrent Work

To effectively rehabilitate a cracked JCP, use of other repair methods in addition to construction of a rigid edge support should be considered. Slab stabilization can be

used to restore uniform support to the slabs. Installation of edge drains and sealing of transverse cracks will inhibit the accumulation of water beneath the slabs, and thus help to prevent pumping and pumping-related distresses in the future. Full-depth repair and dowel bar retrofitting can be used to restore the pavement's structural integrity at transverse crack locations. Diamond grinding of faulted cracks will improve pavement serviceability.

Crack Sealing

Feasible Conditions for Use

Crack sealing can be used to prevent water and incompressibles from entering a transverse crack. Entry of water into a crack can lead to pumping of support material out of the pavement. This can subsequently result in formation of voids beneath the pavement and subsequent faulting and corner breaks near the cracks. Spalling can result if incompressibles become lodged in a crack opening. It is thus recommended that sealing be performed on all transverse cracks that extend fully through the slab depth but do not require full-depth repair or other resurfacing. [39]

Summary of Procedures Involved

If concurrent repair work will be performed on the cracks to be sealed, such repairs should be done prior to crack sealing. The first step in the crack sealing procedure is to saw and shape a reservoir for the crack. The required shape of this reservoir will depend on the type of sealant to be used and the anticipated thermal movements of the crack. A special crack saw, equipped with a pivot wheel and crack-

sawing blades, should be used. Crack wander can be followed with these special saws. [39]

After sawing is completed, the reservoirs must be cleaned to allow for proper sealant adhesion. Cleaning involves three basic steps. A water wash should be performed immediately following sawing to remove slurry residue from the sawing operation. The top of the reservoir should then be sandblasted to remove any remaining debris or contaminants. Just prior to sealant installation, the reservoir should be air blown to remove any sand, dirt, or dust. [39]

The next step involves installing a backer rod into the crack reservoir. A steel roller or any smooth blunt tool can be used to insert the backer rod. It is important that it is installed uniformly at the desired depth. After the backer rod has been installed and the reservoir is clean and dry, the sealant can be installed. A liquid sealant (hot-pour or silicone) should be used. Manufacturer's guidelines should be checked to ensure that the sealant installation temperature complies with any restrictions for the given sealant. The sealant is installed by fitting an injection nozzle into the reservoir and pumping the sealant. If a low-modulus silicone sealant is used, tooling should be performed to achieve proper adhesion to the reservoir walls. The surface of the sealant should be recessed at least 6 to 10 mm below the pavement surface. Manufacturer's guidelines should again be consulted to determine the required curing time. The "knife test" can be used as a simple check to ensure that proper sealant adhesion to the reservoir walls has been attained. After fourteen (14) to twenty-one (21) days, the adequacy of sealant curing can be checked by removing a small sample of sealant, stretching it, and observing the sealant's resilience. [39]

Suggested Concurrent Work

Crack sealing alone should be adequate for full-depth hairline cracks [39]. However, cracks demonstrating poor load transfer should be repaired using dowel bar retrofitting in addition to crack sealing. Deteriorated cracks exhibiting severe spalling should be full-depth repaired rather than sealed and retrofitted. Other types of repairs will help to prevent future distresses from occurring. Slab stabilization, improved edge support, and installation of edge drains will deter void formation and pumping at crack locations. Diamond grinding can be used to restore rideability at faulted cracks.

Diamond Grinding

Feasible Conditions for Use

Diamond grinding is a useful technique in any complete rehabilitation program for cracked JCP's. Because grinding does not actually improve the structural integrity of a pavement, it should usually be used in conjunction with other repair procedures that do restore such integrity [51]. As part of a complete rehabilitation effort, grinding is principally used to restore rideability to faulted transverse cracks and joints and to provide a smooth transition between an existing concrete surface and repair areas (e.g., patches) [51]. It is generally recommended that grinding be used before faulting reaches 6 to 7 mm for a crack or joint [51]. In addition to the noted improvements that result from diamond grinding, this procedure also provides improved skid resistance and rideability on the existing pavement and can be used to improve transverse drainage [42]. Another positive feature of grinding is that it can be done either on only one or all lanes of a highway, depending on the particular needs of the pavement [41].

Summary of Procedures Involved

Prior to selecting equipment and estimating the cost for a diamond grinding job, information on the existing pavement is needed. Data on the concrete aggregate properties should be obtained as this will affect selection of equipment. The existing pavement surface profile should also be obtained (using a profilograph or some other device) to allow for estimation of the amount of grinding required and the locations of areas of roughness [41]. The diamond grinding equipment consists of diamond saw blades mounted to a cutting head. The diamond size, diamond concentration, and bond hardness of the saw blades must be selected. Since these factors depend on the concrete aggregate properties, saw blades should be selected based on the aggregate data collected for the pavement. The saw blade spacing should be selected to provide adequate texture and friction. This factor depends on aggregate hardness. [51]

Diamond grinding should always be done longitudinally (parallel to the pavement centerline). Grinding can be done in either direction, as it has been found not to affect the pavement texture. The direction of grinding should thus be chosen to allow for adequate maneuvering of the equipment. The grinding operation will involve either one pass using multiple machines or several passes using one machine. The size of the project will dictate this decision. [51]

Residual slurry and residue from the grinding operation is removed and collected by vacuums attached to the grinding equipment [41]. In rural areas, the slurry can be deposited onto grassy slopes along the road [41]. In urban areas, the slurry should be dumped into a truck and transported to a suitable off-site location [41]. After completion

of diamond grinding, the pavement should be evaluated to determine if an acceptable profile has been attained [51].

Suggested Concurrent Work

As was noted above, other repair methods should be used concurrently with diamond grinding to properly rehabilitate a cracked JCP. Full-depth repairs can be used to restore structural integrity at deteriorated transverse crack locations. For cracks exhibiting inadequate load transfer without significant deterioration, load transfer restoration is a viable option. Crack sealing and/or installation of edge drains will inhibit water from accumulating in the pavement subsystem and thus deter the formation of voids. Slab stabilization and/or construction of a rigid edge support will reduce corner deflections and further hinder the development of loss of support.

Unbonded Concrete Overlay

Feasible Conditions for Use

An unbonded concrete overlay is a cost-effective resurfacing alternative for cracked JCP's that are badly deteriorated. This type of overlay involves placement of a separation interlayer between the existing pavement and the overlay. The separation layer prevents such distresses as transverse cracking and D-cracking from propagating through the existing slab to the overlay. Due to the effectiveness of the separation layer, the required amount of pre-overlay repair is significantly less for unbonded concrete overlays than that for other overlay methods (i.e., bonded concrete or asphalt overlays). This procedure restores structural integrity to the pavement and improves the ride quality

as any roughness on the existing surface is eliminated with the addition of the overlay. [52]

Summary of Procedures Involved

Unbonded concrete overlays require pre-overlay repairs only where severe distresses in advanced stages exist or where there is a lack of uniform support in the existing pavement. Cracks and joints which are severely deteriorated should be full-depth repaired. Slabs which are severely deteriorated and suffer from a loss of support should be replaced. Slab stabilization and installment of edge drains can be performed if pumping and erosion has occurred in the existing pavement. Localized diamond grinding can be used to remove faulting at cracks and joints with faulting greater than 6 to 7 mm. As an alternative to grinding, a thick separation layer could be used to eliminate the effects of severe faulting. [52]

Once all necessary pre-overlay repairs have been completed, the next step is to clean the existing pavement surface. This provides a suitable surface for placement of the separation interlayer. A mechanical sweeper or an air blower can be used to remove loose debris on the surface. Prior to placing the separation layer, all joints and working cracks (cracks that move and function as a joint) on the existing pavement should be marked if mismatching will be used for the overlay joints [52, 39]. These markings will allow the sawing operation to be performed so that overlay joints are not placed above discontinuities in the existing slab. Mismatching overlay joints is believed to be beneficial in providing good load transfer across the joints in unbonded concrete overlays. It is suggested that the overlay joints be formed on the approach side of an

existing joint or crack. Field adjustment of the joint spacing will be required if mismatching is performed. A maximum spacing should be specified in advance. [52]

The separation layer can be placed after all joint and crack markings have been made. It is recommended that a bituminous mix be used as a separation layer if the existing pavement is severely faulted and/or has excessive cracking. A 25 mm thickness is usually adequate for this layer. If the existing pavement has minimal faulting and surface roughness, a surface treatment may be used as the separation layer. A slurry seal, consisting of a diluted asphalt emulsion mixed with sand aggregate, is a typical material used for these thin separation layers. [52]

If the temperature of the bituminous material in the separation layer is expected to exceed 44°C, whitewash should be applied to the interlayer. Consisting of either white-pigmented curing compound or a lime slurry, whitewash is used to prevent the accumulation of heat in a black-surfaced separation layer. Whitewash provides a cool interlayer surface temperature by creating a white surface that does not absorb sunlight. This helps to deter shrinkage cracking in the concrete and bonding between the concrete and interlayer. [52]

After the separation interlayer is placed and the whitewash is applied and allowed to cool, the concrete can be placed and finished. Epoxy-coated dowel bars should be placed at joint locations to provide load transfer. Following placement and finishing of the concrete, transverse tining can be performed to provide a skid-resistant surface on the concrete. A curing compound can then be applied to prevent moisture loss and shrinkage cracking. Transverse and longitudinal joints should be sawed and sealed as soon as it is practical to do so. Mismatched joints should be created if specified. [52]

Shoulders will also need to be constructed to match the grade of the overlay. Tied concrete shoulders rather than asphalt shoulders are recommended. As was stated in Chapter II of this thesis, tied concrete shoulders can be expected to lead to fewer fatigue cracks in the pavement. If concrete shoulders are used, they can be placed concurrently with the mainline pavement. [52]

Use of an unbonded concrete overlay also warrants other considerations. Ditches and embankments will need to be filled to meet slope requirements. Reconstruction in lieu of an overlay may be necessary at bridge decks and overhead structures. This will provide the necessary vertical transition at bridge decks and the required vertical clearance where overhead structures exist. A smooth transition from overlay slabs to reconstructed slabs can be accomplished by providing an adequate taper. [52]

Bonded Concrete Overlay

Feasible Conditions for Use

A bonded concrete overlay is a useful method for increasing the structural capacity of a JCP that is not appreciably distressed but has become subject to a significantly greater amount of heavy truck traffic than was originally anticipated during design. This overlay method also restores rideability, as a new riding surface replaces roughness on the existing pavement. In this resurfacing procedure, a thin layer of concrete (commonly 76 to 102 mm) is bonded directly to the top of an existing concrete pavement to provide increased structural support. It must be stressed that this overlay type can only be used if the existing pavement is not significantly distressed and has minimal material-related problems. It is not cost-effective to use bonded concrete

overlays on heavily distressed pavements because of the scope of pre-overlay repair that would be required. Without such repairs, distresses in the existing pavement would likely propagate into the overlay. However, when greater structural capacity is desired for a pavement without appreciable damage, bonded concrete overlays do have an advantage over other overlay methods. In such circumstances, bonded concrete overlays are often more cost-effective than asphalt overlays due to their superior structural efficiency. They are also preferred over more costly unbonded concrete overlays, which are unnecessary and unjustified in such cases. [53]

Summary of Procedures Involved

As noted above, bonded concrete overlays should only be attempted on pavements that are not severely distressed. Pre-overlay repairs are required for almost all distresses in the existing pavement. The type of repair required for existing transverse cracks will depend on the severity of the crack. Tight cracks that have no faulting or deterioration can be left untreated. However, reflective cracking will likely result at these crack locations within a couple of years after placement of the overlay. Such reflective cracks will then need to be sealed. Cracks that have a small amount of faulting or deterioration can be treated using "random crack control." This procedure helps to delay - not prevent - reflective cracking. It involves putting tie bars, supported by chairs, across cracks at the existing pavement surface prior to placement of the overlay. Reflective cracks will also likely result at these crack locations and require proper sealing. Cracks and joints that are significantly faulted and/or deteriorated will require full-depth repairs. If pumping and erosion has occurred in the existing pavement, slab stabilization and

installation of edge drains may be useful repair procedures. Slab replacement will be needed for those slabs that are badly deteriorated and demonstrate a loss of support. Localized milling can be used to smoothen faulted cracks and joints, when full-depth repairs or slab replacement are not warranted. [53]

Upon completion of all necessary pre-overlay repairs, a clean and sound surface should be created on the existing pavement. Surface preparation is a three-step procedure. A sound surface free of contaminants is obtained by first either milling or shotblasting the existing pavement surface. Shotblasting is generally the more effective method if sound concrete can be reached close to the surface. When a deeper removal is required to reach sound concrete, milling is the recommended method. Following shotblasting or milling, the second step is to remove dust and other fine residue from the surface. This can be accomplished using either sandblasting or waterblasting. The final step in surface preparation occurs just prior to placing the concrete. Either airblowing or shotblasting can be employed just ahead of the paving operation to ensure that any dust blown on the pavement is removed. [53]

After the sandblasting or waterblasting operation is completed, all transverse joints and working cracks in the existing pavement should be marked. A 25 mm tolerance on each side of the joint/crack should be provided. Marking the joint/crack locations allows for the overlay joints to be matched with the discontinuities in the existing pavement. Matching of the cracks and joints is necessary to prevent reflective cracking. In addition to locations, the type and width of the joints/cracks should be matched in the overlay. It may also be necessary in some cases to mark the longitudinal joint(s) so that it can be matched in the overlay. This will be required if the existing

longitudinal joint(s) meanders. In such cases, offset measurements can be taken from the edge of the pavement to mark the path of the longitudinal joint. [53]

Once the surface is prepared and the joints/cracks have been marked, a bonding grout can be placed on the existing pavement surface if desired. These grouts are cement-based and can help to achieve a good bond between the existing pavement surface and the overlay. While they are commonly utilized, it is debatable whether a bonding grout is needed for these overlays. If a grout is to be used, it should be sprayed on the existing surface at a distance of 2 to 3 m ahead of the paving operation. [53]

Placement and finishing of the concrete takes place following final surface preparation and application of the bonding grout (if used). Transverse tining can be used to provide a skid-resistant texture on the overlay pavement surface. A curing compound should then be applied to inhibit moisture loss and provide the conditions necessary for proper strength gain in the concrete. Sawing and sealing of the transverse and longitudinal joints should be performed as soon as it is practical to do so. The type, width, and location of these joints should match the joints/cracks in the existing pavement. Joint depth should be chosen to ensure that the joint crack aligns with the discontinuity in the existing pavement. Note that dowel bars are usually not used across transverse joints in bonded concrete overlays and thus need not be considered. [53]

Widening of the pavement can often be easily accomplished when applying a bonded concrete overlay. Such widening provides increased roadway capacity and can be used to meet geometric requirements. The widening as well as placement of new tied concrete shoulders can be performed monolithically with the overlay or separately from the overlay. An asphalt shoulder could alternatively be placed with the overlay, but this

is not recommended. Tied concrete shoulders lead to less fatigue cracks than asphalt shoulders, as explained in Chapter II of this thesis. Another consideration to be made during placement of a bonded concrete overlay is provision of smooth vertical transitions at overlay termini and bridges. This can be accomplished by milling the pavement surface to provide an adequate taper. [53]

Asphalt Overlay

Feasible Conditions for Use

Asphalt concrete overlays can be used to improve the structural and functional integrity of a cracked JCP. Two methods of applying an asphalt overlay over a JCP will be discussed here. One method involves placing an asphalt overlay over a rubblized JCP, while the other involves placing the overlay over an existing intact JCP. Constructing an asphalt overlay over a rubblized JCP can be a cost-effective approach if the existing pavement is badly cracked and/or deteriorated. In such a case, the cost of rubblizing the existing pavement is offset by the savings of not having to perform substantial pre-overlay repair. Applying an asphalt overlay over an intact JCP is a feasible alternative if the existing pavement has only a moderate to low amount of deterioration and/or cracking and has little to no material-related problems. This second method requires use of a reflection crack control treatment to inhibit reflective cracking. [1]

Summary of Procedures Involved

The required steps in constructing an asphalt overlay prior to the actual placement of the overlay differ for the two methods noted above. Therefore, these preliminary steps

will be discussed separately for each of the methods. The first method, involving placement of an overlay over a rubblized JCP, requires little pre-overlay repair. It is suggested that any areas on the existing JCP that may lead to nonuniform support following the rubblization process be removed and replaced. If drainage improvements are necessary, edge drains should be installed prior to rubblization. [1]

After the required pre-overlay repairs have been made, the existing JCP can be rubblized. This involves fracturing the slabs into pieces less than 305 mm and then compacting the rubblized layer using several passes of a vibratory roller. If uniform rubblization and proper compaction have been accomplished, there should be no need for an additional reflection crack control treatment. The final step prior to placing the overlay is to apply a tack coat on the rubblized layer. [1]

The second method described here for constructing an asphalt overlay, involving placement of an overlay over an intact JCP, requires pre-overlay repairs to be made wherever significant distresses exist. Deteriorated cracks and joints and all working cracks should be full-depth repaired. If excessive deterioration and/or cracking exists in a slab, the slab should be removed and replaced. Slab stabilization and installation of edge drains can be used if pumping is a problem. Faulting at cracks and joints can be removed by using localized diamond grinding. Upon completion of all necessary pre-overlay repairs, a tack coat should be applied to the existing JCP surface. [1]

A reflection crack control treatment should be selected for use in combination with this second method. One such treatment option is placing a bituminous-stabilized granular interlayer prior to or concurrently with placement of the asphalt overlay. Another approach is to place a synthetic fabric or a stress-absorbing interlayer prior to or

within the asphalt overlay. A treatment method to slow - not prevent – reflective cracking is to increase the thickness of the asphalt overlay. Another option is to saw and seal joints in the overlay to match the joints in the existing JCP. If this last treatment technique is to be used, all joints in the existing JCP should be marked following completion of pre-overlay repairs. [1]

For both asphalt overlay methods (with or without rubblization), the pavement can be overlaid once the tack coat has been applied to the existing surface. This will involve placement of an asphalt concrete overlay over the tack coat (or fabric/interlayer where such a treatment is used). Joints should be sawed and sealed in the overlay if the saw and seal treatment is to be used. [1]

Additional considerations should be made when planning an asphalt overlay. The appropriate action to be taken on the existing shoulder will be determined by its condition. If the shoulder is in fairly good condition, it can be repaired and overlaid. Any deteriorated areas should be patched and an overlay can then be placed over the existing shoulder. However, if the existing shoulder is badly deteriorated, it must be removed and replaced. In either case, the shoulder grade should be matched to that of the overlay mainline pavement. [1]

Widening of the pavement can be performed concurrently with construction of the overlay if desired. This can help in meeting geometric requirements and providing increased roadway capacity. Another consideration that should be made is the use of reconstruction in lieu of an overlay under overhead structures to provide the necessary vertical clearance. An adequate taper should be used to provide a smooth transition from overlay areas to reconstructed areas. [1]

- CHAPTER IV -

Data Collection

DESCRIPTION OF TEST SITES

One of the first tasks of this study was to select test sites from in-service highway pavements in Michigan for use in this field investigation. A set of criteria for choosing sites was developed prior to test site selection to ensure that those chosen would allow for the analyses of all variables to be considered in this study. A listing of the principal criteria used for site selection is given as follows:

- Presence of transverse cracking in the JCP
- Varying concrete coarse aggregate types (carbonate, natural gravel, recycled concrete, and slag) among the test sites
- Varying joint spacing (4.9, 8.2, 12.5, and 21.6 m) among the test sites
- Varying shoulder types (asphalt, tied concrete, and tied concrete with sympathy joints – shoulder joints having a joint spacing less than that which exists in the mainline pavement) among the test sites
- Varying traffic levels among the test sites
- Pavement not scheduled for rehabilitation/reconstruction within the duration of this study
- Test sites dispersed throughout southern Michigan

Using MDOT construction records and consultation with MDOT personnel, various sections of highway in Michigan that met the above criteria were identified. A team of researchers then drove through these highway sections and selected

approximately 150 m sections to be considered for use as test sites. The actual test site locations were selected at the time of field data collection by choosing 25 to 65 m long sections (2 to 8 slabs in length) of pavement from within the 150 m sections initially considered. The outermost traffic lane was used for all test sites. Sites were chosen as far as possible away from entry/exit ramps to prevent traffic flow problems during field data collection.

During the first test cycle (April 1997), thirty-three (33) sites (Sites 1-15, 35-43, 38A, 47-52, 55, and 57) were chosen. In the period between the first and second test cycles (July 1997), three of these sites (Sites 9, 47, and 48) were lost to rehabilitation or reconstruction. In an effort to compensate for the loss of these sites and to provide a sufficient number of sites to allow for proper analysis of the variables considered in this research, fifteen (15) more test sites (Sites 16, 17, 27-29, 31, 32, 44-46, and 58-62) were added during the second test cycle. One additional test site (Site 63) was added during the third test cycle (October 1997) to provide more data on slag aggregate pavements. No new sites were added during the fourth test cycle (June 1998). The database thus consists of a total of forty-nine (49) test sites, where three sites have been "inactive" since the completion of the first test cycle. A discussion of the inventory and field data collected for the test sites is given in the following sections.

INVENTORY DATA

An intensive review of MDOT construction records was performed to collect and compile inventory data for the test sites. This inventory data is compiled in Appendix A of this thesis according to the aggregate type of the pavement. Test site location data as

well as pavement age data can be found in Tables A.1 through A.4 for carbonate, natural gravel, recycled, and slag pavements, respectively. Detailed location information for the test sites is given in these tables, including interstate and route number, mile posts, exit numbers, stationing, and an estimate of the distance of the site from the nearest major city. The sites are located as far west as 35 miles west of Kalamazoo, MI and as far east as 35 miles east of Flint, MI. The northernmost site is located several miles north of Flint, MI, while the southernmost site is located 30 miles south of Ann Arbor, MI. Test sites are found on Interstate 69, Interstate 75, Interstate 94, and U.S. Route 23. Pavement age varied from 3 to 29 years for the test sites.

Some of the physical characteristics of the test site pavements, including the number of slabs within the site, the length and width of the site, the joint spacing, and shoulder information, are given in Tables A.5 through A.8 for the four pavement types, respectively. Tables A.9 through A.12 contain information regarding the pavement layer thickness' and types for the test sites. The slab thickness of the test site pavements ranged from 178 to 305 mm. Information pertaining to the MDOT concrete mixture design designation (grade of concrete) for the test site pavements and the climatic conditions during construction is provided in Tables A.13 through A.16. The final group of inventory data tables, Tables A.17 through A.20, contain all of the traffic data for the test site pavements. This traffic data includes average daily traffic (ADT) and percent commercial data for the years 1987, 1994, 1995, 1996, and 1997 as well as values for the cumulative truck traffic (as of 1998) that has been applied to the test site pavements. The procedure used in determining cumulative truck traffic is described below. Cumulative

truck traffic ranged from 2.3×10^6 to 4.5×10^7 ESAL's (80 kN equivalent single axle loads) for the test sites.

ADT and percent commercial data for 1987, 1994, 1995, 1996, and 1997 were used to estimate the cumulative truck traffic (as of 1998) for the test site pavements. Using these five years of ADT and percent commercial data, an estimate of the ADT and percent commercial existing for a test site at the time of the pavement's construction was interpolated or extrapolated. The ADT and percent commercial data was also used to estimate the annual growth rate of traffic for the test site, which is the percentage by which traffic (ADT and percent commercial) increases per year. The AASHTO "growth factor" was then computed using equation (7) [1]:

$$\mathbf{GF} = \frac{(1+g)^n - 1}{g} \qquad (7)$$

where:

GF	=	growth factor
g	=	annual growth rate / 100%
n	=	age of pavement, yrs.

The cumulative truck traffic (as of 1998) was then calculated using equation (8):

$$\mathbf{Traffic} = (GF)(TF)(ADT_0)(\%\ Com_0)(365) \qquad (8)$$

where:

Traffic	=	cumulative truck traffic (as of 1998), ESAL's
GF	=	growth factor
TF	=	truck factor = 0.85 (supplied by MDOT at time of study)
ADT_0	=	estimated average daily traffic for year pavement constructed, vehicles/day
% Com_0	=	estimated percent commercial for year pavement constructed.

Note that equation (8) contains the factor "365" to convert the average daily traffic to an average annual traffic. The above procedure was used to estimate the cumulative truck traffic for each test site in this study.

FIELD DATA

Overview

Four cycles of field data collection were performed over a fourteen month period for this research. These test cycles corresponded to different seasons of the year and thus allowed for a study of the effects of temperature on crack performance. A traffic closure was set up in the outer traffic lane for the length of the test site during all field testing to allow for data collection. Data collected in this study included manually measured data, FWD test data, and concrete core specimens. Types of data collected varied somewhat from cycle to cycle. A description of the types of testing performed and data collected in this study will therefore be given separately for each test cycle. A discussion concerning the compilation of the manually measured field data in this thesis concludes this section.

Cycle 1 – April 1997

Field data was obtained from thirty-three (33) test sites (all of the test sites at that time) during the first test cycle. The first step taken in the data collection process was to locate all transverse cracks and draw them on field data sheets. As transverse cracks were located, they were marked with spray paint on the pavement. Special marking was used to identify cracks that were to be FWD tested and/or cored. For the purposes of this study, any visible cracking (partial- or full-width) in the transverse direction of the pavement was considered to be a transverse crack, with a couple of notable exceptions. One such exception was hairline shrinkage cracks. These cracks were not considered because they often exist only at the pavement surface and do not significantly affect the structural integrity of JCP's. Furthermore, consideration of these cracks for data collection purposes is impractical, as such cracking can be exhaustively widespread throughout the surface of the pavement. Cracks in the transverse direction due to map cracking were also not considered in this study. Map cracking and transverse cracking are two different types of distresses. Also, it would be impractical to consider map cracking for data collection purposes, as this type of cracking is usually present throughout the pavement surface where it exists.

Two types of FWD testing were performed (by MDOT) during the first test cycle. One type of testing was done at selected cracks and joints to allow for calculation of LTE_δ. In selecting cracks to be tested for LTE_δ, an attempt was made to choose cracks demonstrating a range of widths and conditions to allow for consideration of both poor and acceptably performing cracks. Joints adjacent to the selected cracks were generally chosen for this testing. FWD testing for computation of LTE_δ involved dropping a 40 kN

load in the right wheelpath at the crack/joint location. This testing was done on both the approach (load dropped just before the crack/joint) and leave (load dropped just after the crack/joint) sides of cracks and joints. Upon impact of the load on the pavement, the resulting pavement deflections directly below the FWD load plate and on the opposite side of the crack/joint were measured with the FWD. This deflection data could then be used in equation (5) to compute LTE_{δ}. In addition to measuring deflections, the FWD also measured the ambient and pavement surface temperatures at the time of each test. Further discussion regarding LTE_{δ} values computed in this study is provided in Chapter V of this thesis.

A second type of FWD testing performed during Cycle 1 was midslab testing on uncracked slabs. This testing was done on one uncracked slab per test site. Data obtained from this testing allows for backcalculation of pavement support and stiffness parameters. The backcalculation procedure and results from using the procedure in this study are discussed in Chapter V of this thesis. FWD midslab testing involved dropping a 40 kN load at the center of a slab. Pavement deflections at varying distances from the FWD load plate, resulting from the impact of the applied load, were measured with a series of sensors on the FWD. If an uncracked slab was not available within a given test site, midslab testing was performed either on an uncracked slab adjacent to the test site or as far as possible away from joints and cracks on a minimally cracked slab within the site. For sites where no suitable slabs were available for midslab testing, no such testing was done. In these cases, support and stiffness parametric values had to be either assumed or copied from another test site and/or test cycle.

Coring was also performed (by MDOT) during the first test cycle. 152 mm diameter concrete core specimens were taken from the right wheelpath at one crack and one joint per test site. These cores were taken to examine the type of crack (aggregate or mortar) and to confirm the slab thickness and aggregate type. An aggregate crack refers to a crack that propagates through the concrete aggregate in the core. If the crack propagates around the aggregate, it is deemed a mortar crack. Several of the core specimens were also used for Volumetric Surface Texture (VST) testing in this study. A discussion of the VST test procedure and results obtained using the procedure in this research is given in Chapter VI. An incidental finding from the cores taken at cracks in this study was evidence of dropped and completely sheared off reinforcement. This evidence confirmed the reasons given in Chapter II for why reinforcement effects were not considered in this research. Coring could not be performed at some test sites due to mechanical problems with the coring rig. However, cores were obtained for such sites during subsequent test cycles.

In addition to FWD testing and coring, several other types of data were manually measured during Cycle 1. Crack width, length, and faulting were measured for all transverse cracks within a test site. Joint width and faulting were measured for all joints within a test site. The spacing between cracks for each slab within a site was also measured. All manually measured data, in this cycle and all others, was recorded on field data sheets.

Crack length and crack spacing were measured with a measuring wheel. Joint width was measured with electronic calipers. The arms of the calipers were placed within the edges of the joint to measure the width.

In Cycle 1, an electronic faultmeter was used to measure faulting at cracks and joints. This device recorded positive faulting if the leave side of the discontinuity was lower than the approach side. The fault values measured with the faultmeter were, however, found to be inconsistent, as values often did not agree with visual observations of the faulting (both in sign and magnitude).

Crack width was measured using a "crack comparator" card during the first test cycle. Several measurements were made at various locations along both wheelpaths of each crack. These measurements were then averaged to obtain the crack width. Several problems were encountered, however, in measuring the crack widths. One problem was that using the card to measure crack width required a subjective judgement to be made, as the crack width was basically compared to a series of lines on the card with varying known thickness'. It was thus very difficult to take consistent measurements using this device. Spalls and other forms of crack deterioration were another source of problem in measuring crack widths. Where such deterioration existed, it was difficult to distinguish between the actual crack and the spalling that surrounded it. Another subjective decision thus had to be made to choose where the width would be measured. A third problem in measuring crack widths was that measurements were only taken at the pavement surface. The crack width at the surface is not necessarily indicative of the crack width throughout the depth of the crack. Consideration of the inconsistent and unreliable nature of the crack width measurements was taken into account during data analyses and only general observations were made when using this data.

Cycle 2 – July 1997

Field data was collected from forty-four (44) test sites during the second test cycle. This included fifteen new sites added during this test cycle. One "active" site (Site 10) was not tested during this cycle, as construction was being performed near this test site at the time of testing and an additional traffic closure would have posed traffic flow problems. All transverse cracks identified in Cycle 1 were located and marked on the pavement. In addition, "new" cracks (either cracks that had not been there in Cycle 1 or shrinkage cracks that had developed into more severe cracks between Cycles 1 and 2) were identified and marked, wherever such cracks were found. Cracks to be FWD tested and/or cored were specially marked. All cracks were drawn on the field data sheets.

FWD wheelpath testing for LTE_{δ} computation was performed at the same cracks and joints as were tested during Cycle 1. Note that a few cracks and joints tested in Cycle 1 were not tested in Cycle 2 due to inadequate communication between the FWD technician and the researchers marking the pavement. In addition to the previously tested cracks and joints, testing was also done on some other cracks and joints where it was felt that data on such cracks/joints would be useful.

FWD midslab testing was performed at the same slab locations as were tested in Cycle 1, wherever possible. In some instances, testing could not be performed at the same location because a crack had developed there. In such cases, testing was performed at another slab location if a suitable slab was available. Where no other suitable slabs existed, no testing was done and support and stiffness parametric values were either assumed or copied from another test site and/or test cycle.

Coring was performed at one crack and one joint for some of the sites that had not been cored during Cycle 1. However, coring was not performed on all such test sites that were missing core data, as the coring rig was not available on some testing days. These sites missing data were cored in subsequent test cycles.

Regarding manually measured data, no faulting data was collected during Cycle 2 due to the erred values obtained during the first test cycle. Crack lengths were measured, however, and the spacing between cracks was measured and updated for slabs with "new" cracks. Crack and joint widths were also measured in Cycle 2. Crack widths were again measured using the card method. In an attempt to overcome the subjectivity of the card method, pins were installed at selected cracks (those that were FWD tested for LTE_{δ} computation) in this cycle. These pins, which were installed on either side of a crack in the wheelpath of the pavement, had divots on their top end. The distance between the two pins could be measured by placing the arms of the calipers into these divots. By measuring this distance each test cycle the change in crack width from cycle to cycle could be computed. Actual crack widths could be determined by considering the change in crack width and a card reading that was taken at the time of the first pin reading (reference measurement). Initial pin distances were measured during Cycle 2.

Cycle 3 – October 1997

Data collection was performed at forty (40) test sites during Cycle 3, including the one site (Site 63) that was added during this cycle. Six "active" sites were not tested during this cycle. Sites 16 and 17 were not tested due to the restrictive times that testing was allowed on these sites. Heavy traffic volumes mandated such restrictions. Sites 38,

39, 40, and 41 were not tested during this cycle due to time constraints. All previously identified transverse cracks were again located and marked on the pavement. "New" cracks were identified and marked wherever such cracks were found. Cracks to be FWD tested and/or cored were specially marked. All cracks were drawn on the field data sheets.

Almost all of the cracks and joints that had been previously FWD wheelpath tested for LTE_{δ} computation (in Cycle 1 and/or 2) were again tested during Cycle 3. Inadequate communication between the FWD technician and the researchers did, however, lead to missed testing at some cracks/joints. Testing was done at some cracks and joints that had not been previously tested, where it was felt that data on such cracks/joints would be useful.

In the third test cycle, FWD midslab testing was performed at the same slab locations as were tested in Cycle 2, wherever possible. For sites where "new" cracking prevented testing on such slabs, testing was performed at another slab location if a suitable slab was available. Where no other suitable slabs existed, no testing was done and support and stiffness parametric values were either assumed or copied from another test site and/or test cycle.

In addition to wheelpath and midslab testing, a third type of FWD testing was performed during Cycle 3 – corner testing. This testing was done to provide data for a voids analysis procedure that is described in Chapter V of this thesis. FWD corner testing was performed at corner locations near selected cracks and joints (in the area where the crack/joint and longitudinal lane-shoulder joint intersect). It was done at both visually faulted cracks/joints and at cracks/joint without noticeable faulting (control

tests). This testing involved dropping three loads of varying magnitude (40, 67, and 89 kN) on the leave side of a crack or joint and measuring the consequent pavement deflections directly beneath the load plate. Besides containing a description of the voids analysis procedure, Chapter V also includes a discussion of the results and analysis pertaining to the voids analyses performed in this research.

Coring was performed at one crack and one joint for the sites that had not yet been cored through Cycle 2. Upon completion of coring in this cycle, only site – Site 63 – had not been cored. Site 63 was cored during the fourth test cycle.

Faulting data was not collected in Cycle 3, again due to the erred measurements that the faultmeter was found to provide in Cycle 1. Crack length as well as crack spacing (updated for slabs with "new" cracks) were measured, however. Crack and joint width measurements were also obtained. Crack width was measured using both the card and pin methods. It was found, however, that like the card method, the pin method also leads to unreliable and inconsistent measurements. Inconsistencies were denoted by the measurement of both positive and negative changes in crack width for different cracks within the same test site. Such measurements suggest that some slab fragments are contracting and/or curling upward and some are expanding and/or curling downward. This behavior is contradictory and would certainly not be expected to occur to the extent that the pin measurements indicated. The inconsistent results could probably be attributed to erred pin readings. Such errors are likely the result of looseness between the caliper arms and the pinhead divots into which these arms are placed. This looseness can err the measurements by tenths of millimeters, which is on the same order of magnitude as the changes in crack width being measured. Considering the previously noted

difficulties in measuring crack width along with the inadequacies of both the card and pin methods, it becomes quite clear that there is a need for development of a reliable, consistent method for measuring crack width.

Cycle 4 – June 1998

Field data was collected from forty-six (46) test sites (all "active" sites) during the fourth test cycle. Despite the restrictive times imposed on testing Sites 16 and 17, these sites were tested during Cycle 4 by collecting data at an off-peak time for traffic. All previously identified transverse cracks were identified and marked. "New" cracks were also located and marked, where such cracks existed. Special marking was again applied to cracks that were to be FWD tested and/or cored. All cracks were drawn on the field data sheets.

FWD wheelpath testing was done at all crack and joints that had been tested in Cycles 1, 2, or 3. Inadequate communication between the FWD technician and the researchers again led to a few of these cracks/joints being missed. In addition to the cracks and joints that had been previously tested, testing was also performed at a few other cracks and joints where it was felt that such data would be useful.

FWD midslab testing was not performed during Cycle 4, as it was felt that a sufficient amount of this data had been obtained during the first three cycles. Corner FWD testing was performed, however, during this test cycle. Selected cracks and joints that had not been tested during Cycle 3 were corner tested to provide data for the voids analysis procedure. Note that a few cracks that had been tested in Cycle 3 were also tested during Cycle 4. This was again due to inadequate communication between the

FWD technician and the researchers. The task of coring one crack and one joint per test site was completed during the fourth test cycle. Cores were obtained from Site 63, the only site that had not yet been cored.

Crack length and crack spacing (updated for slabs with "new" cracks) were measured during Cycle 4. Crack and joint widths were also measured in this cycle. Both the card and pin methods were used to measure crack width. Crack and joint faulting were measured again during Cycle 4. Desiring to obtain fault measurements but noting the inconsistent measurements produced with the electronic faultmeter in Cycle 1, it was decided in Cycle 4 to manually measure faulting with a straightedge. Measurements were taken only if a crack or joint had a fault of 2 mm or greater. Cracks and joints that did not have at least 2 mm of faulting were considered to be not faulted. The rationale for this "rule" was that faulting of 1 mm or less could possibly be due to leveling error during construction rather than actual faulting. Requiring at least 2 mm of faulting better ensures that actual faulting exists. Positive fault values were recorded if the leave side was lower than the approach side of the discontinuity.

Visual distress surveys were also taken at each test site during the fourth test cycle. This involved noting such distresses as faulting, spalling, joint sealant problems, and others that existed on the test site pavements. Survey comments were recorded on the field data sheets. These distress surveys were performed for a couple of reasons. One reason for taking these surveys was to provide a visual assessment of crack and joint condition to complement assessments of crack condition obtained through the FWD test procedures that were performed in this study. These surveys were also performed to allow for a cataloging of all visible distresses on the test site pavements. This

information is useful in getting a better perspective on the overall pavement condition of the test sites.

Compilation of Field Data

Manually measured field data collected during Cycles 1 through 4 is compiled in Appendix B of this thesis. Crack and joint width data as well as crack and joint fault data are provided in Tables B.1 through B.4 for carbonate, natural gravel, recycled, and slag pavements, respectively. In these tables and others in this thesis, "C" refers to a crack and "J" refers to a joint under the "Test Type" heading. Data is provided in these tables only for those cracks and joints that were FWD tested for LTE_{δ} computation. Crack width values in these tables were mostly taken from the measurements obtained using the "crack comparator" card. In cases where the card readings gave unreasonable values, crack widths were obtained using the pin measurements (unless these measurements led to even more unreasonable values). It should be noted that although joint width and faulting data are tabulated in this thesis, this data was not considered for analyses purposes. This is because the focus of this research was to investigate crack behavior, not joint behavior. Proper consideration of the joint data would have required additional information (e.g., dowel bar characteristics, etc.) and analysis that is beyond the scope of this study. This joint data (and all other joint data collected in this study) was collected and tabulated because it did not require much additional effort to obtain such data, and it could be used in future research by the sponsoring agency – MDOT.

Information regarding the type of crack (aggregate or mortar) found within each core specimen is given in Tables B.5 through B.8 for carbonate, natural gravel, recycled,

and slag pavements, respectively. The number of existing cracks and average crack spacing for each slab in a test site as well as the joint spacing for the test site are also included in these tables. Note that this crack count and spacing data reflects the data updated through Cycle 4 (i.e., it includes all "new" cracks located through Cycle 4).

The information recorded during the visual distress surveys performed during Cycle 4 is compiled in Tables B.9 through B.12 for the four types of pavements, respectively. In these tables, the nomenclature "CX of SY" refers to crack [number X] of slab [number Y] in the test site. The numbering here considers all cracks in a slab, not just those FWD tested for LTE_{δ} computation. "JX" in these tables corresponds to joint [number X] in the test site. Descriptions and more information concerning all distresses listed in these tables (except for exposed reinforcement, shrinkage cracking, and alkali-silica reactivity (ASR)) can be found in [54]. The noted exceptions are not specifically defined distresses. Exposed reinforcement refers to pavements where the steel reinforcement has risen above the pavement surface. Shrinkage cracking was defined and described in detail in Chapter II of this thesis. It can be a precursor to transverse cracking. Pavements with ASR are denoted by the presence of map-like cracking. Information relating to ASR can be found in [55].

- CHAPTER V -

Results and Discussion I - FWD Analysis Procedures

OVERVIEW

This chapter contains results and discussion pertaining to the various analyses performed in this study using FWD data. Three FWD analysis procedures - backcalculation of pavement support and stiffness parameters, determination of crack performance parameters, and assessment of void potential near cracks – were demonstrated using field data from this study. The latter two procedures can be useful to transportation agencies in determining when and how to repair JCP's with transverse cracking. The backcalculation procedure is also useful, as it allows for determination of support and stiffness parameters that are inputs in the procedure for determining crack performance parameters. An overview of the work performed in this research relating to these analysis procedures is given in the following paragraphs. Results and discussion concerning such work are explained in more detail in subsequent sections of this chapter.

FWD midslab data from this study was used to backcalculate the deflection basin area (AREA), the radius of relative stiffness (ℓ), the concrete modulus of elasticity (E), and the modulus of subgrade reaction (k) of the test site pavements. The procedure that was used to backcalculate these support and stiffness parameters is described in the next section of this chapter. A discussion of the reasonableness of the values obtained through use of this procedure in this research is also provided in the next section.

Several crack performance parameters were determined for selected cracks and joints in the test site pavements using FWD wheelpath data. These parameters, which

characterize the integrity of transverse cracks, included deflection load transfer efficiency (LTE_δ), transferred load efficiency (TLE), the total load transferred across a discontinuity (P_T), and aggregate interlock shear stiffness per unit length of a discontinuity (AGG) [28]. A "standard" procedure for determining these parameters, which is described later in this chapter, was used for computation of parametric values in this study.

Recognizing the practical limitations of this cumbersome procedure for use by a transportation agency, a somewhat simpler, streamlined approach to computing the performance parameters was developed in this research. This streamlined approach, which is also described later in this chapter, provides a more direct method for quickly computing these parameters based on FWD deflection data. Computation of the crack performance parameters can be useful to a transportation agency, as comparison of parametric values to established threshold limits allows for an evaluation of the condition of transverse cracks. Such evaluations can help an agency in planning and selecting rehabilitation activities for cracked JCP's. Threshold limits for the performance parameters were developed in this study using the field data. A discussion concerning the development of these thresholds is provided later in this chapter. Data from this study was also used to determine the effect of temperature on the performance parameters. Discussion related to the findings concerning temperature effects is also contained in this chapter.

A voids analysis procedure was performed at selected cracks and joints in the test site pavements using FWD corner data. This procedure can be used by a transportation agency to determine the likelihood of loss of support at cracks and joints. By identifying areas of loss of support, this procedure allows appropriate rehabilitation actions to be

taken to restore support to a cracked JCP. The voids analysis procedure is described later in this chapter. Results from the voids analyses performed in this research were used to determine appropriate threshold limits for evaluating void potential using this procedure. A discussion concerning the determination of these thresholds is provided later in this chapter.

BACKCALCULATION OF SUPPORT AND STIFFNESS PARAMETERS

Overview

A backcalculation procedure for determining various pavement support and stiffness parameters, based on FWD data, was demonstrated using field data from this research. In Cycles 1 through 3 of this study, FWD midslab data was used to backcalculate the deflection basin area, radius of relative stiffness, concrete modulus of elasticity, and modulus of subgrade reaction of each of the test site pavements. Determination of these parameters allowed for subsequent calculation of the crack performance parameters AGG, TLE, and P_T for selected cracks and joints in this study. Besides allowing for calculation of the crack performance parameters, determination of these parameters also provides information regarding the support and stiffness characteristics of pavements.

An explanation of the backcalculation procedure that was used to compute AREA, ℓ, E, and k values in this research is given later in this section. An illustrative example, using actual data from this study, is also provided later in this section to demonstrate the use of this procedure in determining parametric values. A discussion of the backcalculated values obtained in this study concludes this section. Backcalculated

AREA and ℓ values for Cycles 1 through 3 can be found in Tables B.13 through B.16 of Appendix B for carbonate, natural gravel, recycled, and slag pavements. Backcalculated E and k values for these four pavement types are located in Tables B.17 through B.20, respectively.

Before moving on to a description of the backcalculation procedure, it should first be noted that some of the values in Tables B.13 through B.20 were either assumed or copied from another test site and/or test cycle. Values obtained in such ways are indicated in the tables. Assumed or copied values had to be used in some cases due to one of the following reasons: 1) no midslab data could be collected at a test site during a particular test cycle due to lack of a suitable slab for testing, or 2) backcalculation using the data taken during that test cycle led to unreasonable results. In such circumstances, it was initially attempted to copy parametric values either from those computed for a nearby test site or from values computed during another test cycle for the test site in need of data. If values could not be obtained using either of these methods, reasonable values for AREA, ℓ, E, and k were assumed.

Backcalculation Procedure

The backcalculation procedure that was used to determine values for AREA, ℓ, E, and k in this study is described below. It should be noted that some of the equations used in this procedure are regression equations that were developed using Inch-Pound units. In order to allow the use of SI units in such equations and to produce results in SI units, it was necessary to insert conversion factors into some of the equations. This explains the

presence of the number "25.4," which was used to convert between inches and millimeters, in these modified equations.

The first parameter that needs to be calculated in the backcalculation procedure is AREA. This parameter is defined as the cross-sectional area of the deflection basin between the center of the FWD load plate and the outermost deflection sensor, normalized with respect to the maximum deflection (i.e., deflection at the sensor directly below the center of the load plate, δ_0) [56]. Due to this normalization, AREA has units of length rather than area. It is computed by using deflection data measured at sensors located at various radial distances "r" (0, 203, 305, 457, 610, 914, and 1524 mm) from the center of the FWD load plate. These deflections result from the application of a 40 kN load at a midslab location. Equation (9), modified from [56], is used to calculate this parameter:

$$\mathbf{AREA} = \mathbf{25.4}\left[\begin{array}{l} 4 + 6\left(\frac{\delta_{203}}{\delta_0}\right) + 5\left(\frac{\delta_{305}}{\delta_0}\right) + 6\left(\frac{\delta_{457}}{\delta_0}\right) + \\ 9\left(\frac{\delta_{610}}{\delta_0}\right) + 18\left(\frac{\delta_{914}}{\delta_0}\right) + 12\left(\frac{\delta_{1524}}{\delta_0}\right) \end{array}\right] \quad (9)$$

where:

AREA = deflection basin area, mm
δ_r = deflection of the r^{th} sensor, μm.

Once AREA has been computed, the next parameter to be backcalculated is the radius of relative stiffness. This parameter characterizes the stiffness of the

slab-foundation system [56]. Equation (10), a modification of a regression equation in [57], is used to compute ℓ:

$$\ell = 25.4\left[\ln\left\{\frac{\left(60 - \frac{AREA}{25.4}\right)}{289.708}\right\}/(-0.698)\right]^{2.566} \quad (10)$$

where:

ℓ	=	radius of relative stiffness, mm
AREA	=	deflection basin area, mm.

It should be noted that equation (10) is only valid if the load radius is equal to 150 mm [56]. Most FWD load plates, including the one used in this study, satisfy this requirement.

The next step in the backcalculation procedure is to compute the concrete modulus of elasticity. The procedure for calculating this parameter involves first computing an elastic modulus value, E_c, for each of the FWD sensors, based on the deflection data measured at each of those sensors. These values are computed using equation (11) from [56]:

$$E_c = \frac{12(1-\nu^2)P\ell^2\delta_r^*}{\delta_r h^3} \quad (11)$$

where:

E_c	=	concrete modulus of elasticity based on δ_r, kPa
ν	=	Poisson's ratio for concrete
P	=	applied load, kN
ℓ	=	radius of relative stiffness, m
δ_r	=	deflection of the r^{th} sensor, m
h	=	concrete slab thickness, m
δ_r^*	=	nondimensional deflection coefficient at radial distance "r," defined by equation (12), which is modified from [56]:

$$\delta_r^* = ae^{\left|-be^{\left(\frac{-c\ell}{25.4}\right)}\right|} \qquad (12)$$

where:

a,b,c	=	regression coefficients from [56] (see Table 1)
ℓ	=	radius of relative stiffness, mm.

Note that equation (12) is a regression equation and, as can be seen in Table 1, the regression coefficients for this equation differ for each of the sensor locations. As can be seen from equations (11) and (12), it is necessary to first compute the value of δ_r^* for each sensor location, and then use these values in equation (11) to obtain E_c values based on deflection data measured at each of the sensors. In equation (11), δ_r^* accounts for the dependence of pavement deflection on the distance from the load (i.e., pavement deflection decreases with increasing distance from the load).

Each E_c value represents the estimated value of the concrete modulus of elasticity, a material property of the concrete, based on the pavement deflection (δ_r) measured at a particular sensor location "r." Theoretically, all of these E_c values should be equal, since

Table 1 Regression Coefficients for δ_r^*. (After Smith et al. [56].)

Radial Distance, r (mm)	a	b	c
0	0.12450	0.14707	0.07565
203	0.12323	0.46911	0.07209
305	0.12188	0.79432	0.07074
457	0.11933	1.38363	0.06909
610	0.11634	2.06115	0.06775
914	0.10960	3.62187	0.06568
1524	0.09521	7.41241	0.06255

they are all estimates of the same material property – concrete modulus of elasticity. Identical values are not obtained at all sensors, however, because the δ_r^*'s are computed using regression equations and thus have some error associated with them. This error in the δ_r^* values translates to error in the E_c values. Although identical E_c values are not obtained for all sensors, it is found that these values usually vary only slightly from one another. The E_c values computed in Illustrative Example 1, which can be found later in this section, illustrate this point. Very close values were found for the E_c's computed at the various sensor locations in this example.

After E_c values have been computed using data from each of the sensor locations, the backcalculated concrete modulus of elasticity value for the pavement can be determined. The concrete modulus of elasticity, E, is simply computed as the average of all E_c's. [56]

The final step in the backcalculation procedure is to compute the modulus of subgrade reaction. This parameter characterizes the stiffness of the foundation in the pavement system. It is calculated using equation (13) from [10]:

$$k = \frac{Eh^3}{12(1-\nu^2)\ell^4} \qquad (13)$$

where:

k	=	modulus of subgrade reaction, kPa/mm
E	=	concrete modulus of elasticity, kPa
h	=	concrete slab thickness, mm
ν	=	Poisson's ratio for concrete
ℓ	=	radius of relative stiffness, mm.

An example demonstrating the use of the above procedure in determining values for AREA, ℓ, E, and k for two test sites in this study is given below.

Illustrative Example 1

FWD midslab testing at Sites 38A and 50 during the third test cycle yielded the following data:

Site 38A:

δ_0 = 83.67 μm	δ_{203} = 80.00 μm	δ_{305} = 75.00 μm	δ_{457} = 72.00 μm
δ_{610} = 64.33 μm	δ_{914} = 54.00 μm	δ_{1524} = 36.67 μm	

Site 50:

δ_0 = 90.67 μm	δ_{203} = 86.67 μm	δ_{305} = 83.67 μm	δ_{457} = 80.00 μm
δ_{610} = 73.67 μm	δ_{914} = 66.33 μm	δ_{1524} = 52.00 μm	

Note that these deflection values are the average of three measurements taken during three consecutive tests. Multiple tests were done for data quality control purposes. Other information required for the backcalculation procedure is given as follows:

Site 38A:	Site 50:
h = 241 mm (Site 38A slab thickness)	h = 305 mm (Site 50 slab thickness)
P = 40 kN (FWD applied load)	P = 40 kN (FWD applied load)
ν = 0.15 (assumed Poisson's ratio)	ν = 0.15 (assumed Poisson's ratio)

Using the above data and equation (9), the deflection basin areas for the two sites were first determined:

Site 38A:

$$\text{AREA} = 25.4\left[\begin{array}{l} 4 + 6\left(\frac{80.00\ \mu m}{83.67\ \mu m}\right) + 5\left(\frac{75.00\ \mu m}{83.67\ \mu m}\right) + 6\left(\frac{72.00\ \mu m}{83.67\ \mu m}\right) + \\ 9\left(\frac{64.33\ \mu m}{83.67\ \mu m}\right) + 18\left(\frac{54.00\ \mu m}{83.67\ \mu m}\right) + 12\left(\frac{36.67\ \mu m}{83.67\ \mu m}\right) \end{array}\right] = 1097\ \text{mm}$$

Site 50:

$$\text{AREA} = 25.4\left[\begin{array}{l} 4 + 6\left(\frac{86.67\ \mu m}{90.67\ \mu m}\right) + 5\left(\frac{83.67\ \mu m}{90.67\ \mu m}\right) + 6\left(\frac{80.00\ \mu m}{90.67\ \mu m}\right) + \\ 9\left(\frac{73.67\ \mu m}{90.67\ \mu m}\right) + 18\left(\frac{66.33\ \mu m}{90.67\ \mu m}\right) + 12\left(\frac{52.00\ \mu m}{90.57\ \mu m}\right) \end{array}\right] = 1194\ \text{mm}$$

Next, equation (10) was used to compute the radius of relative stiffness for the two sites:

Site 38A:

$$\ell = 25.4\left[\ln\left\{\frac{\left(60 - \frac{1097\ \text{mm}}{25.4}\right)}{289.708}\right\} / (-0.698)\right]^{2.566} = 936\ \text{mm}$$

Site 50:

$$\ell = 25.4\left[\ln\left\{\frac{\left(60-\frac{1194\text{ mm}}{25.4}\right)}{289.708}\right\}/(-0.698)\right]^{2.566} = 1170\text{ mm}$$

The third parameter computed was the concrete modulus of elasticity. To determine this parameter, E_c and δ_r^* values were first computed for each of the sensor locations. A sample calculation is given below for both Sites 38A and 50 to demonstrate the procedure used to determine these values. At sensor location r = 610 mm, δ_{610}^* was calculated for Site 38A using equation (11):

$$\delta_{610}^* = 0.11634e^{\left[-2.06115e^{\left(\frac{(-0.06775)(936\text{ mm})}{25.4}\right)}\right]} = 0.09818$$

In the above equation, a = 0.11634, b = 2.06115, and c = 0.06775 (corresponding to r = 610 mm) were obtained from Table 1. $E_{c,610}$ was then computed for Site 38A using equation (12):

$$E_{c,610} = \frac{12(1-0.15^2)(40\text{ kN})(0.936\text{ m})^2(0.09818)}{(64.33\times10^{-6}\text{ m})(0.241\text{ m})^3} = 4.48\times10^7\text{ kPa}$$

Values for δ_{610}^* and $E_{c,610}$ were similarly computed for Site 50:

$$\delta_{610}^{*} = 0.11634e^{[-2.06115e^{\left(\frac{(-0.06775)(1170\text{ mm})}{25.4}\right)}]} = 0.10623$$

$$E_{c,610} = \frac{12(1-0.15^2)(40\text{ kN})(1.170\text{ m})^2(0.10623)}{(73.67\times10^{-6}\text{ m})(0.305\text{ m})^3} = 3.26\times10^{7}\text{ kPa}$$

E_c values for the two sites were computed in the same manner for the other six sensors. These values are reported below:

Site 38A:

$E_{c,0} = 4.33 \times 10^7$ kPa $E_{c,203} = 4.38 \times 10^7$ kPa $E_{c,305} = 4.50 \times 10^7$ kPa

$E_{c,457} = 4.37 \times 10^7$ kPa $E_{c,914} = 4.32 \times 10^7$ kPa $E_{c,1524} = 3.64 \times 10^7$ kPa

Site 50:

$E_{c,0} = 3.09 \times 10^7$ kPa $E_{c,203} = 3.16 \times 10^7$ kPa $E_{c,305} = 3.20 \times 10^7$ kPa

$E_{c,457} = 3.19 \times 10^7$ kPa $E_{c,914} = 3.14 \times 10^7$ kPa $E_{c,1524} = 2.74 \times 10^7$ kPa

The seven E_c values for each site, including $E_{c,610}$, were then averaged to determine the concrete modulus of elasticity. Averaging the E_c values yielded concrete modulus of elasticity values of 4.28×10^7 kPa and 3.12×10^7 kPa for Sites 38A and 50, respectively.

The final parameter determined was the modulus of subgrade reaction. It was computed using equation (13). Values for Sites 38A and 50 were thus computed as follows:

Site 38A

$$k = \frac{(4.28 \times 10^7 \text{ kPa})(241 \text{ mm})^3}{12(1-0.15^2)(936 \text{ mm})^4} = 66.3 \text{ kPa / mm}$$

Site 50:

$$k = \frac{(3.12 \times 10^7 \text{ kPa})(305 \text{ mm})^3}{12(1-0.15^2)(1170 \text{ mm})^4} = 40.2 \text{ kPa / mm}$$

Discussion of Backcalculation Results

The backcalculated values obtained for AREA, ℓ, E, and k in Illustrative Example 1 are very reasonable. This was generally found to be true for all of the results obtained from using the backcalculation procedure in this study. AREA values were generally found to range from 1050 to 1250 mm, while ℓ values ranged from 900 to 1300 mm. E values generally ranged from 3.0×10^7 kPa to 6.5×10^7 kPa, while k values ranged from 25 to 85 kPa/mm. All of these ranges are in fair agreement with values typically associated with these four parameters.

In the few cases where the backcalculation procedure yielded values significantly outside the noted ranges, it was usually found that the pavement was actually a concrete overlay. Extremely high E and k values were computed in these cases. Overlays cause erred E and k values when using this backcalculation procedure because of the presence of the old pavement layer beneath the overlay. This old asphalt or concrete layer beneath the overlay essentially acts as a stiff base support layer. Due to the stiffness of this "base" layer, very small deflections result when the FWD applies a load to an overlay

pavement. These small deflections translate to exaggerated E and k values, as was found for the overlay sites in this research. To obtain reasonable values for such pavements in this study, values for the support and stiffness parameters were either assumed or copied from another nearby test site and/or test cycle. The fact that this backcalculation procedure produces extreme values when an anomaly such as an overlay is present could actually be viewed as a beneficial aspect of the procedure. The extreme values encountered in such situations can serve as a warning that there is something unusual about the pavement.

CHARACTERIZATION OF CRACK PERFORMANCE

Overview

There are several parameters that can be used to characterize and quantify the performance of transverse cracks in JCP's. Four such performance parameters, LTE_{δ}, TLE, P_T, and AGG, were considered in this research. These parameters, which can be computed based on FWD data, were introduced in Chapter II of this thesis. They are explained in more detail later in this section. These parameters can be used to evaluate the condition of transverse cracks in a pavement network by comparing parametric values with threshold limits. When integrated into a comprehensive pavement evaluation scheme, these evaluations can act as a useful tool in planning and selecting rehabilitation activities for the pavement network. Load transfer restoration and full-depth patch repair, which are both described in detail in Chapter III, are two such rehabilitation alternatives that can be used to improve the integrity of cracked JCP's by restoring load transfer at cracks in these pavements.

Field data from this study was used to demonstrate a procedure for determining values for the four crack performance parameters noted above. In Cycles 1 through 4 of this study, LTE_{δ}, TLE, P_T, and AGG values were computed for selected cracks and joints in the test site pavements using FWD wheelpath data and a "standard" procedure for determining parametric values. A more detailed description of this procedure is provided later in this section. After careful consideration of this procedure, it was recognized that potential limitations (namely, its cumbersome nature) may exist for its everyday use by a transportation agency. To rectify this problem, a somewhat simpler, more direct approach to computing the performance parameters was developed in this research. This simplified approach, which is also described later in this section, is a streamlined version of the original and provides a more user-friendly method for practical everyday use by a transportation agency. An illustrative example, also included in this section, demonstrates the use of each of these two procedures in computing the performance parameters. In this example, both procedures utilize the same FWD deflection data from two test sites in this study to determine parametric values. This allows for a comparison of the values obtained using each method.

In addition to demonstrating methods for determining parametric values, field data from this study was also used to develop threshold limits for the performance parameters. A discussion on the development of these thresholds, which can be used to evaluate crack condition, is included later this section. An analysis of the effect of pavement surface temperature on the performance parameters, specifically LTE_{δ}, was also performed using the field data from this research. Discussion pertaining to the findings regarding such temperature effects concludes this section.

Determination of Crack Performance Parameters

"Standard" Procedure

The "standard" procedure for determining LTE_{δ}, TLE, P_T, and AGG is described below. This method was used to compute the performance parameters at selected cracks and joints in this study.

The first step in this procedure is to calculate LTE_{δ}. This parameter measures the extent to which load is transferred across a crack in terms of the deflections on either side of the crack under an applied load. As explained in Chapter II, an LTE_{δ} of 100% represents the ideal condition, indicating that the load is being equally shared by both sides of the crack. LTE_{δ} is directly computed by inputting FWD wheelpath data for a crack or joint (as discussed in Chapter IV) into equation (5). LTE_{δ} values computed for the cracks and joints in this study for Cycles 1 through 4 are compiled in Tables B.21 through B.24 of Appendix B for carbonate, natural gravel, recycled, and slag pavements, respectively. In these tables, LTE_{δ} values are given both for tests performed before and after the crack/joint. Note that the cracks and joints in these tables correspond with those cracks and joints listed in Tables B.1 through B.4. Also note that joint data in Tables B.21 through B.24, like that in Tables B.1 through B.4, was not considered for analysis purposes in this research, as consideration of this data was beyond the scope of this study.

Once LTE_{δ} values have been computed, the next step is to determine TLE values. Contrary to deflection load transfer efficiency, transferred load efficiency is a derived parameter that quantifies load transfer in terms of load itself. TLE expresses the actual percentage of the applied load that is transferred across a crack. A TLE of 50% represents the ideal case, indicating that half of the load is transferred across the crack.

To determine this parameter, a plot developed by Ioannides and Korovesis, relating LTE_δ to TLE in terms of the radius of the loaded area (a) and radius of relative stiffness (ℓ), is used. This plot is shown in Figure 7. In order to obtain TLE from LTE_δ using this plot, values for a and ℓ must first be determined. The radius of the loaded area is simply equal to the radius of the FWD load plate, 150 mm. The radius of relative stiffness can either be assumed, based on cross-section information and engineering judgement, or backcalculated using the procedure described in the previous section. Once these two parameters are determined, the a/ℓ ratio is then computed. Knowing a/ℓ and the LTE_δ for a given crack, TLE can be determined by using the curves in Figure 7. Since the actual a/ℓ ratio will most likely not be equal to one of the three values (a/ℓ = 0.047, 0.156, and 0.312) for which there are curves, some interpolation between curves will usually be needed. Thus, to determine TLE, extend a vertical line, starting from the x-axis at the value of LTE_δ for the crack, upward through the three curves. The three points of intersection of this line and the curves are the TLE values corresponding to the respective a/ℓ ratios. The a/ℓ ratio for the pavement in question will fall in between two of the three noted ratios. To find the TLE of the crack in question, interpolate between the two TLE values corresponding to these two a/ℓ ratios. [28]

The TLE values computed for the cracks and joints in this study for all four test cycles are given in Tables B.25 through B.28 for the four pavement types, respectively. The cracks and joints in these tables correspond with those in Tables B.21 through B.24. TLE values in this study were computed based on ℓ values backcalculated from FWD midslab data. To determine TLE values in the fourth test cycle, when no midslab testing

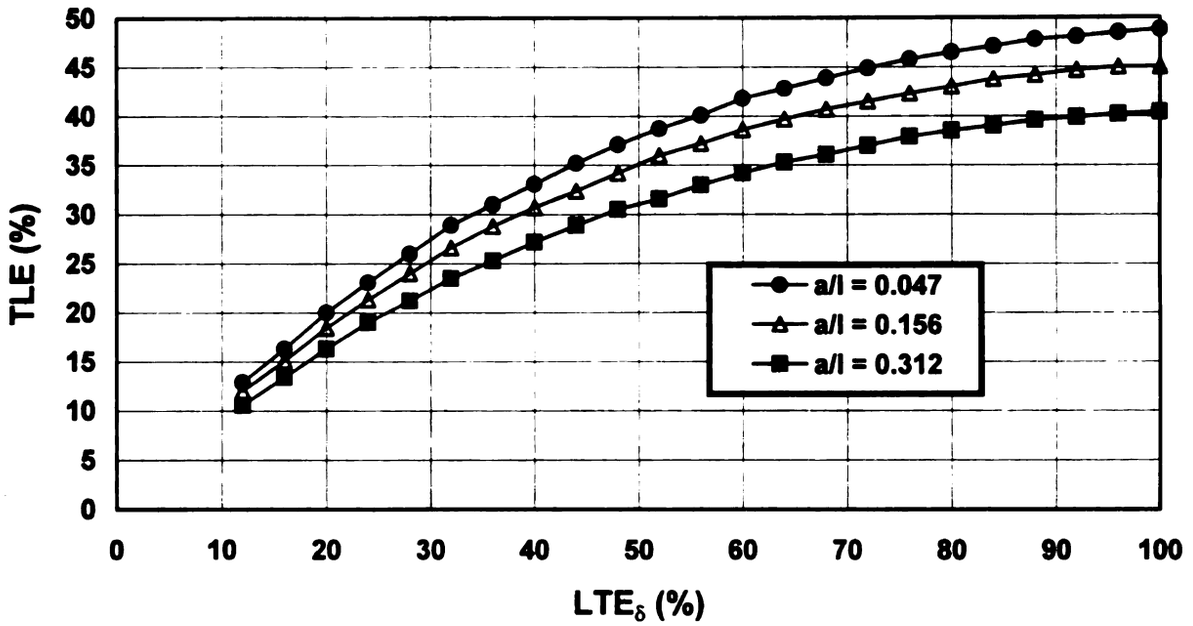

Figure 7 **Relationship between LTE_δ and TLE. (After Ioannides and Korovesis [28].)**

was done, ℓ values had to be taken from values determined in previous test cycles. Thus,for each site, the ℓ value for the most recent test cycle that had such data was used to compute TLE values in Cycle 4.

The third parameter to be computed in this procedure is P_T. This parameter estimates the total amount of load transferred from the loaded to the unloaded side of a crack along its entire length. It is directly derived from TLE using equation (14) from [28]:

$$\mathbf{P_T = \frac{TLE}{100\%} \times P} \qquad \textbf{(14)}$$

where:

P_T	=	total load transferred across crack, kN
TLE	=	transferred load efficiency, %
P	=	applied load, kN.

P_T provides a quantitative sense of the amount of load that is transferred across a crack when a specified load is applied to one side. Ideally, for a 40 kN applied load, P_T would be equal to 20 kN, as half of the load would be transferred across the crack. [28]

Note that TLE and P_T provide the same information regarding characterization of crack performance, only in different forms. It would thus be redundant to use both of these parameters to evaluate cracks. It is suggested that P_T be used rather than TLE, as it has a more physical meaning than its counterpart. Nevertheless, TLE must be computed in this procedure to allow for computation of P_T. [28]

Tables B.29 through B.32 contain the P_T values computed for the cracks and joints in this study. These tables provide values for the four test cycles. The cracks and joints in these tables correspond with those in Tables B.21 through B.24. Note that P_T values computed at joint locations were not considered for analysis purposes in this research, as such consideration would have been beyond the scope of this study.

AGG is the final parameter that is determined in this procedure. This parameter characterizes the shear stiffness per unit length of a crack provided by aggregate interlock. A large AGG value indicates that the crack is relatively stiff and has good potential for aggregate interlock load transfer. To determine AGG in this procedure, a plot developed by Ioannides and Korovesis, relating LTE_δ to AGG/kℓ, is used. This plot is shown in Figure 8. Knowing the LTE_δ of a crack, a value for AGG/kℓ can be determined using the curve in this plot. To determine AGG, values for ℓ and k must next be found. These values can either be assumed, based on cross-section information and engineering judgement, or backcalculated using the procedure described in the previous section. Once AGG/kℓ, ℓ, and k are known, AGG can be determined using simple multiplication. [28]

The AGG values computed for the cracks and joints in this study are catalogued in Tables B.33 through B.36. These tables provide values for the four test cycles. The cracks and joints in these tables correspond with those in Tables B.21 through B.24. Backcalculated k and ℓ values were used to determine AGG values in this research. To determine AGG values in the fourth test cycle, k and ℓ values were taken from values determined in previous test cycles. Thus, for each site, the k and ℓ values for the most recent test cycle that had such data were used to compute AGG values in Cycle 4. Note

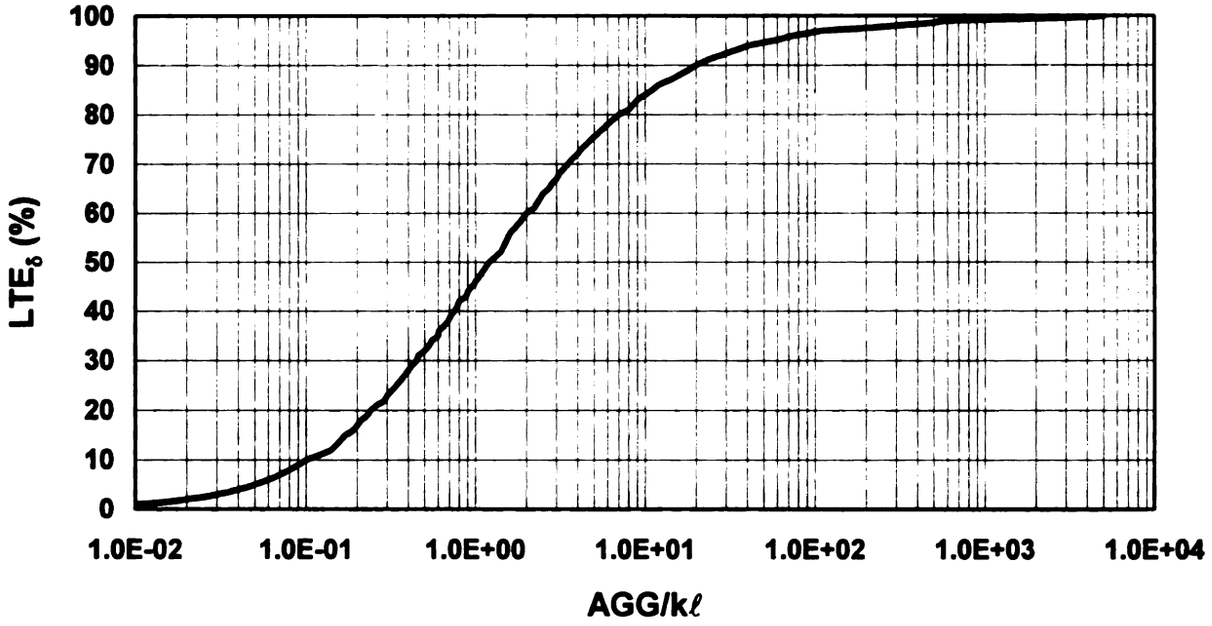

Figure 8 **Relationship between LTE_δ and AGG/kℓ. (After Ioannides and Korovesis [28].)**

that the AGG values computed in this research were not considered for analysis purposes, as such consideration would have been beyond the scope of this study.

In practice, once LTE_{δ}, P_T, and AGG values (TLE values are redundant, as explained earlier) have been obtained at crack locations, the condition of these cracks can be evaluated by comparing the parametric values with established threshold limits. Such evaluations can be useful in deciding when and how to rehabilitate cracked JCP's. The development of threshold values for LTE_{δ}, P_T, and AGG, based on field data from this study, is explained later in this section.

Streamlined Approach

After considering the feasibility of implementing the "standard" procedure for determining crack performance parameters into a transportation agency's pavement evaluation scheme, it was realized that a quicker, more efficient method would be desirable. Use of the "standard" procedure could prove to be quite time-consuming in evaluating the condition of the many transverse cracks found in a typical pavement network. A more efficient approach to determining the performance parameters was thus developed in this project. This simplified procedure is essentially a streamlined version of the "standard" procedure.

In this method, the procedure for determining LTE_{δ} remains exactly the same as that used in the "standard" procedure. That is, LTE_{δ} values are computed based on deflection data obtained from FWD wheelpath testing. However, the procedure for determining P_T and AGG (note that TLE is not computed in this method due to its redundancy) in this method is different. These two parameters are determined by using

direct relationships between LTE_δ and P_T and LTE_δ and AGG. Such relationships are established in the form of a series of LTE_δ versus P_T plots for a range of ℓ values and LTE_δ versus AGG plots for various combinations of k and ℓ.

In order to use this procedure, an initial effort must be undertaken by the transportation agency to develop this series of plots. A sufficient number of k and ℓ values and combinations should be chosen to cover the range of values normally encountered for these parameters (e.g., k: 25-85 kPa/mm and ℓ: 900-1300 mm, as found in this study). For each ℓ value, a plot of LTE_δ versus P_T can be developed for a range of LTE_δ values. This involves first determining TLE values for this range of LTE_δ's using Figure 7 and the method described in the "standard" procedure above, noting that a is a constant equal to the radius of the FWD load plate and ℓ is the value being considered for that plot. These TLE values can then be transformed into P_T values using equation (14), noting the magnitude of load that is generally used for deflection testing. The P_T values can then be plotted against the range of LTE_δ values considered. This process is repeated for each of the ℓ values to develop all of the necessary LTE_δ versus P_T plots.

LTE_δ versus AGG plots must be developed for each k and ℓ combination considered. This involves computing AGG values for a range of LTE_δ's using Figure 8 and the method described in the "standard" procedure above, noting that k and ℓ correspond to the combination being considered for that plot. The AGG values obtained can then be plotted versus LTE_δ for the range of values considered. This process is repeated for each of the k and ℓ combinations to develop all of the necessary LTE_δ versus AGG plots.

Once this initial effort has been completed and LTE_δ versus P_T and LTE_δ versus AGG plots have been developed for all k and ℓ values and combinations to be considered, the process of determining the performance parameters becomes straightforward. First, field deflection data is collected at crack locations, and LTE_δ values are computed using equation (5). P_T and AGG values are then determined by considering the appropriate LTE_δ-P_T and LTE_δ-AGG plots for the pavement in question. These plots correspond to specific ℓ values and k and ℓ combinations, respectively. To select the appropriate plots, the k and ℓ values for the pavement can be backcalculated using the procedure described in the previous section of this chapter. If such backcalculation is performed, the LTE_δ-P_T plot corresponding to the ℓ value closest in magnitude to the backcalculated value should be chosen. Likewise, the LTE_δ-AGG plot corresponding to the k and ℓ combination that best matches the k and ℓ values backcalculated for the pavement should be chosen. Alternatively, if it is not desired to perform backcalculation, LTE_δ-P_T and LTE_δ-AGG plots can be selected by using pavement cross-section information and engineering judgement to choose the most appropriate ℓ value and k and ℓ combination for the pavement from among the values and combinations for which plots are available. Once the appropriate plots have been selected for the pavement, P_T and AGG values can then be determined for the cracks based on the computed LTE_δ values and the selected LTE_δ-P_T and LTE_δ-AGG plots. Like the "standard" procedure, the LTE_δ, P_T, and AGG values obtained from this simplified procedure can be compared to threshold limits to evaluate the condition of the cracks. These evaluations can then be used to help in deciding when and how to rehabilitate cracked JCP's in the pavement network.

Although this streamlined approach requires an initial investment of time in developing the series of LTE_δ versus P_T and LTE_δ versus AGG plots, the ease of use and time saved in determining the performance parameters with this method provide ample compensation in the long-term. An example, using data from two of the test sites in this study, is given below to illustrate the use of this approach as well as that of the "standard" procedure.

Illustrative Example 2

FWD wheelpath testing on cracks at Sites 38A and 50 during the third test cycle yielded the following data:

Site 38A:

Crack 1: $\delta_{U1} = 118.67$ μm $\delta_{L1} = 121.67$ μm

Crack 2: $\delta_{U2} = 111.67$ μm $\delta_{L2} = 134.33$ μm

Site 50:

Crack 1: $\delta_{U1} = 69.67$ μm $\delta_{L1} = 282.67$ μm

Crack 2: $\delta_{U2} = 108.67$ μm $\delta_{L2} = 115.33$ μm

Note that these deflection values are the average of three measurements taken during three consecutive tests. Multiple tests were done for data quality control purposes. All deflections are taken from tests performed before the crack.

Other pertinent information related to this FWD testing is given as follows:

a = 150 mm (radius of FWD load plate)

P = 40 kN (FWD applied load)

In addition to the information given above, values for k and ℓ were also needed to compute the performance parameters. In this study, k and ℓ values were obtained using the backcalculation procedure described earlier in this chapter. Backcalculation of k and ℓ using data collected at Sites 38A and 50 during Cycle 3 was demonstrated in Illustrative Example 1. The results are repeated here for convenience:

Site 38A: k = 66.3 kPa/mm ℓ = 936 mm

Site 50: k = 40.2 kPa/mm ℓ = 1170 mm

All of the information required to determine the performance parameters for the noted cracks has now been given. The use of the two previously described procedures for determining performance parametric values is demonstrated below.

"Standard" Procedure

Using the "standard" procedure, the first step was to compute LTE_δ values for the cracks using equation (5):

Site 38A:

$$LTE_{\delta 1,38A} = \frac{118.67\ \mu m}{121.67\ \mu m} \times 100\% = 97.53\%$$

$$LTE_{\delta 2,38A} = \frac{111.67\ \mu m}{134.33\ \mu m} \times 100\% = 83.13\%$$

Site 50:

$$LTE_{\delta 1,50} = \frac{69.67\ \mu m}{282.67\ \mu m} \times 100\% = 24.65\%$$

$$LTE_{\delta 2,50} = \frac{108.67\ \mu m}{115.33\ \mu m} \times 100\% = 94.22\%$$

Having determined the LTE_δ values, TLE was the next parameter considered. TLE values were determined using Figure 7 and the respective LTE_δ values. In order to use this figure, the a/ℓ ratios for the two sites had to first be determined:

Site 38A: $a / \ell = \frac{150\ mm}{936\ mm} = 0.160$ Site 50: $a / \ell = \frac{150\ mm}{1170\ mm} = 0.128$

Since these values did not match any of the three a/ℓ ratios (0.047, 0.156, and 0.312) in Figure 7, TLE values had to be interpolated. Thus, using the plot in Figure 7, TLE values corresponding to the three noted a/ℓ ratios were found for each LTE_δ value for the two sites by drawing vertical lines from the x-axis through the three curves. These vertical lines are drawn on the LTE_δ-TLE plot in Figure 9. The points of intersection of the vertical lines with the three curves are the TLE values for each of the three a/ℓ ratios. The values thus obtained were:

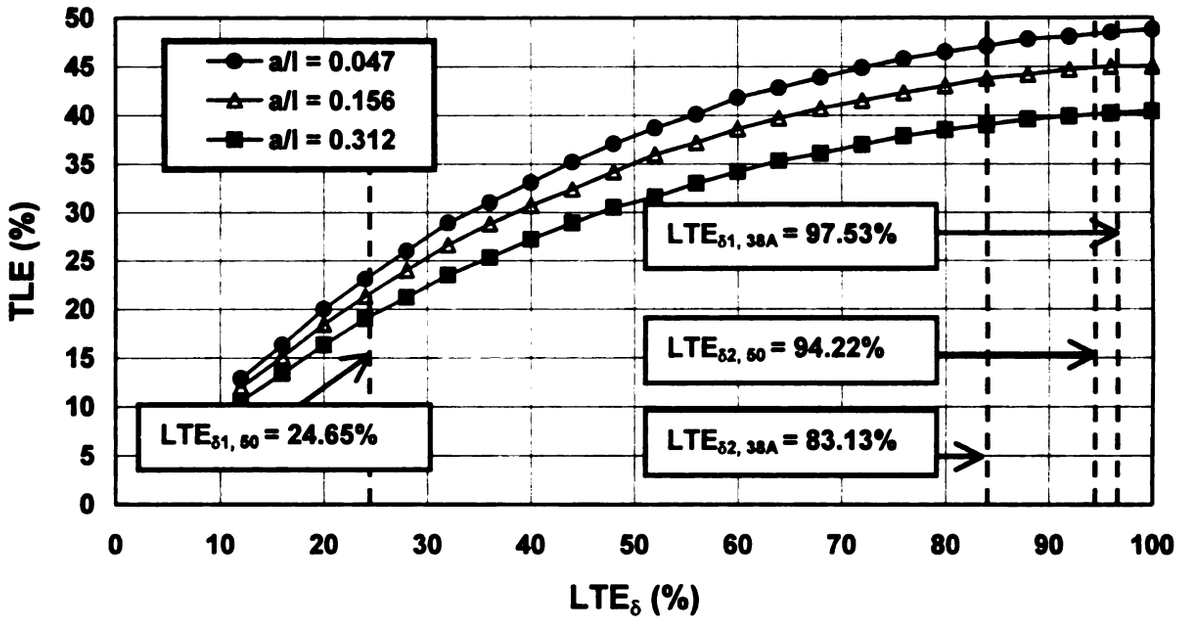

Figure 9 Determination of TLE Using "Standard" Procedure.

Site 38A:

For $LTE_{\delta 1,\ 38A} = 97.53\%$:

$TLE_{a/\ell\ =\ 0.047} = 48.6\%$ $TLE_{a/\ell\ =\ 0.156} = 45.0\%$ $TLE_{a/\ell\ =\ 0.312} = 40.3\%$

For $LTE_{\delta 2,\ 38A} = 83.13\%$:

$TLE_{a/\ell\ =\ 0.047} = 47.0\%$ $TLE_{a/\ell\ =\ 0.156} = 43.6\%$ $TLE_{a/\ell\ =\ 0.312} = 38.9\%$

Site 50:

For $LTE_{\delta 1,\ 50} = 24.65\%$:

$TLE_{a/\ell\ =\ 0.047} = 23.5\%$ $TLE_{a/\ell\ =\ 0.156} = 21.7\%$ $TLE_{a/\ell\ =\ 0.312} = 19.3\%$

For $LTE_{\delta 2,\ 50} = 94.22\%$:

$TLE_{a/\ell\ =\ 0.047} = 48.4\%$ $TLE_{a/\ell\ =\ 0.156} = 44.9\%$ $TLE_{a/\ell\ =\ 0.312} = 40.0\%$

For Site 38A, where the a/ℓ ratio was equal to 0.160, TLE values were determined by interpolating between the values found for a/ℓ ratios of 0.156 and 0.312. Equation (15) was used to calculate these interpolated TLE values:

$$TLE_{a/\ell=0.160} = \frac{(0.160 - 0.156)(TLE_{a/\ell=0.312} - TLE_{a/\ell=0.156})}{0.312 - 0.156} + TLE_{a/\ell=0.156} \qquad \textbf{(15)}$$

where:

$TLE_{a/\ell}$ = transferred load efficiency for the given a/ℓ ratio, %.

The TLE values for the two cracks at Site 38A were thus computed using equation (15):

$$TLE_{1,38A} = \frac{(0.160 - 0.156)(40.3\% - 45.0\%)}{0.312 - 0.156} + 45.0\% = 44.87\%$$

$$TLE_{2,38A} = \frac{(0.160 - 0.156)(38.9\% - 43.6\%)}{0.312 - 0.156} + 43.6\% = 43.47\%$$

For Site 50, where the a/ℓ ratio was equal to 0.128, TLE values were determined by interpolating between the values found for a/ℓ ratios of 0.047 and 0.156. Equation (16) was used to calculate these interpolated TLE values:

$$TLE_{a/\ell=0.128} = \frac{(0.128 - 0.047)(TLE_{a/\ell=0.156} - TLE_{a/\ell=0.047})}{0.156 - 0.047} + TLE_{a/\ell=0.047} \quad \textbf{(16)}$$

where:

$TLE_{a/\ell}$ = transferred load efficiency for the given a/ℓ ratio, %.

The TLE values for the two cracks at Site 50 were thus computed using equation (16):

$$TLE_{1,50} = \frac{(0.128 - 0.047)(21.7\% - 23.5\%)}{0.156 - 0.047} + 23.5\% = 22.16\%$$

$$TLE_{2,50} = \frac{(0.128 - 0.047)(44.9\% - 48.4\%)}{0.156 - 0.047} + 48.4\% = 45.79\%$$

Once the TLE values had been determined, P_T values were computed for the cracks simply by using equation (14):

Site 38A:

$$P_{T1,38A} = \frac{44.87\%}{100\%} \times 40\text{kN} = 17.97\text{ kN}$$

$$P_{T2,38A} = \frac{43.47\%}{100\%} \times 40\text{kN} = 17.41\text{ kN}$$

Site 50:

$$P_{T1,50} = \frac{22.16\%}{100\%} \times 40\text{kN} = 8.87\text{ kN}$$

$$P_{T2,50} = \frac{45.79\%}{100\%} \times 40\text{kN} = 18.34\text{ kN}$$

The final step in this procedure was to determine AGG values for the cracks. This involved determining AGG/kℓ values for each of the LTE_δ values for the two sites using the plot in Figure 8. Determination of these AGG/kℓ values using the LTE_δ-AGG/kℓ plot is depicted in Figure 10. From this plot, the following values were obtained:

Site 38A:	Site 50:
$AGG/k\ell_{1,38A} = 205.00$	$AGG/k\ell_{1,50} = 0.33$
$AGG/k\ell_{2,38A} = 9.00$	$AGG/k\ell_{2,50} = 41.00$

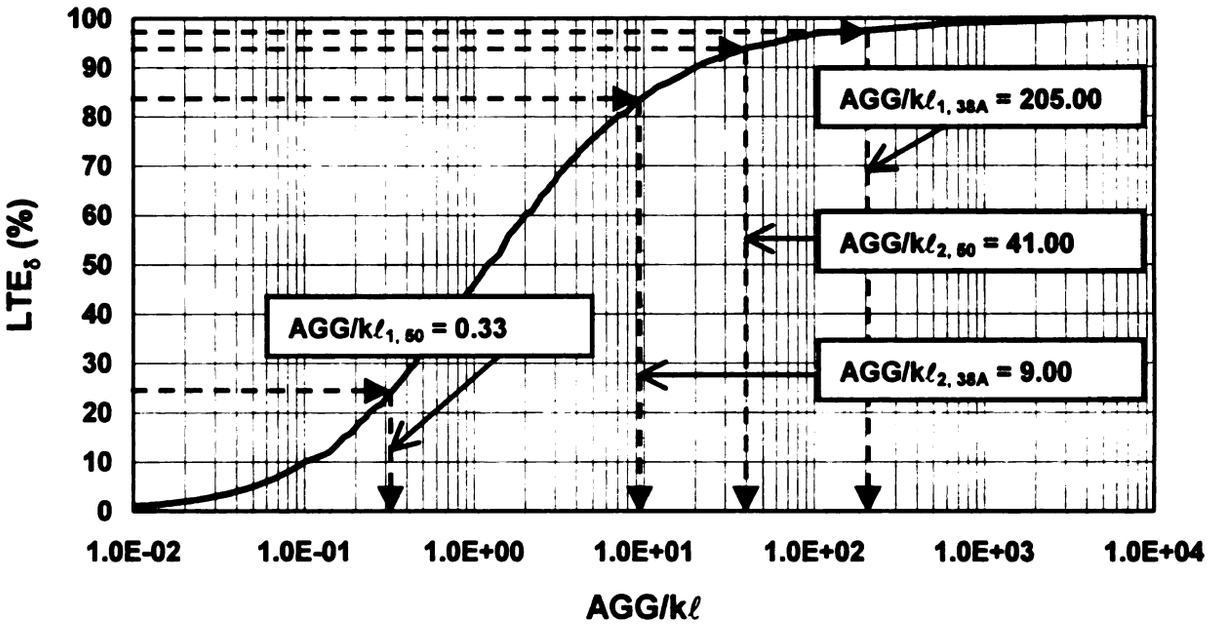

Figure 10 Determination of AGG/kℓ Using "Standard" Procedure.

AGG values were then computed for the cracks by multiplying these AGG/kℓ values by the k and ℓ values for the respective test sites:

Site 38A:

$$AGG_{1,38A} = (205.00)(66.3 \text{ kPa / mm})(936 \text{ mm}) = 1.3 \times 10^7 \text{ kPa}$$

$$AGG_{2,38A} = (9.00)(66.3 \text{ kPa / mm})(936 \text{ mm}) = 5.6 \times 10^5 \text{ kPa}$$

Site 50:

$$AGG_{1,50} = (0.33)(40.2 \text{ kPa / mm})(1170 \text{ mm}) = 1.6 \times 10^4 \text{ kPa}$$

$$AGG_{2,50} = (41.00)(40.2 \text{ kPa / mm})(1170 \text{ mm}) = 1.9 \times 10^6 \text{ kPa}$$

Streamlined Approach

In the streamlined approach to determining crack performance parameters, the first step is identical to that of the "standard" procedure. That is, LTE_δ values are computed using equation (5). Since these calculations were already shown above in the "standard" procedure example, only the results will be repeated here:

Site 38A:	Site 50:
$LTE_{\delta 1,38A} = 97.53\%$	$LTE_{\delta 1,50} = 24.65\%$
$LTE_{\delta 2,38A} = 83.13\%$	$LTE_{\delta 2,50} = 94.22\%$

As was explained earlier in this section, in order to determine P_T and AGG using this method, an initial effort must be undertaken by the transportation agency to develop a series of LTE_δ versus P_T and LTE_δ versus AGG plots for various k and ℓ values and combinations. For the purposes of this example, LTE_δ-P_T plots were developed for three ℓ values – 900, 1100, and 1300 mm. These plots are shown in Figures 11 through 13, respectively. LTE_δ-AGG plots were developed for six k and ℓ combinations – {k = 40 kPa/mm, ℓ = 900 mm}, {70 kPa/mm, 900 mm}, {40 kPa/mm, 1100 mm}, {70 kPa/mm, 1100 mm}, {40 kPa/mm, 1300 mm}, and {70 kPa/mm, 1300 mm} – in this example. These plots are displayed in Figures 14 through 19, respectively. In practice, such plots would need to be developed for a greater variety of k and ℓ values and combinations. A sufficient number of values and combinations should be considered to cover the range of values normally encountered in practice.

Figures 11 through 13 were developed by considering several LTE_δ values ranging from 15 to 100%. For each LTE_δ value, TLE and P_T were determined using the "standard" procedure. These plots were developed based on an applied load of 40 kN and radius of the loaded area of 150 mm, which correspond to the FWD wheelpath test conditions used in this study. The P_T values were then plotted against the respective LTE_δ values and a curve was drawn through these points. Figures 14 through 19 were also developed by considering several LTE_δ values ranging from 15 to 100%. AGG values were determined for each LTE_δ value using the "standard" procedure. These values were then plotted against their respective LTE_δ values and a curve was drawn through these points.

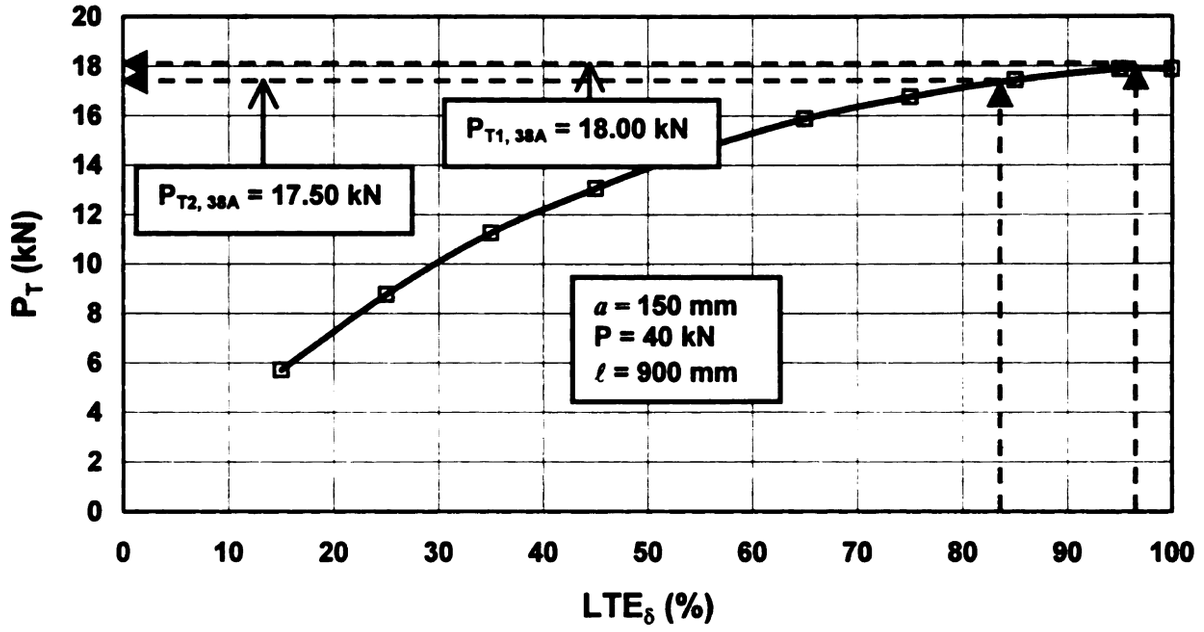

Figure 11 LTE_δ versus P_T Plot, ℓ = 900 mm.

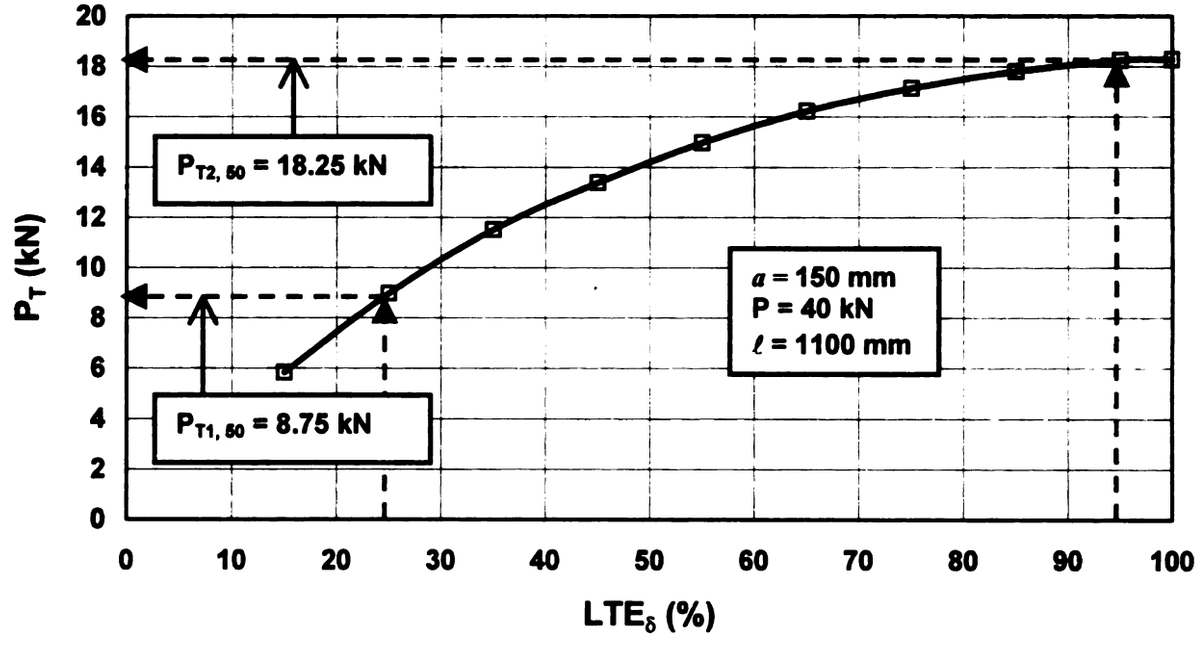

Figure 12 LTE_δ versus P_T Plot, ℓ = 1100 mm.

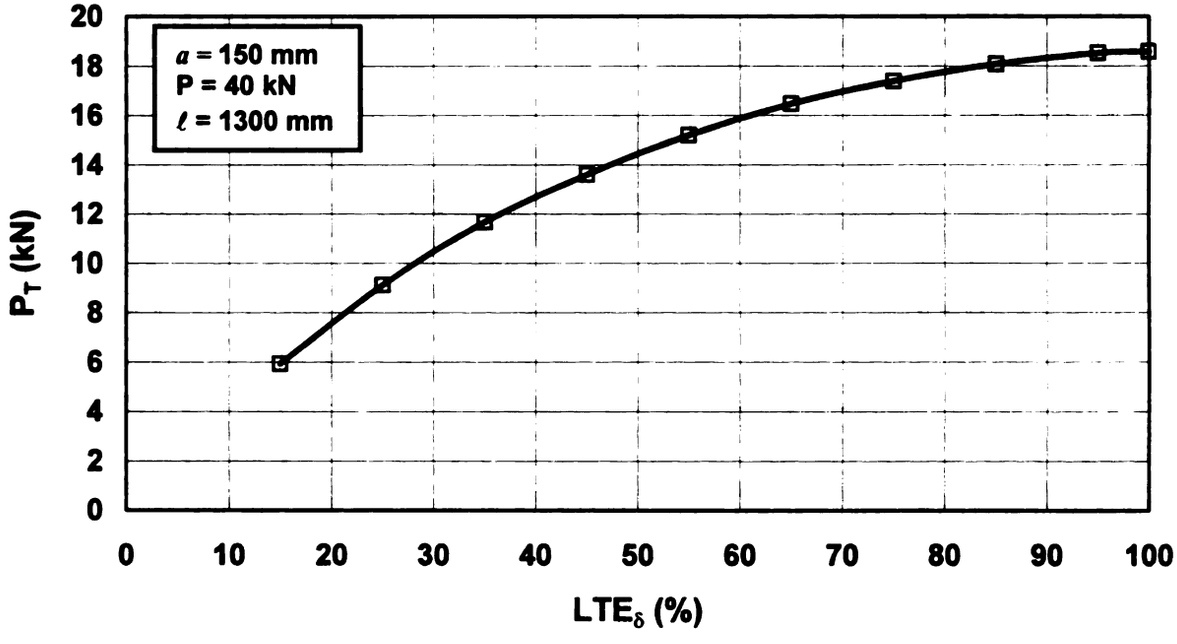

Figure 13 LTE_δ **versus** P_T **Plot,** ℓ **= 1300 mm.**

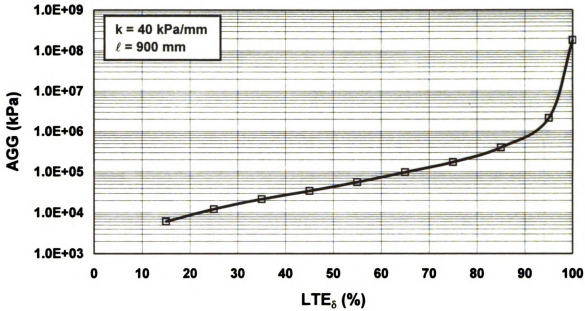

Figure 14 **LTE_{δ} versus AGG Plot, k = 40 kPa/mm and ℓ = 900 mm.**

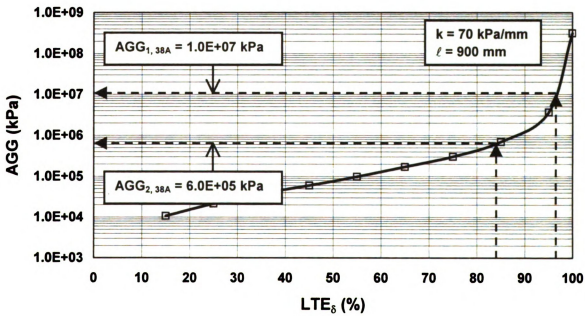

Figure 15 **LTE_{δ} versus AGG Plot, k = 70 kPa/mm and ℓ = 900 mm.**

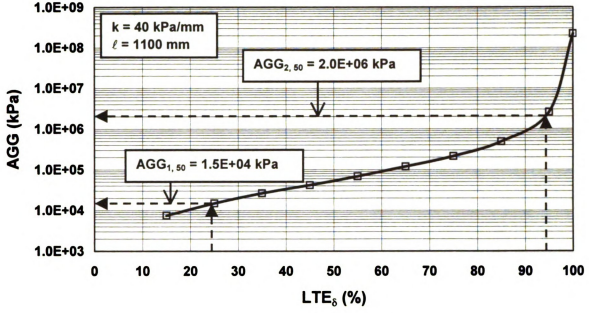

Figure 16 **LTE_δ versus AGG Plot, k = 40 kPa/mm and ℓ = 1100 mm.**

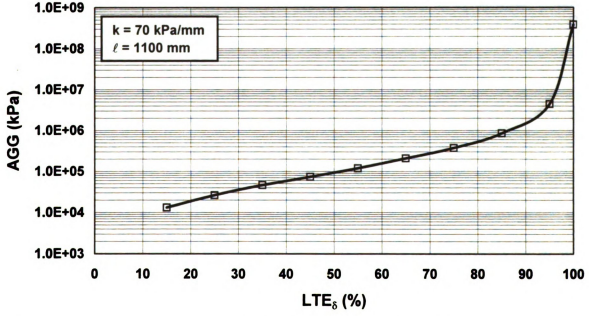

Figure 17 **LTE_δ versus AGG Plot, k = 70 kPa/mm and ℓ = 1100 mm.**

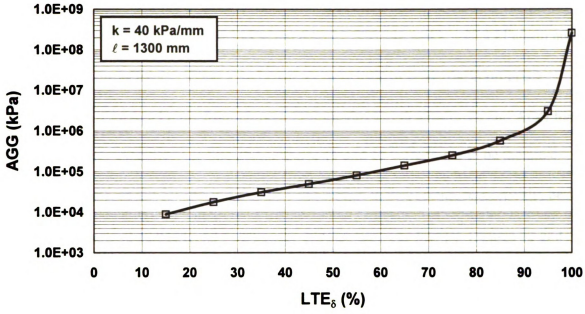

Figure 18 **LTE$_\delta$ versus AGG Plot, k = 40 kPa/mm and ℓ = 1300 mm.**

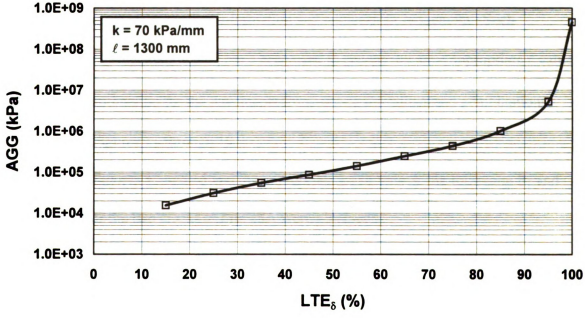

Figure 19 **LTE$_\delta$ versus AGG Plot, k = 70 kPa/mm and ℓ = 1300 mm.**

The backcalculated k and ℓ values for Sites 38A and 50 in Cycle 3 were found in Illustrative Example 1 to be k = 66.3 kPa/mm and ℓ = 936 mm and k = 40.2 kPa/mm and ℓ = 1170 mm, respectively. These k and ℓ values were used to select the appropriate LTE_δ-P_T and LTE_δ-AGG plots from Figures 11 through 19 to determine P_T and AGG for the cracks in this example. For Site 38A, Figures 11 and 15 were found to be the most appropriate plots, as the ℓ value and k and ℓ combination in these plots, respectively, best matched the backcalculated k and ℓ values for this test site. For Site 50, Figures 12 and 16 were found to be the most appropriate plots, as the ℓ value and k and ℓ combination in these plots, respectively, best matched the backcalculated k and ℓ values for this test site. As an alternate method, if k and ℓ had not been backcalculated in this example, the appropriate LTE_δ-P_T and LTE_δ-AGG plots for these two test sites could have been chosen based on pavement cross-section information and engineering judgement. Such information and judgement would have been used to choose the most appropriate ℓ value and k and ℓ combination for the pavements from among the values and combinations considered in Figures 11 through 19.

Using Figures 11 and 15 and the appropriate LTE_δ values, the following P_T and AGG values for the two cracks at Site 38A were obtained:

$P_{T1,\,38A}$ = 18.00 kN $\qquad$ $AGG_{1,\,38A} = 1.0 \times 10^7$ kPa

$P_{T2,\,38A}$ = 17.50 kN $\qquad$ $AGG_{2,\,38A} = 6.0 \times 10^5$ kPa

Using Figures 12 and 16 and the appropriate LTE_δ values, the following P_T and AGG values for the two cracks at Site 50 were obtained:

$P_{T1,\,50} = 8.75$ kN $\qquad$ $AGG_{1,\,50} = 1.5 \times 10^4$ kPa

$P_{T2,\,50} = 18.25$ kN $\qquad$ $AGG_{2,\,50} = 2.0 \times 10^6$ kPa

Comments

In practice, the LTE_δ, P_T, and AGG values computed for the cracks in this example would be compared to threshold limits. Comparison of these parametric values with the thresholds would allow for evaluation of the condition of the cracks. On a global scale, this process could be performed on all transverse cracks in the pavement network. If evaluations were performed on such a global scale, they could be used as a tool in planning and selecting rehabilitation activities for the pavement network.

A comparison of the P_T and AGG values determined in this example using each of the two procedures described in this section shows that fairly similar results are obtained for both methods. Generally, the P_T values computed using each procedure were within 1% of each other. The AGG values determined by each method were generally within 10% of each other. It can be seen that the discrepancy in AGG values obtained using the two procedures is larger than that for the P_T values. This can be attributed to error in reading values off of the log scale of the AGG axis in the LTE_δ-AGG plots when using the streamlined approach. When reading values off of plots, some error inevitably occurs in visually reading the values. Such errors in reading AGG values off of the LTE_δ-AGG plots are magnified due to the log scale of the AGG axis. These

magnified errors lead to a larger discrepancy in the AGG values obtained using the "standard" and streamlined procedures than the discrepancy associated with the P_T values obtained using these two procedures. Nevertheless, the 10% discrepancy found in AGG values between the two methods in this example is still not very great, and the results obtained using each of the two methods can be considered fairly similar.

It should be noted that the accuracy of the results obtained using the streamlined approach depends on the closeness between the k and ℓ values in the plots used to determine P_T and AGG and the actual values for the pavement. To provide sufficient accuracy using this approach, an adequate number of k and ℓ values and combinations should thus be considered when developing LTE_δ-P_T and LTE_δ-AGG plots. This will help to ensure the availability of plots corresponding to k and ℓ values that are close to the actual values for the pavement.

As indicated by the results in this example, the P_T and AGG values obtained using the streamlined approach are close to those determined using the "standard" procedure. Considering the similar results obtained using the two methods and the advantage in time saved by using the streamlined approach, which was evidenced in this example, the streamlined procedure would seem to be the more efficient method for determining parametric values. Thus, if a transportation agency intends to use performance parameters to evaluate transverse crack performance, it would be suggested that the streamlined approach be employed.

Development of Performance Parameter Thresholds

Comparison of crack performance parametric values (LTE_δ, P_T, and AGG) with threshold limits allows for evaluation of cracks in a pavement network. When integrated into a comprehensive pavement evaluation scheme, these evaluations can act as a useful tool in planning and selecting rehabilitation activities for the pavement network. Ideally, rehabilitation activities (e.g., load transfer restoration or full-depth patch repair) would be performed before parametric values reach the threshold limits, allowing the integrity of cracked JCP's to be restored prior to the development of crack-related distresses.

In order to use crack performance parameters as a means for evaluating crack condition, threshold limits must first be established for these parameters. 70% is a commonly accepted threshold value for LTE_δ by many researchers. That is, cracks are considered to have adequate load transfer if they have an LTE_δ of 70% or higher. No such common thresholds exist for P_T and AGG, as these parameters have not been widely used for assessing crack performance to date. Addressing the lack of threshold limits for these parameters, data from this study was used to develop thresholds for P_T and AGG. Field data was also used to check the validity of the 70% threshold for LTE_δ.

To develop such thresholds, it was necessary to establish an indicator of the ability of transverse cracks to transfer load other than the crack performance parameters, so that such an indicator could be compared to the parametric values. Faulting was selected as such an indicator in this study. This distress can be used as an indicator of poor load transfer (and thus poor crack condition), because inadequate load transfer is a mechanism for faulting. It can be assumed that when faulting exists at a crack, poor load transfer also exists at that crack.

Using this logic, Cycle 4 crack fault data and Cycle 4 crack LTE_δ, P_T, and AGG values were compared in an effort to establish threshold limits. Cycle 4 data was used because the fault data collected during this cycle was considered to be reliable. Inaccurate fault data was collected during Cycle 1, and no fault data was collected during Cycles 2 and 3. Since temperature is known to affect the parametric values (effect of temperature on LTE_δ is discussed later in this section), it should be noted that the data used in developing the thresholds in this study was taken at ambient temperatures ranging from 10 to 29°C. This included all Cycle 4 crack data except for that taken at Site 44, which was tested during very high ambient temperatures (> 40°C).

A plot of Cycle 4 fault data (i.e., faulting or no faulting) versus the respective LTE_δ values for all cracks tested during this cycle is given in Figure 20. From this plot, it can be seen that the fault-free cracks generally had very high LTE_δ values, whereas most of the faulted cracks had low values. Considering the relationship between faulting and load transfer capacity discussed above, this trend is very reasonable. Of course, there are a few exceptions to this trend, but these can be attributed to the many sources of error associated with taking field data. In this case, such error could be due to faulty FWD measurements and/or error in the visual assessments of faulting. In any event, there is a clear trend that faulted cracks have lower LTE_δ values than fault-free cracks. To establish an LTE_δ threshold based on faulting using this plot, a breakoff value must be established where most of the faulted data lies below this value and most of the fault-free data lies above this value. It appears that the commonly accepted LTE_δ threshold value of 70% is such an appropriate breakoff value. Thus, based on the data from this study, an LTE_δ threshold value of 70% seems appropriate.

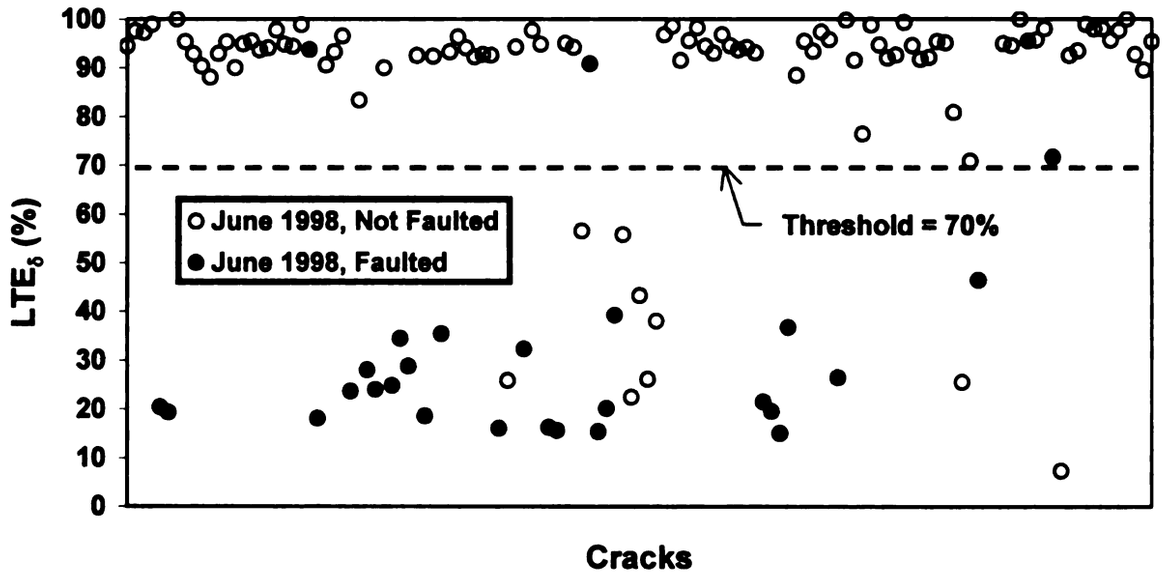

Figure 20 Comparison of Cycle 4 Fault and LTE_δ Crack Data.

Figure 21 contains a plot of Cycle 4 fault data versus the respective P_T values for all cracks tested during this cycle. This plot, of course, shows a similar trend to that observed in Figure 20 for LTE_δ. That is, the fault-free cracks generally had very high P_T values, whereas most of the faulted cracks had low values. Again, there are a few exceptions to this trend, but these can be attributed to the sources of error noted previously. Considering Figure 21, it appears that an appropriate breakoff value for P_T is 16.5 kN. Most of the faulted crack data falls below this value, while the fault-free data generally lies above this value. Thus, a P_T threshold value of 16.5 kN seems appropriate based on the field data from this study.

A plot of fault data versus the respective AGG values for all cracks tested during Cycle 4 is shown in Figure 22. This plot shows a similar trend to that observed in Figures 20 and 21. That is, higher parametric values are found for fault-free cracks than for faulted cracks. Figure 22 shows that fault-free cracks generally had high AGG values, while most of the faulted cracks had low values. There are once again a few exceptions to this trend, but these can be attributed to the sources of error noted previously. Based on Figure 22, it seems that an appropriate breakoff value for AGG is 2.0×10^5 kPa. Most of the faulted crack data falls below this value, while the fault-free data generally lies above this value. Based on the field data from this study, an AGG threshold value of 2.0×10^5 kPa thus seems appropriate.

Based on the results from this study, a suggested criteria for using the performance parameters would be that a crack is considered to be in acceptable condition if all of its parametric values are greater than the thresholds given above. If any of the threshold criteria are not met, the crack is considered to be in unacceptable condition. It

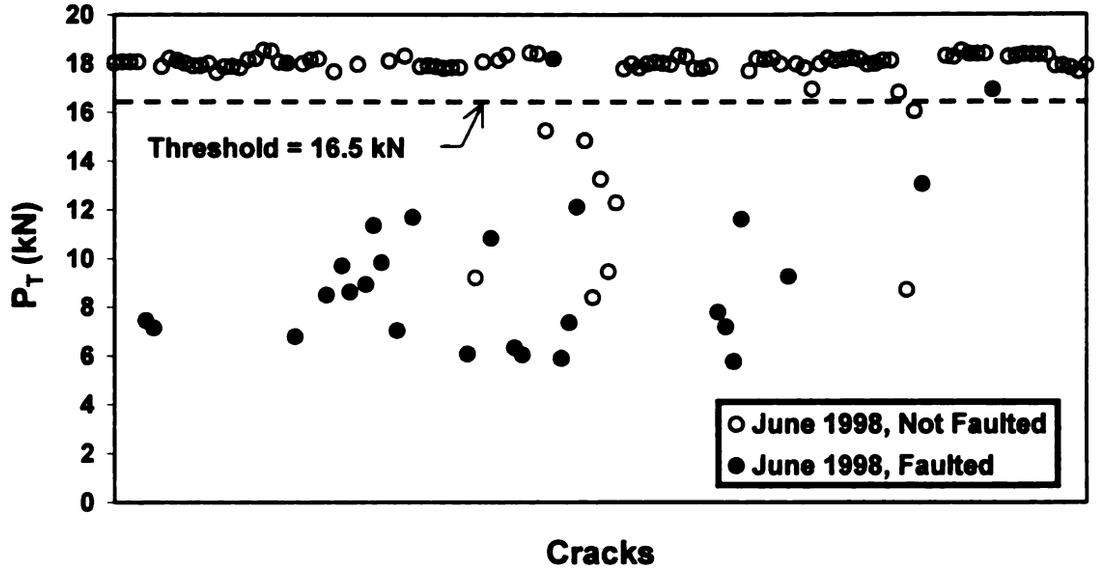

Figure 21 **Comparison of Cycle 4 Fault and P_T Crack Data.**

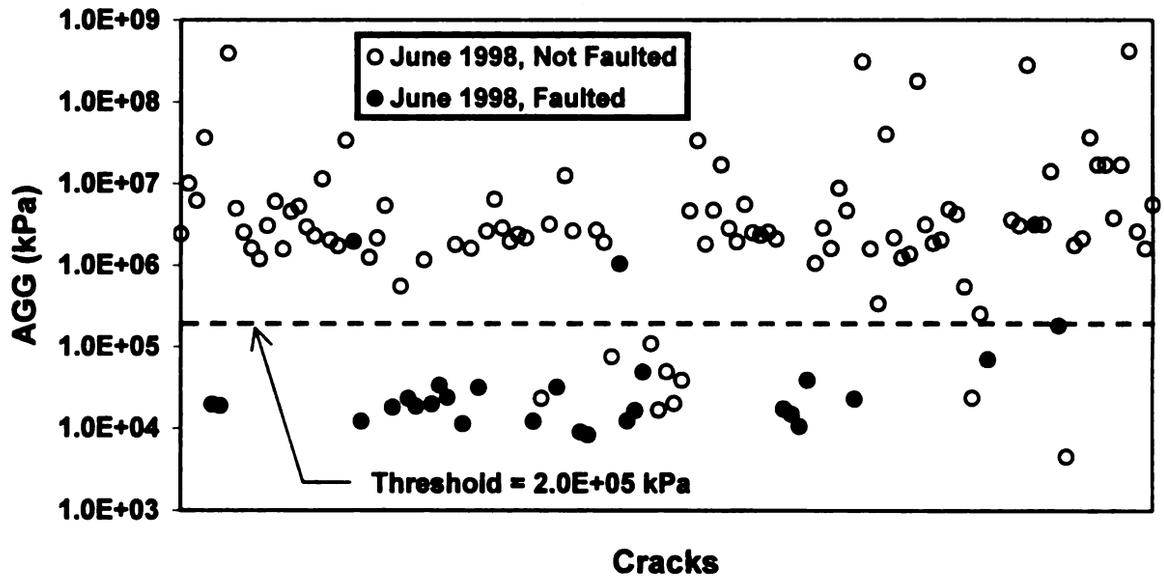

Figure 22 **Comparison of Cycle 4 Fault and AGG Crack Data.**

was previously noted that the data used for developing the thresholds in this study was taken at ambient temperatures ranging from 10 to 29°C. If ambiguous results (see discussion below on temperature effects) are obtained for data taken near the limits or outside of this temperature range, performance parameters alone should not be used to evaluate crack condition. In such cases, a visual distress survey of the crack condition, taken at the time of testing, should also be considered for crack evaluation purposes.

Temperature Effects on Performance Parameters

Effect of Pavement Surface Temperature on LTE_δ

It is well-known that temperature affects the load transfer potential of transverse cracks in JCP's through slab curling and thermal expansion/contraction of the slab. At high temperatures, downward curling and thermal expansion reduce crack widths. This results in a greater potential for contact between opposing crack faces and thus greater potential for aggregate interlock load transfer.

Noting this dependence of load transfer potential on temperature, it was desired to determine how temperature affects the performance parameters discussed in this thesis. Hence, data from this study was used to examine the effect of pavement surface temperature on LTE_δ. Since P_T and AGG are derived from LTE_δ, temperature should have a similar effect on these parameters as for LTE_δ. Before discussing the analysis of temperature effects that was performed in this research, let us first review the temperature data that was collected in this study.

As was noted in Chapter IV, ambient and pavement surface temperature measurements were made at the time of all FWD wheelpath testing. Tables B.37 through

B.40 of Appendix B provide ambient test temperature data for the cracks and joints that were FWD wheelpath tested. These tables contain data for the carbonate, natural gravel, recycled, and slag test site pavements, respectively. Pavement surface test temperatures for such cracks and joints are given in Tables B.41 through B.44 for the four pavement types, respectively. The data in Tables B.37 through B.44 includes measurements taken for both the tests performed before and after the crack/joint for all testing done in Cycles 1 through 4. Note that the cracks and joints in these tables correspond to those listed in Tables B.21 through B.36. Also note that data measured at joint locations was not considered for purposes of analysis, as consideration of this data would have been beyond the scope of this study.

The relationship between pavement surface temperature and LTE_{δ} was examined on a test site-by-test site basis. In this analysis, temperature measurements were compared to LTE_{δ} values for each crack within a test site using the data collected during Cycles 1 through 4. Results from this analysis did indeed show a relationship between temperature and LTE_{δ}. That is, increasing the pavement surface temperature was usually found to result in an increase in LTE_{δ} and, in general, a reduction in crack width. Considering the downward slab curling and thermal expansion that occur at high temperatures, this trend is very reasonable. The reduced crack widths associated with downward curling and slab expansion allow for greater aggregate interlock and thus lead to higher LTE_{δ}'s. Note that the relationship between pavement surface temperature and crack width in this study was not consistent, probably due to the erred nature of the crack width measurements (see Chapter IV).

The trend of increasing LTE_δ with increasing temperature was particularly evident for cracks with wide openings and low LTE_δ's at low temperatures. These cracks were often found to show substantial improvement in LTE_δ with increasing temperature. Such improvement was likely the result of a significant reduction in crack width with increasing temperature. Cracks having LTE_δ's of less than 30% at low pavement surface temperatures (5 to 15°C) were often found to increase by 40 to 80% LTE_δ when temperatures rose to 30 to 40°C. Such behavior is displayed in Figure 23, which presents a plot of pavement surface temperature versus LTE_δ for the two cracks tested at Site 7. From this plot, it can be seen that Crack 2 had an LTE_δ just below 15% at a temperature just above 10°C. As the temperature increased to about 40°C, the LTE_δ of this crack climbed to above 90%.

It should be noted that temperature did not seem to have a significant effect on LTE_δ, however, for cracks that were tight and had high LTE_δ's at low temperatures. Temperature did not significantly affect the LTE_δ's of these cracks, because the crack faces were already in close contact at low temperatures. Cracks demonstrating LTE_δ's of 90 to 100% at low temperatures (5 to 15°C) were usually found to show a change of less than 5% when the temperature was increased to 30 to 40°C. These changes can probably be attributed more to error in the FWD measurements than the effect of temperature. Variation in LTE_δ with temperature for such cracks is shown in Figure 24, which plots pavement surface temperature versus LTE_δ for the two cracks tested at Site 5. It can be seen in this plot that LTE_δ increased by 5% or less for Cracks 1 and 2 as temperature increased from about 10°C to about 40°C. Crack 1 in Figure 23 further demonstrates the

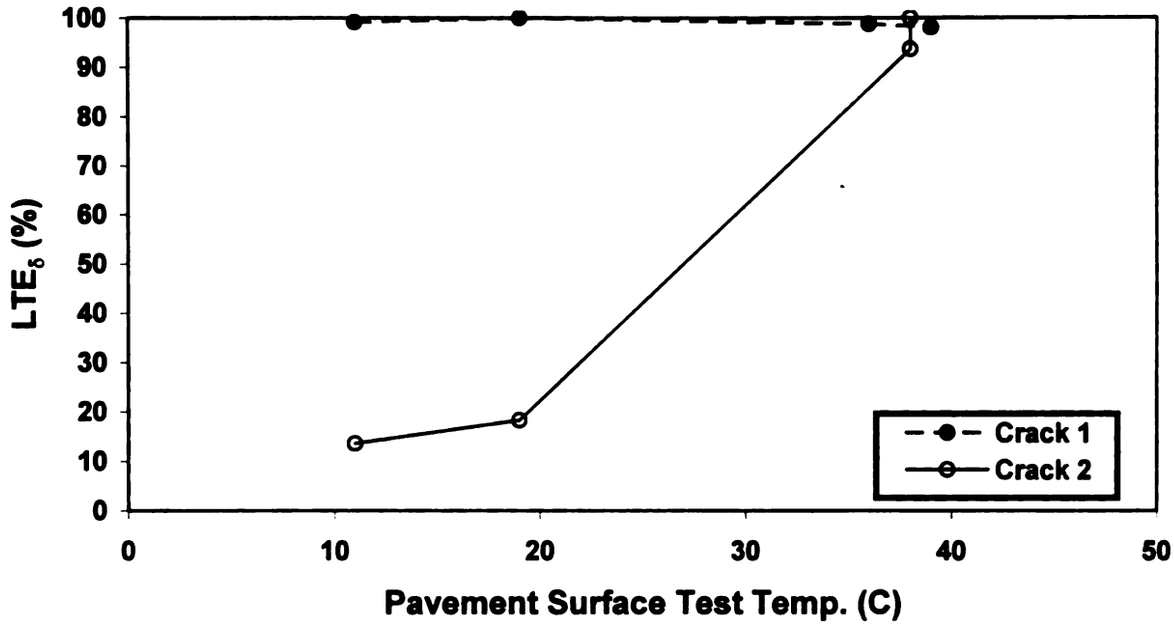

Figure 23 **Effect of Pavement Surface Temperature on LTE_δ, Site 7.**

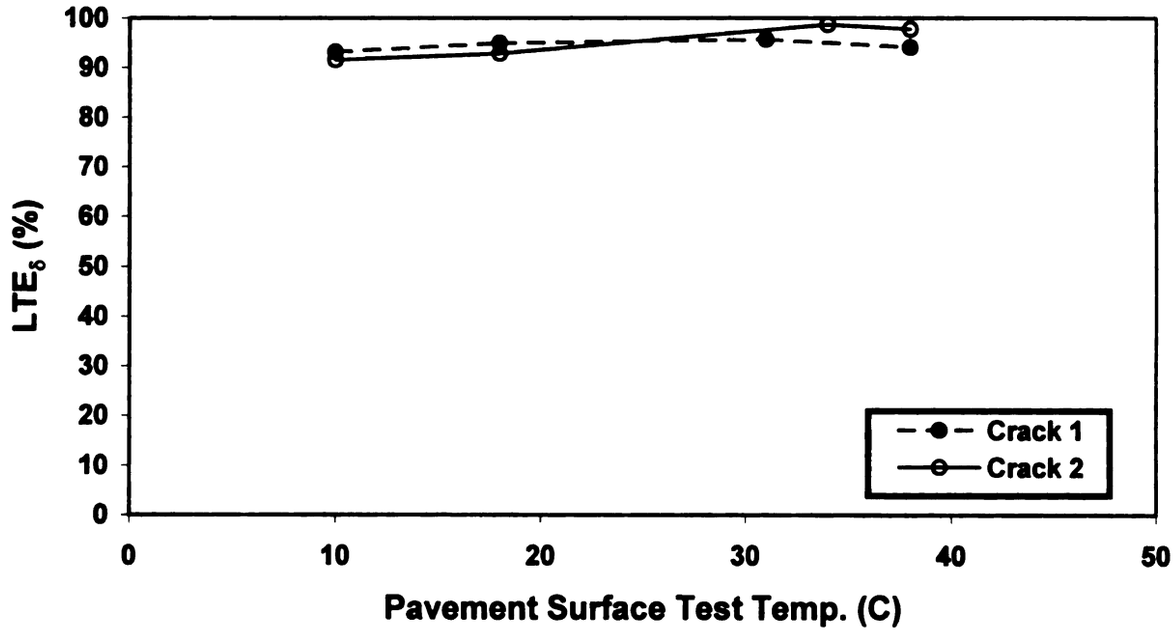

Figure 24 **Effect of Pavement Surface Temperature on LTE_δ, Site 5.**

behavior of such cracks, as its LTE_δ changed by less than 2% as the temperature increased from about 10°C to about 40°C. All three of these cracks had LTE_δ's of 90 to 100% at 10°C.

Consideration of Temperature Effects in Evaluating Performance Parametric Values

The dependence of LTE_δ (and by default, P_T and AGG) on pavement surface temperature suggests that the temperature at the time of FWD testing should be noted and subsequently considered when making crack evaluations based on these parameters. Temperature effects can lead to ambiguous results for LTE_δ, P_T, and AGG. Such ambiguity can occur when low parametric values are obtained at low temperatures or high values are obtained at high temperatures. In these cases, parametric values may not be indicative of the actual crack condition. Cracks exhibiting low values at low temperatures may demonstrate significantly higher, acceptable values at higher temperatures. Similarly, cracks showing high parametric values at high temperatures may exhibit unacceptable values at lower temperatures. In such cases, visual crack distress surveys should be performed and considered in addition to the parametric values to allow for a better assessment of the crack condition. Another approach to dealing with these temperature effects is to minimize the effects by only performing FWD testing when temperatures are within a specified range. Darter et al. suggest testing when ambient temperatures are between 10 and 27°C [41]. Testing during these relatively cool temperatures helps to minimize curling and expansion/contraction effects. It also helps to ensure that if these temperature effects do occur, the result will be upward curling and/or

slab contraction. These conditions would lead to conservative assessments of crack condition.

ASSESSMENT OF VOID POTENTIAL NEAR TRANSVERSE CRACKS

Overview

Field data from this study was used to demonstrate a voids analysis procedure that allows for an assessment of the likelihood of loss of support near transverse cracks and joints. By detecting the presence of voids at cracks and joints, this procedure, which utilizes corner FWD data, allows appropriate rehabilitation actions to be taken to restore support to a cracked JCP. It is particularly useful for identifying void potential near cracks and joints that are in the early stages of void manifestation, but do not yet show visual evidence (faulting, corner breaks, etc.) of loss of support. Detecting the presence of voids at such cracks and joints allows appropriate rehabilitation actions to be taken before distresses develop and allows support to be restored at locations that might otherwise be overlooked. Slab stabilization, which is described in detail in Chapter III of this thesis, is one rehabilitation action that can be used to restore support near cracks or joints associated with a loss of support. The voids analysis procedure described herein can also be useful in ensuring that voids no longer exist after rehabilitation actions have been performed.

FWD corner deflection data collected at selected cracks and joints during Cycles 3 and 4 was used to perform voids analyses in this study. A description of the voids analysis procedure used in this study is given below. An example, using field data from this research, is also provided in this section to illustrate the use of this procedure in

evaluating void potential near transverse cracks. Results from the voids analyses performed on the field data from this study were used to determine appropriate threshold limits for evaluating void potential using this procedure. A discussion concerning the determination of these thresholds concludes this section.

Voids Analysis Procedure

The first step in the voids analysis procedure involves performing FWD tests at crack and/or joint corner locations, as described in Chapter IV of this thesis. This testing should preferably be performed when the ambient temperature is below 27°C. Testing during such cool temperatures helps to ensure conservative results, as any slab curling will be upward in nature. Upward curling leads to higher corner deflections. [41]

From this FWD testing, deflection values are obtained for three magnitudes of load at each crack or joint tested. This data is then used to create a plot of pavement deflection (x-axis) versus load magnitude (y-axis). For each crack or joint, a best-fit line is plotted through the three data points and extrapolated until it intersects the x-axis. The x-intercept obtained from such lines is the parameter that is used to determine the void potential of the crack or joint. If the x-intercept lies above an established threshold value, it would be considered likely that a void exists on the leave side of that crack or joint. An x-intercept below the threshold would indicate that no loss of support exists at that location. A threshold value of 50 μm is suggested by Darter et al., while Wade et al. recommend a value of 75 μm [41, 58]. An evaluation of the validity of these thresholds, based on data from this study, is given later in this section. [41]

An example, using data collected in this research, is given below to demonstrate the use of the voids analysis procedure.

Illustrative Example 3

FWD corner deflection testing on three cracks at Site 13 during Cycle 4 yielded the following load and deflection data:

Crack 1:	P = 40 kN	⟶	δ = 267 μm
	P = 67 kN	⟶	δ = 397 μm
	P = 89 kN	⟶	δ = 499 μm
Crack 2:	P = 40 kN	⟶	δ = 165 μm
	P = 67 kN	⟶	δ = 270 μm
	P = 89 kN	⟶	δ = 352 μm
Crack 3:	P = 40 kN	⟶	δ = 486 μm
	P = 67 kN	⟶	δ = 593 μm
	P = 89 kN	⟶	δ = 720 μm

These load and deflection values were plotted on a deflection (x-axis) versus load (y-axis) graph. Best-fit lines were then drawn through the data points and extrapolated to the x-axis, as shown in Figure 25. From this figure, the following x-intercept values were obtained:

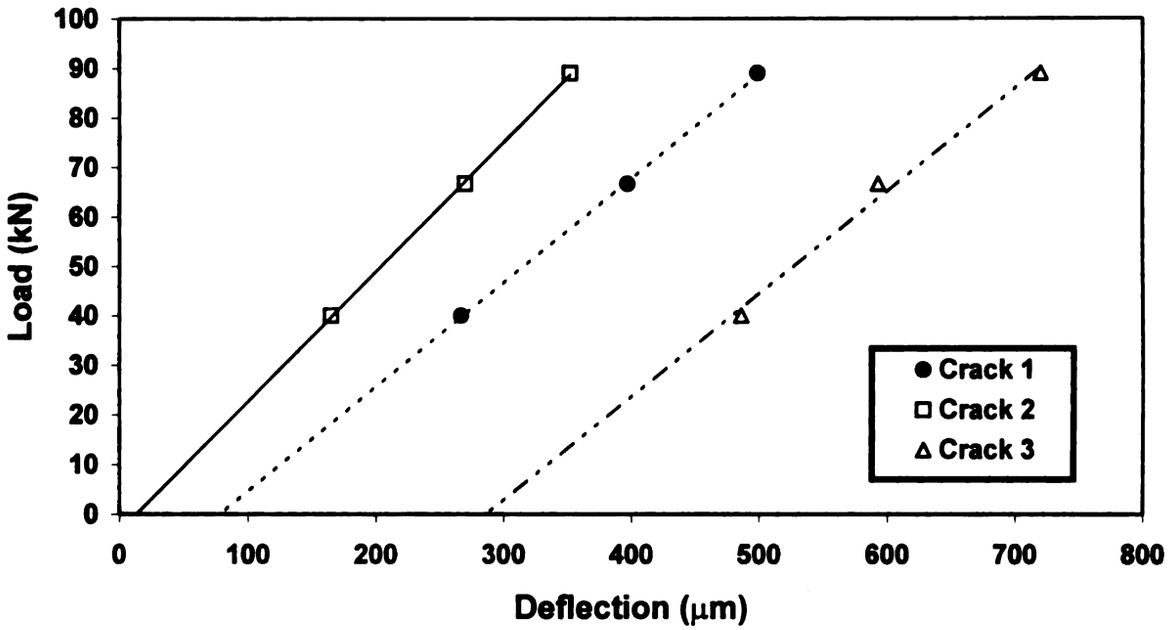

Figure 25 **Determination of x-intercepts for Voids Analysis, Site 13, Cycle 4 Data.**

$x\text{-intercept}_{Crack\ 1} = 78\ \mu m$

$x\text{-intercept}_{Crack\ 2} = 13\ \mu m$

$x\text{-intercept}_{Crack\ 3} = 287\ \mu m$

To evaluate the void potential of these cracks, the x-intercepts found above must be compared to threshold limits. Figure 26 allows for such an evaluation. In addition to the three x-intercepts determined above, this figure contains horizontal lines drawn at the two threshold values from [41] and [58] noted earlier in this section. Data points plotting above these lines indicate the presence of a void, while those plotting below the lines indicate that no loss of support exists. Figure 26 shows that the Crack 2 x-intercept is well below either threshold limit, and thus no void likely exists at this location. Conversely, the Crack 3 x-intercept plots significantly above both threshold limits, and it can thus be considered very likely that some loss of support exists at this location. The x-intercept for Crack 1 plots just above the 75 μm threshold. Thus, it would be considered likely that a void does exist at this crack location. Note, however, that assessment of void potential at Crack 1 cannot be made with as much confidence as for the other two cracks, as its x-intercept is very close to the threshold values. For this test site, rehabilitation action(s) (e.g., slab stabilization) are needed to restore support at Cracks 1 and 3.

In practice, the voids analysis procedure could be performed on all transverse cracks in the vicinity of this test site. Assessing the void potential of all such cracks would allow appropriate rehabilitation actions to be taken on this pavement. Such actions would restore the integrity of the cracked JCP.

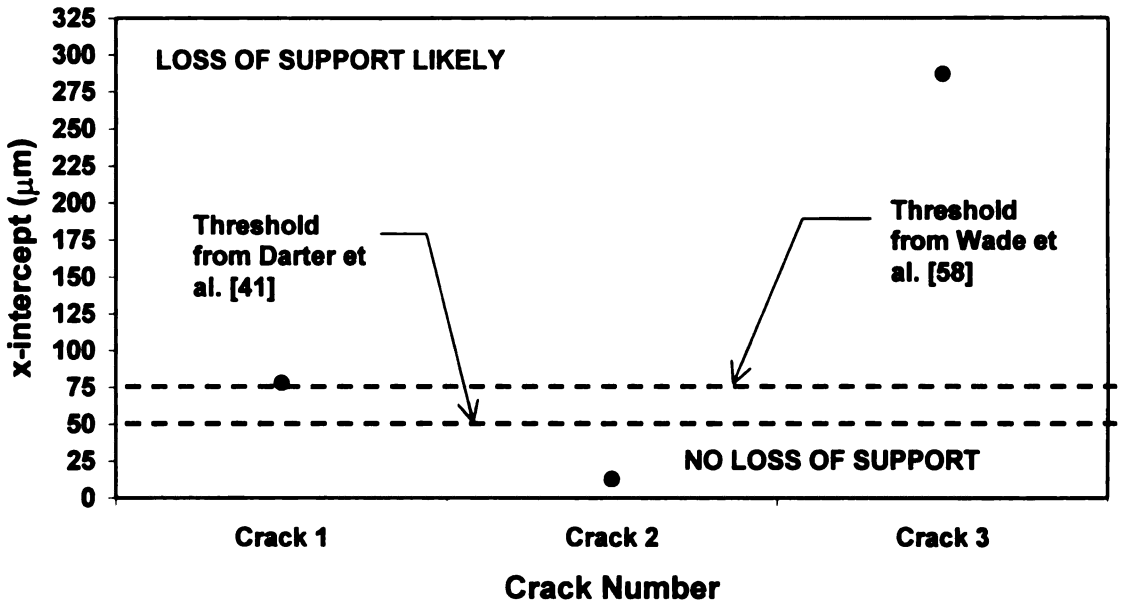

Figure 26 **Determination of Void Potential Using Established Threshold Limits, Site 13, Cycle 4 Data.**

Examination of Threshold Limits for Void Potential

Voids analysis results from this study were used to examine the validity of the two aforementioned thresholds (50 μm and 75 μm) for void potential. It was desired to determine if these thresholds were satisfactory for detecting the presence of voids, or if another threshold would be more appropriate, based on the data from this study. In order to do this, it was necessary to determine x-intercept values for cracks known to have voids and cracks known not to have voids. Comparison of these x-intercept values would then allow an appropriate threshold to be determined.

It was thus necessary to establish a means, other than the voids analysis procedure, for determining which cracks had voids and which did not have voids. In this study, faulting was used as such an indicator to determine whether voids did or did not exist at a crack location. Faulting can be used as an indicator of the existence of voids, because a loss of support is a consequence of the faulting mechanism. As a testimonial to this, Darter et al. assert that voids are definitely present where there is faulting. It should be noted, however, that voids may be present even if there is no faulting. For purposes of this analysis, however, it was assumed that no faulting was equivalent to no loss of support. [41]

Thus, FWD corner testing and the complementary voids analysis were performed on test site pavements in this study at both visually faulted cracks and cracks with no noticeable faulting. Tables B.45 through B.48 of Appendix B contain the results pertaining to the voids analyses performed at crack locations in this study for the carbonate, natural gravel, recycled, and slag pavements, respectively. Similar data obtained for joints in this study is located in Tables B.49 through B.52 for the four

pavement types, respectively. Tables B.45 through B.52 contain the x-intercept values determined using data from Cycles 3 and 4 as well as measurements of faulting taken during Cycle 4. Cycle 1 fault data was not considered in this analysis due to the inconsistent results obtained during that test cycle. It can be seen that corner testing was not usually done in both Cycles 3 and 4 for the same crack/joint. This was done intentionally to allow for as many cracks and joints as possible to be tested in the shortest time possible. It should be noted that the cracks and joints in these tables do not correspond to those in earlier tables of this thesis. Also note that although joint data was collected and tabulated, this data was not considered in the analyses reported in this section, as consideration of joints is beyond the scope of this research.

The validity of the voids analysis procedure itself is supported by the fault and x-intercept data in Tables B.45 through B.48. It can be seen from these tables that faulted cracks generally had significantly larger x-intercepts than cracks without faulting. The average x-intercept for faulted cracks was 165 μm, whereas an average intercept of 52 μm was found for fault-free cracks. This indicates that cracks having voids (based on faulting) have larger x-intercepts. Indeed, that is the premise of the voids analysis procedure.

In order to examine the validity of the 50 μm and 75 μm thresholds, a plot of fault data (i.e., faulting or no faulting) versus the respective x-intercepts for all cracks corner tested in this study was created. This plot is shown in Figure 27. Note that negative x-intercept values were taken as "zero" in this plot, as both negative and zero values essentially have the same interpretation in this analysis – that is, they indicate areas of full support. Horizontal lines were drawn in this figure at the two noted threshold values.

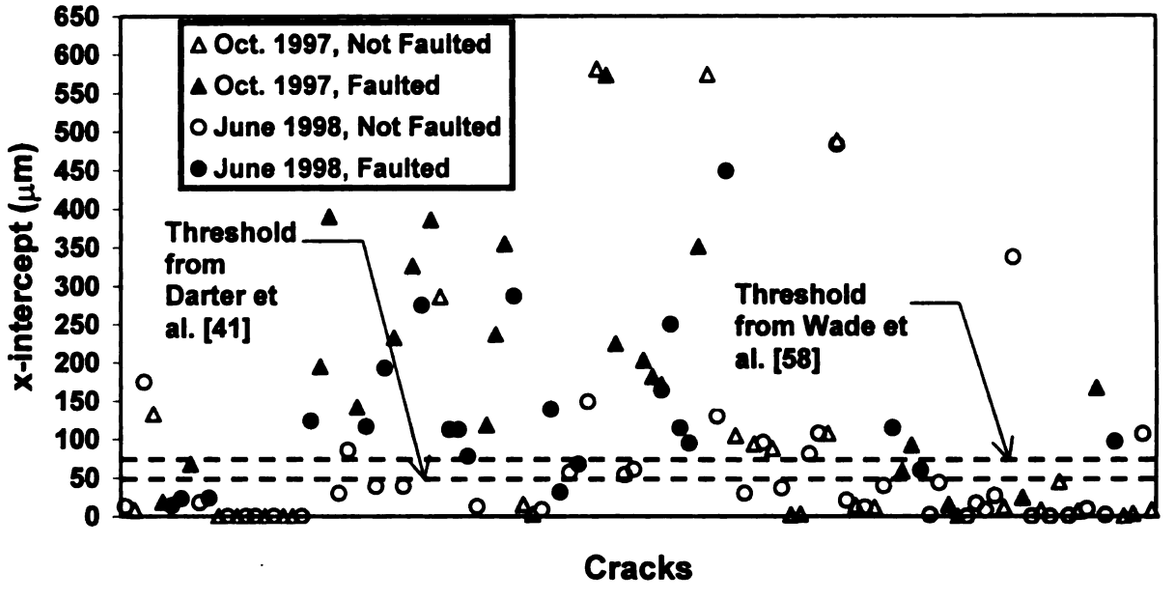

Figure 27 Comparison of Cycles 3 and 4 x-intercepts with Cycle 4 Fault Data.

It appears from this figure that most of the x-intercepts for the faulted cracks plot above the 50 to 75 μm range, while those for the non-faulted cracks plot below this range. Certainly, there are deviations from this trend, but these can be attributed to the many sources of error associated with taking field data (e.g., faulty FWD measurements and/or error in the visual assessments of faulting). Hence, both of these thresholds seem to be fairly reasonable.

Selection of one particular x-intercept value to be used as a threshold in this procedure would be very difficult, as there is no one distinct value that can differentiate between the existence and nonexistence of a void. To improve the usefulness of this method, it might thus be suggested that, rather than using one specific threshold value, a threshold range should be established. Void potential would thus be assessed based on whether x-intercepts plot below, within, or above this range. x-intercepts below the lower limit of this range would indicate no loss of support, while values above the upper limit would signify that there is some loss of support. For those cracks demonstrating x-intercepts within the threshold range, it would be suggested that coring (or some other method) be performed to further investigate if voids exist at those locations. Using this logic and based on field data from this study, it seems that a threshold range of 50 to 75 μm is appropriate for the voids analysis procedure.

When using the voids analysis procedure to evaluate void potential, it should be kept in mind that it is recommended that corner FWD testing for this procedure be performed at ambient temperatures less than 27°C. For data collected at temperatures significantly higher than 27°C, downward slab curling could cause decreased slab deflections, thus hindering the accuracy of this procedure in determining void potential.

- CHAPTER VI -

Results and Discussion II – Factors Affecting Transverse Cracking in JCP's

OVERVIEW

Field data from this research was used to study the effects of various factors on the occurrence and performance of transverse cracks in JCP's. The effects of joint spacing, concrete coarse aggregate type, and shoulder type on transverse crack occurrence were examined using such data. In addition, a relatively new analysis procedure called Volumetric Surface Texture (VST) testing, which was developed at the University of Minnesota, was utilized to investigate the effect of concrete aggregate type on crack face surface texture. Noting that the surface texture of a crack face is related to the potential for aggregate interlock load transfer across a transverse crack, this procedure was used to assess the relative crack performance potential of the four aggregate types considered in this study. Results and discussion pertaining to the analysis of the above factor effects are provided in subsequent sections of this chapter.

EFFECT OF JOINT SPACING ON TRANSVERSE CRACKING

Field data from this study was used to determine the effect of joint spacing on the occurrence of transverse cracks in JCP's. This was done by examining the relationship between joint spacing and number of transverse cracks per slab. Figure 28 depicts this relationship for the data collected in this study. This plot shows that increasing the joint spacing leads to a greater number of cracks per slab. Increasing the joint spacing from 4.9 m to 8.2 m results in almost twice the number of cracks, while an increase to 21.6 m

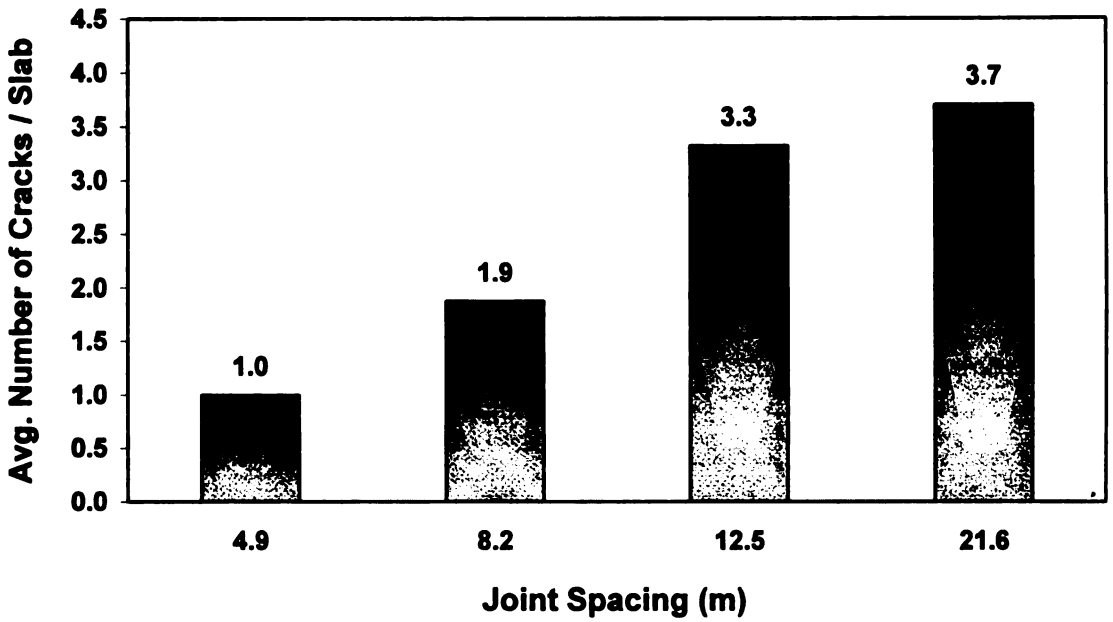

Figure 28 Effect of Joint Spacing on Number of Transverse Cracks per Slab.

leads to almost four times the number of cracks. Other studies performed in Minnesota and Michigan support this finding that the amount of transverse cracking increases with longer joint spacing [59].

Joint spacing affects transverse cracking due to its influence on curling stresses. Longer joint spacing (and thus slab length) generally corresponds to higher curling stresses in a slab. This is evidenced by considering Bradbury's curve (briefly discussed in Chapter II), which relates the correction factor C_x (accounting for the finite length of a concrete slab) to the joint spacing-radius of relative stiffness ratio (L_x/ℓ) [5]. As joint spacing increases, L_x/ℓ also increases, which leads to a higher C_x value according to Bradbury's curve (up to $L_x/\ell = 8.5$) [5]. Consideration of the curling stress equation (equation (1) in this thesis) reveals that higher C_x values result in larger curling stresses. Thus, longer joint spacing is generally associated with higher curling stresses. In a concrete slab, curling stresses manifest themselves as tensile stresses. Eventually, these tensile stresses are relieved by transverse cracking. Hence, due to its effect in producing larger curling stresses, longer joint spacing results in the potential for more transverse cracks in a slab.

EFFECT OF CONCRETE COARSE AGGREGATE TYPE ON TRANSVERSE CRACKING

A study of the effect of coarse aggregate type on transverse crack occurrence was also performed using data from this study. Field data from test sites with a 12.5 m joint spacing was used to investigate the relationship between aggregate type and number of transverse cracks per slab. By considering data only from pavements with this joint spacing, the influence of slab length on transverse cracking was removed. Figure 29

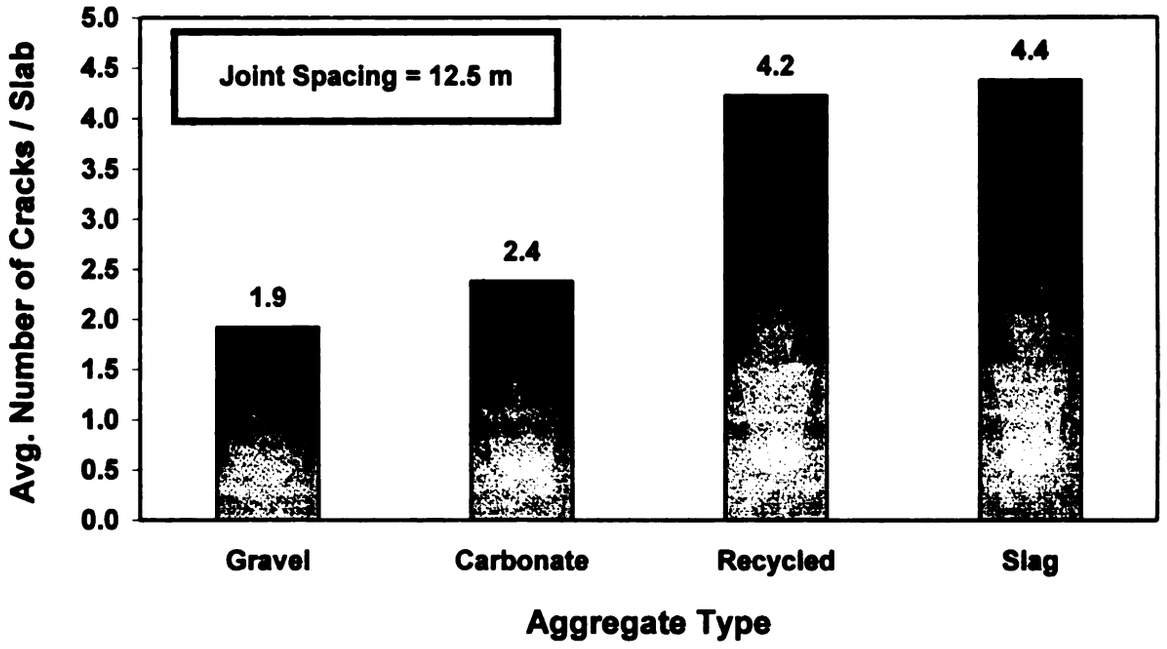

Figure 29 **Effect of Coarse Aggregate Type on Number of Transverse Cracks per Slab.**

shows the relationship between aggregate type and number of transverse cracks per slab for the data from this research. It can be seen that recycled concrete and slag pavements tended to have approximately twice the number of transverse cracks as pavements with natural gravel or carbonate aggregates. This can possibly be attributed to the greater susceptibility of slag and recycled concrete pavements to shrinkage cracking, when proper curing considerations are not made.

Slag aggregates have the potential to absorb a substantial amount of water from the concrete mixture due to their high porosity. If such absorption occurs, the resulting loss of water from the paste can lead to shrinkage cracking. After being subjected to repeated traffic and environmental load applications, these shrinkage cracks can develop into more severe transverse cracks.

Recycled aggregates can also be highly susceptible to shrinkage cracking, as they are associated with a nonuniform, sometimes high moisture absorption capacity [14]. It is suspected that the variability in the absorption capacity of these aggregates is linked to the variability in the amount of old mortar which exists on the aggregate particles. In areas where a large amount of old mortar covers the aggregate particles, a greater tendency for moisture absorption will exist. This is at least partially due to the presence of unhydrated cement particles within the old mortar. Hydration of these particles may occur as they come in contact with the mix water. Such hydration would result in a loss of mix water and could contribute to shrinkage cracking, and eventually, more severe transverse cracks. If the aggregate particles used in recycled pavements have a high moisture absorption capacity, the susceptibility of these pavements to shrinkage cracking would be further heightened.

Natural gravel and carbonate pavements are much less likely to experience significant shrinkage cracking caused by aggregate absorption of mix water. These aggregates generally have low absorption capacities compared to recycled concrete and slag aggregates. If all other variables are assumed constant and proper curing methods are neglected, recycled and slag pavements would thus be expected to be plagued with more transverse cracks than natural gravel and carbonate pavements due to their relatively high proclivity towards shrinkage cracking.

EFFECT OF SHOULDER TYPE ON TRANSVERSE CRACKING

It is believed that the type of shoulder used in conjunction with a JCP can significantly affect the occurrence of transverse cracking in the mainline pavement. To test the validity of this belief, an analysis was performed on the field data from this study. Specifically, field data was used to determine if shoulder type has a significant effect on the number of transverse cracks per slab. Each of the test site pavements in this study had one of three different shoulder types – tied concrete, tied concrete with sympathy joints, or asphalt. Before discussing the results from the analysis performed in this study, let us first consider why pavements with these three shoulder types are expected to behave differently with respect to transverse cracking. Note that a brief explanation of why these shoulder types affect cracking was provided in Chapter II. A somewhat more detailed explanation is given here, however, for convenience.

Pavements with asphalt shoulders are expected to have more transverse cracks than those with tied concrete shoulders. The reason for this can be understood by considering a load that is applied at the midslab edge location of a JCP (see Figure 3). If

an asphalt shoulder exists, the mainline pavement and the shoulder structurally act as two separate entities. The load is essentially applied at a free edge, resulting in the midslab edge load condition. This is considered to be the critical load condition for fatigue cracking. Tensile stresses are greatest in this load condition because the load is located far from the joints, where mechanical load transfer is often provided by dowel bars, and at a free edge, where the maximum bending stress occurs [3]. Thus, pavements with asphalt shoulders are highly susceptible to fatigue cracking if they have not been designed to resist the stresses resulting from this critical load condition.

In contrast, if a tied concrete shoulder is used, the slab and shoulder act as a composite support system for the load. The tied shoulder essentially extends the width of the pavement receiving the load. Consequently, if the same load positioning as described above occurs on a pavement with a tied concrete shoulder, the load is no longer applied at a free edge and the tensile bending stress in the concrete is reduced. Pavements with tied concrete shoulders would thus be expected to be less prone to fatigue cracking than those with asphalt shoulders.

A tied concrete shoulder with sympathy joints is another shoulder type that is sometimes used. Sympathy joints are shoulder joints with a joint spacing less than that which exists in the mainline pavement. For pavements with these shoulders, differential responses to thermal variations between the slab and shoulder (which are tied together) induce tensile stresses in the slab. These stresses frequently result in transverse cracks in the mainline pavement adjacent to the shoulder sympathy joints. Hence, pavements with this shoulder type are expected to demonstrate more transverse cracking than would occur on a pavement with tied concrete shoulders and no sympathy joints.

An analysis of variance (ANOVA) was performed on the field data from this study to determine if the data agreed with the behavior that is expected (according to the above paragraphs) of pavements with the three shoulder types. This analysis procedure allowed for a statistical assessment of whether shoulder type had a significant effect on the average number of transverse cracks per slab. An analysis was performed for each possible pairing of the three shoulder types. To remove the influence of aggregate type on cracking, separate analyses were performed for each of the four concrete aggregate types. Note that there were no recycled test site pavements with asphalt shoulders and no slag test site pavements with tied concrete shoulders having sympathy joints. For the various analyses, an α (confidence level) of 0.05 was used, meaning that if the p-value (smallest α level at which significant results could be obtained) was less than 0.05, the difference in number of cracks per slab between shoulder types was considered statistically significant [60]. One final important note is that several variables believed to affect transverse cracking were not controlled in this analysis. Controlling such variables would not have provided a sufficient amount of data to perform this analysis.

Results from the ANOVA analyses are presented in Table 2. It can be seen that shoulder type did affect transverse cracking for natural gravel pavements. Pavements with asphalt shoulders had a significantly greater number of cracks than those with tied concrete shoulders (with and without sympathy joints). As was previously discussed, this is due to the reduced tensile stresses that result when a tied concrete shoulder is used. Although it would be expected that significantly more cracks would occur in pavements with tied concrete shoulders having sympathy joints than in pavements having tied concrete shoulders without such joints, no significant difference in transverse cracking

Table 2 Effect of Shoulder Type on Number of Transverse Cracks per Slab.

Concrete Coarse Aggregate Type	Shoulder Types	Avg. Number of Cracks per Slab	Significant Difference? ($\alpha = 0.05$)
Natural Gravel	Tied Concrete	1.33	No
	Tied Concrete with Sympathy Joints	1.67	
	Tied Concrete	1.33	Yes
	Asphalt	3.70	
	Tied Concrete with Sympathy Joints	1.67	Yes
	Asphalt	3.70	
Recycled Concrete[a]	Tied Concrete	3.65	Yes
	Tied Concrete with Sympathy Joints	7.20	
Carbonate	Tied Concrete	2.35	No
	Tied Concrete with Sympathy Joints	2.25	
	Tied Concrete	2.35	No
	Asphalt	1.75	
	Tied Concrete with Sympathy Joints	2.25	No
	Asphalt	1.75	
Slag[b]	Tied Concrete	2.83	No
	Asphalt[c]	1.00	

[a] No recycled pavements with asphalt shoulders existed in the database.

[b] No slag pavements with tied concrete shoulders having sympathy joints existed in the database.

[c] All slag pavements with asphalt shoulders in the database had a 4.3 m widened lane with traffic stripes painted 0.6 m from the pavement edge.

was found between natural gravel pavements having the two types of tied concrete shoulders. This may be attributable to variability in the parameters not controlled for this analysis.

Shoulder type also had a significant effect on transverse cracking for recycled pavements. For this aggregate type, a significantly higher number of cracks occurred in pavements having concrete shoulders with sympathy joints compared to those having concrete shoulders without such joints. This is reasonable considering the tendency for cracking in the mainline pavement adjacent to shoulder sympathy joints.

For carbonate pavements, Table 2 shows that shoulder type did not significantly affect the occurrence of transverse cracking. It actually appears that tied concrete shoulders (with and without sympathy joints) tended to result in slightly more cracks than asphalt shoulders - contrary to what is expected. Also, tied concrete shoulders without sympathy joints appear to have resulted in slightly more cracks than such shoulders with sympathy joints. These anomalies can probably both be attributed to variability in the parameters not controlled for this analysis.

No significant difference in number of cracks per slab was found between slag pavements having tied concrete shoulders and those having asphalt shoulders. Although the difference was not significant, it can be seen that the pavements with tied concrete shoulders actually demonstrated more transverse cracking than those with asphalt shoulders – contrary to expectations. One reason for this could again be the variability in the parameters not controlled in this analysis. Another reason could be that the slag pavements with asphalt shoulders had 4.3 m widened lanes with traffic stripes painted at 3.7 m. The combination of widened lanes and painting the stripes 0.6 m from the

pavement edge tends to move traffic loads away from the critical midslab edge position. This results in lower tensile bending stresses and less transverse fatigue cracks.

As the results indicate, several of the shoulder type ANOVA analyses in this study suggested that there was not a significant effect of shoulder type on transverse cracking. Such statistically insignificant results were attributed to variability in parameters that are believed to affect transverse cracking, but were not controlled in these analyses. It is surmised that if such variability in parameters had been able to be controlled, significant relationships between shoulder type and transverse cracking (those described in the beginning of this section) may have been obtained in these cases.

Despite statistically insignificant findings in the cases alluded to above, a significant effect of shoulder type on cracking was found in the analyses involving natural gravel and recycled pavements. These results indicated that a significantly greater number of transverse cracks occur for pavements with asphalt shoulders than for those with tied concrete shoulders. They further indicated that more transverse cracks occur for pavements having tied concrete shoulders with sympathy joints than for those having tied concrete shoulders without such joints. Such results are in direct agreement with the expected cracking behavior of pavements with these shoulder types.

VOLUMETRIC SURFACE TEXTURE (VST) TESTING

A relatively new analysis procedure, VST testing, was utilized in this research to determine, among other things, the effect of aggregate type on crack face surface texture. The surface texture of a crack face is directly related to the potential for aggregate interlock load transfer across a transverse crack. Greater surface texture allows for more

interlocking and friction between aggregates of opposing crack faces, which corresponds to better load transfer across a crack. Considering this relationship between surface texture and load transfer potential, an assessment of the relative crack performance potential of pavements with the aggregates considered in this study was also obtained through the VST test results. A description of the testing performed in this study, the VST test procedure itself, and the results obtained in this study are given below.

Eighteen core specimens taken at cracks in this study were sent to the University of Minnesota, where this test method was developed, to be tested for surface texture using the VST test procedure. A detailed explanation of this test procedure is given by Wade et al. in [58]. Five cores each from carbonate, natural gravel, and recycled concrete pavements were tested. The cores to be tested were selected on the basis of the crack within the core. Wherever possible, cores with full-depth cracks were chosen. Choosing such cores helped to facilitate the VST testing process, as the cores must be split into two halves (along the crack) prior to testing. Full-depth cracks also provide a larger area for testing. Only three cores tested were from slag pavements, as these were the only slag cores available at the time such testing was done. A brief description of the VST test procedure follows.

The VST test procedure involves testing a given area of a crack face (cracked core face in this case) for surface texture. This test area is divided into many smaller individual areas (A_i) in a grid pattern. For each of these individual areas, distances (d_i) are measured from an arbitrary datum plane to the fractured surface within that area. The average distance from the datum plane (d_{ave}) is then calculated, and the differences, $r_i = d_i - d_{ave}$, are computed for each of the individual areas. These differences, r_i, are then

multiplied by their respective areas, A_i. The product of r_i and A_i is V_i, the volume of material above or void space below the plane defined by d_{ave} for the individual area. The absolute values of all V_i's are then summed, and the resulting quantity is divided by the total test area to produce the microtexture volumetric surface texture ratio (VSTR). The VSTR indicates the volume of texture per surface area of the specimen. A high VSTR indicates a rough surface texture, while a low value indicates a smooth texture. [58]

It should be noted that both a microtexture and macrotexture VSTR can be computed. Microtexture VSTR quantifies the surface texture within a fracture plane due to aggregate protrusions or roughness in the paste texture, whereas macrotexture VSTR accounts for both the surface texture of the fracture surface and texture due to multiple fracture planes (adjacent fracture planes oriented at angles to one another). Only microtexture VSTR's were considered in this analysis. [61]

Results from the VST testing in this study are presented in Table 3. For each specimen tested the microtexture VSTR is given as well as a visual assessment of the core's surface texture, which was made at the time of testing. The mode of fracture through the core (i.e., through or around the aggregates) is also included in this table.

The visual assessments of surface texture are found to be mostly in agreement with the VSTR values. That is, higher VSTR values generally correspond to "rougher" texture assessments. Such correspondence between visual observations and test results indicates that this may indeed be a valid procedure for assessing surface texture.

A relationship between the mode of concrete fracture and surface texture is also evident in Table 3. Cracks that propagated through the aggregates were generally found to have smoother surface texture (and lower VSTR's), whereas cracks propagating

Table 3 Volumetric Surface Texture Test Results.

Specimen Name	Aggregate Type	Microtexture VSTR (cm^3/cm^2)	Microtexture	Mode of Fracture (T)hrough / (A)round
CARB-1	Carbonate	0.0678	Smooth	90%T
CARB-2	Carbonate	0.0767	Smooth	99%T
CARB-3	Carbonate	0.0958	Smooth	Poor Visability[a]
CARB-4	Carbonate	0.0691	Smooth	98%A
CARB-5	Carbonate	0.0429	Smooth-Moderate	99%T
NG-1	Natural Gravel	0.1624	Rough	95%A
NG-2	Natural Gravel	0.1238	Rough	60%A
NG-3	Natural Gravel	0.2498	Moderate	90%A
NG-4	Natural Gravel	0.1406	Moderate	80%A
NG-5	Natural Gravel	0.0550	Moderate	98%A
RCY-1	Recycled Concrete	0.1426	Rough	80%T
RCY-2	Recycled Concrete	0.0419	Smooth	99%T
RCY-3	Recycled Concrete	0.1699	Moderate	85%T
RCY-4	Recycled Concrete	0.0878	Moderate	90%T
RCY-5	Recycled Concrete	0.0635	Smooth	95%T
SLAG-1	Slag	0.0663	Smooth	70%T
SLAG-2	Slag	0.0781	Smooth	99%T
SLAG-3	Slag	0.0659	Smooth-Moderate	95%A

[a] Poor visability - was unable to tell whether the fractures went through or around the aggregate particles.

around the aggregates were associated with rougher texture (and higher VSTR's). This relationship can be easily explained, as cracks that propagate around the aggregates result in a greater amount of aggregate protrusions at the crack face and thus more surface texture.

The effect of concrete aggregate type on surface texture is also readily apparent in Table 3. It can be seen that carbonate and slag specimens were generally found to have smooth surface texture, while natural gravel specimens demonstrated rough texture. Recycled concrete specimens showed a range of surface texture from smooth to rough.

The difference in texture between natural gravel specimens and carbonate specimens can be explained in terms of the relative aggregate–paste bond strength and the aggregate strength of each specimen type. Natural gravel aggregates form a relatively weak bond with the paste due to their rounded shape. Cracks are thus more likely to propagate around these aggregates at the aggregate-paste interface rather than through the aggregates, which are relatively strong. Conversely, the angular shape of carbonate aggregates produces a strong aggregate-paste bond for such specimens, and cracks thus tend to propagate through rather than around these aggregates, which can be relatively weak. Considering the relation between mode of fracture and surface texture explained above, it is reasonable that natural gravel specimens have a rougher texture than carbonate specimens. [14]

The smooth surface texture of slag specimens is likely due to the porosity and size of the slag aggregates. These aggregates are often relatively weak due to their high porosity. Consequently, cracks can easily propagate through the aggregates, leading to a smooth texture at the crack face. Even if cracks propagate around slag aggregates, poor

texture often results due to the typically small size of the aggregates, which leads to a reduced volume of protrusions from the crack face.

The variable surface texture found for the recycled concrete specimens can be primarily attributed to the composite nature of these aggregates. Recycled aggregates are composed of old aggregate particles partially covered with old mortar. At a given crack face, a higher old mortar content will translate to a lower amount of aggregate particles protruding from the face. Thus, recycled aggregates with high old mortar contents will result in a relatively smooth crack face. Conversely, if a low old mortar content is obtained, a rough surface texture can be achieved. The old mortar content obtained in practice depends on the crushing process used during recycling. It should be noted that the surface texture of these specimens also depends to a lesser extent on the type of old aggregate used. [35]

Based on these VST results, an assessment of the relative crack performance potential of carbonate, natural gravel, recycled, and slag pavements can be made. Noting the relationship between surface texture and load transfer potential explained earlier in this section (i.e., greater surface texture corresponds to better aggregate interlock load transfer potential), the test results indicate that natural gravel pavements should show the best transverse crack performance. Slag and carbonate pavements are likely to demonstrate relatively poor crack performance, based on these results, due to the smooth crack face texture associated with these pavements. The performance of cracks in recycled pavements is uncertain, according to the VST test results, as the crack face surface texture of these pavements depends on the old mortar content of the aggregates.

A few comments on the VST test procedure itself and its usefulness are warranted here. The results from this study suggest that the VST test method is a promising means for assessing crack face surface texture and aggregate interlock potential. Further work is needed, however, to refine the test procedure and to develop relationships between VSTR and crack performance parameters. Vandenbossche and Snyder developed one such relationship between VSTR and load transfer efficiency [35]. Their work was described in Chapter II. Once relationships between VSTR and performance parameters are established, a better understanding and assessment of aggregate property effects on crack performance will be possible through VST testing.

- CHAPTER VII -

Conclusions, Recommendations, and Future Research Needs

CONCLUSIONS AND RECOMMENDATIONS

Three FWD analysis procedures - backcalculation of pavement support and stiffness parameters, determination of crack performance parameters, and assessment of void potential near cracks – were demonstrated using field data from this study:

- A backcalculation procedure for determining the AREA, ℓ, E, and k of JCP's using FWD midslab data was described in this thesis. Determination of these parameters is useful in characterizing the support and stiffness properties of a pavement system and allows for the computation of several crack performance parameters that were discussed in this thesis. This procedure was used on data collected in this study to determine AREA, ℓ, E, and k values for the test site pavements. The results obtained were very reasonable with the exception of those pavements that were concrete overlays. In general, the following ranges of values were obtained in this study: AREA: 1050 - 1250 mm, ℓ: 900 - 1300 mm, E: 3.0×10^7 - 6.5×10^7 kPa, and k: 25 - 85 kPa/mm. These values are typical of those normally associated with these parameters. Exaggerated E and k values resulted for the overlay pavements due to the presence of the underlying pavement layer, which acted as a stiff base support layer.

- Procedures for determining three crack performance parameters, LTE_δ, P_T, and AGG, were also described in this thesis. Each of these parameters characterizes crack performance in a slightly different way. Determination of these parameters and subsequent comparison of the parametric values with threshold limits allows for evaluation of cracks in a pavement network. When integrated into a comprehensive pavement evaluation scheme, these evaluations can act as a useful tool in planning and selecting rehabilitation activities for the pavement network.

LTE_δ, P_T, and AGG can be determined using FWD wheelpath data and knowledge of the support and stiffness characteristics (k and ℓ) of the pavement. Two procedures for determining these parameters were described in this thesis. One method, the "standard" procedure, was used to determine parametric values for selected cracks and joints in this study. In this method, LTE_δ is directly computed using FWD data, and P_T and AGG are indirectly derived from this LTE_δ value. It was explained that the "standard" procedure may be too cumbersome and time-consuming for practical everyday use by a transportation agency. Thus, a second, streamlined method for computing these parameters was developed in this study. In this streamlined approach, LTE_δ is computed using the same procedure as is used in the "standard" method. However, the procedure for determining P_T and AGG is different in this approach, as these parameters are determined directly from LTE_δ values. This streamlined approach requires an initial effort by a transportation agency to develop direct relationships between LTE_δ and P_T and LTE_δ and AGG, but compensates for this effort through the time saved and ease of use that it affords thereafter.

Based on the parametric values computed and fault data collected in this study, threshold limits were established for the three noted performance parameters. Thresholds of 70%, 16.5 kN, and 2.0×10^5 kPa were found for LTE_δ, P_T, and AGG, respectively. A suggested criteria for using the performance parameters would thus be that a crack is considered to be in acceptable condition if all of its parametric values are greater than the thresholds given above. If any of the threshold criteria are not met, the crack is considered to be in unacceptable condition.

Field data from this study was also used to determine the effect of temperature on the performance parameters. Increasing the pavement surface temperature was found to result in higher LTE_δ's. Since P_T and AGG are derived from LTE_δ, it is assumed that temperature would have a similar effect on these parameters. This temperature effect is caused by downward curling and thermal expansion of slabs at high pavement temperatures, which result in tighter crack widths and better aggregate interlock load transfer potential. This effect mandates that pavement surface temperature at the time of FWD wheelpath testing be considered when using the performance parameters to characterize crack performance. Visual crack distress surveys should accompany FWD testing to aid in assessing crack condition when temperatures render FWD results ambiguous. To limit the effects of temperature on parametric values, temperature restrictions could be placed on when this testing can be performed.

- A voids analysis procedure, which can be used to assess the likelihood of loss of support at cracks and joints in JCP's, was also described in this thesis. By detecting

the presence of voids at cracks and joints, this procedure allows appropriate rehabilitation actions to be taken to restore support to cracked JCP's. This procedure involves the use of FWD deflection data taken at crack and joint corner locations for a range of load magnitudes. It is recommended that voids testing be performed at ambient temperatures less than 27°C to ensure that conservative results will be obtained [41].

In this procedure, deflection (x-axis) data is plotted versus load magnitude (y-axis) for a given crack or joint, and an x-intercept is obtained. This x-intercept is compared to a threshold value to determine void potential for the crack or joint. An x-intercept above the threshold value indicates that there is a loss of support.

The voids analysis procedure was performed at selected cracks and joints in this study. Results from these analyses indicated that this procedure is a valid method for estimating void potential. Based on the voids analysis results and fault data collected in this study, a threshold range of 50 to 75 μm was established for x-intercept values when using this procedure. Values above this range would indicate a loss of support, while values below this range would signify that no voids exist at those locations. Values within the threshold range would require that coring (or some other method) be used to further investigate the void potential at those locations.

In addition to the above analyses involving FWD data, several other analyses were performed on field data from this research to study the effects of various factors on transverse cracking in JCP's. Findings related to these analyses are summarized below.

- Longer joint spacing was found to lead to a greater number of transverse cracks per slab. This was attributed to the larger curling stresses generally associated with longer slabs.

- Pavements containing slag or recycled concrete coarse aggregates demonstrated a larger number of transverse cracks per slab than those using natural gravel or carbonate aggregates. A greater susceptibility to shrinkage cracking for slag and recycled pavements, when proper curing considerations are neglected, was cited as a possible reason for this.

- An analysis of the effect of shoulder type on transverse cracking revealed that natural gravel pavements having tied concrete shoulders (with and without sympathy joints) had significantly less cracks per slab than those having asphalt shoulders. Tied concrete shoulders essentially eliminate the critical midslab free edge load condition and thus reduce the slab tensile stresses that cause fatigue cracking. Less fatigue cracking (and thus transverse cracking) thus occurs for pavements with tied concrete shoulders than for those with asphalt shoulders. This effect was not observed in pavements containing other aggregate types, possibly due to variability in parameters not controlled in this analysis.

The shoulder type analysis also revealed that recycled pavements having tied concrete shoulders with sympathy joints had a significantly greater number of cracks per slab than those having tied concrete shoulders without such joints. This is reasonable, since sympathy joints almost inevitably lead to transverse cracking in the mainline pavement adjacent to these joints, as the slab and shoulder respond differently to thermal variations. No such effect was observed in the pavements containing the other aggregate types, again probably due to variability in parameters not controlled in this analysis.

- A relatively new analysis procedure, VST testing, was performed at the University of Minnesota (where this test method was developed) on cores from this study. This testing was done to determine, among other things, the effect of aggregate type on crack face surface texture. Very reasonable results were obtained from this testing, as good agreement was found between visual assessments of surface texture and values for the surface texture indicator in this procedure, VSTR. Results from this testing also agreed with the intuitively reasonable notion that cracks propagating around aggregates lead to a rougher surface texture than cracks propagating through aggregates.

Concerning aggregate type effects, the VST test results revealed a smooth crack face surface texture for carbonate and slag specimens, whereas natural gravel specimens had a rough texture. Recycled specimens demonstrated a range of textures. These differences in surface texture between aggregate types were attributed primarily to the

bond strengths and aggregate strengths typical of the aggregate types, which affect the mode of fracture. The surface texture of recycled specimens is believed to be dependent on the amount of old mortar clinging to the aggregates. This accounts for the variable texture found for these specimens.

Noting that greater surface texture corresponds to better aggregate interlock load transfer potential, these test results can be used to make inferences regarding the crack performance potential of pavements with the four noted aggregate types. Based on the test results, natural gravel pavements should show the best crack performance, while slag and carbonate pavements should demonstrate relatively poor crack performance. The performance of cracks in recycled pavements is uncertain, based on the test results.

The VST test results from this study suggest that this test method is a promising means for assessing crack face surface texture, and thus, aggregate interlock load transfer potential.

In addition to the factor effects determined using the data in this study, other factors affecting transverse cracking have been determined in previous research studies. A summary of these findings was given in the literature review (Chapter II) section of this thesis. These findings, along with those determined in this study, could prove useful to a transportation agency in improving the performance of JCP's with regard to

transverse cracking. A brief listing of some of these factor effects is therefore given below.

The literature review revealed the following factors to affect the occurrence of transverse cracking in JCP's:

- Provision of good drainage to the pavement leads to less fatigue cracks. Increased slab thickness and high concrete strength also result in less fatigue cracks. Fatigue cracking can also be reduced by using widened slabs (4.0 to 4.3 m in width) with traffic stripes painted at 3.7 m. [11]

- A combination of high aggregate content, moderate cement content, and low moisture content lessen the potential for drying shrinkage cracks. [9]

The following factors were found through the literature review to affect the performance of transverse cracking in JCP's:

- Larger concrete coarse aggregates lead to improved load transfer effectiveness and endurance. Harder aggregates result in better load transfer endurance. [13]

- A coarser aggregate gradation provides higher load transfer efficiency than a finer gradation [22].

- Virgin aggregates lead to better load transfer endurance than recycled aggregates [33].

- Higher concrete strength provides higher load transfer efficiency [24].

- Increased slab thickness leads to better load transfer efficiency [2]. Thicker slabs also increase load transfer endurance [30].

FUTURE RESEARCH NEEDS

The work performed in this study revealed a few areas where future research is warranted. These future research needs are listed below.

- There is a need for development of a reliable, consistent, and accurate method for measuring the width of transverse cracks in JCP's. As was explained in this thesis, several problems currently exist in obtaining crack width measurements. These include: 1) lack of a reliable device for measuring the widths, 2) the difficulty encountered in locating the actual crack opening for cracks with severe surface deterioration, and 3) surface measurements of crack width may not be indicative of the crack width throughout the slab depth, where aggregate interlock occurs. In order to use crack width in future discussions and analyses of transverse crack performance, these difficulties must be addressed.

- Laboratory and/or field studies, where all variables (especially temperature and number/magnitude of load applications) except concrete coarse aggregate properties are controlled, are needed to investigate and better understand the effect of aggregate properties on transverse crack performance.

  This need is being partially addressed by a research study just started at Michigan State University. This research study will involve a laboratory investigation of transverse cracking in JCP's. It is actually being performed as a complement to the field component of the MDOT project under which this thesis work was conducted. In this laboratory investigation, the effect of concrete coarse aggregate type, size, and gradation on the measured performance (in terms of LTE_{δ}, P_T, and AGG) of transverse cracks will be studied.

- Another research need, which is related to the need just discussed, involves VST testing. Further work is needed to refine this relatively new test method and to develop relationships between VSTR and crack performance parameters such as LTE_{δ}, P_T, and AGG. If such relationships can be established, VST testing could be used as a means for better understanding aggregate property effects on crack performance.

APPENDICES

APPENDIX A: INVENTORY DATA

Table A.1 Test Site Location and Age Data, Carbonate Pavements.

Site No.	Location	Year of Const.	Age of Pav't (yrs.)
5	Route: I-69 EB; @ Sta 43+00; Btwn MP 173 & 174; West of Exit 176; West of Martin Rd; ~35 Miles East of Flint, MI	1983	15
6	Route: I-69 EB; Starts @ Sta 78+00; Just East of MP 174; West of Exit 176; Just East of Martin Rd; ~35 Miles East of Flint, MI	1983	15
7	Route: I-69 EB; Starts @ Sta 100+00; Btwn MP 174 & 175; Exit 176 1 Mile Sign; West of Exit 176; ~35 Miles East of Flint, MI	1983	15
8	Route: I-69 WB; Just East of MP 167; Btwn Sta 1197+00 & Sta 1196+00; West of Exit 168; ~30 Miles East of Flint, MI	1984	14
35	Route: I-69 SB; Starts 13' North of Sta 1769+00; Btwn MP 68 & 67; North of Exit 66; ~15 Miles South of Lansing, MI	1991	7
36	Route: I-69 SB; Starts 23' South of Sta 1768+00; Just South of Site #35; Btwn MP 68 & 67; North of Exit 66; ~15 Miles South of Lansing, MI	1991	7
38	Route: I-94 EB; Starts @ Sta 1238+00; Just East of MP 146; Btwn Exits 145 & 147; ~35 Miles West of Ann Arbor, MI	1960	38
39	Route: I-94 EB; Btwn MP 146 & 147; Starts 41' East of Site #38; Btwn Exits 145 & 147; ~35 Miles West of Ann Arbor, MI	1960	38
42	Route: US-23 SB; 5' North of Sta 1048+00; Btwn MP 18 & Exit 17; North of Exit 17; ~20 Miles South of Ann Arbor, MI	1984	14
43	Route: US-23 SB; Btwn MP 18 & Exit 17; Just South of Site #42; Starts 32' South of Sta 1046+00; North of Exit 17; ~20 Miles South of Ann Arbor, MI	1984	14
44	Route: US-23 SB; Btwn MP 18 & Exit 17; Just South of Site #43; Starts 32' South of Sta 1044+00; Ends 25' South of Sta 1042+00; North of Exit 17; ~20 Miles South of Ann Arbor, MI	1984	14
45	Route: US-23 SB; Btwn MP 8 & 7; Starts 22' South of Sta 514+00; South of Exit 9; ~30 Miles South of Ann Arbor, MI	1995	3
46	Route: US-23 SB; Btwn MP 8 & 7; Starts 27' South of Site #45; South of Exit 9; ~30 Miles South of Ann Arbor, MI	1995	3
49	Route: I-75 SB; Starts 12' South of Sta 543+00; Ends 20'-1" South of Sta 542+00; Just North of MP 12; North of Exit 11; ~15 Miles North of Toledo, OH	1989	9
50	Route: I-75 SB; Starts 5'-7" North of Sta 747+00; Ends 2' South of Sta 746+00; Just North of MP 16; North of Exit 15; ~15 Miles North of Toledo, OH	1989	9

Table A.1 (cont'd).

Site No.	Location	Year of Const.	Age of Pav't (yrs.)
51	Route: I-75 SB; Btwn MP 17 & 16; Starts 57' North of Sta 769+00; Just South of Site #52; South of Exit 18; ~20 Miles North of Toledo, OH	1989	9
52	Route: I-75 SB; Starts 50' North of Sta 775+00; Btwn MP 17 & 16; South of Exit 18; ~15 Miles North of Toledo, OH	1989	9

Table A.2 Test Site Location and Age Data, Natural Gravel Pavements.

Site No.	Location	Year of Const.	Age of Pav't (yrs.)
2	Route: I-69 WB; Starts @ Sta 815+00; Ends @ Sta 813+00; ~1 Mile West of MP 104; Btwn MP 104 & 103; Just West of Site #3; West of Exit 105; ~20 Miles East of Lansing, MI	1990	8
3	Route: I-69 WB; Starts @ Sta 818+00; Just West of MP 104; West of Exit 105; ~20 Miles East of Lansing, MI	1990	8
4	Route: I-69 EB; @ Sta 1534+93; Btwn MP 154 & 155; Just East of Turnaround; East of Exit 153; ~20 Miles East of Flint, MI	1970	28
9	Route: I-69 WB; @ Sta 975+00; Btwn MP 144 & 143; East of Exit 143; ~10 Miles East of Flint, MI	1969	Rehab.
10	Route: I-69 WB; Starts 27'-6" West of Sta 969+00; Btwn MP 144 & 143; Just East of Exit 143; ~10 Miles East of Flint, MI	1969	29
37	Route: I-69 SB; Starts 31' North of Sta 2899+00; Ends 12' South of Sta 2898+00; Just North of MP 54; South of Exit 57; ~20 Miles South of Lansing, MI	1971	27
38A	Route: I-69 SB; Starts 24'-6" South of Sta 2898+00; Just South of MP 54; Just South of Site #37; South of Exit 57; ~20 Miles South of Lansing, MI	1971	27
57	Route: I-69 WB; Starts 14'-7" East of Sta 158 (Metric); Just East of MP 86; Just East of Exit 85; ~5 Miles North of Lansing, MI	1981	17

Table A.3 Test Site Location and Age Data, Recycled Pavements.

Site No.	Location	Year of Const.	Age of Pav't (yrs.)
11	Route: I-94 WB; Starts 27' East of Sta 305+00; @ MP 106; Btwn Exits 104 & 108; ~10 Miles East of Battle Creek, MI	1986	12
12	Route: I-94 WB; Starts 37'-6" West of Sta 304+00; Just West of MP 106; Just West of Site #11; Btwn Exits 104 & 108; ~10 Miles East of Battle Creek, MI	1986	12
13	Route: I-94 WB; Starts 1'-4" West of Sta 302+00; Just West of MP 106; Just West of Site #12; Btwn Exits 104 & 108; ~10 Miles East of Battle Creek, MI	1986	12
14	Route: I-94 WB; Starts 12'-3" West of Sta 1281+00; Just West of MP 91; West of Exit 92; ~5 Miles West of Battle Creek, MI	1983	15
15	Route: I-94 WB; Starts 24' East of Sta 1279+00; Btwn MP 91 & 90; Just West of Site #14; West of Exit 92; ~5 Miles West of Battle Creek, MI	1983	15
16	Route: I-94 WB; Starts 12' East of Sta 893+00; Btwn MP 84 & 83; Btwn Exits 85 & 81; ~10 Miles East of Kalamazoo, MI	1986	12
17	Route: I-94 WB; Starts 27' West of Sta 891+00; Btwn MP 84 & 83; Btwn Exits 85 & 81; ~10 Miles East of Kalamazoo, MI	1986	12
27	Route: I-94 WB; Starts 15'-6" East of Sta 1300+00; Btwn MP 65 & 64; West of Exit 66; ~15 Miles West of Kalamazoo, MI	1987	11
28	Route: I-94 WB; Starts 11' East of Sta 1298+00; Starts 41' West of Site #27; Btwn MP 65 & 64; West of Exit 66; ~15 Miles West of Kalamazoo, MI	1987	11
29	Route: I-94 WB; Starts 8'-6" East of Sta 1116+00; Btwn MP 62 & 61; Just West of Exit 60 Sign; East of Exit 60; ~15 Miles West of Kalamazoo, MI	1988	10
31	Route: I-94 EB; Starts 39'-7" East of Sta 658+00; Btwn MP 112 & 113; East of Exit 112; ~20 Miles East of Battle Creek, MI	1988	10
32	Route: I-94 EB; Starts 15' West of Sta 661+00; Btwn MP 112 & 113; Just East of Site #31; East of Exit 112; ~20 Miles East of Battle Creek, MI	1988	10
47	Route: I-75 NB; Starts 11' South of Sta 73+00; @ MP 1; ~5 Miles North of Toledo, OH	1987	Rehab.
48	Route: I-75 NB; Just North of Site #47; ~5 Miles North of Toledo, OH	1987	Rehab.

Table A.4 Test Site Location and Age Data, Slag Pavements.

Site No.	Location	Year of Const.	Age of Pav't (yrs.)
1	Route: I-69 WB; Starts @ Sta 610+00 (Just East of Peacock Rd); Just West of MP 97; West of Exit 98; ~10 Miles East of Lansing, MI	1990	8
40	Route: I-94 WB; Starts 54' East of Sta 321+00; Btwn MP 186 & 185; Wash. Co.; Just West of Exit 186; ~5 Miles East of Ann Arbor, MI	1987	11
41	Route: I-94 WB; Starts @ Sta 306+00; Btwn MP 186 & 185; West of Site #40; Just West of Exit 186; ~5 Miles East of Ann Arbor, MI	1987	11
55	Route: I-94 EB; Starts 7'-2" East of Sta 1791+00; Btwn MP 38 & 39; West of Exit 39; ~35 Miles West of Kalamazoo, MI	1995	3
58	Route: US-23 NB; Starts 13'-6" North of Sta 603+00; Just South of MP 89; Btwn Exits 88 & 90; ~10 Miles South of Flint, MI	1992	6
59	Route: US-23 NB; Starts 51' South of Sta 605+00; Starts Just South of MP 89; Just North of Site #58; Btwn Exits 88 & 90; ~10 Miles South of Flint, MI	1992	6
60	Route: US-23 NB; Starts 25' North of Sta 608+00; Just North of MP 89; Btwn Exits 88 & 90; ~10 Miles South of Flint, MI	1992	6
61	Route: US-23 SB; Starts 44' North of Sta 566+00; Btwn MP 89 & 88; Btwn Exits 88 & 90; ~10 Miles South of Flint, MI	1992	6
62	Route: US-23 SB; Starts 8' North of Sta 565+00; Btwn MP 89 & 88; Just South of Site #61; Btwn Exits 88 & 90; ~10 Miles South of Flint, MI	1992	6
63	Route: I-94 EB; Starts @ Sta 1793+00; Btwn MP 38 & 39; West of Exit 39; ~35 Miles West of Kalamazoo, MI	1995	3

Table A.5 Geometric Layout of Test Sites[a], Carbonate Pavements.

Site No.	Number of Slabs	Joint Spacing (m)	Length of Test Site (m)	Shoulder Width (m)	Shoulder Type
5	4	12.5	50.0	2.4	Concrete / Sympathy Joints
6	4	12.5	50.0	2.4	Concrete / Sympathy Joints
7	4	12.5	50.0	2.4	Concrete / Sympathy Joints
8	4	12.5	50.0	2.4	Concrete / Sympathy Joints
35	3	8.2	24.7	3.0	Asphalt
36	4	8.2	32.9	3.0	Asphalt
38	5	12.5	62.5	2.7	Concrete
39	4	12.5	50.0	2.7	Concrete
42	4	12.5	50.0	2.4	Concrete
43	3	12.5	37.5	2.4	Concrete
44	5	12.5	62.5	2.4	Concrete
45	4	8.2	32.9	3.0	Concrete
46	3	8.2	24.7	3.0	Concrete
49	4	8.2	32.9	3.7	Concrete
50	4	8.2	32.9	3.7	Concrete
51	3	By Slab: 12.5/12.5/8.2	33.2	3.7	Concrete
52	4	8.2	32.9	3.7	Concrete

[a] All sites in this table have a 3.7 m lane width.

Table A.6 Geometric Layout of Test Sites[a], Natural Gravel Pavements.

Site No.	Number of Slabs	Joint Spacing (m)	Length of Test Site (m)	Shoulder Width (m)	Shoulder Type
2	5	12.5	62.5	2.7	Concrete
3	4	12.5	50.0	2.7	Concrete
4	3	21.6	64.9	2.7	Asphalt
9	3	21.6	64.9	2.7	Asphalt
10	2	21.6	43.3	2.7	Asphalt
37	2	21.6	43.3	2.7	Asphalt
38A	2	21.6	43.3	2.7	Asphalt
57	4	12.5	50.0	2.7	Concrete / Sympathy Joints

[a] All sites in this table have a 3.7 m lane width.

Table A.7 Geometric Layout of Test Sites[a], Recycled Pavements.

Site No.	Number of Slabs	Joint Spacing (m)	Length of Test Site (m)	Shoulder Width (m)	Shoulder Type
11	3	12.5	37.5	2.7	Concrete
12	3	12.5	37.5	2.7	Concrete
13	3	12.5	37.5	2.7	Concrete
14	3	12.5	37.5	2.7	Concrete / Sympathy Joints
15	3	12.5	37.5	2.7	Concrete / Sympathy Joints
16	3	12.5	37.5	2.7	Concrete
17	4	12.5	50.0	2.7	Concrete
27	4	12.5	50.0	2.7	Concrete
28	4	12.5	50.0	2.7	Concrete
29	4	12.5	50.0	2.7	Concrete
31	3	12.5	37.5	2.7	Concrete
32	3	12.5	37.5	2.7	Concrete
47	2	12.5	25.0	3.7	Concrete
48	2	12.5	25.0	3.7	Concrete

[a] All sites in this table have a 3.7 m lane width.

Table A.8 Geometric Layout of Test Sites[a], Slag Pavements.

Site No.	Number of Slabs	Joint Spacing (m)	Length of Test Site (m)	Shoulder Width (m)	Shoulder Type
1	4	12.5	50.0	2.7	Concrete
40	3	12.5	37.5	3.4	Concrete
41	4	12.5	50.0	3.4	Concrete
55	8	4.9	39.0	2.6	Asphalt
58	4	8.2	32.9	3.0	Concrete
59	4	8.2	32.9	3.0	Concrete
60	4	8.2	32.9	3.0	Concrete
61	4	8.2	32.9	3.0	Concrete
62	4	8.2	32.9	3.0	Concrete
63	6	4.9	29.3	2.6	Asphalt

[a] All sites in this table have a 3.7 m lane width, except Sites 55 and 63, which have a 4.3 m widened lane.

Table A.9 Pavement Cross-Section Data, Carbonate Pavements.

Site No.	Cross-Section			Base Type	Subbase Type	Subgrade Type
	PCC (mm)	Base (mm)	Subbase (mm)			
5	254	102	203	O.G.D.C.	No Data	No Data
6	254	102	203	O.G.D.C.	No Data	No Data
7	254	102	203	O.G.D.C.	No Data	No Data
8	241	102	203	O.G.D.C.	No Data	No Data
35	241	127	254	O.G.D.C.	No Data	Locke Conover
36	241	127	254	O.G.D.C.	No Data	Locke Conover
38	216 (Possible Overlay)	76	No Data	"Select Subbase"	No Data	No Data
39	216 (Possible Overlay)	76	No Data	"Select Subbase"	No Data	No Data
42	178 (Unbonded Conc. Overlay)	76	229	"Select Subbase"	No Data	No Data
43	178 (Unbonded Conc. Overlay)	76	229	"Select Subbase"	No Data	No Data
44	178 (Unbonded Conc. Overlay)	76	229	"Select Subbase"	No Data	No Data
45	267	76	305	Agg. Base	No Data	No Data
46	267	76	305	Agg. Base	No Data	No Data
49	305	102	406	O.G.D.C. w/ Geotextile Separator	No Data	No Data
50	305	102	No Data	O.G.D.C. w/ Geotextile Separator	No Data	No Data
51	305	102	No Data	O.G.D.C. w/ Geotextile Separator	No Data	No Data

Table A.9 (cont'd).

Site No.	Cross-Section			Base Type	Subbase Type	Subgrade Type
	PCC (mm)	Base (mm)	Subbase (mm)			
52	305	102	No Data	O.G.D.C. w/ Geotextile Separator	No Data	No Data

Table A.10 Pavement Cross-Section Data, Natural Gravel Pavements.

Site No.	Cross-Section			Base Type	Subbase Type	Subgrade Type
	PCC (mm)	Base (mm)	Subbase (mm)			
2	241	102	254	O.G.D.C.	Sand	Clay
3	241	102	254	O.G.D.C.	Sand	Clay
4	229	102	356	"Select Subbase"	No Data	No Data
9	229	102	254	"Select Subbase"	No Data	No Data
10	229	102	254	"Select Subbase"	No Data	No Data
37	241	102	No Data	"Select Subbase"	No Data	No Data
38A	241	102	No Data	"Select Subbase"	No Data	No Data
57	241	102	254	Agg. Base	Silt	Clay

Table A.11 Pavement Cross-Section Data, Recycled Pavements.

Site No.	Cross-Section			Base Type	Subbase Type	Subgrade Type
	PCC (mm)	Base (mm)	Subbase (mm)			
11	267	102	432	O.G.D.C.	Sand	No Data
12	267	102	432	O.G.D.C.	Sand	No Data
13	267	102	432	O.G.D.C.	Sand	No Data
14	254	76	305	"Condit.'d Agg. Base"	No Data	No Data
15	254	76	305	"Condit.'d Agg. Base"	No Data	No Data
16	254	102	No Data	O.G.D.C.	No Data	No Data
17	254	102	No Data	O.G.D.C.	No Data	No Data
27	279	102	432	O.G.D.C.	Sand	No Data
28	279	102	432	O.G.D.C.	Sand	No Data
29	279	102	432	O.G.D.C.	Sand	No Data
31	267	102	305	O.G.D.C.	Sand	No Data
32	267	102	305	O.G.D.C.	Sand	No Data
47	305	102	305	O.G.D.C.	No Data	Silty Clay; Loamy Sand
48	305	102	305	O.G.D.C.	No Data	Silty Clay; Loamy Sand

Table A.12 Pavement Cross-Section Data, Slag Pavements.

Site No.	Cross-Section			Base Type	Subbase Type	Subgrade Type
	PCC (mm)	Base (mm)	Subbase (mm)			
1	254	102	254	O.G.D.C.	Sand	Clay
40	305	102	254	O.G.D.C.	No Data	No Data
41	305	102	254	O.G.D.C.	No Data	No Data
55	305	102	203	O.G.D.C. w/ Geotextile Separator	No Data	No Data
58	254	178	No Data	Asphalt Stab. O.G.D.C. + Agg. Base	No Data	No Data
59	254	178	No Data	Asphalt Stab. O.G.D.C. + Agg. Base	No Data	No Data
60	254	178	No Data	Asphalt Stab. O.G.D.C. + Agg. Base	No Data	No Data
61	254	178	No Data	Asphalt Stab. O.G.D.C. + Agg. Base	No Data	No Data
62	254	178	No Data	Asphalt Stab. O.G.D.C. + Agg. Base	No Data	No Data
63	305	102	203	O.G.D.C. w/ Geotextile Separator	No Data	No Data

Table A.13 Material and Construction Properties, Carbonate Pavements.

Site No.	Grade of Concrete	Construction Conditions					
		Ambient Temp.'s (C)		Concrete Temp.'s (C)		Weather	
		A.M.	P.M.	A.M.	P.M.	A.M.	P.M.
5	35P (Mod)	21	32	29	31	No Data	No Data
6	35P (Mod)	21	30	31	32	No Data	No Data
7	35P (Mod)	21	30	31	32	No Data	No Data
8	35P	17	20	23	24	Cloudy	Cloudy
35	35P	15	30	24	26	Clear	Clear
36	35P	15	30	24	26	Clear	Clear
38	No Data	17	29	No Data	No Data	Clear	Clear
39	No Data	17	29	No Data	No Data	Clear	Clear
42	35P	30	30	27	29	No Data	No Data
43	35P	30	30	27	29	No Data	No Data
44	35P	30	30	27	29	No Data	No Data
45	35P	8	12	No Data	No Data	No Data	No Data
46	35P	8	12	No Data	No Data	No Data	No Data
49	35P (Mod)	17	20	21	26	Sunny	Sunny
50	35P (Mod)	18	25	22	29	No Data	No Data
51	35P (Mod)	26	27	27	27	Cloudy, Humid	Overcast
52	35P (Mod)	24	26	27	27	Cloudy, Rain	Windy, Overcast

Table A.14 Material and Construction Properties, Natural Gravel Pavements.

Site No.	Grade of Concrete	Construction Conditions					
		Ambient Temp.'s (C)		Concrete Temp.'s (C)		Weather	
		A.M.	P.M.	A.M.	P.M.	A.M.	P.M.
2	35P	16	26	No Data	No Data	No Data	No Data
3	35P	16	26	No Data	No Data	No Data	No Data
4	No Data	22	No Data	25	No Data	Cloudy, Rain	No Data
9	35P	18	22	23	26	Cloudy	Cloudy
10	35P	18	22	23	26	Cloudy	Cloudy
37	No Data	No Data	No Data	No Data	No Data	No Data	No Data
38A	No Data	No Data	No Data	No Data	No Data	No Data	No Data
57	35P	12	15	12	15	Clear	Clear

Table A.15 Material and Construction Properties, Recycled Pavements.

Site No.	Grade of Concrete	Construction Conditions					
		Ambient Temp.'s (C)		Concrete Temp.'s (C)		Weather	
		A.M.	P.M.	A.M.	P.M.	A.M.	P.M.
11	35P	21	30	26	27	Clear	Clear
12	35P	21	30	26	27	Clear	Clear
13	35P	21	30	26	27	Clear	Clear
14	35P	11	22	22	24	No Data	No Data
15	35P	11	22	22	24	No Data	No Data
16	35P	21	27	21	22	Overcast	Overcast
17	35P	21	27	21	22	Overcast	Overcast
27	35P (Mod)	27	35	28	31	Clear	Clear
28	35P (Mod)	27	35	28	31	Clear	Clear
29	35P (Mod)	-1	17	8	8	No Data	No Data
31	35P	16	24	21	23	Sunny	Sunny
32	35P	7	No Data	16	No Data	Sunny	Sunny
47	35P	8	8	19	21	Cloudy	Cloudy
48	35P	8	8	19	21	Cloudy	Cloudy

Table A.16 Material and Construction Properties, Slag Pavements.

Site No.	Grade of Concrete	Construction Conditions					
		Ambient Temp.'s (C)		Concrete Temp.'s (C)		Weather	
		A.M.	P.M.	A.M.	P.M.	A.M.	P.M.
1	35P	21	27	No Data	No Data	No Data	No Data
40	35S	3	12	11	No Data	Clear	Clear
41	35S	0	11	13	15	Clear	Clear
55	35P	No Data	No Data	29	31	Cloudy	Cloudy
58	35P	17	26	20	28	Sunny	Sunny
59	35P	17	26	20	28	Sunny	Sunny
60	35P	17	26	20	28	Sunny	Sunny
61	35P	16	30	18	24	Sunny	Sunny
62	35P	16	30	18	24	Sunny	Sunny
63	35P	No Data	No Data	29	31	Cloudy	Cloudy

Table A.17 Traffic Data, Carbonate Pavements.

Site No.	Traffic										1998
	1987		1994		1995		1996		1997		
	ADT	% Com.	ADT	% Com.	ADT	% Com.	ADT	% Com.	ADT	% Com.	Cum. Traffic (10^6 ESALs)
5	3,226	10	6,000	20	5,500	22	6,500	19	12,500	22	5.3
6	3,226	10	6,000	20	5,500	22	6,500	19	12,500	22	5.3
7	3,226	10	6,000	20	5,500	22	6,500	19	12,500	22	5.3
8	7,495	14	8,500	17	8,500	18	9,000	24	7,000	30	8.7
35	12,000	13	12,500	16	12,500	16	13,000	16	13,500	15	4.2
36	12,000	13	12,500	16	12,500	16	13,000	16	13,500	15	4.2
38	14,900	28	19,500	20	18,500	22	17,500	23	18,500	27	45
39	14,900	28	19,500	20	18,500	22	17,500	23	18,500	27	45
42	11,650	16	13,000	21	13,000	21	13,500	17	15,500	25	15
43	11,650	16	13,000	21	13,000	21	13,500	17	15,500	25	15
44	11,650	16	13,000	21	13,000	21	13,500	17	15,500	25	15
45	9,353	16	12,500	16	12,500	16	11,500	23	13,000	20	2.3
46	9,353	16	12,500	16	12,500	16	11,500	23	13,000	20	2.3
49	22,300	27	27,000	20	27,000	21	26,000	22	29,000	19	16
50	25,150	26	27,500	20	27,000	21	28,500	20	30,500	19	17
51	25,150	26	27,500	20	27,000	21	28,500	20	30,500	19	17
52	25,150	26	27,500	20	27,000	21	28,500	20	30,500	19	17

Table A.18 Traffic Data, Natural Gravel Pavements.

Site No.	Traffic										1998
	1987		1994		1995		1996		1997		
	ADT	% Com.	ADT	% Com.	ADT	% Com.	ADT	% Com.	ADT	% Com.	Cum. Traffic (10^6 ESALs)
2	10,486	12	13,000	19	12,500	21	12,500	21	13,000	22	6.0
3	10,486	12	13,000	19	12,500	21	12,500	21	13,000	22	6.0
4	10,000	14	10,000	12	12,000	20	12,000	20	12,500	22	11
9	14,350	7	15,500	9	15,500	11	16,500	16	16,500	16	N/A
10	14,350	7	15,500	9	15,500	11	16,500	16	16,500	16	13
37	7,250	11	9,500	26	9,000	29	9,500	27	9,500	27	15
38A	7,250	11	9,500	26	9,000	29	9,500	27	9,500	27	15
57	3,747	10	12,000	19	13,500	19	14,000	20	14,500	19	16

Table A.19 Traffic Data, Recycled Pavements.

Site No.	Traffic										1998
	1987		1994		1995		1996		1997		
	ADT	% Com.	ADT	% Com.	ADT	% Com.	ADT	% Com.	ADT	% Com.	Cum. Traffic (10^6 ESALs)
11	16,500	22	18,000	24	18,000	34	19,500	31	20,000	30	19
12	16,500	22	18,000	24	18,000	34	19,500	31	20,000	30	19
13	16,500	22	18,000	24	18,000	34	19,500	31	20,000	30	19
14	19,150	19	19,500	23	17,000	36	14,000	43	19,000	32	25
15	19,150	19	19,500	23	17,000	36	14,000	43	19,000	32	25
16	17,767	13	22,000	23	22,500	27	16,500	37	18,000	34	25
17	17,767	13	22,000	23	22,500	27	16,500	37	18,000	34	25
27	11,100	20	15,500	26	14,500	33	13,000	37	18,000	27	15
28	11,100	20	15,500	26	14,500	33	13,000	37	18,000	27	15
29	11,100	20	15,500	26	14,500	33	13,000	37	18,000	27	15
31	10,600	21	15,000	28	14,000	31	13,500	36	14,500	34	13
32	10,600	21	15,000	28	14,000	31	13,500	36	14,500	34	13
47	19,000	27	24,000	23	23,500	24	19,500	29	21,000	27	N/A
48	19,000	27	24,000	23	23,500	24	19,500	29	21,000	27	N/A

Table A.20 Traffic Data, Slag Pavements.

Site No.	Traffic										1998
	1987		1994		1995		1996		1997		
	ADT	% Com.	ADT	% Com.	ADT	% Com.	ADT	% Com.	ADT	% Com.	Cum. Traffic (10^6 ESALs)
1	10,486	12	13,000	19	12,500	21	12,500	21	12,500	22	5.9
40	27,768	21	24,500	11	24,500	12	36,000	8	37,500	8	15
41	27,768	21	24,500	11	24,500	12	36,000	8	37,500	8	15
55	14,400	18	16,000	24	15,500	25	13,000	30	13,000	30	3.6
58	21,250	9	22,500	10	25,500	13	26,000	12	26,000	11	5.2
59	21,250	9	22,500	10	25,500	13	26,000	12	26,000	11	5.2
60	21,250	9	22,500	10	25,500	13	26,000	12	26,000	11	5.2
61	21,250	9	22,500	10	25,500	13	26,000	12	26,000	11	5.2
62	21,250	9	22,500	10	25,500	13	26,000	12	26,000	11	5.2
63	14,400	18	16,000	24	15,500	25	13,000	30	13,000	30	3.6

APPENDIX B: MEASURED AND DERIVED FIELD DATA

Table B.1 Measured Crack and Joint Field Data I, Carbonate Pavements.

Site No.	Test Type	Crack/Joint Width (mm)				Faulting[a,b] (mm)	
		Apr. 1997	July 1997	Oct. 1997	June 1998	Apr. 1997[c]	June 1998[d,e]
5	C	0.14	0.12	0.45	0.58	0.80	No
	C	0.14	0.17	0.42	0.45	0.05	No
	J	14.80	14.00	16.15	15.20	-0.50	No
6	C	0.08	0.12	0.19	0.19	0.15	No
	C	0.05	0.03	0.40	0.39	0.70	No
	J	14.62	16.91	17.72	17.73	-0.45	No
7	C	0.99	0.60	0.62	0.43	-0.25	No
	C	0.50	Fault	0.50	0.40	-1.05	5
	J	15.72	15.28	18.13	17.89	-0.85	No
8	C	0.13	0.15	0.40	0.33	0.30	No
	C	0.15	0.17	0.18	0.14	0.40	No
	J	15.86	16.46	17.50	16.84	-1.05	No
35	C	0.20	0.15	0.15	0.13	0.50	No
	C	0.19	0.17	0.24	0.19	0.15	No
	J	14.29	13.38	14.22	13.72	-0.15	No
36	C	0.08	0.08	0.08	0.10	-1.00	No
	C	0.05	0.05	0.20	0.17	0.80	No
	J	13.40	13.51	13.19	13.32	-0.50	No
38	C	0.20	0.16	No Data	0.10	-0.30	No
	C	0.16	0.18	No Data	0.10	-0.10	No
	C	0.08	0.10	No Data	0.08	0.35	No
	J	16.06	15.05	No Data	16.69	-0.70	No
39	C	0.11	0.10	No Data	0.08	0.55	No
	C	0.14	0.10	No Data	0.08	-0.35	No
	C	0.09	0.10	No Data	0.08	0.30	No
	J	16.64	14.42	No Data	16.11	0.00	No
42	C	0.13	0.16	0.59	0.58	0.80	No
	C	0.33	0.41	0.19	0.51	-0.70	No
	J	15.50	15.40	16.11	No Data	-0.30	No
43	C	0.20	0.20	0.19	0.40	-0.50	No
	C	0.90	1.00	Spall	Spall	-1.30	3
	J	14.92	14.33	15.46	No Data	-0.10	No

[a] Faulting was not measured during July and Oct. 1997 testing cycles.

[b] Positive fault values mean that leave side was lower than approach side.

[c] April 1997 faulting was measured using electronic faultmeter.

[d] June 1998 faulting was measured manually using a straightedge.

[e] No faulting is reported for cracks/joints that had less than 2 mm of faulting (if any).

Table B.1 (cont'd).

Site No.	Test Type	Crack/Joint Width (mm)				Faulting[a,b] (mm)	
		Apr. 1997	July 1997	Oct. 1997	June 1998	Apr. 1997[c]	June 1998[d,e]
43	J	15.83	15.31	16.09	No Data	-0.30	No
44	C	No Data	0.15	0.10	0.18	No Data	No
	C	No Data	1.00	Spall	Spall	No Data	-3
	J	No Data	15.09	16.18	16.27	No Data	No
	J	No Data	15.14	16.85	No Data	No Data	No
	J	No Data	17.64	15.71	No Data	No Data	6
	J	No Data	15.17	15.33	No Data	No Data	No
45	C	No Data	0.10	0.24	0.28	No Data	No
	J	No Data	17.99	18.28	18.87	No Data	No
	J	No Data	18.18	18.74	18.62	No Data	No
46	C	No Data	0.30	0.41	0.43	No Data	No
	J	No Data	17.26	14.84	18.15	No Data	No
	J	No Data	16.82	16.92	17.45	No Data	No
49	C	0.30	0.11	0.23	0.16	-0.25	No
	J	20.05	16.93	17.35	17.32	-0.65	No
50	C	0.25	1.53	Spall	Spall	-1.65	3
	C	0.05	0.07	0.24	0.33	-0.15	No
	C	0.09	0.11	0.49	0.46	0.35	No
	C	0.06	0.07	0.33	Spall	-0.25	4
	J	18.67	15.89	16.92	16.58	-1.15	No
51	C	1.00	1.50	Spall	Spall	-0.15	No
	C	0.03	0.01	0.62	0.55	0.20	No
	C	0.11	0.14	0.44	0.46	0.30	No
	C	0.24	0.20	0.26	0.23	-0.50	No
52	C	0.29	0.30	0.31	0.32	0.00	No
	C	0.37	0.25	0.34	0.32	0.15	No
	C	0.09	0.10	0.30	0.32	0.95	No
	J	20.31	18.12	18.09	17.80	-0.70	No

[a] Faulting was not measured during July and Oct. 1997 testing cycles.

[b] Positive fault values mean that leave side was lower than approach side.

[c] April 1997 faulting was measured using electronic faultmeter.

[d] June 1998 faulting was measured manually using a straightedge.

[e] No faulting is reported for cracks/joints that had less than 2 mm of faulting (if any).

Table B.2 Measured Crack and Joint Field Data I, Natural Gravel Pavements.

Site No.	Test Type	Crack/Joint Width (mm)				Faulting[a,b] (mm)	
		Apr. 1997	July 1997	Oct. 1997	June 1998	Apr. 1997[c]	June 1998[d,e]
2	C	0.37	0.20	0.21	0.31	0.85	No
	C	0.40	0.30	0.35	0.26	0.40	No
	C	0.32	0.20	0.23	0.19	0.35	No
	J	19.42	16.67	20.15	17.90	0.80	No
3	C	0.18	0.20	0.25	0.15	-1.60	No
	C	0.21	0.23	0.44	0.42	-0.05	No
	C	0.19	0.18	0.70	0.65	0.00	No
	J	18.62	15.81	19.33	17.41	-0.35	No
4	C	0.18	0.20	0.90	0.68	1.10	No
	C	0.41	0.45	0.75	0.69	0.40	No
	J	15.64	12.55	17.46	19.93	-3.65	6
9	C	0.40	No Data	No Data	No Data	-0.80	No Data
	C	Fault	No Data	No Data	No Data	-6.40	No Data
	J	12.59	No Data	No Data	No Data	-1.85	No Data
10	C	4.11	No Data	Spall	Spall	-5.35	5
	C	4.04	No Data	Spall	Spall	-4.05	4
	C	0.45	No Data	0.25	0.31	-0.50	No
	J	12.96	No Data	13.82	13.50	-0.45	No
37	C	0.22	0.25	0.90	0.57	1.05	No
	C	Spall	1.24	Spall	Spall	-4.90	5
	C	Spall	0.18	Spall	Spall	-8.85	10
	C	Fault	1.08	0.80	Spall	-9.30	11
	C	Spall	0.73	Spall	Spall	-6.20	5
	C	0.55	0.16	Spall	Spall	0.85	No
	J	10.19	9.40	11.92	11.26	-7.35	8
38A	C	0.12	0.15	1.38	0.76	0.60	No
	C	Spall	0.30	Spall	Spall	-10.05	11
	C	0.11	0.15	Spall	Spall	0.55	No
	C	0.11	0.13	Spall	Spall	0.10	No
	C	0.35	0.39	Spall	Spall	0.45	No
	C	0.65	0.48	0.53	0.58	0.35	No
	J	10.19	9.72	12.07	9.41	-8.15	9

[a] Faulting was not measured during July and Oct. 1997 testing cycles.

[b] Positive fault values mean that leave side was lower than approach side.

[c] April 1997 faulting was measured using electronic faultmeter.

[d] June 1998 faulting was measured manually using a straightedge.

[e] No faulting is reported for cracks/joints that had less than 2 mm of faulting (if any).

Table B.2 (cont'd).

Site No.	Test Type	Crack/Joint Width (mm)				Faulting[a,b] (mm)	
		Apr. 1997	July 1997	Oct. 1997	June 1998	Apr. 1997[c]	June 1998[d,e]
57	C	0.07	0.08	0.41	0.33	0.75	No
	C	0.06	0.09	0.69	0.49	0.65	No
	C	0.06	0.04	0.37	0.27	0.35	No
	C	0.04	0.05	0.48	0.41	1.05	No
	C	0.29	0.48	0.32	0.35	0.00	No
	J	14.09	15.37	16.64	15.20	0.05	No
	J	13.17	13.00	15.41	13.88	-0.75	No

[a] Faulting was not measured during July and Oct. 1997 testing cycles.

[b] Positive fault values mean that leave side was lower than approach side.

[c] April 1997 faulting was measured using electronic faultmeter.

[d] June 1998 faulting was measured manually using a straightedge.

[e] No faulting is reported for cracks/joints that had less than 2 mm of faulting (if any).

Table B.3 Measured Crack and Joint Field Data I, Recycled Pavements.

Site No.	Test Type	Crack/Joint Width (mm)				Faulting[a,b] (mm)	
		Apr. 1997	July 1997	Oct. 1997	June 1998	Apr. 1997[c]	June 1998[d,e]
11	C	0.80	0.85	Spall	Spall	-5.40	9
	C	0.25	0.30	0.30	0.46	0.20	No
	C	0.28	0.27	0.38	0.44	-0.50	No
	C	0.12	0.20	0.21	0.22	-0.35	No
	C	1.38	1.30	Spall	Spall	-4.35	5
	C	0.55	0.50	0.37	0.63	0.15	No
	C	0.37	0.30	Spall	Spall	-2.10	5
	J	17.30	16.81	19.12	17.65	-0.85	No
12	C	0.90	1.40	Spall	Spall	-2.95	4
	C	0.27	0.20	0.22	0.28	0.80	No
	C	0.65	0.70	0.10	Spall	-5.85	5
	C	0.55	0.60	Spall	Spall	-6.15	6
	C	0.40	0.44	Spall	Spall	-3.65	5
	C	0.40	0.25	0.30	0.30	0.50	No
	J	15.96	17.10	16.27	16.29	-0.25	No
13	C	0.13	0.15	Spall	Spall	-0.60	4
	C	0.12	0.15	0.29	0.23	0.05	No
	C	0.90	1.42	Spall	Spall	-3.60	4
	J	14.85	15.09	16.07	15.88	-0.40	No
	J	17.54	19.26	19.27	19.38	-0.85	No
14	C	0.28	0.25	0.16	0.16	-0.20	No
	C	0.12	0.15	0.18	0.22	-0.05	No
	C	0.19	0.20	0.20	0.10	-0.15	No
	C	0.08	0.15	0.18	0.08	0.00	No
	J	13.42	12.88	14.88	13.10	-1.15	No
15	C	0.15	0.10	0.12	0.08	-0.30	No
	C	0.10	0.10	0.08	0.08	-0.40	No
	C	0.13	0.16	0.25	0.30	0.55	No
	J	14.61	14.31	16.25	15.88	-1.20	No
	J	13.93	12.85	15.51	14.24	-0.90	No
16	C	No Data	0.70	No Data	Fault	No Data	4
	C	No Data	0.27	No Data	0.40	No Data	No

[a] Faulting was not measured during July and Oct. 1997 testing cycles.

[b] Positive fault values mean that leave side was lower than approach side.

[c] April 1997 faulting was measured using electronic faultmeter.

[d] June 1998 faulting was measured manually using a straightedge.

[e] No faulting is reported for cracks/joints that had less than 2 mm of faulting (if any).

Table B.3 (cont'd).

Site No.	Test Type	Crack/Joint Width (mm)				Faulting[a,b] (mm)	
		Apr. 1997	July 1997	Oct. 1997	June 1998	Apr. 1997[c]	June 1998[d,e]
16	C	No Data	0.33	No Data	0.67	No Data	No
	J	No Data	15.97	No Data	15.33	No Data	No
	J	No Data	16.92	No Data	16.70	No Data	3
	J	No Data	16.43	No Data	17.17	No Data	No
	J	No Data	16.80	No Data	16.43	No Data	No
17	C	No Data	0.92	No Data	Spall	No Data	7
	C	No Data	0.30	No Data	0.29	No Data	No
	J	No Data	14.76	No Data	15.32	No Data	No
	J	No Data	15.34	No Data	15.48	No Data	No
	J	No Data	15.13	No Data	15.31	No Data	2
27	C	No Data	0.33	0.35	0.26	No Data	No
	C	No Data	0.65	Spall	Spall	No Data	4
	J	No Data	16.49	18.86	16.57	No Data	No
	J	No Data	15.19	18.80	15.11	No Data	No
	J	No Data	16.17	17.84	16.16	No Data	No
28	C	No Data	0.40	0.45	Spall	No Data	3
	C	No Data	0.38	0.34	0.41	No Data	No
	C	No Data	0.36	0.32	0.32	No Data	No
	J	No Data	16.52	18.84	16.98	No Data	No
	J	No Data	16.40	19.06	17.03	No Data	No
	J	No Data	16.02	18.17	16.25	No Data	No
29	C	No Data	0.20	0.18	0.10	No Data	No
	C	No Data	0.20	Spall	Spall	No Data	6
	J	No Data	16.87	18.35	16.99	No Data	No
	J	No Data	16.23	18.72	16.59	No Data	No
	J	No Data	16.81	17.89	16.93	No Data	No
	J	No Data	15.76	17.59	15.98	No Data	3
31	C	No Data	0.44	0.45	0.25	No Data	2
	C	No Data	0.30	Spall	Spall	No Data	5
	J	No Data	16.09	18.32	17.45	No Data	No
	J	No Data	16.61	18.73	17.17	No Data	No
	J	No Data	16.33	17.32	16.40	No Data	No

[a] Faulting was not measured during July and Oct. 1997 testing cycles.

[b] Positive fault values mean that leave side was lower than approach side.

[c] April 1997 faulting was measured using electronic faultmeter.

[d] June 1998 faulting was measured manually using a straightedge.

[e] No faulting is reported for cracks/joints that had less than 2 mm of faulting (if any).

Table B.3 (cont'd).

Site No.	Test Type	Crack/Joint Width (mm)				Faulting[a,b] (mm)	
		Apr. 1997	July 1997	Oct. 1997	June 1998	Apr. 1997[c]	June 1998[d,e]
32	C	No Data	Patch	0.45	0.23	No Data	7
	C	No Data	0.33	0.45	0.20	No Data	No
	C	No Data	0.15	Spall	Spall	No Data	No
	J	No Data	16.89	19.18	17.96	No Data	No
	J	No Data	16.21	18.48	17.87	No Data	No
	J	No Data	16.43	18.34	16.45	No Data	No
47	C	0.30	No Data	No Data	No Data	0.55	No Data
	C	0.50	No Data	No Data	No Data	0.00	No Data
	C	0.24	No Data	No Data	No Data	-0.40	No Data
	C	Spall	No Data	No Data	No Data	-3.20	No Data
	J	15.17	No Data	No Data	No Data	-0.95	No Data
48	C	Spall	No Data	No Data	No Data	-5.10	No Data
	C	0.25	No Data	No Data	No Data	-0.35	No Data
	C	0.20	No Data	No Data	No Data	-2.50	No Data
	C	0.33	No Data	No Data	No Data	-1.95	No Data
	C	0.32	No Data	No Data	No Data	-0.25	No Data
	J	18.41	No Data	No Data	No Data	-1.40	No Data
	J	17.43	No Data	No Data	No Data	-0.95	No Data

[a] Faulting was not measured during July and Oct. 1997 testing cycles.

[b] Positive fault values mean that leave side was lower than approach side.

[c] April 1997 faulting was measured using electronic faultmeter.

[d] June 1998 faulting was measured manually using a straightedge.

[e] No faulting is reported for cracks/joints that had less than 2 mm of faulting (if any).

Table B.4 Measured Crack and Joint Field Data I, Slag Pavements.

Site No.	Test Type	Crack/Joint Width (mm)				Faulting[a,b] (mm)	
		Apr. 1997	July 1997	Oct. 1997	June 1998	Apr. 1997[c]	June 1998[d,e]
1	C	0.37	0.33	0.42	0.20	0.20	No
	C	0.16	0.18	0.23	0.22	0.05	No
	C	0.22	0.20	0.28	0.25	0.25	No
	C	0.15	0.17	0.47	0.33	0.45	No
	J	14.38	13.70	14.42	14.29	-0.15	No
40	C	0.55	0.22	No Data	0.58	0.30	No
	C	0.23	0.18	No Data	0.20	0.30	No
	J	16.48	18.20	No Data	16.77	-0.65	No
41	C	0.45	0.14	No Data	0.63	0.07	No
	C	0.40	0.30	No Data	0.34	-0.30	No
	C	0.21	0.31	No Data	0.60	-0.13	No
	C	0.19	0.21	No Data	0.21	-0.45	No
	J	14.37	14.42	No Data	14.59	0.05	No
55	C	0.32	0.13	0.37	0.17	-0.65	No
	C	0.32	0.27	0.24	0.15	-0.65	No
	J	12.09	11.19	12.38	11.70	0.10	No
	J	11.90	10.94	12.04	11.71	-0.25	No
	J	12.13	11.24	12.07	11.73	-0.60	No
	J	11.94	11.29	12.29	12.09	-0.25	No
58	C	No Data	0.15	0.12	0.10	No Data	No
	C	No Data	0.15	0.29	0.28	No Data	No
	J	No Data	13.83	14.45	12.95	No Data	No
	J	No Data	14.93	15.77	14.36	No Data	No
	J	No Data	13.92	15.06	13.51	No Data	No
	J	No Data	14.57	15.65	13.95	No Data	No
59	C	No Data	0.13	0.15	0.15	No Data	No
	C	No Data	0.15	0.17	0.19	No Data	No
	J	No Data	14.32	15.74	14.46	No Data	No
	J	No Data	14.26	15.26	14.44	No Data	No
	J	No Data	13.11	14.03	12.56	No Data	No
60	C	No Data	0.20	0.17	0.16	No Data	No
	C	No Data	0.25	0.25	0.27	No Data	No

[a] Faulting was not measured during July and Oct. 1997 testing cycles.

[b] Positive fault values mean that leave side was lower than approach side.

[c] April 1997 faulting was measured using electronic faultmeter.

[d] June 1998 faulting was measured manually using a straightedge.

[e] No faulting is reported for cracks/joints that had less than 2 mm of faulting (if any).

Table B.4 (cont'd).

Site No.	Test Type	Crack/Joint Width (mm)				Faulting[a,b] (mm)	
		Apr. 1997	July 1997	Oct. 1997	June 1998	Apr. 1997[c]	June 1998[d,e]
60	J	No Data	12.74	13.96	13.13	No Data	No
	J	No Data	14.86	15.95	15.16	No Data	No
	J	No Data	14.09	15.20	14.88	No Data	No
61	C	No Data	0.15	0.23	0.18	No Data	No
	C	No Data	0.20	0.24	0.23	No Data	No
	J	No Data	15.42	15.70	16.52	No Data	No
	J	No Data	13.38	15.09	13.59	No Data	No
	J	No Data	14.24	14.68	13.45	No Data	No
	J	No Data	14.26	15.41	14.77	No Data	No
62	C	No Data	0.15	0.21	0.16	No Data	No
	C	No Data	0.15	0.18	0.16	No Data	No
	J	No Data	14.72	16.27	14.90	No Data	No
	J	No Data	14.26	15.32	14.10	No Data	No
	J	No Data	13.79	15.24	14.68	No Data	No
63	C	No Data	No Data	0.27	0.16	No Data	No
	C	No Data	No Data	0.15	0.15	No Data	No
	J	No Data	No Data	12.80	11.40	No Data	No
	J	No Data	No Data	12.82	No Data	No Data	No
	J	No Data	No Data	13.05	No Data	No Data	No

[a] Faulting was not measured during July and Oct. 1997 testing cycles.

[b] Positive fault values mean that leave side was lower than approach side.

[c] April 1997 faulting was measured using electronic faultmeter.

[d] June 1998 faulting was measured manually using a straightedge.

[e] No faulting is reported for cracks/joints that had less than 2 mm of faulting (if any).

Table B.5 Measured Crack and Joint Field Data II, Carbonate Pavements.

Site No.	Type of Core	Crack Type (Core Specimen)	Slab Number	Number of Cracks	Avg. Crack Spacing (m)	Joint Spacing (m)
5	Crack	Aggregate	1	4	2.4	12.5
	Joint	Mortar	2	2	4.2	12.5
			3	3	2.8	12.5
			4	2	4.1	12.5
6	Crack	Mortar	1	3	2.8	12.5
	Joint	Mortar	2	2	3.9	12.5
			3	3	2.8	12.5
			4	3	2.5	12.5
7	Crack	Aggregate	1	3	2.7	12.5
	Joint	Mortar	2	2	3.9	12.5
			3	6	1.3	12.5
			4	3	2.8	12.5
8	Crack	Mortar	1	1	7.4	12.5
	Joint	Mortar	2	3	2.7	12.5
			3	2	3.8	12.5
			4	1	7.4	12.5
35	Crack	Surface Crack	1	4	1.4	8.2
	Joint	Mortar	2	1	4.0	8.2
			3	0	-----	8.2
36	Crack	Aggregate	1	3	1.9	8.2
	Joint	Mortar	2	1	5.2	8.2
			3	1	5.2	8.2
			4	0	-----	8.2
38	Crack	Mortar	1	5	1.8	12.5
	Joint	Mortar	2	1	9.1	12.5
			3	3	3.0	12.5
			4	6	1.4	12.5
			5	2	4.2	12.5
39	Crack	Surface Crack	1	2	3.0	12.5
	Joint	Mortar	2	2	3.7	12.5
			3	2	3.0	12.5
			4	2	2.3	12.5
42	Crack	Aggregate	1	2	2.2	12.5
	Joint	Mortar	2	0	-----	12.5
			3	1	6.4	12.5
			4	1	8.1	12.5
43	Crack	Aggregate	1	2	3.5	12.5

Table B.5 (cont'd).

Site No.	Type of Core	Crack Type (Core Specimen)	Slab Number	Number of Cracks	Avg. Crack Spacing (m)	Joint Spacing (m)
43	Joint	Mortar	2	1	6.7	12.5
			3	0	-----	12.5
44	Crack	Aggregate	1	2	3.4	12.5
	Joint	Mortar	2	2	3.3	12.5
			3	1	4.9	12.5
			4	1	5.8	12.5
			5	3	2.7	12.5
45	Crack	Aggregate	1	1	3.9	8.2
	Joint	Mortar	2	3	1.7	8.2
			3	1	4.3	8.2
			4	1	4.3	8.2
46	Crack	Aggregate	1	1	4.4	8.2
	Joint	Mortar	2	1	4.0	8.2
			3	2	2.1	8.2
49	Crack	Aggregate	1	0	-----	8.2
	Joint	Mortar	2	3	1.7	8.2
			3	1	4.3	8.2
			4	1	3.6	8.2
50	Crack	Aggregate	1	3	1.8	8.2
	Joint	Mortar	2	2	2.7	8.2
			3	4	1.3	8.2
			4	2	2.9	8.2
51	Crack	Aggregate	1	5	1.7	12.5
	Joint	Expansion	2	4	2.2	12.5
		Joint	3	2	2.4	8.2
52	Crack	Aggregate	1	5	1.0	8.2
	Joint	Mortar	2	2	2.2	8.2
			3	1	3.1	8.2
			4	4	1.3	8.2

Table B.6 Measured Crack and Joint Field Data II, Natural Gravel Pavements.

Site No.	Type of Core	Crack Type (Core Specimen)	Slab Number	Number of Cracks	Avg. Crack Spacing (m)	Joint Spacing (m)
2	Crack	Mortar	1	2	3.3	12.5
	Joint	Mortar	2	1	6.2	12.5
			3	0	-----	12.5
			4	1	7.1	12.5
			5	1	5.9	12.5
3	Crack	Aggregate	1	1	6.1	12.5
	Joint	Mortar	2	0	-----	12.5
			3	1	7.0	12.5
			4	2	2.3	12.5
4	Crack	Aggregate	1	5	3.7	21.6
	Joint	No Data	2	2	5.6	21.6
			3	6	3.0	21.6
9	Crack	Mortar	1	3	4.6	21.6
	Joint	No Data	2	3	4.8	21.6
			3	3	5.8	21.6
10	Crack	Mortar	1	3	4.8	21.6
	Joint	Mortar	2	4	3.8	21.6
37	Crack	Mortar	1	3	5.1	21.6
	Joint	Mortar	2	3	5.2	21.6
38A	Crack	Mortar	1	6	3.0	21.6
	Joint	No Data	2	5	3.6	21.6
57	Crack	Mortar	1	1	6.1	12.5
	Joint	Mortar	2	2	4.1	12.5
			3	2	3.7	12.5
			4	1	4.0	12.5

Table B.7 Measured Crack and Joint Field Data II, Recycled Pavements.

Site No.	Type of Core	Crack Type (Core Specimen)	Slab Number	Number of Cracks	Avg. Crack Spacing (m)	Joint Spacing (m)
11	Crack	Mortar	1	3	3.0	12.5
	Joint	No Data	2	6	1.6	12.5
			3	3	3.0	12.5
12	Crack	Aggregate	1	4	2.2	12.5
	Joint	Mortar	2	4	3.7	12.5
			3	6	1.5	12.5
13	Crack	Mortar	1	3	3.1	12.5
	Joint	Mortar	2	3	3.4	12.5
			3	3	3.4	12.5
14	Crack	Mortar	1	10	0.9	12.5
	Joint	Mortar	2	5	1.8	12.5
			3	7	1.2	12.5
15	Crack	Aggregate	1	3	2.9	12.5
	Joint	Mortar	2	7	1.1	12.5
			3	7	1.4	12.5
16	Crack	Mortar	1	5	1.9	12.5
	Joint	Aggregate	2	3	2.4	12.5
			3	2	3.2	12.5
17	Crack	No Data	1	4	2.3	12.5
	Joint	Mortar	2	2	2.4	12.5
			3	4	2.5	12.5
			4	2	2.8	12.5
27	Crack	Mortar	1	3	3.1	12.5
	Joint	Mortar	2	5	1.6	12.5
			3	2	4.7	12.5
			4	1	9.4	12.5
28	Crack	Mortar	1	4	2.2	12.5
	Joint	Mortar	2	2	4.2	12.5
			3	2	4.8	12.5
			4	5	2.0	12.5
29	Crack	Mortar	1	1	3.4	12.5
	Joint	Mortar	2	4	2.3	12.5
			3	3	2.7	12.5
			4	4	2.3	12.5
31	Crack	Mortar	1	4	2.6	12.5
	Joint	Mortar	2	5	2.0	12.5
			3	5	1.8	12.5

Table B.7 (cont'd).

Site No.	Type of Core	Crack Type (Core Specimen)	Slab Number	Number of Cracks	Avg. Crack Spacing (m)	Joint Spacing (m)
32	Crack	Mortar	1	3	2.6	12.5
	Joint	Mortar	2	4	2.4	12.5
			3	5	1.8	12.5
47	Crack	Aggregate	1	3	3.1	12.5
	Joint	Mortar	2	3	3.4	12.5
48	Crack	Aggregate	1	4	2.6	12.5
	Joint	Mortar	2	5	1.7	12.5

Table B.8 Measured Crack and Joint Field Data II, Slag Pavements.

Site No.	Type of Core	Crack Type (Core Specimen)	Slab Number	Number of Cracks	Avg. Crack Spacing (m)	Joint Spacing (m)
1	Crack	Aggregate	1	4	2.3	12.5
	Joint	Mortar	2	3	3.5	12.5
			3	2	5.0	12.5
			4	3	3.1	12.5
40	Crack	Aggregate	1	3	2.7	12.5
	Joint	Mortar	2	0	-----	12.5
			3	1	7.8	12.5
41	Crack	Mortar	1	11	0.8	12.5
	Joint	Expansion	2	5	1.7	12.5
		Joint	3	3	3.0	12.5
			4	4	2.2	12.5
55	Crack	Aggregate	1	1	2.9	4.9
	Joint	Mortar	2	1	2.7	4.9
			3	1	2.4	4.9
			4	1	2.7	4.9
			5	1	2.1	4.9
			6	2	1.5	4.9
			7	2	2.0	4.9
			8	2	1.7	4.9
58	Crack	Aggregate	1	1	4.5	8.2
	Joint	Mortar	2	1	4.0	8.2
			3	1	4.2	8.2
			4	1	4.4	8.2
59	Crack	Aggregate	1	2	2.5	8.2
	Joint	Aggregate	2	0	-----	8.2
			3	1	4.4	8.2
			4	1	4.1	8.2
60	Crack	Mortar	1	1	3.8	8.2
	Joint	Aggregate	2	1	4.0	8.2
			3	1	4.1	8.2
			4	0	-----	8.2
61	Crack	Aggregate	1	2	2.6	8.2
	Joint	Mortar	2	1	3.7	8.2
			3	2	3.0	8.2
			4	3	1.8	8.2
62	Crack	Aggregate	1	2	2.3	8.2
	Joint	Mortar	2	3	1.2	8.2

Table B.8 (cont'd).

Site No.	Type of Core	Crack Type (Core Specimen)	Slab Number	Number of Cracks	Avg. Crack Spacing (m)	Joint Spacing (m)
62			3	3	2.1	8.2
			4	4	1.3	8.2
63	Crack	Aggregate	1	1	2.4	4.9
	Joint	Aggregate	2	1	2.1	4.9
			3	1	2.7	4.9
			4	1	2.4	4.9
			5	1	2.4	4.9
			6	2	1.4	4.9

Table B.9 Visual Distress Data, Carbonate Pavements.

Site No.	Distress Comments
5	Faulting: C1 & C2 of S1, C2 of S2; Spalling: C1 & C2 of S1, C1 & C2 of S2, C3 of S3, C1 & C2 of S4, J3; Exposed Reinforcement; Lane-Shoulder Dropoff
6	Faulting: C2 of S2; Spalling: C2 of S2, C2 of S3
7	Faulting: C1 of S2, C2 of S3, C2 & C3 of S4, Lane-Lane; Spalling: C1 of S2, C2 of S3, C3 of S4; Lane-Shoulder Dropoff
8	Lane-Shoulder Dropoff; Scaling on S1
35	Popouts; Shrinkage Cracking
36	Popouts; Shrinkage Cracking
38	Spalling: J3; Shrinkage Cracking
39	Shrinkage Cracking
42	Spalling: J1; Dropped Sealant: J1 & J5
43	Faulting: C1 of S2, J3; Spalling: C1 of S2; Dropped Sealant: J1, J2, J3, & J4; Lane-Shoulder Dropoff
44	Faulting: C1 of S5, J5; Spalling: C1 of S5, J5; Dropped Sealant: J4
45	Shrinkage Cracking
46	Shrinkage Cracking
49	Faulting: Lane-Lane; Sealant Damage: Lane-Lane; Polished Aggregate; Shrinkage Cracking
50	Faulting: C1 of S1, C1 of S4; Spalling: C1 of S1, C1 of S4; Sealant Damage: J5, Lane-Lane; Popouts; Polished Aggregate
51	Faulting: C1 & C4 of S2, J2, J3, Lane-Lane; Spalling: C2 of S1, C1 & C4 of S2; Sealant Damage: J1, J2, J4, Lane-Shoulder; Exposed Reinforcement; Lane-Shoulder Dropoff; Polished Aggregate
52	Faulting: Lane-Lane; Popouts; Polished Aggregate

Table B.10 Visual Distress Data, Natural Gravel Pavements.

Site No.	Distress Comments
2	Popouts
3	Spalling: C1 & C2 of S4
4	Faulting: J3, Lane-Lane; Spalling: C3 & C5 of S1, C2 of S2, J1, J3, J4; C4 of S1 is Concrete Patched; Popouts; Exposed Reinforcement; Lane-Shoulder Dropoff; Lane-Lane Separation; Polished Aggregate
9	No Data
10	Faulting: C1, C2, & C3 of S1, C2 & C4 of S2, Lane-Lane; Spalling: C1, C2, & C3 of S1, C2 & C4 of S2, J2, J3; Dropped Sealant: J1 & J3; C2 & C3 of S1 are Asphalt Patched; Lane-Shoulder Dropoff; Lane-Lane Separation; Polished Aggregate
37	Faulting: C2 & C3 of S1, C1 & C2 of S2, J1, J2, J3, Lane-Lane; Spalling: C1, C2, & C3 of S1, C1, C2, & C3 of S2, J2; Dropped Sealant: J3; Sealant Damage: J1, J2, & J3; C3 of S2 is Asphalt Patched; Lane-Shoulder Dropoff; Polished Aggregate
38A	Faulting: C2 of S1, C4 of S2, J1, J2, J3, Lane-Lane; Spalling: C1, C2, C3, & C6 of S1, C1, C2, & C4 of S2, J2; Sealant Damage: J1, J2, & J3; C2 & C3 of S1, C1, C2, & C4 of S2, J2 is Asphalt Patched; Lane-Shoulder Dropoff; Polished Aggregate
57	Scaling

Table B.11 Visual Distress Data, Recycled Pavements.

Site No.	Distress Comments
11	Faulting: C1 of S1, C1 & C3 of S3; Spalling: C1 of S1, C1 & C3 of S3; Lane-Shoulder Dropoff; Polished Aggregate; Shrinkage Cracking
12	Faulting: C1 & C4 of S1; C2 & C3 of S2; C3 of S3; Spalling: C1 & C4 of S1; C2 & C3 of S2; C3 of S3; Lane-Shoulder Dropoff; Shrinkage Cracking
13	Faulting: C1 of S1, C1 & C2 of S2, C1 & C2 of S3; Spalling: C1 of S1, C1 & C2 of S2, C1 & C2 of S3; Polished Aggregate; Shrinkage Cracking
14	Dropped Sealant: J1, J3, & J4; Lane-Shoulder Dropoff; Polished Aggregate; Shrinkage Cracking
15	Spalling: C2 & C4 of S3; Dropped Sealant: J1, J2, J3, & J4; Polished Aggregate; Shrinkage Cracking
16	Faulting: C1 & C4 of S1, C1 of S2, J2; Spalling: C1, C4, & C5 of S1, C1 & C3 of S2; Dropped Sealant: J1, J2, J3, & J4
17	Faulting: C2 of S1, C2 of S3, J3; Spalling: C1 & C2 of S1, C2 of S3; Dropped Sealant: J1, J2, & J3; Shrinkage Cracking
27	Faulting: C3 of S2; Spalling: C2 of S1, C3 of S2, C1 & C2 of S3; Dropped Sealant: J2; Alkali-Silica Reactivity; Lane-Shoulder Dropoff; Polished Aggregate; Shrinkage Cracking
28	Faulting: C2 of S1; Spalling: C2 of S1, C1 & C2 of S2; Alkali-Silica Reactivity; Lane-Shoulder Dropoff; Polished Aggregate; Shrinkage Cracking
29	Faulting: C1 of S4, J5; Spalling: C1 & C2 of S4; Dropped Sealant: J1, J2, J3, J4, & J5; Alkali-Silica Reactivity; Lane-Shoulder Dropoff; Polished Aggregate
31	Faulting: C2 & C3 of S1, C1 & C3 of S2, C3 of S3; Spalling: C2 & C3 of S1, C1 & C3 of S2, C3 of S3; Popouts; Lane-Shoulder Dropoff; Polished Aggregate
32	Faulting: C1 of S1, C1of S2, C4 of S3; Spalling: C1 & C3 of S1, C1 & C3 of S2, C4 of S3; Lane-Shoulder Dropoff; Polished Aggregate
47	No Data
48	No Data

Table B.12 Visual Distress Data, Slag Pavements.

Site No.	Distress Comments
1	Alkali-Silica Reactivity; Lane-Shoulder Dropoff
40	Faulting: J1; Dropped Sealant: J2 & J4; Lane-Shoulder Dropoff; Shrinkage Cracking
41	Polished Aggregate; Shrinkage Cracking
55	Spalling: C1 of S1, C1 of S2, C1 of S3, C1 of S4, C1 of S5, C1 of S7, C1 of S8; Dropped Sealant: J6, J7, J8
58	Sealant Damage: J1, J2, J3, J4, & J5; Longitudinal Cracking; Polished Aggregate
59	Sealant Damage: J1, J2, J3, J4, & J5; Longitudinal Cracking; Lane-Shoulder Dropoff; Polished Aggregate
60	Sealant Damage: J1, J2, J3, J4, & J5; Longitudinal Cracking
61	Alkali-Silica Reactivity; Polished Aggregate
62	Longitudinal Cracking; Alkali-Silica Reactivity; Durability Cracking; Polished Aggregate
63	Spalling: C1 of S1, C1 of S2, C1 of S3, C1 of S4, C1 of S5; Dropped Sealant: J4, J5, J6, & J7

Table B.13 Backcalculated Parameters I[a], Carbonate Pavements.

Site No.	AREA (mm)			ℓ (mm)		
	April 1997	July 1997	Oct. 1997	April 1997	July 1997	Oct. 1997
5	1127	1128	1148	998	1001	1048
6	1209	1202	1233	1216	1195	1295
7	1160	1158	1115	1078	1073	972
8	1180	1147	1118	1130	1045	980
35	1172	1155	1179	1107	1066	1127
36	1079	1220	1064	902	1251	875
38	1248	1151	No Data	1349	1055	No Data
39	1218	1162	No Data	1245	1083	No Data
42	987	987[b]	987[b]	755	755[b]	755[b]
43	987[b]	987[b]	987[b]	755[b]	755[b]	755[b]
44	No Data	987[b]	987[b]	No Data	755[b]	755[b]
45	No Data	1114	1175	No Data	972	1115
46	No Data	1088	1175[b]	No Data	919	1115[b]
49	1235	1216	1219	1301	1239	1247
50	1213[b]	1290	1194	1228[b]	1529	1170
51	1213[b]	1035	1186[b]	1228[b]	825	1148[b]
52	1213	1204	1186	1228	1198	1148

[a] Midslab deflection data was not collected for June 1998 testing cycle.

[b] This data was either assumed or copied from another test site and/or test cycle.

Table B.14 Backcalculated Parameters I[a], Natural Gravel Pavements.

Site No.	AREA (mm)			ℓ (mm)		
	April 1997	July 1997	Oct. 1997	April 1997	July 1997	Oct. 1997
2	1097	1152	1100	936	1057	942
3	1122	1104	1116	989	951	974
4	1139	1111	1117	1025	965	977
9	1133	No Data	No Data	1013	No Data	No Data
10	1110	No Data	1072	964	No Data	889
37	1130[b]	1170[b]	1097[b]	1006[b]	1104[b]	936[b]
38A	1130	1170	1097	1006	1104	936
57	1126	1077	1081	997	898	905

[a] Midslab deflection data was not collected for June 1998 testing cycle.

[b] This data was either assumed or copied from another test site and/or test cycle.

Table B.15 Backcalculated Parameters I[a], Recycled Pavements.

Site No.	AREA (mm)			ℓ (mm)		
	April 1997	July 1997	Oct. 1997	April 1997	July 1997	Oct. 1997
11	1233	1150	1148[b]	1296	1052	1046[b]
12	1175	1081	1148	1116	905	1046
13	1179	1113	1198	1126	968	1182
14	1136	1071	1084[b]	1018	886	911[b]
15	1260	1275	1084	1396	1462	911
16	No Data	1128	No Data	No Data	1000	No Data
17	No Data	1133	No Data	No Data	1011	No Data
27	No Data	1171	1185	No Data	1107	1145
28	No Data	1162	1207	No Data	1082	1208
29	No Data	1200	1187	No Data	1188	1149
31	No Data	1154	1105	No Data	1062	952
32	No Data	1146	1105[b]	No Data	1043	952[b]
47	1143[b]	No Data	No Data	1036[b]	No Data	No Data
48	1143[b]	No Data	No Data	1036[b]	No Data	No Data

[a] Midslab deflection data was not collected for June 1998 testing cycle.

[b] This data was either assumed or copied from another test site and/or test cycle.

Table B.16 Backcalculated Parameters I[a], Slag Pavements.

Site No.	AREA (mm)			ℓ (mm)		
	April 1997	July 1997	Oct. 1997	April 1997	July 1997	Oct. 1997
1	1150	1261	1052	1052	1400	854
40	1179	1152	No Data	1127	1058	No Data
41	1188	1130	No Data	1153	1005	No Data
55	1247	1290	1245	1348	1531	1340
58	No Data	1146	1154[b]	No Data	1043	1061[b]
59	No Data	1110	1154	No Data	963	1061
60	No Data	1098	1102	No Data	938	947
61	No Data	1078	1073	No Data	901	891
62	No Data	1110	1073[b]	No Data	964	891[b]
63	No Data	No Data	1245[b]	No Data	No Data	1340[b]

[a] Midslab deflection data was not collected for June 1998 testing cycle.

[b] This data was either assumed or copied from another test site and/or test cycle.

Table B.17 Backcalculated Parameters II[a], Carbonate Pavements.

Site No.	E (kPa)			k (kPa/mm)		
	April 1997	July 1997	Oct. 1997	April 1997	July 1997	Oct. 1997
5	3.49E+07	3.86E+07	4.61E+07	49.0	53.8	53.3
6	4.23E+07	4.54E+07	5.43E+07	27.0	31.1	26.9
7	3.81E+07	3.79E+07	3.42E+07	39.4	39.8	53.5
8	5.81E+07	5.92E+07	4.44E+07	42.5	59.3	57.4
35	7.42E+07	5.61E+07	6.10E+07	58.8	51.9	45.1
36	4.23E+07	6.11E+07	3.49E+07	76.2	29.7	70.9
38	1.57+08[b]	5.86E+07[b]	No Data	40.7[b]	40.7[b]	No Data
39	1.14E+08[b]	6.51E+07[b]	No Data	40.7[b]	40.7[b]	No Data
42	6.05E+07	6.05E+07[b]	6.05E+07[b]	89.3	89.3[b]	89.3[b]
43	6.05E+07[b]	6.05E+07[b]	6.05E+07[b]	89.3[b]	89.3[b]	89.3[b]
44	No Data	6.05E+07[b]	6.05E+07[b]	No Data	89.3[b]	89.3[b]
45	No Data	4.52E+07	5.26E+07	No Data	82.2	55.1
46	No Data	3.64E+07	5.26E+07[b]	No Data	82.9	55.1[b]
49	4.93E+07	4.30E+07	4.49E+07	41.6	44.1	44.9
50	3.92E+07[b]	6.01E+07	3.12E+07	41.7[b]	26.6	40.2
51	3.92E+07[b]	9.81E+06	3.55E+07[b]	41.7[b]	51.1	49.4[b]
52	3.92E+07	4.09E+07	3.55E+07	41.7	47.9	49.4

[a] Midslab deflection data was not collected for June 1998 testing cycle.

[b] This data was either assumed or copied from another test site and/or test cycle.

Table B.18 Backcalculated Parameters II[a], Natural Gravel Pavements.

Site No.	E (kPa)			k (kPa/mm)		
	April 1997	July 1997	Oct. 1997	April 1997	July 1997	Oct. 1997
2	4.83E+07	5.68E+07	4.97E+07	75.1	54.2	75.1
3	4.12E+07	3.36E+07	4.42E+07	51.3	49.1	58.5
4	4.41E+07	4.35E+07	4.45E+07	40.8	51.3	49.9
9	6.02E+07	No Data	No Data	58.5	No Data	No Data
10	5.55E+07	No Data	5.37E+07	65.8	No Data	88.0
37	4.38E+07[b]	3.87E+07[b]	4.28E+07[b]	51.0[b]	31.1[b]	66.3[b]
38A	4.38E+07	3.87E+07	4.28E+07	51.0	31.1	66.3
57	5.39E+07	5.29E+07	5.17E+07	65.1	97.1	92.1

[a] Midslab deflection data was not collected for June 1998 testing cycle.

[b] This data was either assumed or copied from another test site and/or test cycle.

Table B.19 Backcalculated Parameters II[a], Recycled Pavements.

Site No.	E (kPa)			k (kPa/mm)		
	April 1997	July 1997	Oct. 1997	April 1997	July 1997	Oct. 1997
11	3.83E+07	3.83E+07	4.09E+07[b]	22.0	50.7	55.3[b]
12	3.32E+07	2.88E+07	4.09E+07	34.7	69.7	55.3
13	3.39E+07	3.32E+07	5.25E+07	34.2	61.3	43.7
14	2.91E+07	2.34E+07	3.77E+07[b]	37.8	52.9	76.4[b]
15	6.53E+07	7.67E+07	3.77E+07	24.0	23.4	76.4
16	No Data	4.59E+07	No Data	No Data	64.0	No Data
17	No Data	4.55E+07	No Data	No Data	60.6	No Data
27	No Data	3.76E+07	3.66E+07	No Data	46.4	39.5
28	No Data	3.86E+07	4.42E+07	No Data	52.0	38.4
29	No Data	4.47E+07	3.71E+07	No Data	41.5	39.4
31	No Data	4.68E+07	3.64E+07	No Data	59.6	71.8
32	No Data	3.67E+07	3.64E+07[b]	No Data	50.3	71.8[b]
47	1.93E+07[b]	No Data	No Data	40.7[b]	No Data	No Data
48	1.93E+07[b]	No Data	No Data	40.7[b]	No Data	No Data

[a] Midslab deflection data was not collected for June 1998 testing cycle.

[b] This data was either assumed or copied from another test site and/or test cycle.

Table B.20 Backcalculated Parameters II[a], Slag Pavements.

Site No.	E (kPa)			k (kPa/mm)		
	April 1997	July 1997	Oct. 1997	April 1997	July 1997	Oct. 1997
1	4.40E+07	4.02E+07	1.88E+07	50.2	14.6	49.3
40	2.98E+07	3.12E+07	No Data	44.7	60.1	No Data
41	3.03E+07	3.07E+07	No Data	41.3	72.6	No Data
55	4.93E+07	4.34E+07	5.56E+07	36.1	19.1	41.7
58	No Data	5.72E+07	6.37E+07[b]	No Data	67.4	70.1[b]
59	No Data	5.20E+07	6.37E+07	No Data	84.5	70.1
60	No Data	5.06E+07	5.48E+07	No Data	91.1	95.1
61	No Data	3.46E+07	3.98E+07	No Data	73.3	88.2
62	No Data	4.87E+07	3.98E+07[b]	No Data	78.9	88.2[b]
63	No Data	No Data	5.56E+07[b]	No Data	No Data	41.7[b]

[a] Midslab deflection data was not collected for June 1998 testing cycle.

[b] This data was either assumed or copied from another test site and/or test cycle.

Table B.21 LTE_δ Data, Carbonate Pavements.

Site No.	Test Type	April 1997 LTE_δ (%)		July 1997 LTE_δ (%)		Oct. 1997 LTE_δ (%)		June 1998 LTE_δ (%)	
		Before	After	Before	After	Before	After	Before	After
5	C	94.98	100.00	95.69	99.77	93.20	97.88	94.10	96.88
	C	92.84	96.83	98.66	98.42	91.54	96.15	97.73	95.25
	J	75.85	67.07	97.95	94.81	65.80	53.87	92.23	92.37
6	C	99.84	99.49	100.00	95.18	95.03	94.83	94.84	91.88
	C	100.00	95.86	100.00	96.69	99.15	97.24	94.43	94.05
	J	88.53	84.58	90.57	87.11	86.44	84.51	97.74	93.46
7	C	100.00	90.46	98.06	93.17	99.14	88.87	98.83	91.01
	C	18.32	30.75	100.00	95.10	13.62	13.08	93.73	96.77
	J	80.61	79.61	85.02	85.67	78.97	82.03	88.69	89.00
8	C	94.96	96.06	94.16	90.91	95.87	93.41	97.19	92.07
	C	100.00	92.92	95.51	88.19	94.23	89.64	98.93	91.78
	J	100.00	93.71	100.00	89.42	89.17	74.81	100.00	91.10
35	C	94.06	94.62	93.27	92.00	93.76	93.05	96.83	92.55
	C	93.54	92.71	92.48	93.29	94.27	93.55	94.56	96.03
	J	92.32	99.36	95.46	90.05	86.34	88.65	93.59	87.56
36	C	91.98	91.92	90.19	89.31	92.29	90.66	93.68	93.43
	C	93.80	94.42	92.55	94.35	90.14	96.96	94.18	93.90
	J	82.73	97.68	97.85	90.07	67.93	85.72	97.92	90.78
38	C	90.96	87.23	87.79	86.23	No Data	No Data	95.45	87.79
	C	91.59	90.36	88.21	91.10	No Data	No Data	93.45	91.98
	C	92.79	86.61	89.00	82.33	No Data	No Data	97.35	87.51
	J	87.49	79.65	61.71	73.59	No Data	No Data	52.62	59.72
39	C	91.06	90.75	89.05	88.59	No Data	No Data	94.70	91.33
	C	92.50	88.86	89.87	86.86	No Data	No Data	92.01	87.80
	C	90.91	87.28	91.21	85.16	No Data	No Data	92.58	86.08
	J	84.84	80.82	94.62	87.38	No Data	No Data	55.36	61.68
42	C	90.97	88.02	81.14	94.76	87.55	94.10	80.83	100.00
	C	91.19	83.10	81.76	75.32	86.94	78.40	25.51	29.59
	J	92.17	82.92	90.06	86.51	89.54	78.58	96.05	88.64
43	C	88.95	84.50	88.08	87.91	82.23	80.61	70.83	67.80
	C	66.17	75.72	63.51	58.99	52.98	60.84	46.39	28.70
	J	90.11	81.86	82.02	74.17	82.67	72.35	89.97	95.87
	J	83.75	80.75	79.88	71.98	82.31	71.00	72.45	85.52
44	C	No Data	No Data	88.33	85.21	89.55	88.10	93.57	88.59
	C	No Data	No Data	63.41	70.90	53.17	66.78	49.11	64.39
	J	No Data	No Data	76.51	54.15	77.40	72.76	91.05	72.51
	J	No Data	No Data	64.19	81.26	79.39	72.74	62.27	70.82

Table B.21 (cont'd).

Site No.	Test Type	April 1997 LTE_{δ} (%)		July 1997 LTE_{δ} (%)		Oct. 1997 LTE_{δ} (%)		June 1998 LTE_{δ} (%)	
		Before	After	Before	After	Before	After	Before	After
44	J	No Data	No Data	72.98	42.10	72.57	39.75	71.04	65.64
	J	No Data	No Data	77.45	74.17	77.13	78.84	81.54	79.53
45	C	No Data	No Data	93.25	91.00	96.79	93.63	94.98	93.18
	J	No Data	No Data	89.92	90.10	76.82	93.92	91.35	98.36
	J	No Data	No Data	No Data	No Data	98.81	79.31	93.06	93.97
46	C	No Data	No Data	93.93	95.19	88.14	98.20	94.55	100.00
	J	No Data	No Data	94.44	87.50	92.29	87.34	91.77	93.36
	J	No Data	No Data	90.52	74.88	70.46	70.95	82.43	81.11
49	C	98.60	95.97	95.62	90.18	97.92	98.92	100.00	94.61
	J	93.62	89.97	97.83	94.91	66.41	64.56	98.30	91.63
50	C	20.66	23.48	93.95	97.84	24.65	21.21	95.50	89.09
	C	94.15	93.12	90.35	96.82	99.01	95.37	95.69	89.26
	C	100.00	92.04	97.29	93.41	94.22	91.29	98.06	91.91
	C	100.00	92.97	96.27	96.92	77.98	73.10	71.62	56.90
	J	61.68	56.17	89.41	95.23	58.48	50.64	85.84	81.72
51	C	11.26	6.99	9.88	6.72	10.44	9.03	7.41	5.94
	C	98.49	95.49	100.00	99.01	100.00	93.34	92.55	92.61
	C	99.65	89.69	97.28	95.56	94.43	96.26	93.52	90.75
	C	88.75	94.30	92.56	93.52	94.25	95.71	98.89	90.42
52	C	99.59	95.38	94.70	90.32	97.82	93.53	97.94	91.87
	C	100.00	96.38	94.93	95.65	91.02	95.42	98.02	95.94
	C	97.89	98.54	93.97	95.66	97.68	96.91	95.65	89.97
	J	100.00	97.78	99.52	100.00	98.37	88.95	95.12	97.38

Table B.22 LTE_δ Data, Natural Gravel Pavements.

Site No.	Test Type	April 1997 LTE_δ (%)		July 1997 LTE_δ (%)		Oct. 1997 LTE_δ (%)		June 1998 LTE_δ (%)	
		Before	After	Before	After	Before	After	Before	After
2	C	93.68	95.28	92.64	92.00	83.25	98.70	98.59	100.00
	C	97.83	93.64	92.34	95.59	85.88	96.06	91.51	93.82
	C	96.97	98.29	95.31	90.97	87.54	95.52	95.57	100.00
	J	55.60	81.43	94.81	92.09	46.98	77.19	51.32	82.75
3	C	97.55	100.00	98.90	92.53	97.80	93.11	98.23	95.02
	C	100.00	100.00	95.24	96.57	97.65	99.57	94.47	98.71
	C	No Data	No Data	88.11	99.76	46.06	82.07	93.01	No Data
	J	54.22	74.89	60.68	71.51	52.70	78.51	43.41	70.84
4	C	97.03	95.28	99.69	93.81	98.02	97.71	94.47	90.14
	C	100.00	99.72	100.00	95.63	97.48	98.69	97.55	92.41
	J	77.83	67.80	80.19	80.91	22.94	28.87	77.12	58.84
9	C	97.63	95.57	No Data	No Data	No Data	No Data	No Data	No Data
	C	22.03	29.47	No Data	No Data	No Data	No Data	No Data	No Data
	J	70.19	63.77	No Data	No Data	No Data	No Data	No Data	No Data
10	C	39.35	34.28	No Data	No Data	25.79	28.02	20.43	40.10
	C	No Data	No Data	No Data	No Data	No Data	No Data	19.30	31.54
	C	100.00	96.71	No Data	No Data	22.26	29.28	100.00	100.00
	J	73.87	67.35	No Data	No Data	66.35	67.45	71.51	67.77
37	C	92.81	92.93	100.00	90.11	89.37	94.58	93.06	91.02
	C	31.55	51.94	100.00	95.02	21.68	26.31	21.53	34.90
	C	No Data	No Data	97.99	100.00	21.10	25.00	19.54	19.02
	C	27.55	89.41	96.30	96.68	16.07	21.53	15.09	39.85
	C	67.37	83.04	100.00	90.06	34.47	26.41	36.68	30.32
	C	90.56	93.06	100.00	84.25	96.24	97.92	88.44	90.24
	J	45.20	51.11	88.09	84.93	29.53	44.01	30.4598	28.68
38A	C	96.44	94.31	100.00	95.62	91.49	97.24	95.83	90.02
	C	67.75	87.10	99.56	89.82	25.81	26.66	26.45	20.80
	C	100.00	94.72	99.28	91.07	97.53	91.43	99.77	92.70
	C	94.21	97.53	99.78	91.27	91.43	92.90	91.54	96.98
	C	78.98	93.17	91.64	64.16	83.13	93.83	76.42	95.94
	C	No Data	No Data	No Data	No Data	No Data	No Data	98.78	93.73
	J	47.30	40.57	83.05	66.82	34.65	32.79	34.21	31.88
57	C	96.96	90.54	93.64	88.11	93.67	89.86	97.61	91.95
	C	98.85	93.33	99.44	92.53	84.93	93.65	100.00	98.56
	C	98.15	92.06	96.22	83.21	97.46	94.59	92.74	93.97
	C	93.39	93.80	95.60	97.49	91.62	100.00	89.54	91.10
	C	No Data	No Data	No Data	No Data	No Data	No Data	95.37	92.44

Table B.22 (cont'd).

Site No.	Test Type	April 1997 LTE_{δ} (%)		July 1997 LTE_{δ} (%)		Oct. 1997 LTE_{δ} (%)		June 1998 LTE_{δ} (%)	
		Before	After	Before	After	Before	After	Before	After
57	J	92.37	90.63	80.13	84.39	82.78	85.36	78.75	81.50
	J	93.08	89.73	72.06	86.12	65.35	86.90	68.11	81.41

Table B.23 LTE_δ Data, Recycled Pavements.

Site No.	Test Type	April 1997 LTE_δ (%)		July 1997 LTE_δ (%)		Oct. 1997 LTE_δ (%)		June 1998 LTE_δ (%)	
		Before	After	Before	After	Before	After	Before	After
11	C	47.57	46.37	19.98	95.05	12.94	16.21	18.12	18.55
	C	100.00	96.57	91.44	93.34	97.50	92.80	90.55	88.40
	C	96.99	98.57	91.83	92.79	94.49	100.00	93.27	93.67
	C	95.81	90.48	95.42	82.68	99.50	91.25	96.57	85.37
	C	No Data	No Data	21.43	17.62	16.85	12.81	23.65	15.55
	C	92.78	87.41	80.98	88.30	91.24	89.40	83.29	93.19
	C	No Data	No Data	No Data	No Data	No Data	No Data	27.99	18.35
	J	70.56	69.61	64.88	76.51	67.94	74.96	73.17	71.80
12	C	42.33	43.64	26.89	40.73	18.75	20.89	24.02	37.00
	C	96.63	95.17	89.80	91.84	No Data	No Data	90.01	92.82
	C	36.62	35.35	24.62	34.09	21.32	17.27	24.82	15.97
	C	42.30	39.09	28.57	25.22	30.07	40.48	34.44	24.69
	C	54.73	58.40	No Data	No Data	19.88	44.25	28.74	29.98
	C	100.00	97.50	92.15	93.01	96.42	91.95	92.51	94.38
	J	63.29	73.50	81.32	90.36	80.93	76.74	74.26	74.28
13	C	100.00	87.76	23.15	86.43	21.92	71.26	18.56	86.16
	C	96.18	97.72	92.77	92.31	94.31	99.38	92.41	92.17
	C	51.65	63.82	37.85	37.01	26.81	35.89	35.39	38.72
	J	65.43	70.61	67.29	65.71	72.09	78.08	66.50	74.27
	J	82.33	76.94	81.33	67.83	83.36	81.62	86.54	78.74
14	C	97.41	94.52	94.28	93.33	88.63	90.80	93.31	90.87
	C	95.93	90.19	95.34	87.86	92.71	89.28	96.37	89.65
	C	92.58	90.03	92.89	83.38	94.29	89.35	94.07	89.52
	C	93.21	95.08	91.35	92.08	93.14	89.03	92.25	90.59
	J	95.56	88.69	92.03	87.43	75.86	65.50	90.78	91.38
15	C	95.03	89.87	97.12	89.06	90.54	87.40	92.76	90.09
	C	97.49	90.07	97.32	88.03	92.28	88.47	92.57	88.35
	C	96.40	96.06	94.34	93.42	94.56	93.48	No Data	No Data
	J	86.45	81.58	82.27	79.99	83.84	72.80	82.11	77.26
	J	No Data	79.12	87.61	81.25	No Data	No Data	78.42	71.40
16	C	No Data	No Data	17.45	34.85	No Data	No Data	16.07	22.90
	C	No Data	No Data	No Data	No Data	No Data	No Data	25.82	16.53
	C	No Data	No Data	97.79	91.09	No Data	No Data	94.27	99.03
	J	No Data	No Data	81.49	70.95	No Data	No Data	75.26	74.91
	J	No Data	No Data	49.66	30.38	No Data	No Data	26.17	31.80
	J	No Data	No Data	67.01	62.70	No Data	No Data	83.70	85.02
	J	No Data	No Data	76.21	73.11	No Data	No Data	75.56	68.36

Table B.23 (cont'd).

Site No.	Test Type	April 1997 LTE_δ (%)		July 1997 LTE_δ (%)		Oct. 1997 LTE_δ (%)		June 1998 LTE_δ (%)	
		Before	After	Before	After	Before	After	Before	After
17	C	No Data	No Data	24.56	23.36	No Data	No Data	32.32	29.22
	C	No Data	No Data	97.56	90.53	No Data	No Data	97.68	94.56
	J	No Data	No Data	31.55	30.56	No Data	No Data	38.53	25.63
	J	No Data	No Data	61.46	46.73	No Data	No Data	59.15	45.18
	J	No Data	No Data	31.75	30.71	No Data	No Data	32.63	29.75
27	C	No Data	No Data	96.52	90.39	98.67	96.22	94.84	97.21
	C	No Data	No Data	24.71	41.34	11.08	13.00	16.27	15.45
	J	No Data	No Data	60.37	84.99	52.30	75.82	49.24	78.28
	J	No Data	No Data	77.02	85.25	71.86	75.39	63.55	65.83
	J	No Data	No Data	70.11	74.29	68.78	77.22	64.18	64.78
28	C	No Data	No Data	57.41	77.76	14.92	37.84	15.70	35.28
	C	No Data	No Data	96.81	78.09	100.00	100.00	95.06	100.00
	C	No Data	No Data	No Data	No Data	No Data	No Data	94.20	96.12
	J	No Data	No Data	52.68	79.30	52.88	73.94	47.07	63.89
	J	No Data	No Data	79.18	77.24	70.88	78.57	75.42	67.27
	J	No Data	No Data	67.89	78.35	76.93	84.61	70.30	84.85
29	C	No Data	No Data	94.82	95.00	95.24	83.10	56.52	73.90
	C	No Data	No Data	99.86	94.54	21.00	22.50	90.83	98.70
	J	No Data	No Data	96.82	93.99	60.14	51.21	54.12	40.97
	J	No Data	No Data	100.00	91.51	60.02	91.51	49.66	66.28
	J	No Data	No Data	96.45	91.17	59.44	61.70	49.11	38.85
	J	No Data	No Data	62.85	69.34	53.53	53.46	48.20	44.39
31	C	No Data	No Data	48.26	85.12	41.87	43.48	15.42	65.31
	C	No Data	No Data	93.13	95.84	19.58	16.58	20.13	41.68
	J	No Data	No Data	90.62	73.69	66.15	59.76	76.17	63.62
	J	No Data	No Data	82.39	83.40	57.30	52.47	59.26	42.54
	J	No Data	No Data	96.94	92.11	57.05	46.61	51.79	38.02
32	C	No Data	No Data	No Data	No Data	No Data	No Data	39.23	32.69
	C	No Data	No Data	89.27	76.66	54.15	16.86	No Data	28.78
	C	No Data	No Data	99.85	90.56	33.71	11.54	55.73	25.55
	J	No Data	No Data	96.77	88.36	64.21	47.24	55.03	38.41
	J	No Data	No Data	91.30	88.57	59.53	68.25	49.85	44.49
	J	No Data	No Data	100.00	91.33	83.13	73.77	62.87	68.17
47	C	100.00	96.65	No Data	No Data	No Data	No Data	No Data	No Data
	C	99.70	92.57	No Data	No Data	No Data	No Data	No Data	No Data
	C	97.17	89.56	No Data	No Data	No Data	No Data	No Data	No Data
	C	35.08	27.35	No Data	No Data	No Data	No Data	No Data	No Data

Table B.23 (cont'd).

Site No.	Test Type	April 1997 LTE_{δ} (%)		July 1997 LTE_{δ} (%)		Oct. 1997 LTE_{δ} (%)		June 1998 LTE_{δ} (%)	
		Before	After	Before	After	Before	After	Before	After
47	J	54.72	50.96	No Data	No Data	No Data	No Data	No Data	No Data
48	C	31.15	26.06	No Data	No Data	No Data	No Data	No Data	No Data
	C	97.14	88.14	No Data	No Data	No Data	No Data	No Data	No Data
	C	79.36	77.43	No Data	No Data	No Data	No Data	No Data	No Data
	C	97.56	90.51	No Data	No Data	No Data	No Data	No Data	No Data
	C	96.72	96.17	No Data	No Data	No Data	No Data	No Data	No Data
	J	39.80	34.37	No Data	No Data	No Data	No Data	No Data	No Data
	J	50.59	58.37	No Data	No Data	No Data	No Data	No Data	No Data

Table B.24 LTE_δ Data, Slag Pavements.

Site No.	Test Type	April 1997 LTE_δ (%)		July 1997 LTE_δ (%)		Oct. 1997 LTE_δ (%)		June 1998 LTE_δ (%)	
		Before	After	Before	After	Before	After	Before	After
1	C	100.00	87.12	97.17	91.63	94.46	84.23	96.79	91.64
	C	100.00	93.41	98.81	93.89	91.07	87.53	No Data	No Data
	C	97.77	90.34	98.38	92.80	90.42	86.52	No Data	No Data
	C	98.81	89.76	95.95	94.05	99.29	87.74	No Data	No Data
	J	72.14	56.19	99.26	92.05	68.11	55.40	96.38	88.33
40	C	89.94	92.26	97.68	85.39	No Data	No Data	99.33	87.12
	C	No Data	No Data	No Data	No Data	No Data	No Data	94.57	88.33
	J	88.95	85.77	93.44	90.01	No Data	No Data	95.71	90.88
41	C	97.68	91.31	95.47	94.79	No Data	No Data	91.70	92.92
	C	No Data	No Data	No Data	No Data	No Data	No Data	92.12	93.70
	C	94.49	93.95	95.14	91.42	No Data	No Data	95.36	92.10
	C	98.35	90.13	97.24	91.52	No Data	No Data	95.10	92.88
	J	88.54	87.61	95.18	87.08	No Data	No Data	92.21	87.18
55	C	27.15	46.62	88.80	93.40	28.08	24.65	22.45	30.35
	C	46.24	80.64	95.20	87.13	25.79	24.80	43.23	66.89
	J	No Data	54.54	61.84	64.62	36.87	48.21	27.08	34.64
	J	27.19	No Data	78.77	96.23	34.26	40.97	24.83	26.29
	J	No Data	No Data	80.69	90.42	37.07	64.08	28.85	46.39
	J	No Data	No Data	75.24	91.42	30.98	69.13	29.76	44.34
58	C	No Data	No Data	90.12	92.72	94.76	90.13	95.41	93.80
	C	No Data	No Data	89.93	91.54	92.62	92.51	92.86	93.89
	J	No Data	No Data	71.73	69.29	78.03	73.38	80.20	73.48
	J	No Data	No Data	69.86	66.45	73.05	69.86	89.46	92.04
	J	No Data	No Data	47.57	43.24	38.47	37.69	95.12	89.43
	J	No Data	No Data	48.02	72.40	45.81	49.07	95.04	92.05
59	C	No Data	No Data	90.80	92.83	91.22	90.06	90.36	91.17
	C	No Data	No Data	96.00	89.17	88.28	90.11	88.05	90.84
	J	No Data	No Data	47.19	79.03	47.40	59.95	87.80	91.42
	J	No Data	No Data	56.04	56.49	50.37	54.00	88.52	91.87
	J	No Data	No Data	58.15	66.55	45.09	49.65	85.36	84.51
60	C	No Data	No Data	93.07	89.80	88.14	90.95	92.94	87.94
	C	No Data	No Data	92.34	88.66	89.39	94.86	95.29	92.63
	J	No Data	No Data	91.48	89.95	51.99	65.91	92.11	90.48
	J	No Data	No Data	69.34	80.25	37.79	49.00	94.85	88.80
	J	No Data	No Data	67.95	69.20	36.33	38.80	91.84	85.14
61	C	No Data	No Data	88.40	87.61	88.93	84.60	90.00	86.31
	C	No Data	No Data	92.50	88.73	92.14	89.22	94.92	87.86

Table B.24 (cont'd).

Site No.	Test Type	April 1997 LTE_δ (%)		July 1997 LTE_δ (%)		Oct. 1997 LTE_δ (%)		June 1998 LTE_δ (%)	
		Before	After	Before	After	Before	After	Before	After
61	J	No Data	No Data	97.01	87.65	74.49	76.90	92.39	78.38
	J	No Data	No Data	93.19	85.85	59.65	64.54	90.84	85.00
	J	No Data	No Data	90.82	90.81	58.49	52.49	95.67	86.77
	J	No Data	No Data	92.03	92.11	36.17	36.10	98.77	88.57
62	C	No Data	No Data	91.50	89.16	91.10	86.86	95.54	89.45
	C	No Data	No Data	91.63	87.45	89.03	91.34	93.72	89.11
	J	No Data	No Data	93.01	87.92	66.17	57.27	94.47	89.03
	J	No Data	No Data	95.94	89.34	55.72	65.52	95.45	90.04
	J	No Data	No Data	94.66	84.62	57.17	62.40	92.44	87.33
63	C	No Data	No Data	No Data	No Data	33.86	24.16	26.12	No Data
	C	No Data	No Data	No Data	No Data	78.59	74.49	38.01	67.37
	J	No Data	No Data	No Data	No Data	34.20	58.00	30.77	44.18
	J	No Data	No Data	No Data	No Data	25.13	35.72	25.03	39.55
	J	No Data	No Data	No Data	No Data	26.45	33.31	28.75	37.20

Table B.25 TLE Data, Carbonate Pavements.

Site No.	Test Type	April 1997 TLE (%)		July 1997 TLE (%)		Oct. 1997 TLE (%)		June 1998 TLE (%)	
		Before	After	Before	After	Before	After	Before	After
5	C	45.18	45.20	45.19	45.21	45.21	45.42	45.31	45.42
	C	44.98	45.19	45.20	45.20	45.01	45.41	45.42	45.41
	J	42.48	40.66	45.20	45.19	40.56	36.93	45.10	45.20
6	C	46.13	46.13	46.06	45.97	46.29	46.29	46.29	45.95
	C	46.13	46.04	46.06	45.97	46.36	46.33	46.19	46.19
	J	45.37	44.88	45.47	45.10	45.39	45.11	46.33	46.15
7	C	45.58	45.04	45.53	45.32	45.05	44.35	45.05	44.65
	C	17.41	26.34	45.56	45.52	13.21	12.81	44.95	45.05
	J	43.64	43.44	44.40	44.50	42.95	43.45	44.35	44.35
8	C	45.74	45.74	45.29	44.99	45.09	44.99	45.09	44.79
	C	45.81	45.54	45.39	44.61	44.99	44.49	45.10	44.79
	J	45.81	45.62	45.43	44.81	44.39	42.29	45.10	44.69
35	C	45.56	45.56	45.37	45.17	45.63	45.53	45.75	45.51
	C	45.54	45.44	45.27	45.37	45.63	45.61	45.63	45.73
	J	45.44	45.71	45.49	44.90	44.83	45.05	45.61	44.93
36	C	44.38	44.38	45.59	45.59	44.31	44.03	44.41	44.41
	C	44.57	44.58	45.92	46.06	43.93	44.53	44.41	44.41
	J	43.19	44.69	46.19	45.59	40.24	43.52	44.53	44.12
38	C	46.04	45.58	44.65	44.44	No Data	No Data	45.44	44.65
	C	46.04	45.94	44.65	45.04	No Data	No Data	45.33	45.13
	C	46.24	45.54	44.75	43.94	No Data	No Data	45.45	44.64
	J	45.64	44.34	39.39	42.33	No Data	No Data	36.54	38.89
39	C	45.74	45.74	44.87	44.87	No Data	No Data	45.46	45.16
	C	45.91	45.47	44.97	44.67	No Data	No Data	45.24	44.77
	C	45.74	45.34	45.16	44.44	No Data	No Data	45.34	44.56
	J	45.01	44.34	45.46	44.76	No Data	No Data	37.55	39.49
42	C	43.28	42.94	41.97	43.66	42.91	43.56	41.97	43.74
	C	43.28	42.31	42.14	40.99	42.81	41.54	21.76	24.21
	J	43.38	42.31	43.11	42.78	43.11	41.54	43.68	43.01
43	C	43.04	42.58	42.94	42.94	42.14	41.87	40.07	39.44
	C	38.99	40.99	38.39	37.09	35.09	37.72	32.59	23.53
	J	43.11	42.14	42.14	40.74	42.24	40.37	43.11	43.68
	J	42.48	41.97	41.77	40.27	42.24	40.07	40.37	42.68
44	C	No Data	No Data	43.01	42.58	43.11	42.94	43.56	43.01
	C	No Data	No Data	38.39	40.07	35.09	39.27	33.63	38.59
	J	No Data	No Data	41.19	35.39	41.37	40.54	43.28	40.37
	J	No Data	No Data	38.49	42.04	41.67	40.37	38.12	40.07

Table B.25 (cont'd).

Site No.	Test Type	April 1997 TLE (%)		July 1997 TLE (%)		Oct. 1997 TLE (%)		June 1998 TLE (%)	
		Before	After	Before	After	Before	After	Before	After
44	J	No Data	No Data	40.54	30.57	40.37	29.74	40.07	38.89
	J	No Data	No Data	41.37	40.74	41.27	41.64	42.04	41.67
45	C	No Data	No Data	44.85	44.65	45.71	45.57	45.69	45.49
	J	No Data	No Data	44.45	44.45	43.17	45.59	45.29	45.73
	J	No Data	No Data	No Data	No Data	45.73	43.59	45.49	45.59
46	C	No Data	No Data	44.67	44.77	44.91	45.71	45.59	45.75
	J	No Data	No Data	44.67	43.98	45.47	44.89	45.37	45.57
	J	No Data	No Data	44.28	41.99	41.77	41.95	44.19	43.89
49	C	46.38	46.30	46.12	45.55	46.18	46.21	46.24	46.04
	J	46.17	45.74	46.15	46.12	41.35	40.81	46.21	45.74
50	C	19.30	21.53	46.76	46.91	22.16	19.61	45.89	45.21
	C	45.98	45.88	46.36	46.91	45.94	45.89	45.89	45.31
	C	46.18	45.75	46.91	46.70	45.79	45.49	45.91	45.56
	C	46.18	45.88	46.86	46.91	43.54	42.66	42.26	38.34
	J	39.96	38.10	46.31	46.86	38.94	36.01	44.89	44.19
51	C	Low[a]	Low[a]	Low[a]	Low[a]	Low[a]	Low[a]	Low[a]	Low[a]
	C	46.15	46.08	44.24	44.24	45.88	45.69	45.59	45.59
	C	46.18	45.51	44.22	44.20	45.71	45.81	45.69	45.41
	C	45.41	45.98	43.99	44.09	45.71	45.81	45.86	45.31
52	C	46.18	46.08	45.89	45.49	45.83	45.69	45.83	45.49
	C	46.18	46.08	45.99	45.99	45.41	45.81	45.83	45.81
	C	46.11	46.15	45.89	45.99	45.83	45.83	45.81	45.23
	J	46.18	46.11	46.07	46.07	45.86	45.13	45.81	45.83

[a] "Low" indicates that the LTE_δ was below 12% and thus no value could be determined for TLE, as this is out of the range of the LTE_δ-TLE plot.

Table B.26 TLE Data, Natural Gravel Pavements.

Site No.	Test Type	April 1997 TLE (%)		July 1997 TLE (%)		Oct. 1997 TLE (%)		June 1998 TLE (%)	
		Before	After	Before	After	Before	After	Before	After
2	C	44.76	44.86	45.24	45.14	43.50	44.90	44.90	44.90
	C	44.87	44.76	45.24	45.45	43.90	44.90	44.50	44.80
	C	44.87	44.87	45.45	45.05	44.10	44.90	44.90	44.90
	J	36.98	43.17	45.45	45.14	33.72	42.40	35.71	43.40
3	C	45.14	45.15	44.94	44.74	45.06	44.86	45.06	45.06
	C	45.15	45.15	44.94	44.94	45.06	45.07	44.96	45.07
	C	No Data	No Data	44.14	44.94	33.45	43.46	44.86	No Data
	J	36.71	42.33	38.65	41.34	36.25	42.86	32.25	41.36
4	C	45.32	45.31	45.02	44.92	45.08	45.08	44.98	44.48
	C	45.33	45.33	45.02	45.02	45.08	45.08	45.08	44.88
	J	42.99	40.98	43.02	43.22	20.64	24.75	42.58	38.37
9	C	45.26	45.25	No Data	No Data	No Data	No Data	No Data	No Data
	C	20.01	25.15	No Data	No Data	No Data	No Data	No Data	No Data
	J	41.23	39.92	No Data	No Data	No Data	No Data	No Data	No Data
10	C	30.50	28.10	No Data	No Data	22.67	23.77	18.62	30.41
	C	No Data	No Data	No Data	No Data	No Data	No Data	17.83	26.04
	C	45.01	45.01	No Data	No Data	20.11	24.76	44.62	44.62
	J	42.01	40.61	No Data	No Data	39.94	40.22	41.03	40.32
37	C	45.02	45.02	45.70	45.06	44.27	44.77	44.67	44.47
	C	26.44	36.17	45.70	45.64	19.44	23.12	19.44	28.30
	C	No Data	No Data	45.66	45.70	19.14	22.03	17.94	17.54
	C	23.82	44.62	45.64	45.64	15.05	19.44	14.35	30.60
	C	40.80	43.81	45.70	45.06	28.01	23.12	29.00	25.52
	C	44.72	45.02	45.70	44.41	44.87	44.87	44.17	44.27
	J	33.08	35.77	44.86	44.52	24.9196	32.303	25.5196	24.22
38A	C	45.22	45.12	45.70	45.64	44.47	44.87	44.87	44.27
	C	40.90	44.32	45.70	45.06	22.82	23.12	23.12	19.14
	C	45.24	45.12	45.70	45.24	44.87	44.47	44.87	44.66
	C	45.12	45.22	45.70	45.24	44.47	44.67	44.47	44.87
	C	43.11	45.02	45.24	40.27	43.47	44.76	42.28	44.87
	C	No Data	No Data	No Data	No Data	No Data	No Data	44.87	44.76
	J	34.18	31.05	44.22	41.07	28.01	27.21	27.81	26.51
57	C	45.18	44.67	44.55	43.87	44.59	44.10	44.70	44.39
	C	45.18	45.07	44.67	44.45	43.59	44.59	44.71	44.70
	C	45.18	44.87	44.65	43.26	44.70	44.59	44.49	44.59
	C	45.07	45.07	44.65	44.66	44.30	44.71	44.10	44.29
	C	No Data	No Data	No Data	No Data	No Data	No Data	44.69	44.49

Table B.26 (cont'd).

Site No.	Test Type	April 1997 TLE (%)		July 1997 TLE (%)		Oct. 1997 TLE (%)		June 1998 TLE (%)	
		Before	After	Before	After	Before	After	Before	After
57	J	44.97	44.67	42.68	43.55	43.30	43.69	42.51	43.01
	J	44.97	44.58	41.18	43.65	39.82	43.80	40.41	43.01

Table B.27 TLE Data, Recycled Pavements.

Site No.	Test Type	April 1997 TLE (%)		July 1997 TLE (%)		Oct. 1997 TLE (%)		June 1998 TLE (%)	
		Before	After	Before	After	Before	After	Before	After
11	C	35.07	34.67	18.60	45.43	12.92	15.24	16.95	17.36
	C	46.40	46.29	45.03	45.31	45.41	45.20	44.90	44.71
	C	46.33	46.36	45.11	45.23	45.30	45.44	45.29	45.29
	C	46.29	45.79	45.43	43.93	45.44	45.00	45.40	44.39
	C	No Data	No Data	19.70	16.56	16.14	12.92	21.20	14.84
	C	46.09	45.49	43.63	44.74	45.00	44.81	44.09	45.20
	C	No Data	No Data	No Data	No Data	No Data	No Data	24.23	17.36
	J	42.35	42.12	40.38	42.83	41.07	42.59	42.19	41.89
12	C	32.25	32.75	23.32	30.68	17.36	19.38	21.51	29.55
	C	45.69	45.69	44.10	44.40	No Data	No Data	44.81	45.20
	C	29.53	29.03	21.55	27.69	19.68	16.55	22.31	15.24
	C	32.25	30.75	24.12	21.94	25.55	31.19	28.35	21.91
	C	37.35	38.77	No Data	No Data	18.58	33.02	24.54	25.55
	C	45.75	45.71	44.40	44.50	45.40	45.09	45.19	45.30
	J	40.21	42.57	43.01	44.20	43.60	42.80	42.49	42.49
13	C	45.79	44.95	20.61	44.13	20.33	42.30	17.57	44.93
	C	45.73	45.75	44.83	44.83	45.83	46.01	45.70	45.60
	C	36.36	40.34	29.82	29.32	24.00	29.38	29.18	30.61
	J	40.74	41.81	40.63	40.13	42.40	43.58	41.15	43.00
	J	44.23	43.21	43.33	40.73	44.60	44.23	45.03	43.68
14	C	45.28	45.18	44.49	44.48	44.03	44.33	44.62	44.33
	C	45.28	44.68	44.59	43.81	44.52	44.13	44.73	44.13
	C	45.07	44.68	44.39	43.30	44.63	44.13	44.62	44.13
	C	45.08	45.28	44.20	44.29	44.53	44.04	44.43	44.23
	J	45.28	44.58	44.29	43.80	42.05	39.85	44.33	44.33
15	C	46.56	46.00	46.76	46.06	44.23	43.93	44.53	44.13
	C	46.60	46.00	46.76	45.96	44.52	44.03	44.52	44.03
	C	46.56	46.56	46.61	46.56	44.63	44.62	No Data	No Data
	J	45.66	44.86	45.21	44.71	43.53	41.54	43.14	42.35
	J	No Data	44.41	45.91	45.01	No Data	No Data	42.54	41.15
16	C	No Data	No Data	16.47	28.51	No Data	No Data	15.16	20.69
	C	No Data	No Data	No Data	No Data	No Data	No Data	23.00	15.57
	C	No Data	No Data	45.19	44.79	No Data	No Data	45.09	45.20
	J	No Data	No Data	43.49	41.48	No Data	No Data	42.39	42.38
	J	No Data	No Data	35.05	25.72	No Data	No Data	23.00	26.72
	J	No Data	No Data	40.67	39.47	No Data	No Data	43.88	44.08
	J	No Data	No Data	42.49	41.98	No Data	No Data	42.39	40.97

Table B.27 (cont'd).

Site No.	Test Type	April 1997 TLE (%)		July 1997 TLE (%)		Oct. 1997 TLE (%)		June 1998 TLE (%)	
		Before	After	Before	After	Before	After	Before	After
17	C	No Data	No Data	21.83	21.12	No Data	No Data	27.06	24.85
	C	No Data	No Data	45.25	44.74	No Data	No Data	45.25	45.14
	J	No Data	No Data	26.46	25.76	No Data	No Data	30.16	22.63
	J	No Data	No Data	39.22	33.80	No Data	No Data	38.52	33.10
	J	No Data	No Data	26.46	25.76	No Data	No Data	27.06	25.45
27	C	No Data	No Data	45.65	45.15	45.84	45.80	45.80	45.82
	C	No Data	No Data	22.04	31.79	Low[a]	13.03	15.80	14.97
	J	No Data	No Data	39.30	44.53	36.82	43.10	35.34	43.55
	J	No Data	No Data	43.13	44.53	42.28	43.00	40.31	40.91
	J	No Data	No Data	41.62	42.73	41.63	43.28	40.41	40.71
28	C	No Data	No Data	38.26	43.22	14.72	30.44	15.05	29.24
	C	No Data	No Data	45.57	43.22	46.11	46.11	46.02	46.11
	C	No Data	No Data	No Data	No Data	No Data	No Data	45.92	46.02
	J	No Data	No Data	36.63	43.45	37.11	42.99	34.64	40.60
	J	No Data	No Data	43.44	43.04	42.26	43.76	43.22	41.53
	J	No Data	No Data	41.21	43.32	43.49	44.86	42.09	44.89
29	C	No Data	No Data	45.95	45.95	45.81	44.39	38.07	42.79
	C	No Data	No Data	46.03	45.85	19.57	20.67	45.41	45.86
	J	No Data	No Data	45.98	45.85	39.34	36.23	37.25	31.70
	J	No Data	No Data	46.03	45.55	39.34	45.41	35.55	41.04
	J	No Data	No Data	45.95	45.55	39.22	39.72	35.35	30.84
	J	No Data	No Data	40.24	41.80	37.13	37.13	34.87	33.35
31	C	No Data	No Data	34.79	44.36	31.46	32.16	14.68	40.05
	C	No Data	No Data	45.27	45.47	17.98	15.48	18.38	31.26
	J	No Data	No Data	44.97	42.36	40.15	38.55	42.25	39.55
	J	No Data	No Data	43.97	44.16	37.75	36.15	38.45	31.66
	J	No Data	No Data	45.49	45.16	37.55	33.56	35.95	29.76
32	C	No Data	No Data	No Data	No Data	No Data	No Data	30.26	26.87
	C	No Data	No Data	44.80	42.79	36.55	15.98	No Data	24.67
	C	No Data	No Data	45.42	44.89	27.56	Low[a]	37.05	22.47
	J	No Data	No Data	45.40	44.70	39.65	33.76	36.85	29.96
	J	No Data	No Data	44.99	44.70	38.45	40.75	35.06	32.66
	J	No Data	No Data	45.42	44.99	43.55	41.95	39.35	40.65
47	C	45.38	45.35	No Data	No Data	No Data	No Data	No Data	No Data

[a] "Low" indicates that the LTE_δ was below 12% and thus no value could be determined for TLE, as this is out of the range of the LTE_δ-TLE plot.

Table B.27 (cont'd).

Site No.	Test Type	April 1997 TLE (%)		July 1997 TLE (%)		Oct. 1997 TLE (%)		June 1998 TLE (%)	
		Before	After	Before	After	Before	After	Before	After
47	C	45.38	45.14	No Data	No Data	No Data	No Data	No Data	No Data
	C	45.36	44.76	No Data	No Data	No Data	No Data	No Data	No Data
	C	28.61	23.90	No Data	No Data	No Data	No Data	No Data	No Data
	J	37.08	35.87	No Data	No Data	No Data	No Data	No Data	No Data
48	C	26.22	23.08	No Data	No Data	No Data	No Data	No Data	No Data
	C	45.36	44.56	No Data	No Data	No Data	No Data	No Data	No Data
	C	43.25	42.94	No Data	No Data	No Data	No Data	No Data	No Data
	C	45.36	44.85	No Data	No Data	No Data	No Data	No Data	No Data
	C	45.35	45.35	No Data	No Data	No Data	No Data	No Data	No Data
	J	30.94	28.32	No Data	No Data	No Data	No Data	No Data	No Data
	J	35.58	38.49	No Data	No Data	No Data	No Data	No Data	No Data

Table B.28 TLE Data, Slag Pavements.

Site No.	Test Type	April 1997 TLE (%)		July 1997 TLE (%)		Oct. 1997 TLE (%)		June 1998 TLE (%)	
		Before	After	Before	After	Before	After	Before	After
1	C	45.46	44.54	46.61	46.17	44.29	43.19	44.40	44.00
	C	45.46	45.31	46.66	46.47	43.99	43.60	No Data	No Data
	C	45.44	44.93	46.66	46.37	43.90	43.49	No Data	No Data
	C	45.45	44.84	46.57	46.47	44.42	43.60	No Data	No Data
	J	41.91	37.55	46.70	46.22	40.12	36.56	44.39	43.70
40	C	45.15	45.51	45.47	44.44	No Data	No Data	45.49	44.57
	C	No Data	No Data	No Data	No Data	No Data	No Data	45.35	44.77
	J	45.05	44.73	45.34	44.87	No Data	No Data	45.45	45.05
41	C	45.85	45.43	45.21	45.21	No Data	No Data	44.81	45.01
	C	No Data	No Data	No Data	No Data	No Data	No Data	44.91	45.11
	C	45.73	45.73	45.21	44.81	No Data	No Data	45.21	44.91
	C	45.88	45.25	45.22	44.81	No Data	No Data	45.21	45.01
	J	45.15	45.03	45.21	44.32	No Data	No Data	44.91	44.32
55	C	24.28	34.79	46.21	46.71	24.81	22.43	20.95	26.53
	C	34.59	44.53	46.86	46.01	23.63	22.83	33.09	41.75
	J	No Data	37.95	40.75	41.45	30.19	35.37	24.27	28.99
	J	24.28	No Data	44.71	46.86	28.99	32.15	22.83	23.93
	J	No Data	No Data	44.96	46.36	30.19	40.95	25.55	34.77
	J	No Data	No Data	44.01	46.46	26.89	42.19	26.19	33.83
58	C	No Data	No Data	44.80	45.18	45.47	44.88	45.47	45.37
	C	No Data	No Data	44.80	44.99	45.25	45.25	45.27	45.37
	J	No Data	No Data	41.78	41.27	43.14	42.35	43.47	42.35
	J	No Data	No Data	41.37	40.66	42.25	41.44	44.88	45.15
	J	No Data	No Data	34.32	32.30	30.31	29.89	45.47	44.88
	J	No Data	No Data	34.52	41.98	33.79	35.07	45.47	45.15
59	C	No Data	No Data	44.60	44.80	45.07	44.88	44.97	45.07
	C	No Data	No Data	45.00	44.30	44.78	44.88	44.68	45.07
	J	No Data	No Data	33.80	42.90	34.39	39.03	44.68	45.07
	J	No Data	No Data	37.20	37.40	35.67	36.97	44.78	45.15
	J	No Data	No Data	38.00	40.30	33.29	35.27	44.45	44.34
60	C	No Data	No Data	44.68	44.28	44.13	44.52	44.72	44.13
	C	No Data	No Data	44.67	44.18	44.32	44.92	44.92	44.72
	J	No Data	No Data	44.48	44.28	35.93	40.13	44.62	44.42
	J	No Data	No Data	40.79	42.89	29.74	34.64	44.92	44.23
	J	No Data	No Data	40.58	40.79	29.04	30.24	44.62	43.82
61	C	No Data	No Data	43.98	43.88	43.93	43.51	44.02	43.71
	C	No Data	No Data	44.47	43.98	44.31	43.93	44.61	43.83

Table B.28 (cont'd).

Site No.	Test Type	April 1997 TLE (%)		July 1997 TLE (%)		Oct. 1997 TLE (%)		June 1998 TLE (%)	
		Before	After	Before	After	Before	After	Before	After
61	J	No Data	No Data	44.68	43.88	41.73	42.14	44.41	42.43
	J	No Data	No Data	44.47	43.67	38.15	39.45	44.21	43.51
	J	No Data	No Data	44.27	44.27	37.85	35.85	44.61	43.72
	J	No Data	No Data	44.37	44.37	28.52	28.52	44.63	43.92
62	C	No Data	No Data	44.61	44.31	44.21	43.72	44.61	44.02
	C	No Data	No Data	44.61	44.21	43.93	44.22	44.51	43.93
	J	No Data	No Data	44.81	44.21	39.85	37.45	44.51	43.93
	J	No Data	No Data	45.01	44.41	36.75	39.75	44.61	44.02
	J	No Data	No Data	44.91	43.91	37.25	38.95	44.41	43.82
63	C	No Data	No Data	No Data	No Data	28.75	22.03	23.63	No Data
	C	No Data	No Data	No Data	No Data	44.13	43.47	30.69	41.89
	J	No Data	No Data	No Data	No Data	28.75	39.17	26.89	33.53
	J	No Data	No Data	No Data	No Data	22.83	29.49	22.83	31.43
	J	No Data	No Data	No Data	No Data	23.93	28.45	25.55	30.19

Table B.29 P_T Data, Carbonate Pavements.

Site No.	Test Type	April 1997 P_T (kN)		July 1997 P_T (kN)		Oct. 1997 P_T (kN)		June 1998 P_T (kN)	
		Before	After	Before	After	Before	After	Before	After
5	C	18.10	18.10	18.10	18.11	18.11	18.19	18.15	18.19
	C	18.02	18.10	18.10	18.10	18.03	18.19	18.19	18.19
	J	17.01	16.28	18.10	18.10	16.25	14.79	18.06	18.10
6	C	18.48	18.48	18.45	18.41	18.54	18.54	18.54	18.40
	C	18.48	18.44	18.45	18.41	18.57	18.55	18.50	18.50
	J	18.17	17.98	18.21	18.06	18.18	18.07	18.55	18.48
7	C	18.26	18.04	18.24	18.15	18.04	17.76	18.04	17.88
	C	6.97	10.55	18.25	18.23	5.29	5.13	18.00	18.04
	J	17.48	17.40	17.78	17.82	17.20	17.40	17.76	17.76
8	C	18.32	18.32	18.14	18.02	18.06	18.02	18.06	17.94
	C	18.35	18.24	18.18	17.86	18.02	17.82	18.06	17.94
	J	18.35	18.27	18.19	17.94	17.78	16.94	18.06	17.90
35	C	18.25	18.25	18.17	18.09	18.28	18.24	18.32	18.23
	C	18.24	18.20	18.13	18.17	18.28	18.27	18.28	18.32
	J	18.20	18.31	18.22	17.98	17.96	18.04	18.27	18.00
36	C	17.77	17.77	18.26	18.26	17.75	17.63	17.79	17.79
	C	17.85	17.85	18.39	18.45	17.59	17.84	17.79	17.79
	J	17.30	17.90	18.50	18.26	16.12	17.43	17.84	17.67
38	C	18.44	18.25	17.88	17.80	No Data	No Data	18.20	17.88
	C	18.44	18.40	17.88	18.04	No Data	No Data	18.15	18.07
	C	18.52	18.24	17.92	17.60	No Data	No Data	18.20	17.88
	J	18.28	17.76	15.78	16.95	No Data	No Data	14.63	15.58
39	C	18.32	18.32	17.97	17.97	No Data	No Data	18.21	18.09
	C	18.39	18.21	18.01	17.89	No Data	No Data	18.12	17.93
	C	18.32	18.16	18.09	17.80	No Data	No Data	18.16	17.85
	J	18.02	17.76	18.21	17.93	No Data	No Data	15.04	15.82
42	C	17.34	17.20	16.81	17.48	17.19	17.44	16.81	17.52
	C	17.34	16.95	16.88	16.42	17.15	16.64	8.71	9.69
	J	17.38	16.95	17.27	17.14	17.27	16.64	17.50	17.23
43	C	17.24	17.05	17.20	17.20	16.88	16.77	16.05	15.80
	C	15.62	16.42	15.38	14.86	14.06	15.11	13.05	9.42
	J	17.27	16.88	16.88	16.32	16.92	16.17	17.27	17.50
	J	17.01	16.81	16.73	16.13	16.92	16.05	16.17	17.10
44	C	No Data	No Data	17.23	17.05	17.27	17.20	17.44	17.23
	C	No Data	No Data	15.38	16.05	14.06	15.73	13.47	15.46
	J	No Data	No Data	16.50	14.18	16.57	16.24	17.34	16.17
	J	No Data	No Data	15.42	16.84	16.69	16.17	15.27	16.05

Table B.29 (cont'd).

Site No.	Test Type	April 1997 P_T (kN)		July 1997 P_T (kN)		Oct. 1997 P_T (kN)		June 1998 P_T (kN)	
		Before	After	Before	After	Before	After	Before	After
44	J	No Data	No Data	16.24	12.24	16.17	11.91	16.05	15.58
	J	No Data	No Data	16.57	16.32	16.53	16.68	16.84	16.69
45	C	No Data	No Data	17.96	17.88	18.31	18.25	18.30	18.22
	J	No Data	No Data	17.80	17.80	17.29	18.26	18.14	18.31
	J	No Data	No Data	No Data	No Data	18.31	17.46	18.22	18.26
46	C	No Data	No Data	17.89	17.93	17.99	18.31	18.26	18.32
	J	No Data	No Data	17.89	17.61	18.21	17.98	18.17	18.25
	J	No Data	No Data	17.73	16.82	16.73	16.80	17.70	17.58
49	C	18.57	18.54	18.47	18.24	18.49	18.51	18.52	18.44
	J	18.49	18.32	18.48	18.47	16.56	16.35	18.51	18.32
50	C	7.73	8.62	18.73	18.79	8.87	7.85	18.38	18.11
	C	18.42	18.38	18.57	18.79	18.40	18.38	18.38	18.15
	C	18.49	18.32	18.79	18.70	18.34	18.22	18.39	18.25
	C	18.49	18.38	18.77	18.79	17.44	17.09	16.93	15.35
	J	16.00	15.26	18.55	18.77	15.59	14.42	17.98	17.70
51	C	Low[a]	Low[a]	Low[a]	Low[a]	Low[a]	Low[a]	Low[a]	Low[a]
	C	18.48	18.46	17.72	17.72	18.37	18.30	18.26	18.26
	C	18.49	18.23	17.71	17.70	18.31	18.35	18.30	18.19
	C	18.19	18.42	17.62	17.66	18.31	18.35	18.37	18.15
52	C	18.49	18.46	18.38	18.22	18.36	18.30	18.36	18.22
	C	18.49	18.46	18.42	18.42	18.19	18.35	18.36	18.35
	C	18.47	18.48	18.38	18.42	18.36	18.36	18.35	18.12
	J	18.49	18.47	18.45	18.45	18.37	18.08	18.35	18.36

[a] "Low" indicates that the LTE_δ was below 12% and thus no value could be determined for P_T, as this is out of the range of the LTE_δ-TLE plot.

Table B.30 P_T Data, Natural Gravel Pavements.

Site No.	Test Type	April 1997 P_T (kN)		July 1997 P_T (kN)		Oct. 1997 P_T (kN)		June 1998 P_T (kN)	
		Before	After	Before	After	Before	After	Before	After
2	C	17.93	17.97	18.12	18.08	17.42	17.98	17.98	17.98
	C	17.97	17.93	18.12	18.20	17.58	17.98	17.82	17.94
	C	17.97	17.97	18.20	18.04	17.66	17.98	17.98	17.98
	J	14.81	17.29	18.20	18.08	13.51	16.98	14.30	17.38
3	C	18.08	18.08	18.00	17.92	18.05	17.97	18.05	18.05
	C	18.08	18.08	18.00	18.00	18.05	18.05	18.01	18.05
	C	No Data	No Data	17.68	18.00	13.40	17.41	17.97	No Data
	J	14.70	16.95	15.48	16.56	14.52	17.16	12.92	16.56
4	C	18.15	18.15	18.03	17.99	18.05	18.05	18.01	17.81
	C	18.16	18.16	18.03	18.03	18.05	18.06	18.05	17.97
	J	17.22	16.41	17.23	17.31	8.27	9.91	17.05	15.37
9	C	18.13	18.12	No Data	No Data	No Data	No Data	No Data	No Data
	C	8.02	10.07	No Data	No Data	No Data	No Data	No Data	No Data
	J	16.51	15.99	No Data	No Data	No Data	No Data	No Data	No Data
10	C	12.22	11.26	No Data	No Data	9.08	9.52	7.46	12.18
	C	No Data	No Data	No Data	No Data	No Data	No Data	7.14	10.43
	C	18.03	18.03	No Data	No Data	8.05	9.92	17.87	17.87
	J	16.82	16.26	No Data	No Data	15.99	16.11	16.43	16.15
37	C	18.03	18.03	18.30	18.05	17.73	17.93	17.89	17.81
	C	10.59	14.48	18.30	18.28	7.79	9.26	7.79	11.34
	C	No Data	No Data	18.29	18.30	7.67	8.82	7.19	7.03
	C	9.54	17.87	18.28	18.28	6.03	7.79	5.75	12.26
	C	16.34	17.55	18.30	18.05	11.22	9.26	11.62	10.22
	C	17.91	18.03	18.30	17.78	17.97	17.97	17.69	17.73
	J	13.25	14.32	17.97	17.83	9.98	12.94	10.22	9.70
38A	C	18.11	18.07	18.30	18.28	17.81	17.97	17.97	17.73
	C	16.38	17.75	18.30	18.05	9.14	9.26	9.26	7.67
	C	18.12	18.07	18.30	18.12	17.97	17.81	17.97	17.89
	C	18.07	18.11	18.30	18.12	17.81	17.89	17.81	17.97
	C	17.27	18.03	18.12	16.13	17.41	17.93	16.93	17.97
	C	No Data	No Data	No Data	No Data	No Data	No Data	17.97	17.93
	J	13.69	12.44	17.71	16.45	11.22	10.90	11.14	10.62
57	C	18.09	17.89	17.84	17.57	17.86	17.66	17.90	17.78
	C	18.10	18.05	17.89	17.80	17.46	17.86	17.91	17.90
	C	18.09	17.97	17.88	17.33	17.90	17.86	17.82	17.86
	C	18.05	18.05	17.88	17.89	17.74	17.91	17.66	17.74
	C	No Data	No Data	No Data	No Data	No Data	No Data	17.90	17.82

Table B.30 (cont'd).

Site No.	Test Type	April 1997 P_T (kN)		July 1997 P_T (kN)		Oct. 1997 P_T (kN)		June 1998 P_T (kN)	
		Before	After	Before	After	Before	After	Before	After
57	J	18.01	17.89	17.09	17.44	17.34	17.50	17.02	17.22
	J	18.01	17.85	16.49	17.48	15.95	17.54	16.18	17.22

Table B.31 P_T Data, Recycled Pavements.

Site No.	Test Type	April 1997 P_T (kN)		July 1997 P_T (kN)		Oct. 1997 P_T (kN)		June 1998 P_T (kN)	
		Before	After	Before	After	Before	After	Before	After
11	C	14.05	13.89	7.45	18.19	5.17	6.10	6.79	6.95
	C	18.58	18.54	18.03	18.15	18.19	18.10	17.98	17.91
	C	18.55	18.57	18.07	18.11	18.14	18.20	18.14	18.14
	C	18.54	18.34	18.19	17.59	18.20	18.02	18.18	17.78
	C	No Data	No Data	7.89	6.63	6.46	5.17	8.49	5.94
	C	18.46	18.22	17.47	17.92	18.02	17.95	17.66	18.10
	C	No Data	No Data	No Data	No Data	No Data	No Data	9.70	6.95
	J	16.96	16.87	16.17	17.15	16.45	17.06	16.90	16.78
12	C	12.92	13.12	9.34	12.29	6.95	7.76	8.61	11.84
	C	18.30	18.30	17.66	17.78	No Data	No Data	17.95	18.10
	C	11.83	11.63	8.63	11.09	7.88	6.63	8.93	6.10
	C	12.92	12.32	9.66	8.79	10.23	12.49	11.36	8.77
	C	14.96	15.53	No Data	No Data	7.44	13.23	9.83	10.23
	C	18.32	18.31	17.78	17.82	18.18	18.06	18.10	18.14
	J	16.10	17.05	17.23	17.70	17.46	17.14	17.02	17.02
13	C	18.34	18.00	8.26	17.67	8.14	16.94	7.04	17.99
	C	18.31	18.32	17.95	17.95	18.35	18.43	18.30	18.26
	C	14.56	16.16	11.94	11.74	9.61	11.77	11.69	12.26
	J	16.32	16.74	16.27	16.07	16.98	17.45	16.48	17.22
	J	17.71	17.30	17.35	16.31	17.86	17.71	18.03	17.49
14	C	18.14	18.09	17.82	17.81	17.64	17.75	17.87	17.75
	C	18.13	17.90	17.86	17.54	17.83	17.68	17.91	17.68
	C	18.05	17.90	17.78	17.34	17.87	17.68	17.87	17.68
	C	18.05	18.13	17.70	17.74	17.83	17.64	17.79	17.72
	J	18.13	17.86	17.74	17.54	16.84	15.96	17.75	17.76
15	C	18.65	18.42	18.73	18.45	17.72	17.60	17.83	17.68
	C	18.66	18.42	18.73	18.41	17.83	17.64	17.83	17.64
	C	18.65	18.65	18.67	18.65	17.87	17.87	No Data	No Data
	J	18.29	17.96	18.11	17.91	17.43	16.64	17.28	16.96
	J	No Data	17.79	18.39	18.03	No Data	No Data	17.04	16.48
16	C	No Data	No Data	6.60	11.42	No Data	No Data	6.07	8.29
	C	No Data	No Data	No Data	No Data	No Data	No Data	9.21	6.24
	C	No Data	No Data	18.10	17.94	No Data	No Data	18.06	18.10
	J	No Data	No Data	17.42	16.61	No Data	No Data	16.98	16.97
	J	No Data	No Data	14.04	10.30	No Data	No Data	9.21	10.70
	J	No Data	No Data	16.29	15.81	No Data	No Data	17.58	17.66
	J	No Data	No Data	17.02	16.81	No Data	No Data	16.98	16.41

Table B.31 (cont'd).

Site No.	Test Type	April 1997 P_T (kN)		July 1997 P_T (kN)		Oct. 1997 P_T (kN)		June 1998 P_T (kN)	
		Before	After	Before	After	Before	After	Before	After
17	C	No Data	No Data	8.74	8.46	No Data	No Data	10.84	9.95
	C	No Data	No Data	18.12	17.92	No Data	No Data	18.12	18.08
	J	No Data	No Data	10.60	10.32	No Data	No Data	12.08	9.06
	J	No Data	No Data	15.71	13.54	No Data	No Data	15.43	13.26
	J	No Data	No Data	10.60	10.32	No Data	No Data	10.84	10.19
27	C	No Data	No Data	18.28	18.08	18.36	18.34	18.34	18.35
	C	No Data	No Data	8.83	12.73	Low[a]	5.22	6.33	6.00
	J	No Data	No Data	15.74	17.84	14.74	17.26	14.15	17.44
	J	No Data	No Data	17.28	17.84	16.93	17.22	16.14	16.38
	J	No Data	No Data	16.67	17.12	16.67	17.33	16.18	16.30
28	C	No Data	No Data	15.32	17.31	5.90	12.19	6.03	11.71
	C	No Data	No Data	18.25	17.31	18.47	18.47	18.43	18.47
	C	No Data	No Data	No Data	No Data	No Data	No Data	18.39	18.43
	J	No Data	No Data	14.67	17.40	14.86	17.22	13.87	16.26
	J	No Data	No Data	17.40	17.24	16.93	17.53	17.31	16.63
	J	No Data	No Data	16.50	17.35	17.42	17.97	16.86	17.98
29	C	No Data	No Data	18.40	18.40	18.35	17.78	15.25	17.14
	C	No Data	No Data	18.44	18.36	7.84	8.28	18.19	18.37
	J	No Data	No Data	18.42	18.36	15.76	14.51	14.92	12.70
	J	No Data	No Data	18.44	18.24	15.76	18.19	14.24	16.44
	J	No Data	No Data	18.40	18.24	15.71	15.91	14.16	12.35
	J	No Data	No Data	16.12	16.74	14.87	14.87	13.97	13.36
31	C	No Data	No Data	13.93	17.77	12.60	12.88	5.88	16.04
	C	No Data	No Data	18.13	18.21	7.20	6.20	7.36	12.52
	J	No Data	No Data	18.01	16.96	16.08	15.44	16.92	15.84
	J	No Data	No Data	17.61	17.69	15.12	14.48	15.40	12.68
	J	No Data	No Data	18.22	18.09	15.04	13.44	14.40	11.92
32	C	No Data	No Data	No Data	No Data	No Data	No Data	12.12	10.76
	C	No Data	No Data	17.94	17.14	14.64	6.40	No Data	9.88
	C	No Data	No Data	18.19	17.98	11.04	Low[a]	14.84	9.00
	J	No Data	No Data	18.18	17.90	15.88	13.52	14.76	12.00
	J	No Data	No Data	18.02	17.90	15.40	16.32	14.04	13.08
	J	No Data	No Data	18.19	18.02	17.44	16.80	15.76	16.28
47	C	18.18	18.16	No Data	No Data	No Data	No Data	No Data	No Data

[a] "Low" indicates that the LTE_δ was below 12% and thus no value could be determined for P_T, as this is out of the range of the LTE_δ-TLE plot.

Table B.31 (cont'd).

Site No.	Test Type	April 1997 P_T (kN)		July 1997 P_T (kN)		Oct. 1997 P_T (kN)		June 1998 P_T (kN)	
		Before	After	Before	After	Before	After	Before	After
47	C	18.18	18.08	No Data	No Data	No Data	No Data	No Data	No Data
	C	18.17	17.93	No Data	No Data	No Data	No Data	No Data	No Data
	C	11.46	9.57	No Data	No Data	No Data	No Data	No Data	No Data
	J	14.85	14.37	No Data	No Data	No Data	No Data	No Data	No Data
48	C	10.50	9.24	No Data	No Data	No Data	No Data	No Data	No Data
	C	18.17	17.85	No Data	No Data	No Data	No Data	No Data	No Data
	C	17.32	17.20	No Data	No Data	No Data	No Data	No Data	No Data
	C	18.17	17.96	No Data	No Data	No Data	No Data	No Data	No Data
	C	18.16	18.16	No Data	No Data	No Data	No Data	No Data	No Data
	J	12.39	11.34	No Data	No Data	No Data	No Data	No Data	No Data
	J	14.25	15.42	No Data	No Data	No Data	No Data	No Data	No Data

Table B.32 P_T Data, Slag Pavements.

Site No.	Test Type	April 1997 P_T (kN)		July 1997 P_T (kN)		Oct. 1997 P_T (kN)		June 1998 P_T (kN)	
		Before	After	Before	After	Before	After	Before	After
1	C	18.21	17.84	18.67	18.49	17.74	17.30	17.78	17.62
	C	18.21	18.15	18.69	18.61	17.62	17.46	No Data	No Data
	C	18.20	17.99	18.69	18.57	17.58	17.42	No Data	No Data
	C	18.20	17.96	18.65	18.61	17.79	17.46	No Data	No Data
	J	16.79	15.04	18.70	18.51	16.07	14.64	17.78	17.50
40	C	18.08	18.23	18.21	17.80	No Data	No Data	18.22	17.85
	C	No Data	No Data	No Data	No Data	No Data	No Data	18.16	17.93
	J	18.04	17.92	18.16	17.97	No Data	No Data	18.20	18.04
41	C	18.36	18.19	18.11	18.11	No Data	No Data	17.95	18.03
	C	No Data	No Data	No Data	No Data	No Data	No Data	17.99	18.07
	C	18.31	18.31	18.11	17.95	No Data	No Data	18.11	17.99
	C	18.37	18.12	18.11	17.95	No Data	No Data	18.11	18.03
	J	18.08	18.03	18.11	17.75	No Data	No Data	17.99	17.75
55	C	9.72	13.93	18.51	18.71	9.94	8.98	8.39	10.62
	C	13.85	17.84	18.77	18.43	9.46	9.14	13.25	16.72
	J	No Data	15.20	16.32	16.60	12.09	14.17	9.72	11.61
	J	9.72	No Data	17.91	18.77	11.61	12.88	9.14	9.58
	J	No Data	No Data	18.01	18.57	12.09	16.40	10.23	13.93
	J	No Data	No Data	17.63	18.61	10.77	16.90	10.49	13.55
58	C	No Data	No Data	17.94	18.09	18.21	17.97	18.21	18.17
	C	No Data	No Data	17.94	18.02	18.12	18.12	18.13	18.17
	J	No Data	No Data	16.73	16.53	17.28	16.96	17.41	16.96
	J	No Data	No Data	16.57	16.28	16.92	16.60	17.97	18.08
	J	No Data	No Data	13.75	12.94	12.14	11.97	18.21	17.97
	J	No Data	No Data	13.83	16.81	13.53	14.05	18.21	18.08
59	C	No Data	No Data	17.86	17.94	18.05	17.97	18.01	18.05
	C	No Data	No Data	18.02	17.74	17.93	17.97	17.89	18.05
	J	No Data	No Data	13.54	17.18	13.77	15.63	17.89	18.05
	J	No Data	No Data	14.90	14.98	14.29	14.81	17.93	18.08
	J	No Data	No Data	15.22	16.14	13.33	14.13	17.80	17.76
60	C	No Data	No Data	17.89	17.73	17.67	17.83	17.91	17.67
	C	No Data	No Data	17.89	17.69	17.75	17.99	17.99	17.91
	J	No Data	No Data	17.81	17.73	14.39	16.07	17.87	17.79
	J	No Data	No Data	16.34	17.18	11.91	13.87	17.99	17.71
	J	No Data	No Data	16.25	16.33	11.63	12.11	17.87	17.55
61	C	No Data	No Data	17.61	17.57	17.59	17.43	17.63	17.51
	C	No Data	No Data	17.81	17.61	17.75	17.59	17.86	17.55

Table B.32 (cont'd).

Site No.	Test Type	April 1997 P_T (kN)		July 1997 P_T (kN)		Oct. 1997 P_T (kN)		June 1998 P_T (kN)	
		Before	After	Before	After	Before	After	Before	After
61	J	No Data	No Data	17.89	17.57	16.71	16.88	17.78	16.99
	J	No Data	No Data	17.81	17.49	15.28	15.80	17.71	17.43
	J	No Data	No Data	17.73	17.73	15.16	14.36	17.87	17.51
	J	No Data	No Data	17.77	17.77	11.42	11.42	17.87	17.59
62	C	No Data	No Data	17.87	17.74	17.71	17.51	17.87	17.63
	C	No Data	No Data	17.87	17.70	17.59	17.71	17.82	17.59
	J	No Data	No Data	17.95	17.70	15.96	15.00	17.83	17.59
	J	No Data	No Data	18.03	17.79	14.72	15.92	17.87	17.63
	J	No Data	No Data	17.99	17.58	14.92	15.60	17.78	17.55
63	C	No Data	No Data	No Data	No Data	11.51	8.82	9.46	No Data
	C	No Data	No Data	No Data	No Data	17.67	17.41	12.29	16.78
	J	No Data	No Data	No Data	No Data	11.51	15.69	10.77	13.43
	J	No Data	No Data	No Data	No Data	9.14	11.81	9.14	12.59
	J	No Data	No Data	No Data	No Data	9.58	11.39	10.23	12.09

Table B.33 AGG Data, Carbonate Pavements.

Site No.	Test Type	April 1997 AGG (kPa)		July 1997 AGG (kPa)		Oct. 1997 AGG (kPa)		June 1998 AGG (kPa)	
		Before	After	Before	After	Before	After	Before	After
5	C	2.8E+06	2.4E+08	3.6E+06	2.7E+08	1.9E+06	1.7E+07	2.3E+06	6.2E+06
	C	1.7E+06	5.4E+06	2.6E+07	2.6E+07	1.4E+06	4.2E+06	1.1E+07	3.7E+06
	J	2.5E+05	1.5E+05	1.6E+07	3.1E+06	1.6E+05	8.4E+04	1.6E+06	1.7E+06
6	C	1.6E+08	9.3E+07	1.9E+08	2.2E+06	2.0E+06	2.0E+06	2.0E+06	9.8E+05
	C	1.6E+08	2.5E+06	1.9E+08	3.4E+06	2.3E+07	3.8E+06	1.7E+06	1.4E+06
	J	5.6E+05	3.5E+05	8.0E+05	5.2E+05	4.5E+05	3.7E+05	7.1E+06	1.3E+06
7	C	2.1E+08	9.1E+05	1.3E+07	1.5E+06	3.4E+07	9.4E+05	3.4E+07	1.2E+06
	C	9.3E+03	2.0E+04	2.1E+08	2.5E+06	8.3E+03	7.8E+03	2.0E+06	5.7E+06
	J	3.2E+05	2.9E+05	4.7E+05	4.9E+05	3.4E+05	4.4E+05	8.8E+05	9.4E+05
8	C	2.8E+06	3.6E+06	2.5E+06	1.4E+06	4.2E+06	2.1E+06	6.2E+06	1.6E+06
	C	2.4E+08	1.6E+06	4.1E+06	9.9E+05	2.3E+06	1.1E+06	3.7E+07	1.6E+06
	J	2.4E+08	1.8E+06	3.1E+08	1.2E+06	1.0E+06	2.7E+05	2.8E+08	1.3E+06
35	C	2.7E+06	3.2E+06	2.1E+06	1.5E+06	2.1E+06	1.7E+06	5.6E+06	1.6E+06
	C	2.4E+06	2.0E+06	1.7E+06	2.1E+06	2.5E+06	1.9E+06	2.5E+06	3.8E+06
	J	2.0E+06	1.8E+08	3.7E+06	1.1E+06	6.6E+05	8.6E+05	1.9E+06	7.6E+05
36	C	1.9E+06	1.9E+06	7.4E+05	7.1E+05	1.9E+06	1.3E+06	2.3E+06	2.3E+06
	C	2.8E+06	3.4E+06	1.2E+06	1.8E+06	1.2E+06	6.8E+06	2.5E+06	2.5E+06
	J	6.0E+05	1.4E+07	1.1E+07	7.4E+05	1.9E+05	7.1E+05	1.9E+07	1.4E+06
38	C	1.3E+06	7.7E+05	6.9E+05	5.2E+05	No Data	No Data	2.9E+06	6.9E+05
	C	1.4E+06	1.2E+06	6.9E+05	9.9E+05	No Data	No Data	1.6E+06	1.2E+06
	C	1.9E+06	7.1E+05	7.7E+05	3.8E+05	No Data	No Data	8.8E+06	6.4E+05
	J	8.2E+05	3.7E+05	9.7E+04	1.9E+05	No Data	No Data	6.1E+04	8.4E+04
39	C	1.2E+06	1.2E+06	7.9E+05	7.5E+05	No Data	No Data	2.2E+06	1.1E+06
	C	5.6E+05	4.1E+05	8.8E+05	6.2E+05	No Data	No Data	1.2E+06	7.0E+05
	C	1.2E+06	7.6E+05	1.0E+06	4.8E+05	No Data	No Data	1.4E+06	5.3E+05
	J	5.6E+05	4.1E+05	2.2E+06	6.6E+05	No Data	No Data	7.0E+04	9.9E+04
42	C	1.6E+06	1.1E+06	5.4E+05	3.9E+06	1.0E+06	2.8E+06	5.4E+05	3.4E+08
	C	1.6E+06	6.1E+05	5.7E+05	3.4E+05	9.4E+05	4.2E+05	2.4E+04	3.0E+04
	J	1.9E+06	6.1E+05	1.3E+06	8.8E+05	1.3E+06	4.2E+05	5.1E+06	1.1E+06
43	C	1.2E+06	7.1E+05	1.1E+06	1.1E+06	5.7E+05	5.1E+05	2.5E+05	2.1E+05
	C	1.9E+05	3.4E+05	1.7E+05	1.3E+05	9.8E+04	1.5E+05	7.0E+04	2.8E+04
	J	1.3E+06	5.7E+05	5.7E+05	3.0E+05	5.9E+05	2.8E+05	1.3E+06	5.1E+06
	J	6.7E+05	5.4E+05	4.7E+05	2.7E+05	5.9E+05	2.5E+05	2.8E+05	7.8E+05
44	C	No Data	No Data	1.1E+06	7.4E+05	1.3E+06	1.1E+06	2.5E+06	1.1E+06
	C	No Data	No Data	1.7E+05	2.5E+05	9.8E+04	2.0E+05	7.8E+04	1.8E+05
	J	No Data	No Data	3.6E+05	1.0E+05	3.9E+05	2.8E+05	1.6E+06	2.8E+05
	J	No Data	No Data	1.7E+05	5.6E+05	4.6E+05	2.8E+05	1.6E+05	2.5E+05

Table B.33 (cont'd).

Site No.	Test Type	April 1997 AGG (kPa)		July 1997 AGG (kPa)		Oct. 1997 AGG (kPa)		June 1998 AGG (kPa)	
		Before	After	Before	After	Before	After	Before	After
44	J	No Data	No Data	2.8E+05	5.4E+04	2.8E+05	5.1E+04	2.5E+05	1.9E+05
	J	No Data	No Data	3.9E+05	3.0E+05	3.8E+05	4.4E+05	5.6E+05	4.6E+05
45	C	No Data	No Data	2.7E+06	1.8E+06	6.8E+06	2.3E+06	3.6E+06	2.1E+06
	J	No Data	No Data	1.6E+06	1.6E+06	3.4E+05	2.5E+06	1.6E+06	2.9E+07
	J	No Data	No Data	No Data	No Data	4.0E+07	4.2E+05	2.1E+06	2.5E+06
46	C	No Data	No Data	3.1E+06	4.4E+06	9.8E+05	1.8E+07	3.0E+06	3.1E+08
	J	No Data	No Data	3.8E+06	1.1E+06	1.9E+06	9.2E+05	1.7E+06	2.3E+06
	J	No Data	No Data	1.6E+06	3.7E+05	2.2E+05	2.3E+05	5.4E+05	4.9E+05
49	C	2.6E+07	4.1E+06	3.6E+06	1.1E+06	1.7E+07	3.6E+07	2.8E+08	2.8E+06
	J	2.0E+06	1.1E+06	1.6E+07	3.2E+06	1.6E+05	1.5E+05	2.7E+07	1.4E+06
50	C	1.3E+04	1.6E+04	1.7E+06	1.2E+07	1.6E+04	1.2E+04	3.1E+06	8.5E+05
	C	2.1E+06	1.7E+06	8.8E+05	4.5E+06	3.1E+07	3.1E+06	3.1E+06	9.0E+05
	C	2.6E+08	1.4E+06	8.3E+06	1.5E+06	1.9E+06	1.2E+06	1.4E+07	1.3E+06
	C	2.6E+08	1.7E+06	3.8E+06	4.5E+06	2.8E+05	2.0E+05	1.8E+05	8.0E+04
	J	1.2E+05	8.2E+04	7.7E+05	2.4E+06	8.7E+04	5.9E+04	5.7E+05	3.9E+05
51	C	6.7E+03	3.6E+03	4.2E+03	3.0E+03	6.2E+03	5.1E+03	4.5E+03	3.4E+03
	C	2.4E+07	3.4E+06	2.1E+08	2.7E+07	2.8E+08	2.1E+06	1.8E+06	1.8E+06
	C	1.4E+08	9.7E+05	8.7E+06	2.8E+06	2.8E+06	5.2E+06	2.1E+06	1.3E+06
	C	9.2E+05	2.5E+06	1.3E+06	1.6E+06	2.3E+06	3.8E+06	3.7E+07	1.2E+06
52	C	1.4E+08	3.4E+06	2.8E+06	1.2E+06	1.7E+07	2.1E+06	1.7E+07	1.6E+06
	C	2.6E+08	4.7E+06	3.3E+06	3.8E+06	1.3E+06	3.8E+06	1.7E+07	4.3E+06
	C	1.5E+07	2.4E+07	2.4E+06	3.8E+06	1.2E+07	6.2E+06	3.8E+06	1.1E+06
	J	2.6E+08	1.5E+07	1.6E+08	2.9E+08	2.7E+07	1.0E+06	3.3E+06	1.2E+07

Table B.34 AGG Data, Natural Gravel Pavements.

Site No.	Test Type	April 1997 AGG (kPa)		July 1997 AGG (kPa)		Oct. 1997 AGG (kPa)		June 1998 AGG (kPa)	
		Before	After	Before	After	Before	After	Before	After
2	C	2.6E+06	4.7E+06	1.8E+06	1.6E+06	6.4E+05	3.4E+07	3.4E+07	3.5E+08
	C	2.1E+07	2.6E+06	1.8E+06	3.8E+06	8.5E+05	5.3E+06	1.8E+06	2.9E+06
	C	7.7E+06	3.3E+07	3.8E+06	1.3E+06	1.1E+06	4.7E+06	4.7E+06	3.5E+08
	J	1.1E+05	5.8E+05	3.3E+06	1.6E+06	7.4E+04	4.0E+05	9.6E+04	6.2E+05
3	C	1.0E+07	2.5E+08	3.0E+07	1.4E+06	1.7E+07	1.9E+06	1.7E+07	3.3E+06
	C	2.5E+08	2.5E+08	2.7E+06	4.3E+06	1.2E+07	1.6E+08	2.8E+06	2.7E+07
	C	No Data	No Data	7.5E+05	2.3E+08	5.7E+04	4.8E+05	1.9E+06	No Data
	J	7.6E+04	2.4E+05	9.8E+04	1.8E+05	8.2E+04	3.6E+05	5.1E+04	2.1E+05
4	C	4.6E+06	2.8E+06	1.4E+08	2.0E+06	1.5E+07	1.0E+07	2.4E+06	9.8E+05
	C	2.1E+08	1.2E+08	2.5E+08	3.3E+06	1.0E+07	2.3E+07	1.0E+07	1.5E+06
	J	2.5E+05	1.3E+05	3.5E+05	4.0E+05	1.5E+04	2.0E+04	2.7E+05	9.3E+04
9	C	1.2E+07	3.9E+06	No Data	No Data	No Data	No Data	No Data	No Data
	C	1.7E+04	2.6E+04	No Data	No Data	No Data	No Data	No Data	No Data
	J	2.1E+05	1.5E+05	No Data	No Data	No Data	No Data	No Data	No Data
10	C	4.6E+04	3.7E+04	No Data	No Data	2.8E+04	3.1E+04	2.0E+04	5.9E+04
	C	No Data	No Data	No Data	No Data	No Data	No Data	1.9E+04	3.8E+04
	C	3.2E+08	5.9E+06	No Data	No Data	2.3E+04	3.4E+04	3.9E+08	3.9E+08
	J	2.9E+05	1.9E+05	No Data	No Data	2.3E+05	2.4E+05	3.0E+05	2.4E+05
37	C	1.7E+06	1.7E+06	1.7E+08	6.9E+05	1.2E+06	3.1E+06	2.1E+06	1.4E+06
	C	2.5E+04	7.2E+04	1.7E+08	2.0E+06	1.7E+04	2.3E+04	1.7E+04	3.7E+04
	C	No Data	No Data	1.0E+07	1.7E+08	1.6E+04	2.1E+04	1.5E+04	1.4E+04
	C	2.0E+04	9.8E+05	3.2E+06	3.2E+06	1.2E+04	1.7E+04	1.1E+04	4.7E+04
	C	1.6E+05	4.6E+05	1.7E+08	6.9E+05	3.6E+04	2.3E+04	3.9E+04	2.9E+04
	C	1.1E+06	1.7E+06	1.7E+08	3.4E+05	4.7E+06	1.9E+07	1.1E+06	1.2E+06
	J	4.9E+04	6.7E+04	5.5E+05	3.8E+05	2.7E+04	5.6E+04	2.9E+04	2.5E+04
38A	C	4.7E+06	2.5E+06	1.7E+08	2.3E+06	1.6E+06	6.8E+06	4.7E+06	1.2E+06
	C	1.6E+05	7.2E+05	9.7E+07	6.9E+05	2.2E+04	2.3E+04	2.3E+04	1.6E+04
	C	2.6E+08	2.5E+06	9.7E+07	7.9E+05	1.3E+07	1.6E+06	3.1E+08	1.9E+06
	C	2.1E+06	1.1E+07	1.7E+08	8.8E+05	1.6E+06	2.1E+06	1.6E+06	6.8E+06
	C	3.3E+05	1.7E+06	8.8E+05	8.6E+04	5.6E+05	2.5E+06	3.4E+05	4.7E+06
	C	No Data	No Data	No Data	No Data	No Data	No Data	4.0E+07	2.3E+06
	J	5.5E+04	4.0E+04	3.1E+05	1.0E+05	3.6E+04	3.3E+04	3.4E+04	3.1E+04
57	C	7.1E+06	1.4E+06	3.3E+06	1.4E+06	3.1E+06	1.7E+06	1.7E+07	2.3E+06
	C	4.2E+07	2.4E+06	2.5E+08	2.7E+06	9.2E+05	3.1E+06	4.2E+08	4.0E+07
	C	1.9E+07	1.8E+06	6.5E+06	7.9E+05	1.7E+07	4.1E+06	2.6E+06	3.4E+06
	C	2.4E+06	2.7E+06	5.8E+06	1.8E+07	2.1E+06	4.2E+08	1.6E+06	1.9E+06
	C	No Data	No Data	No Data	No Data	No Data	No Data	5.5E+06	2.6E+06

Table B.34 (cont'd).

Site No.	Test Type	April 1997 AGG (kPa)		July 1997 AGG (kPa)		Oct. 1997 AGG (kPa)		June 1998 AGG (kPa)	
		Before	After	Before	After	Before	After	Before	After
57	J	2.0E+06	1.4E+06	6.1E+05	9.2E+05	7.5E+05	9.6E+05	5.2E+05	6.9E+05
	J	2.2E+06	1.2E+06	3.5E+05	1.0E+06	2.3E+05	1.2E+06	2.6E+05	6.9E+05

Table B.35 AGG Data, Recycled Pavements.

Site No.	Test Type	April 1997 AGG (kPa)		July 1997 AGG (kPa)		Oct. 1997 AGG (kPa)		June 1998 AGG (kPa)	
		Before	After	Before	After	Before	After	Before	After
11	C	3.1E+04	2.9E+04	1.3E+04	3.1E+06	8.7E+03	1.1E+04	1.2E+04	1.3E+04
	C	1.4E+08	2.6E+06	1.4E+06	2.0E+06	1.2E+07	2.0E+06	1.2E+06	9.8E+05
	C	3.1E+06	1.4E+07	1.5E+06	1.8E+06	2.9E+06	2.9E+08	2.2E+06	2.2E+06
	C	2.1E+06	6.1E+05	3.6E+06	4.7E+05	1.6E+08	1.5E+06	5.4E+06	6.7E+05
	C	No Data	No Data	1.5E+04	1.1E+04	1.2E+04	8.7E+03	1.8E+04	1.0E+04
	C	9.7E+05	4.3E+05	4.3E+05	9.1E+05	1.3E+06	1.1E+06	5.5E+05	2.0E+06
	C	No Data	No Data	No Data	No Data	No Data	No Data	2.3E+04	1.3E+04
	J	1.0E+05	9.7E+04	1.4E+05	2.9E+05	1.8E+05	2.8E+05	2.4E+05	2.3E+05
12	C	3.3E+04	3.5E+04	2.4E+04	4.9E+04	1.3E+04	1.5E+04	1.9E+04	3.8E+04
	C	3.6E+06	2.3E+06	1.3E+06	1.8E+06	No Data	No Data	1.2E+06	2.0E+06
	C	2.4E+04	2.4E+04	2.1E+04	3.5E+04	1.6E+04	1.2E+04	2.0E+04	1.1E+04
	C	3.3E+04	2.8E+04	2.6E+04	2.1E+04	2.6E+04	4.5E+04	3.4E+04	1.9E+04
	C	5.9E+04	7.2E+04	No Data	No Data	1.4E+04	5.4E+04	2.4E+04	2.6E+04
	C	1.9E+08	8.0E+06	1.8E+06	2.1E+06	5.4E+06	1.6E+06	1.8E+06	2.9E+06
	J	9.5E+04	1.7E+05	5.2E+05	1.4E+06	4.6E+05	3.1E+05	2.7E+05	2.7E+05
13	C	1.9E+08	6.2E+05	1.8E+04	7.7E+05	1.5E+04	2.0E+05	1.1E+04	6.2E+05
	C	2.9E+06	7.9E+06	2.0E+06	1.8E+06	2.6E+06	1.5E+08	1.6E+06	1.4E+06
	C	5.2E+04	9.6E+04	4.1E+04	3.9E+04	2.0E+04	3.2E+04	3.2E+04	3.6E+04
	J	1.1E+05	1.4E+05	1.8E+05	1.6E+05	2.1E+05	3.1E+05	1.5E+05	2.4E+05
	J	3.4E+05	2.2E+05	4.9E+05	1.8E+05	4.9E+05	4.3E+05	6.7E+05	3.2E+05
14	C	7.9E+06	1.9E+06	2.3E+06	1.8E+06	1.2E+06	1.6E+06	2.6E+06	1.6E+06
	C	2.9E+06	7.7E+05	3.1E+06	7.5E+05	2.2E+06	1.3E+06	6.4E+06	1.3E+06
	C	1.2E+06	7.7E+05	1.6E+06	4.5E+05	3.4E+06	1.3E+06	2.9E+06	1.3E+06
	C	1.3E+06	2.2E+06	1.2E+06	1.3E+06	2.4E+06	1.3E+06	2.0E+06	1.5E+06
	J	2.6E+06	6.6E+05	1.3E+06	7.0E+05	3.6E+05	1.9E+05	1.6E+06	1.8E+06
15	C	1.9E+06	6.7E+05	3.8E+06	6.2E+05	1.5E+06	1.0E+06	2.4E+06	1.4E+06
	C	6.9E+06	6.7E+05	7.0E+06	5.5E+05	2.2E+06	1.2E+06	2.2E+06	1.2E+06
	C	3.1E+06	2.5E+06	1.7E+06	1.3E+06	3.4E+06	2.6E+06	No Data	No Data
	J	4.4E+05	2.8E+05	3.0E+05	2.4E+05	7.0E+05	2.9E+05	5.9E+05	4.0E+05
	J	No Data	2.2E+05	5.1E+05	2.8E+05	No Data	No Data	4.4E+05	2.7E+05
16	C	No Data	No Data	1.3E+04	3.8E+04	No Data	No Data	1.2E+04	1.9E+04
	C	No Data	No Data	No Data	No Data	No Data	No Data	2.3E+04	1.3E+04
	C	No Data	No Data	1.9E+07	1.5E+06	No Data	No Data	3.2E+06	4.2E+07
	J	No Data	No Data	5.3E+05	2.4E+05	No Data	No Data	3.2E+05	3.1E+05
	J	No Data	No Data	7.6E+04	2.9E+04	No Data	No Data	2.3E+04	3.2E+04
	J	No Data	No Data	1.9E+05	1.5E+05	No Data	No Data	6.1E+05	7.0E+05
	J	No Data	No Data	3.3E+05	2.7E+05	No Data	No Data	3.2E+05	2.1E+05

Table B.35 (cont'd).

Site No.	Test Type	April 1997 AGG (kPa)		July 1997 AGG (kPa)		Oct. 1997 AGG (kPa)		June 1998 AGG (kPa)	
		Before	After	Before	After	Before	After	Before	After
17	C	No Data	No Data	2.0E+04	1.9E+04	No Data	No Data	3.2E+04	2.6E+04
	C	No Data	No Data	1.3E+07	1.3E+06	No Data	No Data	1.3E+07	3.0E+06
	J	No Data	No Data	2.9E+04	2.8E+04	No Data	No Data	4.3E+04	2.1E+04
	J	No Data	No Data	1.4E+05	6.3E+04	No Data	No Data	1.2E+05	5.8E+04
	J	No Data	No Data	2.9E+04	2.8E+04	No Data	No Data	3.2E+04	2.8E+04
27	C	No Data	No Data	4.8E+06	1.1E+06	2.1E+07	3.4E+06	2.6E+06	5.0E+06
	C	No Data	No Data	1.7E+04	4.1E+04	5.4E+03	6.8E+03	9.0E+03	8.1E+03
	J	No Data	No Data	1.1E+05	5.7E+05	6.5E+04	2.4E+05	5.2E+04	2.8E+05
	J	No Data	No Data	2.9E+05	5.7E+05	1.8E+05	2.3E+05	1.1E+05	1.3E+05
	J	No Data	No Data	1.8E+05	2.4E+05	1.5E+05	2.5E+05	1.1E+05	1.2E+05
28	C	No Data	No Data	9.9E+04	3.4E+05	7.9E+03	3.2E+04	8.4E+03	2.8E+04
	C	No Data	No Data	6.2E+06	3.4E+05	2.3E+08	2.3E+08	2.7E+06	2.3E+08
	C	No Data	No Data	No Data	No Data	No Data	No Data	1.9E+06	3.5E+06
	J	No Data	No Data	8.1E+04	3.8E+05	6.7E+04	2.1E+05	4.9E+04	1.2E+05
	J	No Data	No Data	3.7E+05	3.2E+05	1.7E+05	2.9E+05	2.3E+05	1.4E+05
	J	No Data	No Data	1.7E+05	3.5E+05	2.6E+05	4.9E+05	1.7E+05	5.1E+05
29	C	No Data	No Data	2.9E+06	2.9E+06	2.6E+06	4.1E+05	7.5E+04	2.0E+05
	C	No Data	No Data	2.5E+08	2.4E+06	1.2E+04	1.4E+04	1.0E+06	2.2E+07
	J	No Data	No Data	5.4E+06	2.0E+06	9.1E+04	5.9E+04	6.8E+04	3.5E+04
	J	No Data	No Data	2.5E+08	1.3E+06	9.1E+04	1.2E+06	5.3E+04	1.3E+05
	J	No Data	No Data	4.6E+06	1.1E+06	8.8E+04	1.0E+05	5.2E+04	3.2E+04
	J	No Data	No Data	1.2E+05	1.7E+05	6.7E+04	6.7E+04	5.0E+04	4.2E+04
31	C	No Data	No Data	7.2E+04	7.0E+05	5.5E+04	6.1E+04	1.2E+04	1.9E+05
	C	No Data	No Data	2.2E+06	4.7E+06	1.6E+04	1.4E+04	1.6E+04	5.4E+04
	J	No Data	No Data	1.4E+06	2.8E+05	1.9E+05	1.4E+05	3.6E+05	1.7E+05
	J	No Data	No Data	5.5E+05	6.0E+05	1.2E+05	9.8E+04	1.3E+05	5.7E+04
	J	No Data	No Data	7.0E+06	1.8E+06	1.2E+05	7.0E+04	9.6E+04	4.7E+04
32	C	No Data	No Data	No Data	No Data	No Data	No Data	4.9E+04	3.6E+04
	C	No Data	No Data	1.0E+06	2.8E+05	1.0E+05	1.4E+04	No Data	2.9E+04
	C	No Data	No Data	2.6E+08	1.1E+06	3.7E+04	8.9E+03	1.1E+05	2.4E+04
	J	No Data	No Data	5.8E+06	8.9E+05	1.7E+05	7.2E+04	1.1E+05	4.8E+04
	J	No Data	No Data	1.3E+06	8.9E+05	1.3E+05	2.2E+05	8.2E+04	6.4E+04
	J	No Data	No Data	2.6E+08	1.3E+06	6.2E+05	3.1E+05	1.6E+05	2.1E+05
47	C	2.1E+08	3.9E+06	No Data	No Data	No Data	No Data	No Data	No Data
	C	1.2E+08	1.3E+06	No Data	No Data	No Data	No Data	No Data	No Data
	C	4.6E+06	8.0E+05	No Data	No Data	No Data	No Data	No Data	No Data
	C	2.5E+04	1.6E+04	No Data	No Data	No Data	No Data	No Data	No Data

Table B.35 (cont'd).

Site No.	Test Type	April 1997 AGG (kPa)		July 1997 AGG (kPa)		Oct. 1997 AGG (kPa)		June 1998 AGG (kPa)	
		Before	After	Before	After	Before	After	Before	After
47	J	6.4E+04	5.5E+04	No Data	No Data	No Data	No Data	No Data	No Data
48	C	1.9E+04	1.5E+04	No Data	No Data	No Data	No Data	No Data	No Data
	C	4.6E+06	6.7E+05	No Data	No Data	No Data	No Data	No Data	No Data
	C	2.8E+05	2.4E+05	No Data	No Data	No Data	No Data	No Data	No Data
	C	8.6E+06	9.1E+05	No Data	No Data	No Data	No Data	No Data	No Data
	C	3.9E+06	3.2E+06	No Data	No Data	No Data	No Data	No Data	No Data
	J	3.2E+04	2.4E+04	No Data	No Data	No Data	No Data	No Data	No Data
	J	5.3E+04	7.8E+04	No Data	No Data	No Data	No Data	No Data	No Data

Table B.36 AGG Data, Slag Pavements.

Site No.	Test Type	April 1997 AGG (kPa)		July 1997 AGG (kPa)		Oct. 1997 AGG (kPa)		June 1998 AGG (kPa)	
		Before	After	Before	After	Before	After	Before	After
1	C	2.6E+08	7.4E+05	2.3E+06	5.2E+05	2.1E+06	4.2E+05	4.6E+06	1.1E+06
	C	2.6E+08	2.0E+06	1.3E+07	8.4E+05	9.7E+05	6.3E+05	No Data	No Data
	C	1.6E+07	1.1E+06	9.7E+06	7.0E+05	9.1E+05	5.5E+05	No Data	No Data
	C	3.4E+07	1.1E+06	1.5E+06	8.4E+05	1.2E+08	6.3E+05	No Data	No Data
	J	2.1E+05	8.5E+04	5.8E+07	5.7E+05	1.3E+05	6.7E+04	3.9E+06	7.2E+05
40	C	1.0E+06	1.6E+06	1.3E+07	7.3E+05	No Data	No Data	1.8E+08	8.9E+05
	C	No Data	No Data	No Data	No Data	No Data	No Data	3.1E+06	1.1E+06
	J	9.1E+05	6.0E+05	2.4E+06	1.3E+06	No Data	No Data	4.2E+06	1.5E+06
41	C	9.8E+06	1.2E+06	4.9E+06	4.2E+06	No Data	No Data	1.9E+06	2.5E+06
	C	No Data	No Data	No Data	No Data	No Data	No Data	2.0E+06	2.7E+06
	C	2.4E+06	2.0E+06	4.2E+06	1.9E+06	No Data	No Data	4.9E+06	2.0E+06
	C	2.3E+07	9.5E+05	8.0E+06	1.9E+06	No Data	No Data	4.2E+06	2.5E+06
	J	8.1E+05	7.2E+05	4.2E+06	1.0E+06	No Data	No Data	2.0E+06	1.0E+06
55	C	1.9E+04	5.0E+04	5.3E+05	1.1E+06	2.2E+04	1.8E+04	1.7E+04	2.6E+04
	C	4.9E+04	3.7E+05	1.7E+06	4.1E+05	2.0E+04	1.9E+04	4.9E+04	1.7E+05
	J	No Data	7.5E+04	6.7E+04	7.6E+04	3.6E+04	6.1E+04	2.1E+04	3.2E+04
	J	1.9E+04	No Data	1.9E+05	2.2E+06	3.2E+04	4.4E+04	1.9E+04	2.1E+04
	J	No Data	No Data	2.2E+05	6.3E+05	3.6E+04	1.4E+05	2.3E+04	5.8E+04
	J	No Data	No Data	1.4E+05	7.5E+05	2.6E+04	1.8E+05	2.5E+04	5.2E+04
58	C	No Data	No Data	1.4E+06	2.2E+06	4.3E+06	1.5E+06	4.9E+06	3.1E+06
	C	No Data	No Data	1.4E+06	1.8E+06	2.3E+06	2.3E+06	2.5E+06	3.1E+06
	J	No Data	No Data	2.7E+05	2.4E+05	4.5E+05	3.2E+05	5.2E+05	3.2E+05
	J	No Data	No Data	2.5E+05	2.0E+05	3.1E+05	2.6E+05	1.4E+06	2.1E+06
	J	No Data	No Data	7.6E+04	6.2E+04	5.2E+04	5.0E+04	4.3E+06	1.4E+06
	J	No Data	No Data	7.7E+04	2.9E+05	7.4E+04	8.6E+04	4.3E+06	2.1E+06
59	C	No Data	No Data	1.9E+06	2.8E+06	1.7E+06	1.5E+06	1.6E+06	1.7E+06
	C	No Data	No Data	6.1E+06	1.5E+06	1.3E+06	1.5E+06	1.2E+06	1.7E+06
	J	No Data	No Data	8.5E+04	5.3E+05	8.0E+04	1.5E+05	1.2E+06	1.9E+06
	J	No Data	No Data	1.3E+05	1.3E+05	9.3E+04	1.1E+05	1.3E+06	2.1E+06
	J	No Data	No Data	1.5E+05	2.4E+05	7.1E+04	8.8E+04	8.6E+05	7.8E+05
60	C	No Data	No Data	2.9E+06	1.7E+06	1.4E+06	2.1E+06	3.1E+06	1.4E+06
	C	No Data	No Data	2.7E+06	1.5E+06	1.7E+06	5.2E+06	6.0E+06	2.8E+06
	J	No Data	No Data	2.2E+06	1.7E+06	1.3E+05	2.5E+05	2.5E+06	1.9E+06
	J	No Data	No Data	2.9E+05	6.0E+05	6.2E+04	1.0E+05	5.2E+06	1.6E+06
	J	No Data	No Data	2.7E+05	2.8E+05	5.7E+04	6.4E+04	2.5E+06	9.9E+05
61	C	No Data	No Data	1.1E+06	9.9E+05	1.4E+06	8.3E+05	1.6E+06	1.0E+06
	C	No Data	No Data	2.1E+06	1.1E+06	2.2E+06	1.4E+06	4.6E+06	1.3E+06

Table B.36 (cont'd).

Site No.	Test Type	April 1997 AGG (kPa)		July 1997 AGG (kPa)		Oct. 1997 AGG (kPa)		June 1998 AGG (kPa)	
		Before	After	Before	After	Before	After	Before	After
61	J	No Data	No Data	7.3E+06	9.9E+05	3.7E+05	4.4E+05	2.4E+06	4.9E+05
	J	No Data	No Data	2.2E+06	7.9E+05	1.5E+05	2.0E+05	1.8E+06	8.6E+05
	J	No Data	No Data	1.5E+06	1.5E+06	1.5E+05	1.1E+05	5.2E+06	1.1E+06
	J	No Data	No Data	1.9E+06	1.9E+06	4.8E+04	4.8E+04	5.1E+07	1.3E+06
62	C	No Data	No Data	1.9E+06	1.4E+06	1.8E+06	1.1E+06	5.2E+06	1.5E+06
	C	No Data	No Data	1.9E+06	1.1E+06	1.4E+06	2.0E+06	2.9E+06	1.4E+06
	J	No Data	No Data	2.6E+06	1.2E+06	2.2E+05	1.4E+05	3.9E+06	1.4E+06
	J	No Data	No Data	5.7E+06	1.4E+06	1.2E+05	2.2E+05	5.2E+06	1.6E+06
	J	No Data	No Data	3.8E+06	8.0E+05	1.3E+05	1.8E+05	2.4E+06	1.2E+06
63	C	No Data	No Data	No Data	No Data	3.1E+04	1.8E+04	2.0E+04	No Data
	C	No Data	No Data	No Data	No Data	3.5E+05	2.6E+05	3.9E+04	1.7E+05
	J	No Data	No Data	No Data	No Data	3.1E+04	1.0E+05	2.6E+04	5.0E+04
	J	No Data	No Data	No Data	No Data	1.9E+04	3.4E+04	1.9E+04	4.1E+04
	J	No Data	No Data	No Data	No Data	2.1E+04	3.0E+04	2.3E+04	3.6E+04

Table B.37 Ambient Test Temperatures, Carbonate Pavements.

Site No.	Test Type	April 1997 Ambient Test Temp. (C)		July 1997 Ambient Test Temp. (C)		Oct. 1997 Ambient Test Temp. (C)		June 1998 Ambient Test Temp. (C)	
		Before	After	Before	After	Before	After	Before	After
5	C	17	17	28	29	10	10	29	29
	C	17	17	29	29	10	10	29	28
	J	16	17	29	29	9	10	29	29
6	C	18	18	30	29	10	10	28	29
	C	17	17	29	29	10	10	27	27
	J	18	18	29	30	10	10	28	28
7	C	17	17	30	30	10	11	28	27
	C	18	18	29	29	11	11	28	27
	J	17	17	30	29	10	11	28	27
8	C	15	15	33	34	11	11	24	24
	C	16	17	34	34	11	11	23	24
	J	15	16	34	34	11	11	23	24
35	C	15	16	33	33	11	12	24	24
	C	16	15	33	34	12	12	24	23
	J	16	16	34	34	12	12	25	24
36	C	16	16	34	35	11	11	23	24
	C	16	16	35	33	11	12	24	24
	J	16	16	34	34	11	11	24	24
38	C	11	11	25	26	No Data	No Data	17	16
	C	12	12	26	26	No Data	No Data	17	17
	C	12	12	26	26	No Data	No Data	17	17
	J	11	11	25	25	No Data	No Data	17	17
39	C	12	12	26	27	No Data	No Data	18	17
	C	13	13	27	26	No Data	No Data	17	17
	C	14	14	27	27	No Data	No Data	18	18
	J	12	13	26	27	No Data	No Data	17	17
42	C	18	17	22	22	15	15	10	10
	C	19	19	22	22	16	16	10	10
	J	18	18	22	22	15	15	10	10
43	C	18	19	22	22	16	16	11	12
	C	19	19	22	23	16	16	18	20
	J	19	19	22	22	16	16	14	14
	J	18	18	22	23	16	17	23	27
44	C	No Data	No Data	22	23	16	17	43	46
	C	No Data	No Data	23	23	17	16	45	45
	J	No Data	No Data	23	22	16	16	26	26

Table B.37 (cont'd).

Site No.	Test Type	April 1997 Ambient Test Temp. (C)		July 1997 Ambient Test Temp. (C)		Oct. 1997 Ambient Test Temp. (C)		June 1998 Ambient Test Temp. (C)	
		Before	After	Before	After	Before	After	Before	After
44	J	No Data	No Data	23	23	16	17	50	52
	J	No Data	No Data	23	23	17	17	47	42
	J	No Data	No Data	23	23	17	17	44	42
45	C	No Data	No Data	23	23	19	19	10	10
	J	No Data	No Data	23	23	19	19	12	10
	J	No Data	No Data	No Data	No Data	21	21	11	11
46	C	No Data	No Data	23	23	21	20	10	10
	J	No Data	No Data	23	23	20	20	10	10
	J	No Data	No Data	22	23	20	20	10	10
49	C	13	13	25	25	12	12	22	23
	J	14	14	26	25	11	13	22	22
50	C	13	13	26	26	10	10	22	22
	C	14	13	26	26	10	11	20	21
	C	14	14	26	27	11	11	20	20
	C	13	14	27	26	10	11	20	20
	J	14	14	26	27	10	10	20	20
51	C	13	12	25	25	11	10	18	19
	C	12	11	25	25	10	10	19	19
	C	11	10	24	25	10	10	18	20
	C	11	11	25	25	10	11	19	20
52	C	10	10	24	24	11	10	19	17
	C	12	12	24	25	10	10	18	18
	C	13	13	24	24	10	10	19	17
	J	12	11	24	24	10	10	18	17

Table B.38 Ambient Test Temperatures, Natural Gravel Pavements.

Site No.	Test Type	April 1997 Ambient Test Temp. (C)		July 1997 Ambient Test Temp. (C)		Oct. 1997 Ambient Test Temp. (C)		June 1998 Ambient Test Temp. (C)	
		Before	After	Before	After	Before	After	Before	After
2	C	11	12	33	33	10	11	17	17
	C	12	12	34	35	10	11	17	16
	C	11	12	35	33	11	10	17	18
	J	12	12	33	34	11	11	17	16
3	C	9	9	35	35	4	4	15	15
	C	9	9	33	34	5	5	15	16
	C	No Data	No Data	33	33	5	5	16	No Data
	J	9	9	34	34	5	5	16	16
4	C	15	14	28	29	8	8	24	24
	C	14	14	28	28	8	8	24	24
	J	16	16	28	28	8	8	24	24
9	C	9	9	No Data	No Data	No Data	No Data	No Data	No Data
	C	10	10	No Data	No Data	No Data	No Data	No Data	No Data
	J	9	9	No Data	No Data	No Data	No Data	No Data	No Data
10	C	8	8	No Data	No Data	10	10	13	13
	C	No Data	No Data	No Data	No Data	No Data	No Data	13	13
	C	7	9	No Data	No Data	10	10	13	13
	J	8	8	No Data	No Data	10	10	14	13
37	C	19	19	35	35	6	6	17	17
	C	18	20	36	35	7	6	17	17
	C	No Data	No Data	36	36	6	5	17	17
	C	21	21	36	37	6	5	17	18
	C	21	21	37	36	6	5	17	17
	C	21	20	36	36	6	6	17	17
	J	20	20	36	36	5	5	17	17
38A	C	19	19	35	35	6	6	17	17
	C	21	21	35	36	2	6	17	17
	C	19	20	36	37	5	5	17	17
	C	20	20	36	36	6	6	17	17
	C	20	20	39	36	6	6	16	17
	C	No Data	No Data	No Data	No Data	No Data	No Data	17	17
	J	21	21	36	37	6	6	17	17
57	C	23	24	33	33	5	5	16	16
	C	24	24	33	33	4	4	16	16
	C	23	23	31	30	4	4	17	16
	C	23	24	31	30	4	4	16	17

Table B.38 (cont'd).

Site No.	Test Type	April 1997 Ambient Test Temp. (C)		July 1997 Ambient Test Temp. (C)		Oct. 1997 Ambient Test Temp. (C)		June 1998 Ambient Test Temp. (C)	
		Before	After	Before	After	Before	After	Before	After
57	C	No Data	No Data	No Data	No Data	No Data	No Data	16	17
	J	24	24	33	33	5	5	16	17
	J	23	22	32	31	4	4	16	16

Table B.39 Ambient Test Temperatures, Recycled Pavements.

Site No.	Test Type	April 1997 Ambient Test Temp. (C)		July 1997 Ambient Test Temp. (C)		Oct. 1997 Ambient Test Temp. (C)		June 1998 Ambient Test Temp. (C)	
		Before	After	Before	After	Before	After	Before	After
11	C	21	21	27	26	5	5	17	17
	C	21	21	26	27	5	5	17	16
	C	21	21	27	25	5	5	17	16
	C	21	20	27	27	6	5	17	17
	C	No Data	No Data	27	28	6	6	17	17
	C	21	21	27	29	6	6	16	16
	C	No Data	No Data	No Data	No Data	No Data	No Data	17	17
	J	21	21	26	26	5	6	16	17
12	C	21	21	27	27	6	6	17	18
	C	21	20	27	28	No Data	No Data	18	17
	C	21	20	28	27	6	6	18	17
	C	21	21	28	27	5	6	18	18
	C	21	21	No Data	No Data	6	6	17	17
	C	21	21	27	28	6	6	18	17
	J	20	20	28	27	6	5	18	18
13	C	22	22	28	28	5	5	18	18
	C	22	21	28	28	6	6	18	17
	C	22	21	28	29	5	6	18	18
	J	22	21	29	29	5	6	18	18
	J	22	22	28	29	5	5	19	19
14	C	23	23	31	30	7	7	20	20
	C	23	22	32	31	6	7	20	20
	C	23	23	31	31	6	7	20	19
	C	23	23	31	31	6	6	19	19
	J	22	23	33	32	6	6	19	20
15	C	23	23	32	32	7	8	20	20
	C	22	22	32	32	7	8	21	21
	C	23	24	33	33	7	8	No Data	No Data
	J	23	23	32	32	6	7	20	20
	J	No Data	23	34	34	No Data	No Data	21	21
16	C	No Data	No Data	22	22	No Data	No Data	19	19
	C	No Data	No Data	No Data	No Data	No Data	No Data	19	19
	C	No Data	No Data	22	22	No Data	No Data	19	20
	J	No Data	No Data	21	22	No Data	No Data	20	20
	J	No Data	No Data	22	24	No Data	No Data	20	19
	J	No Data	No Data	22	21	No Data	No Data	20	20

Table B.39 (cont'd).

Site No.	Test Type	April 1997 Ambient Test Temp. (C)		July 1997 Ambient Test Temp. (C)		Oct. 1997 Ambient Test Temp. (C)		June 1998 Ambient Test Temp. (C)	
		Before	After	Before	After	Before	After	Before	After
16	J	No Data	No Data	23	23	No Data	No Data	20	20
17	C	No Data	No Data	22	22	No Data	No Data	22	22
	C	No Data	No Data	23	23	No Data	No Data	21	21
	J	No Data	No Data	22	22	No Data	No Data	22	21
	J	No Data	No Data	22	23	No Data	No Data	22	22
	J	No Data	No Data	23	24	No Data	No Data	22	21
27	C	No Data	No Data	25	26	6	5	19	19
	C	No Data	No Data	27	28	6	6	19	19
	J	No Data	No Data	25	25	6	6	18	18
	J	No Data	No Data	26	26	6	6	19	18
	J	No Data	No Data	25	24	6	6	19	19
28	C	No Data	No Data	25	25	7	7	20	19
	C	No Data	No Data	24	24	7	7	20	20
	C	No Data	No Data	No Data	No Data	No Data	No Data	20	19
	J	No Data	No Data	25	24	7	7	19	19
	J	No Data	No Data	24	24	7	7	20	20
	J	No Data	No Data	26	25	7	7	20	20
29	C	No Data	No Data	27	27	8	8	23	23
	C	No Data	No Data	27	26	9	8	23	23
	J	No Data	No Data	27	27	8	8	23	23
	J	No Data	No Data	27	27	8	8	23	23
	J	No Data	No Data	27	27	8	8	23	23
	J	No Data	No Data	27	28	8	8	23	24
31	C	No Data	No Data	27	26	4	4	19	19
	C	No Data	No Data	25	25	4	4	19	19
	J	No Data	No Data	27	27	4	4	19	18
	J	No Data	No Data	26	26	4	4	19	19
	J	No Data	No Data	26	26	4	5	19	19
32	C	No Data	No Data	No Data	No Data	No Data	No Data	19	20
	C	No Data	No Data	28	28	4	4	No Data	20
	C	No Data	No Data	29	29	4	5	19	19
	J	No Data	No Data	28	28	5	4	20	20
	J	No Data	No Data	29	29	4	4	19	19
	J	No Data	No Data	28	28	4	5	19	19
47	C	15	15	No Data	No Data	No Data	No Data	No Data	No Data
	C	16	17	No Data	No Data	No Data	No Data	No Data	No Data

Table B.39 (cont'd).

Site No.	Test Type	April 1997 Ambient Test Temp. (C)		July 1997 Ambient Test Temp. (C)		Oct. 1997 Ambient Test Temp. (C)		June 1998 Ambient Test Temp. (C)	
		Before	After	Before	After	Before	After	Before	After
47	C	17	16	No Data	No Data	No Data	No Data	No Data	No Data
	C	16	15	No Data	No Data	No Data	No Data	No Data	No Data
	J	17	17	No Data	No Data	No Data	No Data	No Data	No Data
48	C	17	17	No Data	No Data	No Data	No Data	No Data	No Data
	C	17	18	No Data	No Data	No Data	No Data	No Data	No Data
	C	18	17	No Data	No Data	No Data	No Data	No Data	No Data
	C	16	17	No Data	No Data	No Data	No Data	No Data	No Data
	C	17	18	No Data	No Data	No Data	No Data	No Data	No Data
	J	16	17	No Data	No Data	No Data	No Data	No Data	No Data
	J	16	16	No Data	No Data	No Data	No Data	No Data	No Data

Table B.40 Ambient Test Temperatures, Slag Pavements.

Site No.	Test Type	April 1997 Ambient Test Temp. (C)		July 1997 Ambient Test Temp. (C)		Oct. 1997 Ambient Test Temp. (C)		June 1998 Ambient Test Temp. (C)	
		Before	After	Before	After	Before	After	Before	After
1	C	10	11	37	36	12	11	21	22
	C	11	11	37	36	11	12	No Data	No Data
	C	11	11	35	36	12	12	No Data	No Data
	C	10	11	35	34	13	13	No Data	No Data
	J	10	11	37	36	12	12	22	22
40	C	20	21	26	25	No Data	No Data	23	24
	C	No Data	No Data	No Data	No Data	No Data	No Data	25	25
	J	21	20	26	26	No Data	No Data	25	24
41	C	21	21	27	27	No Data	No Data	24	24
	C	No Data	No Data	No Data	No Data	No Data	No Data	24	23
	C	20	21	27	27	No Data	No Data	24	24
	C	20	20	28	28	No Data	No Data	23	23
	J	20	21	26	26	No Data	No Data	23	24
55	C	17	15	29	28	9	9	25	24
	C	16	16	29	30	10	10	24	24
	J	No Data	16	29	29	10	10	24	25
	J	16	No Data	29	29	9	10	24	25
	J	No Data	No Data	30	29	9	10	25	24
	J	No Data	No Data	29	30	9	9	24	24
58	C	No Data	No Data	21	20	7	6	18	19
	C	No Data	No Data	21	21	6	6	18	18
	J	No Data	No Data	20	20	6	7	19	19
	J	No Data	No Data	21	21	6	6	19	17
	J	No Data	No Data	20	21	6	6	19	19
	J	No Data	No Data	20	21	6	6	18	17
59	C	No Data	No Data	21	21	6	6	19	19
	C	No Data	No Data	21	21	7	6	18	19
	J	No Data	No Data	20	21	6	7	18	18
	J	No Data	No Data	21	21	7	6	18	18
	J	No Data	No Data	22	21	6	6	19	19
60	C	No Data	No Data	22	22	6	6	20	19
	C	No Data	No Data	22	22	7	6	21	19
	J	No Data	No Data	22	22	7	7	20	20
	J	No Data	No Data	22	22	7	6	19	19
	J	No Data	No Data	23	23	6	7	18	19
61	C	No Data	No Data	22	23	4	4	14	14

Table B.40 (cont'd).

Site No.	Test Type	April 1997 Ambient Test Temp. (C)		July 1997 Ambient Test Temp. (C)		Oct. 1997 Ambient Test Temp. (C)		June 1998 Ambient Test Temp. (C)	
		Before	After	Before	After	Before	After	Before	After
61	C	No Data	No Data	24	23	5	5	14	14
	J	No Data	No Data	23	23	4	5	14	14
	J	No Data	No Data	23	23	5	5	14	14
	J	No Data	No Data	23	23	5	5	14	14
	J	No Data	No Data	23	23	4	5	14	14
62	C	No Data	No Data	23	23	6	6	14	14
	C	No Data	No Data	23	23	6	6	14	15
	J	No Data	No Data	23	23	6	6	14	15
	J	No Data	No Data	23	23	6	6	14	15
	J	No Data	No Data	23	23	6	6	15	15
63	C	No Data	No Data	No Data	No Data	10	10	23	No Data
	C	No Data	No Data	No Data	No Data	10	10	23	23
	J	No Data	No Data	No Data	No Data	10	10	23	23
	J	No Data	No Data	No Data	No Data	10	10	23	23
	J	No Data	No Data	No Data	No Data	10	10	23	23

Table B.41 Pavement Surface Test Temperatures, Carbonate Pavements.

Site No.	Test Type	April 1997 Pavement Test Temp. (C)		July 1997 Pavement Test Temp. (C)		Oct. 1997 Pavement Test Temp. (C)		June 1998 Pavement Test Temp. (C)	
		Before	After	Before	After	Before	After	Before	After
5	C	18	17	31	32	10	9	38	34
	C	18	18	34	34	10	10	38	36
	J	18	18	32	31	9	8	39	37
6	C	19	18	34	33	10	10	35	35
	C	19	19	34	35	10	10	36	35
	J	23	20	36	35	13	12	37	36
7	C	19	19	39	38	11	11	36	36
	C	19	20	38	39	11	10	38	36
	J	22	20	40	39	13	12	38	36
8	C	20	20	40	49	11	11	34	33
	C	22	21	41	40	14	14	33	32
	J	20	19	40	41	11	11	32	32
35	C	11	11	32	32	14	15	33	33
	C	15	15	31	32	15	16	34	33
	J	11	12	32	33	15	15	33	32
36	C	12	11	33	33	15	15	33	33
	C	16	15	38	36	18	18	37	34
	J	12	12	35	34	16	14	34	34
38	C	11	11	26	26	No Data	No Data	22	20
	C	14	13	27	27	No Data	No Data	22	21
	C	14	13	27	28	No Data	No Data	22	21
	J	13	12	25	25	No Data	No Data	21	20
39	C	15	14	27	27	No Data	No Data	21	21
	C	17	16	29	29	No Data	No Data	24	24
	C	16	15	29	28	No Data	No Data	24	24
	J	15	14	27	28	No Data	No Data	22	21
42	C	22	22	22	21	12	13	13	13
	C	21	21	22	22	13	13	12	12
	J	23	23	24	22	12	13	13	12
43	C	22	22	22	22	14	13	11	11
	C	24	24	23	24	14	13	12	12
	J	22	22	22	22	13	13	12	12
	J	22	22	23	23	15	14	12	10
44	C	No Data	No Data	23	23	14	13	11	11
	C	No Data	No Data	24	23	14	14	10	10
	J	No Data	No Data	23	23	13	14	11	10

Table B.41 (cont'd).

Site No.	Test Type	April 1997 Pavement Test Temp. (C)		July 1997 Pavement Test Temp. (C)		Oct. 1997 Pavement Test Temp. (C)		June 1998 Pavement Test Temp. (C)	
		Before	After	Before	After	Before	After	Before	After
44	J	No Data	No Data	25	24	15	15	12	13
	J	No Data	No Data	23	24	14	14	10	11
	J	No Data	No Data	25	24	14	14	11	11
45	C	No Data	No Data	24	24	18	18	16	15
	J	No Data	No Data	24	23	18	17	17	17
	J	No Data	No Data	No Data	No Data	23	22	15	16
46	C	No Data	No Data	24	24	19	18	16	17
	J	No Data	No Data	24	23	22	20	18	16
	J	No Data	No Data	25	25	20	19	20	18
49	C	14	14	31	31	16	16	33	32
	J	13	13	30	30	17	16	32	31
50	C	11	11	31	31	17	17	34	32
	C	12	11	32	31	16	15	30	30
	C	12	12	32	31	17	17	31	30
	C	14	14	33	32	15	15	33	31
	J	11	11	32	31	16	15	30	30
51	C	14	12	25	24	16	15	25	23
	C	11	12	25	25	15	16	24	22
	C	11	11	25	25	17	18	27	27
	C	10	10	25	24	16	16	26	25
52	C	9	9	23	22	15	15	22	22
	C	12	12	24	24	17	17	21	22
	C	12	12	23	25	16	16	24	23
	J	9	9	24	23	15	15	21	21

Table B.42 Pavement Surface Test Temperatures, Natural Gravel Pavements.

Site No.	Test Type	April 1997 Pavement Test Temp. (C)		July 1997 Pavement Test Temp. (C)		Oct. 1997 Pavement Test Temp. (C)		June 1998 Pavement Test Temp. (C)	
		Before	After	Before	After	Before	After	Before	After
2	C	13	12	39	38	12	11	24	23
	C	13	13	41	40	13	14	26	24
	C	14	14	42	39	14	13	27	25
	J	14	13	39	39	13	12	26	25
3	C	9	8	38	38	6	6	20	19
	C	10	9	38	38	8	6	22	22
	C	No Data	No Data	41	38	9	8	23	No Data
	J	10	10	38	36	8	7	21	21
4	C	13	12	31	30	6	6	25	26
	C	20	18	31	30	7	7	26	25
	J	14	14	32	30	10	7	28	26
9	C	8	7	No Data	No Data	No Data	No Data	No Data	No Data
	C	8	8	No Data	No Data	No Data	No Data	No Data	No Data
	J	8	8	No Data	No Data	No Data	No Data	No Data	No Data
10	C	8	9	No Data	No Data	10	9	15	15
	C	No Data	No Data	No Data	No Data	No Data	No Data	18	18
	C	11	9	No Data	No Data	10	10	17	16
	J	9	8	No Data	No Data	9	10	17	16
37	C	15	15	41	41	5	5	18	19
	C	16	16	40	38	6	5	18	18
	C	No Data	No Data	42	41	7	6	19	19
	C	17	16	43	42	6	5	19	19
	C	18	16	43	40	6	6	19	19
	C	17	17	41	41	7	6	20	20
	J	19	18	43	42	6	6	19	19
38A	C	18	18	45	43	6	6	19	18
	C	18	18	43	42	7	7	18	19
	C	19	18	44	42	9	8	20	20
	C	20	19	44	42	9	8	19	19
	C	20	19	43	41	10	8	20	20
	C	No Data	No Data	No Data	No Data	No Data	No Data	19	19
	J	20	19	44	43	9	8	20	20
57	C	26	25	26	26	3	3	16	16
	C	26	25	26	26	3	3	17	16
	C	26	26	26	26	3	4	17	18
	C	25	26	27	28	4	4	18	17

Table B.42 (cont'd).

Site No.	Test Type	April 1997 Pavement Test Temp. (C)		July 1997 Pavement Test Temp. (C)		Oct. 1997 Pavement Test Temp. (C)		June 1998 Pavement Test Temp. (C)	
		Before	After	Before	After	Before	After	Before	After
57	C	No Data	No Data	No Data	No Data	No Data	No Data	19	19
	J	27	26	27	27	3	4	17	18
	J	27	26	27	28	3	4	18	18

Table B.43 Pavement Surface Test Temperatures, Recycled Pavements.

Site No.	Test Type	April 1997 Pavement Test Temp. (C)		July 1997 Pavement Test Temp. (C)		Oct. 1997 Pavement Test Temp. (C)		June 1998 Pavement Test Temp. (C)	
		Before	After	Before	After	Before	After	Before	After
11	C	23	23	25	24	4	4	16	16
	C	21	22	25	24	4	4	17	17
	C	22	21	24	24	4	5	16	17
	C	25	24	25	25	9	7	21	19
	C	No Data	No Data	24	25	7	7	19	18
	C	24	23	25	25	6	4	18	16
	C	No Data	No Data	No Data	No Data	No Data	No Data	17	16
	J	24	24	25	24	7	6	18	18
12	C	23	23	27	26	5	5	18	17
	C	23	23	27	27	No Data	No Data	17	18
	C	22	23	27	27	6	5	18	17
	C	25	24	30	30	7	8	20	20
	C	24	22	No Data	No Data	6	5	18	18
	C	24	22	28	27	5	6	17	17
	J	24	24	29	28	8	7	19	20
13	C	24	23	29	29	6	5	18	19
	C	25	24	29	28	6	6	18	19
	C	24	24	29	30	7	6	20	20
	J	27	27	31	30	9	8	21	21
	J	32	29	36	34	8	7	22	21
14	C	27	26	38	35	8	7	21	20
	C	26	25	37	36	8	7	21	21
	C	26	26	38	38	9	10	22	21
	C	29	27	38	38	8	8	20	21
	J	27	27	39	37	9	8	23	21
15	C	29	28	41	40	10	10	22	22
	C	26	26	39	38	9	10	23	22
	C	28	28	43	43	12	10	No Data	No Data
	J	29	28	41	40	8	8	20	20
	J	No Data	27	39	39	No Data	No Data	21	21
16	C	No Data	No Data	23	24	No Data	No Data	22	21
	C	No Data	No Data	No Data	No Data	No Data	No Data	23	23
	C	No Data	No Data	25	24	No Data	No Data	22	22
	J	No Data	No Data	23	23	No Data	No Data	22	22
	J	No Data	No Data	27	27	No Data	No Data	23	22
	J	No Data	No Data	25	25	No Data	No Data	22	21

Table B.43 (cont'd).

Site No.	Test Type	April 1997 Pavement Test Temp. (C)		July 1997 Pavement Test Temp. (C)		Oct. 1997 Pavement Test Temp. (C)		June 1998 Pavement Test Temp. (C)	
		Before	After	Before	After	Before	After	Before	After
16	J	No Data	No Data	28	28	No Data	No Data	25	25
17	C	No Data	No Data	26	25	No Data	No Data	25	24
	C	No Data	No Data	27	26	No Data	No Data	26	24
	J	No Data	No Data	26	25	No Data	No Data	24	24
	J	No Data	No Data	26	27	No Data	No Data	25	25
	J	No Data	No Data	31	29	No Data	No Data	28	27
27	C	No Data	No Data	21	20	5	5	19	18
	C	No Data	No Data	23	23	7	7	19	19
	J	No Data	No Data	22	21	5	5	19	17
	J	No Data	No Data	25	23	8	7	19	19
	J	No Data	No Data	23	22	6	6	18	17
28	C	No Data	No Data	23	23	6	7	19	18
	C	No Data	No Data	23	23	7	6	19	20
	C	No Data	No Data	No Data	No Data	No Data	No Data	19	19
	J	No Data	No Data	24	24	5	6	18	19
	J	No Data	No Data	23	24	7	7	20	19
	J	No Data	No Data	27	27	9	8	22	21
29	C	No Data	No Data	30	30	7	8	25	24
	C	No Data	No Data	32	32	8	8	26	25
	J	No Data	No Data	30	29	7	7	25	25
	J	No Data	No Data	33	32	11	9	27	26
	J	No Data	No Data	33	33	7	8	26	26
	J	No Data	No Data	36	35	11	10	29	28
31	C	No Data	No Data	35	34	6	6	22	22
	C	No Data	No Data	36	35	5	5	22	22
	J	No Data	No Data	36	36	6	6	23	21
	J	No Data	No Data	37	37	7	7	24	23
	J	No Data	No Data	38	36	9	7	26	23
32	C	No Data	No Data	No Data	No Data	No Data	No Data	24	23
	C	No Data	No Data	40	39	7	7	No Data	25
	C	No Data	No Data	40	39	7	6	27	26
	J	No Data	No Data	35	35	8	8	24	23
	J	No Data	No Data	38	37	5	6	26	25
	J	No Data	No Data	39	37	4	5	24	23
47	C	21	21	No Data	No Data	No Data	No Data	No Data	No Data
	C	19	19	No Data	No Data	No Data	No Data	No Data	No Data

Table B.43 (cont'd).

Site No.	Test Type	April 1997 Pavement Test Temp. (C)		July 1997 Pavement Test Temp. (C)		Oct. 1997 Pavement Test Temp. (C)		June 1998 Pavement Test Temp. (C)	
		Before	After	Before	After	Before	After	Before	After
47	C	23	21	No Data	No Data	No Data	No Data	No Data	No Data
	C	24	24	No Data	No Data	No Data	No Data	No Data	No Data
	J	22	22	No Data	No Data	No Data	No Data	No Data	No Data
48	C	23	22	No Data	No Data	No Data	No Data	No Data	No Data
	C	21	21	No Data	No Data	No Data	No Data	No Data	No Data
	C	23	22	No Data	No Data	No Data	No Data	No Data	No Data
	C	24	24	No Data	No Data	No Data	No Data	No Data	No Data
	C	24	25	No Data	No Data	No Data	No Data	No Data	No Data
	J	23	22	No Data	No Data	No Data	No Data	No Data	No Data
	J	22	23	No Data	No Data	No Data	No Data	No Data	No Data

Table B.44 Pavement Surface Test Temperatures, Slag Pavements.

Site No.	Test Type	April 1997 Pavement Test Temp. (C)		July 1997 Pavement Test Temp. (C)		Oct. 1997 Pavement Test Temp. (C)		June 1998 Pavement Test Temp. (C)	
		Before	After	Before	After	Before	After	Before	After
1	C	12	11	47	45	15	15	34	33
	C	13	12	45	43	16	16	No Data	No Data
	C	13	14	46	45	18	18	No Data	No Data
	C	13	13	46	44	16	17	No Data	No Data
	J	15	14	47	46	20	17	36	34
40	C	26	25	29	28	No Data	No Data	36	33
	C	No Data	No Data	No Data	No Data	No Data	No Data	34	33
	J	30	27	31	31	No Data	No Data	35	33
41	C	26	26	30	29	No Data	No Data	35	34
	C	No Data	No Data	No Data	No Data	No Data	No Data	33	34
	C	27	25	31	30	No Data	No Data	35	33
	C	29	28	34	33	No Data	No Data	36	35
	J	31	29	34	32	No Data	No Data	34	35
55	C	20	20	39	37	10	10	27	27
	C	26	24	39	40	12	11	29	29
	J	No Data	21	40	39	10	10	28	28
	J	21	No Data	37	37	10	9	27	27
	J	No Data	No Data	40	38	12	11	28	29
	J	No Data	No Data	39	39	10	10	28	27
58	C	No Data	No Data	20	20	5	6	25	25
	C	No Data	No Data	20	21	5	5	26	25
	J	No Data	No Data	20	20	6	5	27	26
	J	No Data	No Data	23	23	7	7	27	26
	J	No Data	No Data	23	23	6	6	27	25
	J	No Data	No Data	24	22	8	8	28	26
59	C	No Data	No Data	22	22	6	6	27	26
	C	No Data	No Data	23	24	8	7	28	28
	J	No Data	No Data	20	22	6	7	28	26
	J	No Data	No Data	24	24	8	8	29	27
	J	No Data	No Data	25	25	8	9	29	29
60	C	No Data	No Data	23	22	7	6	31	30
	C	No Data	No Data	26	25	8	8	32	31
	J	No Data	No Data	23	22	6	7	32	31
	J	No Data	No Data	26	26	8	8	33	30
	J	No Data	No Data	27	25	8	7	32	31
61	C	No Data	No Data	25	25	6	5	17	18

Table B.44 (cont'd).

Site No.	Test Type	April 1997 Pavement Test Temp. (C)		July 1997 Pavement Test Temp. (C)		Oct. 1997 Pavement Test Temp. (C)		June 1998 Pavement Test Temp. (C)	
		Before	After	Before	After	Before	After	Before	After
61	C	No Data	No Data	26	25	4	4	18	17
	J	No Data	No Data	26	25	4	3	19	17
	J	No Data	No Data	27	26	5	5	18	18
	J	No Data	No Data	26	26	6	6	20	19
	J	No Data	No Data	28	26	7	8	19	18
62	C	No Data	No Data	26	26	5	5	17	17
	C	No Data	No Data	29	28	6	6	20	18
	J	No Data	No Data	27	26	5	4	17	17
	J	No Data	No Data	29	29	7	6	18	19
	J	No Data	No Data	29	28	7	8	19	19
63	C	No Data	No Data	No Data	No Data	10	10	24	No Data
	C	No Data	No Data	No Data	No Data	11	11	24	23
	J	No Data	No Data	No Data	No Data	11	11	24	23
	J	No Data	No Data	No Data	No Data	10	11	24	23
	J	No Data	No Data	No Data	No Data	12	12	25	24

Table B.45 Voids Analysis Results - Cracks, Carbonate Pavements.

Site No.	Crack Number[a]	Faulting[b,c,d] (mm)	x-intercept (μm)	
			October 1997	June 1998
5	1	3	No Data	124
	2	6	195	No Data
	3	3	390	No Data
	4	No	No Data	30
6	1	No	No Data	86
	2	4	142	No Data
7	1	6	No Data	117
	2	No	No Data	39
	3	3	No Data	193
8	1	No	No Data	175
	2	No	133	No Data
35	1	No	No Data	21
	2	No	14	No Data
36	1	No	No Data	12
	2	No	12	No Data
38	1	No	No Data	2
39	1	No	No Data	-1
42	1	No	No Data	27
	2	No	12	No Data
43	1	No	No Data	337
	2	3	25	No Data
44	1	No	No Data	0
	2	-3	-4	No Data
45	1	No	8	No Data
	2	No	No Data	-9
46	1	No	45	No Data
	2	No	No Data	1
49	1	No	7	No Data
	2	No	No Data	10
50	1	3	167	No Data
	2	No	No Data	2
	3	4	No Data	97
51	1	No	-613	No Data
52	1	No	4	No Data

[a] Crack numbers in this table do not correspond with those in other tables.

[b] Faulting values here refer to data collected in June 1998.

[c] Positive fault values mean that leave side was lower than approach side.

[d] No faulting is reported for cracks that had less than 2 mm (if any) of faulting.

Table B.46 Voids Analysis Results - Cracks, Natural Gravel Pavements.

Site No.	Crack Number[a]	Faulting[b,c,d] (mm)	x-intercept (μm)	
			October 1997	June 1998
2	1	No	3	No Data
	2	No	No Data	81
3	1	No	No Data	108
	2	No	108	No Data
	3	No	488	483
4	1	No	No Data	13
	2	No	8	No Data
9	No Data	No Data	No Data	No Data
10	1	5	19	No Data
	2	7	No Data	14
	3	4	No Data	23
	4	9	68	No Data
	5	No	No Data	18
	6	5	No Data	24
37	1	No	No Data	40
	2	5	No Data	115
	3	10	59	No Data
	4	11	93	No Data
	5	5	No Data	60
38A	1	No	No Data	44
	2	11	16	No Data
	3	7	-8	No Data
57	1	No	No Data	107
	2	No	8	No Data

[a] Crack numbers in this table do not correspond with those in other tables.

[b] Faulting values here refer to data collected in June 1998.

[c] Positive fault values mean that leave side was lower than approach side.

[d] No faulting is reported for cracks that had less than 2 mm (if any) of faulting.

Table B.47 Voids Analysis Results - Cracks, Recycled Pavements.

Site No.	Crack Number[a]	Faulting[b,c,d] (mm)	x-intercept (μm)	
			October 1997	June 1998
11	1	9	233	No Data
	2	No	No Data	39
	3	5	326	No Data
	4	5	No Data	275
12	1	5	386	No Data
	2	No	286	No Data
	3	6	No Data	113
	4	5	No Data	113
13	1	4	No Data	78
	2	No	No Data	13
	3	4	119	No Data
	4	5	237	No Data
	5	5	355	No Data
	6	4	No Data	287
14	1	No	16	No Data
15	1	No	3	No Data
	2	No	No Data	9
16	1	3	No Data	139
17	1	7	No Data	32
	2	No	No Data	57
	3	4	No Data	68
27	1	No	No Data	149
	2	No	581	No Data
	3	4	573	No Data
28	1	3	225	No Data
	2	No	No Data	54
29	1	No	No Data	61
	2	6	203	No Data
31	1	4	182	No Data
	2	5	172	164
	3	3	No Data	250
	4	6	No Data	115
32	1	7	No Data	95
	2	5	351	No Data

[a] Crack numbers in this table do not correspond with those in other tables.

[b] Faulting values here refer to data collected in June 1998.

[c] Positive fault values mean that leave side was lower than approach side.

[d] No faulting is reported for cracks that had less than 2 mm (if any) of faulting.

Table B.47 (cont'd).

Site No.	Crack Number[a]	Faulting[b,c,d] (mm)	x-intercept (μm)	
			October 1997	June 1998
32	3	No	574	No Data
	4	No	No Data	130
	5	4	No Data	449
47	No Data	No Data	No Data	No Data
48	No Data	No Data	No Data	No Data

[a] Crack numbers in this table do not correspond with those in other tables.

[b] Faulting values here refer to data collected in June 1998.

[c] Positive fault values mean that leave side was lower than approach side.

[d] No faulting is reported for cracks that had less than 2 mm (if any) of faulting.

Table B.48 Voids Analysis Results - Cracks, Slag Pavements.

Site No.	Crack Number[a]	Faulting[b,c,d] (mm)	x-intercept (μm)	
			October 1997	June 1998
1	1	No	No Data	37
	2	No	2	No Data
40	1	No	No Data	17
41	1	No	No Data	8
55	1	No	105	No Data
	2	No	No Data	30
	3	No	94	No Data
58	1	No	-3	No Data
	2	No	No Data	-5
59	1	No	-13	No Data
	2	No	No Data	-6
60	1	No	No Data	-6
	2	No	-10	No Data
61	1	No	No Data	-4
	2	No	-2	No Data
62	1	No	-4	No Data
	2	No	No Data	-8
63	1	No	No Data	96
	2	No	88	No Data

[a] Crack numbers in this table do not correspond with those in other tables.

[b] Faulting values here refer to data collected in June 1998.

[c] Positive fault values mean that leave side was lower than approach side.

[d] No faulting is reported for cracks that had less than 2 mm (if any) of faulting.

Table B.49 Voids Analysis Results - Joints, Carbonate Pavements.

Site No.	Joint Number[a]	Faulting[b,c,d] (mm)	x-intercept (μm)	
			October 1997	June 1998
5	1	No	9	No Data
	2	No	No Data	9
6	1	No	No Data	31
	2	No	47	No Data
7	1	No	81	No Data
	2	No	No Data	44
8	1	No	No Data	-13
	2	No	154	No Data
35	1	No	No Data	7
	2	No	57	No Data
36	1	No	No Data	35
	2	No	33	No Data
38	1	No	No Data	26
39	1	No	No Data	27
42	1	No	9	No Data
	2	No	No Data	239
43	1	No	No Data	196
44	1	No	80	No Data
	2	No	No Data	307
	3	6	50	No Data
45	1	No	No Data	402
	2	No	78	No Data
46	1	No	75	No Data
	2	No	No Data	192
49	1	No	No Data	9
	2	No	26	No Data
50	1	No	49	No Data
	2	No	No Data	25
51	No Data	No Data	No Data	No Data
52	1	No	13	No Data

[a] Joint numbers in this table do not correspond with those in other tables.

[b] Faulting values here refer to data collected in June 1998.

[c] Positive fault values mean that leave side was lower than approach side.

[d] No faulting is reported for joints that had less than 2 mm (if any) of faulting.

Table B.50 Voids Analysis Results - Joints, Natural Gravel Pavements.

Site No.	Joint Number[a]	Faulting[b,c,d] (mm)	x-intercept (μm)	
			October 1997	June 1998
2	1	No	4	No Data
	2	No	No Data	31
	3	No	No Data	23
	4	No	No Data	24
	5	No	No Data	-14
3	1	No	133	No Data
	2	No	No Data	46
	3	No	No Data	204
	4	No	11	No Data
4	1	No	No Data	9
	2	6	120	No Data
	3	No	116	No Data
9	No Data	No Data	No Data	No Data
10	1	No	0	No Data
	2	No	No Data	63
37	1	10	No Data	131
	2	12	10	No Data
	3	8	No Data	110
38A	1	10	33	No Data
	2	8	53	No Data
57	1	No	39	No Data
	2	No	15	No Data
	3	No	No Data	66

[a] Joint numbers in this table do not correspond with those in other tables.

[b] Faulting values here refer to data collected in June 1998.

[c] Positive fault values mean that leave side was lower than approach side.

[d] No faulting is reported for joints that had less than 2 mm (if any) of faulting.

Table B.51 Voids Analysis Results - Joints, Recycled Pavements.

Site No.	Joint Number[a]	Faulting[b,c,d] (mm)	x-intercept (μm)	
			October 1997	June 1998
11	1	No	No Data	102
	2	No	113	No Data
12	1	No	No Data	125
	2	No	70	No Data
13	1	No	No Data	73
	2	No	47	No Data
14	1	No	31	No Data
15	1	No	8	No Data
	2	No	No Data	-3
16	1	No	No Data	121
	2	3	No Data	478
17	1	2	No Data	88
	2	No	No Data	61
27	1	No	321	No Data
	2	No	134	No Data
	3	No	No Data	198
28	1	No	No Data	180
	2	No	117	No Data
29	1	No	No Data	109
	2	No	332	No Data
	3	3	293	No Data
31	1	No	No Data	318
32	1	No	No Data	346
47	No Data	No Data	No Data	No Data
48	No Data	No Data	No Data	No Data

[a] Joint numbers in this table do not correspond with those in other tables.

[b] Faulting values here refer to data collected in June 1998.

[c] Positive fault values mean that leave side was lower than approach side.

[d] No faulting is reported for joints that had less than 2 mm (if any) of faulting.

Table B.52 Voids Analysis Results - Joints, Slag Pavements.

Site No.	Joint Number[a]	Faulting[b,c,d] (mm)	x-intercept (μm)	
			October 1997	June 1998
1	1	No	No Data	10
	2	No	3	No Data
40	1	3	No Data	3
	2	No	No Data	5
41	1	No	No Data	7
55	1	No	No Data	26
	2	No	57	No Data
58	1	No	-15	No Data
	2	No	No Data	-7
59	1	No	No Data	-1
	2	No	-1	No Data
60	1	No	No Data	-8
	2	No	0	No Data
61	1	No	2	No Data
	2	No	No Data	-2
62	1	No	No Data	-3
	2	No	2	No Data
63	1	No	118	No Data
	2	No	No Data	127

[a] Joint numbers in this table do not correspond with those in other tables.

[b] Faulting values here refer to data collected in June 1998.

[c] Positive fault values mean that leave side was lower than approach side.

[d] No faulting is reported for joints that had less than 2 mm (if any) of faulting.

REFERENCES

- REFERENCES -

1. *AASHTO Guide for Design of Pavement Structures*. American Association of State Highway and Transportation Officials, Washington, D.C., 1993.

2. McGhee, K.H. *Design, Construction, and Maintenance of PCC Pavement Joints*. NCHRP Synthesis of Highway Practice 211. Transportation Research Board (TRB), National Research Council, 1995.

3. Huang, Y.H. *Pavement Analysis and Design*. Prentice-Hall, Inc., Englewood Cliffs, NJ, 1993.

4. Westergaard, H.M. Analysis of Stresses in Concrete Pavement Due to Variations of Temperature. *Proceedings, Highway Research Board*, Vol. 6, 1926, pp. 201-215.

5. Bradbury, R.D. *Reinforced Concrete Pavements*. Wire Reinforcement Institute, Washington, D.C., 1938.

6. Westergaard, H.M. New Formulas for Stresses in Concrete Pavements of Airfields. *ASCE Transactions*, Vol. 113, 1948, pp. 425-444.

7. Miner, M.A. Cumulative Damage in Fatigue. *Transactions of the ASME*, Vol. 67, 1945, pp. A159-A164.

8. Ioannides, A.M. Pavement Fatigue Concepts: A Historical Review. *Proceedings, Sixth International Purdue Conference on Concrete Pavement Design and Materials for High Performance, Vol. 3*, Indianapolis, IN, Nov. 18-21, 1997, pp. 147-159.

9. Mindess, S., and J.F. Young. *Concrete*. Prentice-Hall, Inc., Englewood Cliffs, NJ, 1981.

10. Darter, M.I., K.T. Hall, and C. Kuo. *Support under Portland Cement Concrete Pavements*. NCHRP Report 372. TRB, National Research Council, 1995.

11. Smith, K.D., M.J. Wade, H.T. Yu, and M.I. Darter. Design Considerations for Improved JPCP Performance. *Proceedings, Sixth International Purdue Conference on Concrete Pavement Design and Materials for High Performance, Vol. 1*, Indianapolis, IN, Nov. 18-21, 1997, pp. 89-109.

12. Darter, M.I. *Initial Evaluation of Michigan JRCP Crack Deterioration in JRCP*. Revised Report. Michigan Concrete Paving Association, 1989.

13. Nowlen, W.J. Influence of Aggregate Properties on Effectiveness of Interlock Joints in Concrete Pavements. *Journal of the PCA, Research and Development Laboratories*, Vol. 10, No. 2, May 1968, pp. 2-8.

14. Raja, Z.I., and M.B. Snyder. Factors Affecting Deterioration of Transverse Cracks in Jointed Reinforced Concrete Pavements. *Transportation Research Record 1307*, TRB, National Research Council, Washington, D.C., 1991, pp. 162-168.

15. Khazanovich, L., M.I. Darter, and K.D. Smith. Transverse Crack Deterioration Model for JRCP. *Proceedings, Sixth International Purdue Conference on Concrete Pavement Design and Materials for High Performance, Vol. 1*, Indianapolis, IN, Nov. 18-21, 1997, pp. 311-327.

16. Poblete, M., R. Valenzuela, and R. Salsilli. Load Transfer in Undoweled Transverse Joints of PCC Pavements. *Transportation Research Record 1207*, TRB, National Research Council, Washington, D.C., 1988, pp. 39-49.

17. Paulay, T., and P.J. Loeber. Shear Transfer by Aggregate Interlock. *Shear in Reinforced Concrete*. ACI Special Publication SP 42-1, Vol. 1. American Concrete Institute (ACI), Detroit, MI, 1974, pp. 1-15.

18. Benkelman, A.C. Tests of Aggregate Interlock at Joints and Cracks. *Engineering News-Record*, Vol. 111, No. 8, Aug. 24, 1933, pp. 227-232.

19. Laible, J.P., R.N. White, and P. Gergely. Experimental Investigation of Seismic Shear Transfer Across Cracks in Concrete Nuclear Containment Vessels. *Reinforced Concrete Structures in Seismic Zones*. ACI Special Publication SP 53-9. ACI, Detroit, MI, 1977, pp. 203-226.

20. Jimenez, R., P. Gergely, and R.N. White. *Shear Transfer across Cracks in Reinforced Concrete*. Report 78-4. Cornell University, 1978.

21. Fardis, M.N., and O. Buyukozturk. Shear Transfer Model for Reinforced Concrete. *Proceedings, ASCE*, Vol. 105, No. EM2, April 1979, pp. 225-275.

22. Walraven, J.C. Fundamental Analysis of Aggregate Interlock. *Journal of the Structural Division, ASCE*, Vol. 107, No. 11, Nov. 1981, pp. 2245-2270.

23. Millard, S.G., and R.P. Johnson. Shear Transfer Across Cracks in Reinforced Concrete Due to Aggregate Interlock and to Dowel Action. *Magazine of Concrete Research*, Vol. 36, No. 126, Mar. 1984, pp. 9-21.

24. Soroushian, P., K. Obaseki, and K. Choi. Analysis of Aggregate Interlock Behaviour at Cracks in Reinforced Concrete. *Magazine of Concrete Research*, Vol. 40, No. 142, Mar. 1988, pp. 43-49.

25. Paulay, T., R. Park, and M.H. Phillips. Horizontal Construction Joints in Cast-in-Place Reinforced Concrete. *Shear in Reinforced Concrete*. ACI Special Publication SP 42, Vol. 2. ACI, Detroit, MI, 1974, pp. 599-616.

26. Mills, G.M. A Partial Kinking Criterion for Reinforced Concrete Slabs. *Magazine of Concrete Research*, Vol. 27, No. 90, Mar. 1975, pp. 13-22.

27. Millard, S.G. *Shear Transfer in Cracked Reinforced Concrete*. Ph.D. Thesis. University of Warwick, 1983.

28. Ioannides, A.M., and G.T. Korovesis. Aggregate Interlock: A Pure-Shear Load Transfer Mechanism. *Transportation Research Record 1286*, TRB, National Research Council, Washington, D.C., 1990, pp. 14-24.

29. Buch, N.J. *Development of Empirical-Mechanistic Based Faulting Models in the Design of Plain Jointed Concrete Pavements*. Ph.D. Dissertation. Texas A&M University, College Station, TX, 1995.

30. Colley, B.E., and H.A. Humphrey. Aggregate Interlock at Joints in Concrete Pavements. *Highway Research Record 189*, Highway Research Board (HRB), National Research Council, Washington, D.C., 1967, pp. 1-18.

31. Fenwick, R.C., and T. Paulay. Mechanisms of Shear Resistance of Concrete Beams. *Journal of the Structural Division, ASCE*, Vol. 94, No. 10, Oct. 1968, pp. 2325-2350.

32. *Design, Construction, and Maintenance of PCC Pavement Joints*. NCHRP Synthesis of Highway Practice 19. HRB, National Research Council, 1973.

33. Bruinsma, J.E., Z.I. Raja, M.B. Snyder, and J.M. Vandenbossche. *Factors Affecting the Deterioration of Transverse Cracks in JRCP*. Final Report. Michigan Department of Transportation, 1995.

34. Sutherland, E.C., and H.D. Cashell. Structural Efficiency of Transverse Weakened-Plane Joints. *Public Roads*, Vol. 24, No. 4, Apr.-June 1945, pp. 83-97.

35. Vandenbossche, J.M., and M.B. Snyder. Estimating Potential Aggregate Interlock Load Transfer Based upon Measurements of Volumetric Surface Texture of the Fracture Plane. *A Paper Prepared for the Open Paper Session of ACI Annual Meeting*, Denver, CO, Mar. 1996.

36. Armaghani, J.M., J.M. Lybas, M. Tia, and B.E. Ruth. Concrete Pavement Joint Stiffness Evaluation. *Transportation Research Record 1099*, TRB, National Research Council, Washington, D.C., 1986, pp. 22-36.

37. Smith, K.D., D.G. Peshkin, M.I. Darter, A.L. Mueller, and S.H. Carpenter. *Performance of Jointed Concrete Pavements, Phase I, Volume IV - Appendix A.* Report FHWA-RD-89-139. Federal Highway Administration (FHWA), U.S. Department of Transportation, 1990.

38. Neville, A. *Properties of Concrete.* Pittman Publishing, Ltd., Aulander Cliffs, NC, 1975.

39. *Joint and Crack Sealing and Repair for Concrete Pavements.* Report TB-012P. American Concrete Pavement Association (ACPA), 1993.

40. *Guidelines for Full-Depth Repair.* Report TB-002P. ACPA, 1995.

41. Darter, M.I., E.J. Barenberg, and W.A. Yrjanson. *Joint Repair Methods for Portland Cement Concrete Pavements.* NCHRP Report 281. TRB, National Research Council, 1985.

42. Snyder, M.B., M.J. Reiter, K.T. Hall, and M.I. Darter. *Rehabilitation of Concrete Pavements: Volume I – Repair Rehabilitation Techniques.* Report FHWA-RD-88-071. FHWA, U.S. Department of Transportation, 1989.

43. Pierce, L.M. Design, Construction, Performance, and Future Direction of Dowel Bar Retrofit in Washington State. *Proceedings, Sixth International Purdue Conference on Concrete Pavement Design and Materials for High Performance, Vol. 2,* Indianapolis, IN, Nov. 18-21, 1997, pp. 87-100.

44. *Slab Stabilization Guidelines for Concrete Pavements.* Report TB-018P. ACPA, 1994.

45. Hossain, M., and A.J. Gisi. Detection of Voids under Concrete Pavements Using Deflection Testing – Kansas Experience. *Proceedings, Fourth International Conference on the Bearing Capacity of Roads and Airfield,* Minneapolis, MN, July 17-21, 1994, pp. 1703-1718.

46. *Construction Handbook on PCC Pavement Rehabilitation.* FHWA, Washington, D.C., 1984.

47. *Cement-Grout Subsealing and Slabjacking of Concrete Pavements.* Report IS212.01P. Portland Cement Association, 1982.

48. Taha, R., A. Salim, S. Hasan, and B. Lunde. Evaluation of Highway Undersealing Practices of PCC Pavements. *Paper No. 940104, Presented at the 1994 Transportation Research Board Annual Meeting,* Washington, D.C., Jan.1994.

49. Sawan, J.S., M.I. Darter, and B.J. Dempsey. *Structural Analysis and Design of PCC Shoulders*. Report FHWA-RD-81-122. FHWA, U.S. Department of Transportation, 1982.

50. Colley, B.E., C.G. Ball, and P. Arrigavat. Evaluation of Concrete Pavements with Tied Shoulders or Widened Lanes. *Transportation Research Record 666*, TRB, National Research Council, Washington, D.C., 1978, pp. 39-45.

51. *Diamond Grinding and Concrete Pavement Restoration 2000*. Report TB-008P. ACPA, 1990.

52. *Guidelines for Unbonded Concrete Overlays*. Report TB-005P. ACPA, 1990.

53. *Guidelines for Bonded Concrete Overlays*. Report TB-007P. ACPA, 1990.

54. *Distress Identification Manual for the Long-Term Pavement Performance Studies*. Report SHRP-LTPP-FR-90-001. Strategic Highway Research Program (SHRP), National Research Council, 1990.

55. Helmuth, R., D. Stark, S. Diamond, and M. Moranville-Regourd. *Alkali-Silica Reactivity: An Overview of Research*. Report SHRP-C-342. SHRP, National Research Council, 1993.

56. Smith, K.D., H.T. Yu, M.J. Wade, D.G. Peshkin, and M.I. Darter. *Performance of Concrete Pavements, Volume I - Field Investigation*. Report FHWA-RD-94-177. FHWA, U.S. Department of Transportation, 1997.

57. Hall, K.T. Backcalculation Solutions for Concrete Pavements. *A Paper Prepared for Long-Term Pavement Performance Data Analysis*. Report SHRP-P-20. SHRP, National Research Council, 1992.

58. Wade, M.J., G.D. Cuttell, J.M. Vandenbossche, H.T. Yu, K.D. Smith, and M.B. Snyder. *Performance of Concrete Pavements Containing Recycled Concrete Aggregate*. Report FHWA-RD-96-164. FHWA, U.S. Department of Transportation, 1997.

59. Darter, M.I. *Design of Zero-Maintenance Plain Jointed Pavements*. Report FHWA-RD-77-111. FHWA, U.S. Department of Transportation, 1977.

60. Milton, J.S., and J.C. Arnold. *Introduction to Probability and Statistics: Principles and Applications for Engineering and Computing Sciences*. McGraw-Hill, Inc., New York, NY, 1990.

61. Snyder, M.B. VSTR Test Results and Interpretation. *Letter to Neeraj Buch*, Mar. 25, 1998.